This is to certify that the

dissertation entitled

The Scattering and Receiving Characteristics Of Monopoles and Slots in Tri-Layered Media

presented by

Wang-jie Gesang

has been accepted towards fulfillment of the requirements for

Ph.D. degree in Electrical Engineering

Major professor

Date 11/21/91

PLACE IN RETURN BOX to remove this checkout from your record.
TO AVOID FINES return on or before date due.

DATE DUE	DATE DUE	DATE DUE

TH

OF

THE SCATTERING AND RECEIVING CHARACTERISTICS OF MONOPOLES AND SLOTS IN TRI-LAYERED MEDIA

By

Wang-jie Gesang

A DISSERTATION

Submitted to
Michigan State University
in partial fulfillment of the requirements
for the degree of

DOCTOR OF PHILOSOPHY

Department of Electrical Engineering

1991

THE

OF

In this dis

slots in tri-laye

niques are use

and electromag

the magnetic

integral equatio

induced curre

impedance, ra

numeric-analyt

admittance ma

Theoretic

observed. Ant

power, and ra

in tri-layered

interaction of

that, for an an

ABSTRACT

THE SCATTERING AND RECEIVING CHARACTERISTICS OF MONOPOLES AND SLOTS IN TRI-LAYERED MEDIA

by

Wang-jie Gesang

In this dissertation, the scattering and receiving characteristics of monopoles and slots in tri-layered media have been studied. Two-dimensional Fourier transform techniques are used to derive the dyadic Green's functions for vector Hertzian potentials and electromagnetic fields. The electric field integral equation for a thin monopole and the magnetic field integral equation for a narrow slot are converted to Hallen-type integral equations. Galerkin's method is used to solve the integral equations to obtain induced currents on the antennas. Antenna parameters investigated are input impedance, radiation pattern, received power, and radar cross section. Various numeric-analytical techniques are exploited to evaluate the entries of impedance and admittance matrices accurately and efficiently.

Theoretical results are compared against published data and good agreement is observed. Antenna current distribution, input impedance, radiation pattern, received power, and radar cross section are obtained for a vertical imaged monopole and a slot in tri-layered media with various substrates and superstrates. Emphasis is placed on the interaction of a lossy superstrate with an antenna. The theoretical results demonstrate that, for an antenna in tri-layered media with a lossy superstrate, the reduction in radar

cross section is

this dissertation

capabilities and

cross section is greater than the reduction in received power. The theory developed in this dissertation can aid in the design of antennas with good transmission and receiving capabilities and low radar cross section.

To my wife

Wei Cha

First, I wish
and support throu
have had the opp
also like to expre
for their generous
and rewarding ex

I am much
grateful to the fe
their help.

I owe a gre
not least, I must
stant encourage
my graduate stu

ACKNOWLEDGMENTS

First, I wish to thank Dr. Kun-Mu Chen, my academic advisor, for his guidance and support throughout my study at Michigan State University. I feel very fortunate to have had the opportunity to work under his supervision and to learn from him. I would also like to express my gratitude to Dr. Dennis P. Nyquist and Dr. Edward J. Rothwell for their generous advice and help. Working closely with them has been an enjoyable and rewarding experience.

I am much obliged to Dr. Byron Drachman for his time and direction. I am also grateful to the fellow graduate students working in the Electromagnetics Laboratory for their help.

I owe a great deal to my parents for their love and continuous support. Last but not least, I must acknowledge my wonderful wife, Wei Cha. Her love, sacrifice, constant encouragement and support have been invaluable in the successful completion of my graduate study.

TABLE OF CONTENTS

LIST OF FIGURES

1.1 Introductio

In some ap
such as an aircr
there are many
ing antenna sub
of the aircraft.
an antenna syst
system.

An effecti
preserve the rec
that while the
once and endur
and suffers two

It is neces
coating and to
radar absorbing
simplified mode
an antenna, is
substrate, a sup
is a very vers
essential antenn
are studied in

CHAPTER ONE
INTRODUCTION

1.1 Introduction

In some applications, it is necessary to reduce the radar cross section of a system, such as an aircraft. In order to communication with other airplanes and ground control, there are many conformal antenna subsystems on board. However an effective receiving antenna subsystem is also an effective contributor to the overall radar cross section of the aircraft. In other words, the requirement to maintain the receiving capability of an antenna system contradicts the requirement to reduce the radar cross section of the system.

An effective way to decrease the radar cross section of an antenna and to preserve the receiving ability of the antenna is lossy coating. The physical intuition is that while the received signal or transmitted signal passes through the lossy coating once and endures one loss, the scattered signal must go through the lossy layer twice and suffers two losses.

It is necessary to develop a theoretical model to analyze an antenna with lossy coating and to provide design guidelines. A practical conformal antenna coated with radar absorbing material on board an aircraft is too complicated to handle at once. A simplified model, which highlights the effects of lossy coating on the characteristics of an antenna, is established. The geometry is tri-layered media with a ground plane, a substrate, a superstrate, and a half space. The superstrate can be a lossy coating. This is a very versatile structure and includes major electromagnetic phenomena. Two essential antenna elements, a vertical imaged monopole and a slot, in tri-layered media are studied in the dissertation. A detailed description of the geometry is provided in the next section.

A vertical i

geneous medium

Sommerfeld pio

planarly layered

ject. A recent b

waves and fields

work on the sub

One of the

problems in ele

functions in la

Transform tech

[6][10][11] The

The scatte

research for ye

antennas, which

works on printe

pared with micr

Sommerfel

layered media

tral integrals in

ous analytical,

tional time [35]

There are

this research. I

solved.

the next section.

A vertical imaged monopole is equivalent to a dipole. A dipole or a slot in homogeneous medium is a classical antenna problem and is treated in many books [1]-[4]. Sommerfeld pioneered the study of the propagation of electromagnetic (EM) waves in planarly layered media [5]. There are extensive research and publications on the subject. A recent book by Chew [6] presents a comprehensive and updated treatment of waves and fields in inhomogeneous media. From this book, all the important historical work on the subject can be traced.

One of the most powerful and commonly used technique to solve boundary value problems in electromagnetics is the integral equation approach [7]-[9]. Dyadic Green's functions in layered media are needed to arrive at appropriate integral equations. Transform techniques can be used to derive Green's functions in layered media [6][10][11] The singularity of dyadic Green's function has been studied in [12].

The scattering and radiation of apertures in ground plane has been the subject of research for years [13]-[17]. There is a vast amount of publication on microstrip antennas, which are closely related to slots, [18]-[26]. Of particular interest are the the works on printed circuit antenna in a superstrate-substrate configuration [27][28]. Compared with microstrip antenna, printed slot has received less attention [29]-[34].

Sommerfeld integral approach can solve the EM wave propagation in planarly layered media rigorously. The price to pay for the analytical elegance is that the spectral integrals involved in matrix filling are very difficult to compute numerically. Various analytical, asymptotic, and numerical techniques can be used to reduce computational time [35]-[44].

There are eight chapters in this dissertation. Chapter one gives the motivation for this research. It also contains a literature survey and describes the problems to be solved.

Chapter two presents in detail the derivation of dyadic Green's functions in tri-layered media. Electric and magnetic Hertzian potentials are used to facilitate the development of Green's functions. The planar layers are homogeneous and have arbitrary electric and magnetic contrasts. The Green's functions for Hertzian potentials and EM fields maintained by a vertical electric current or a horizontal magnetic current in the substrate are derived.

Plane wave propagation in tri-layered media is investigated in chapter three. This information is needed to determine the excitation terms of the integral equations developed in chapter four.

An electric field integral equation (EFIE) and a magnetic field integral equation (MFIE) are developed in chapter four. Then under certain approximation conditions, both EFIE and MFIE are converted to Hallen-type integral equations (HTIE).

Chapter five presents solutions of the integral equations developed in the previous chapter by moment methods. Special effort is made to find accurate and efficient ways to calculate the spectral integrals encountered in matrix filling. Induced current on a monopole or a slot in tri-layered media illuminated by an incident plane wave is obtained. Input impedance and received power are computed.

Chapter six deals with the evaluation of scattered field. A stationary phase method is used to calculate far field. The expressions for radar cross section and radiation pattern are presented.

Numerical results generated by the theory developed in this dissertation are compared with published results and experimental data whenever possible in chapter seven to validate the theory. Then computer simulation are conducted for several sets of representative parameters of a monopole or a slot in tri-layered media. Results of input impedance, received power, radar cross section, and radiation pattern are plotted.

In the final

is drawn from th

mended.

1.2 Problem De

Two proble

media, have bee

to analyze slots

layered media is

that the lossy co

more complicate

phenomena of s

plicated problem

Consider th

a conducting gr

of thickness t,

length h and rad

and have arbitr

respectively. Th

θ. The monopol

magnetically los

The geome

thin conducting

length 2l is cut

substrate of thic

the ground plan

In the final chapter, chapter eight, the work done are summarized. A conclusion is drawn from the results of chapter seven. Some ideas on further research are recommended.

1.2 Problem Description and Decomposition

Two problems, an imaged monopole in tri-layered media and a slot in tri-layered media, have been studied. The ultimate goal is to develop a theory and computer codes to analyze slots in tri-layered media. The main reason to study a vertical monopole in layered media is that this is the simplist problem in tri-layered media. It is conjectured that the lossy coating interacts with this simple antenna in much the same way as with more complicated antenna systems. This simple model keeps all the electromagnetic phenomena of scattering and radiation in layered media and can lead to the more complicated problem of slots in stratified media.

Consider the geometry pictured in Figure 1.1. The tri-layered media are made of a conducting ground plane in the z=-d plane, a substrate of thickness d, a superstrate of thickness t, and a half space on top of the superstrate. A vertical monopole of length h and radius a is immersed in the substrate. The planar layers are homogeneous and have arbitrary complex permittivity and permeability ε_1, ε_2, ε_3, μ_1, μ_2 and μ_3 respectively. The entire structure is illuminated by a plane wave with an incident angle θ. The monopole has a load Z_L attached to it. The superstrate can be a electrically or magnetically lossy coating.

The geometry of a slot in tri-layered media is shown in Figure 1.2. An infinitely thin conducting ground is placed in z=0 plane. A rectangular slot of width 2w and length 2l is cut in the ground plane. There are three layers above the ground plane, a substrate of thickness d, a superstrate of thickness t, and a semi-infinite space. Beneath the ground plane is another semi-infinite space. All four layers are assumed to be homogeneous and

is illuminated by

placed at the cen

lossy coating.

In practice,

to make it radiat

in Figure 1.2 is

interaction betwe

waves in tri-laye

include backing

In the recei

of the energy is

superposition pri

ing problem and

linear.

First consid

figure 1.3. A rec

wave. The curre

$$V = -I$$

In the scatt

ing mode curren

the gap between

is generated by

of the monopole

$$Z_{in} = $$

homogeneous and can have arbitrary complex permittivity and permeability. The slot is illuminated by a plane wave with incident angle θ . A load impedance Z_L can be placed at the center of the slot. The superstrate can be a electrically or magnetically lossy coating.

In practice, a slot usually is backed by either a cavity or another conducting plate to make it radiate in only one direction. The reason to choose the structure described in Figure 1.2 is to simplify the problem and to concentrate on the effects of the EM interaction between a slot and a lossy coating. Once the radiation and scattering of EM waves in tri-layered media have been well understood, the research can be extended to include backing and complicated and practical feeding mechanism for slots.

In the receiving case, an incident plane wave induces current on a antenna. Part of the energy is delivered to the load and part of it is radiated out in the space. The superposition principle can be used to decompose the receiving problem into a scattering problem and a transmitting one as shown in Figure 1.3 because the problems are linear.

First consider the decomposition of a receiving monopole shown in part a of figure 1.3. A receiving mode current I is induced on a monopole by an incident plane wave. The current causes a voltage drop V across the load Z_L.

$$V = -IZ_L \tag{1.2.1}$$

In the scattering case, the monopole is shorted to the ground plane and a scattering mode current I_s is induced by an incident plane. There is no voltage drop across the gap between the monopole and the ground plane. A transmitting mode current I_t is generated by a voltage source V_t. There is no incident wave. The input impedance of the monopole is defined as

$$Z_{in} = \frac{V_t}{I_t} \tag{1.2.2}$$

The receiving

current I_s and load

$$I = I_s + I_t$$

$$V = V_t$$

From (1.2.1-4

$$I_t = -I\frac{Z}{Z}$$

The transmi

current by solvin

$$I_t = -I_s$$

The the re

current by solvi

$$I = I_s$$

Finally, th

$$P_L =$$

where

$$Z_L =$$

Then co

1.3. An ape

This apertur

flowing alo

The receiving mode current I can be expressed in terms of scattering mode current I_s and load and input impedance Z_{in} and Z_L by some straight manipulation.

$$I = I_s + I_t \tag{1.2.3}$$

$$V = V_t \tag{1.2.4}$$

From (1.2.1-4)

$$I_t = -I\frac{Z_L}{Z_{in}} = -(I_t + I_s)\frac{Z_L}{Z_{in}} \tag{1.2.5}$$

The transmitting mode current can be expressed in terms of scattering mode current by solving (1.2.5)

$$I_t = -I_s\frac{Z_L}{Z_L + Z_{in}} \tag{1.2.6}$$

The the receiving mode current can be expressed in terms of scattering mode current by solving (1.2.6).

$$I = I_s + I_t = I_s\frac{Z_{in}}{Z_{in} + Z_L} \tag{1.2.7}$$

Finally, the power delivered to the load Z_L can be written as

$$P_L = \frac{1}{2}\mathrm{Re}(VI^*) = \frac{1}{2}|I_s|^2 R_L \left|\frac{Z_{in}}{Z_{in} + Z_L}\right|^2 \tag{1.2.8}$$

where

$$Z_L = R_L + jX_L$$

Then consider the decomposition of a receiving slot shown in part b of Figure 1.3. An aperture electric field $\mathbf{E}_a$ is induced in the slot by an incident plane wave. This aperture field generates a voltage V across the slot and an electric current I flowing along a load impedance Z_L. For a narrow slot ($w \ll l$; $w \ll \lambda$), the voltage across the slot is expressed as

$$V = \int_{-w}^{w} E_{ay}\, dy \tag{1.2.9}$$

where the orientation of the slot is shown in Figure 1.2.

$$I = -\frac{V}{Z_L} \tag{1.2.10}$$

The slot is open and illuminated by a plane wave in the scattering case. An scattering mode voltage V_s can be obtained from (1.2.9). Notice that there is no conduction electric current flowing across the slot. A transmitting mode voltage V_t is generated by a electric current source I_t placed in the slot. There is no incident wave. The input impedance of a slot is defined as

$$Z_{in} = \frac{V_t}{I_t} \tag{1.2.11}$$

This definition of input impedance of a slot depends on the position of the current source in the slot.

The receiving mode voltage V can be expressed in terms of the scattering mode voltage V_s and input and load impedance Z_{in} , Z_L through some straight forward derivation.

$$I = I_t \tag{1.2.12}$$

$$V = V_s + V_t \tag{1.2.13}$$

From (1.2.10-13)

$$V_t = -V\frac{Z_{in}}{Z_L} = -(V_s+V_t)\frac{Z_{in}}{Z_L} \tag{1.2.14}$$

Solve (1.2.14

$$V_t = -V_s$$

Substituting (

$$V = V_s \frac{}{Z}$$

The power re

$$P_L = \frac{1}{2}\mathrm{R}$$

According to

by an equivalent m

$$\mathbf{M} = -\hat{n}\times$$

Then the problem

shown in Figure 1

Green's function in

Green's function i

development of MI

Solve (1.2.14) to get

$$V_t = -V_s \frac{Z_{in}}{Z_L + Z_{in}} \tag{1.2.15}$$

Substituting (1.2.15) into (1.2.13) leads to

$$V = V_s \frac{Z_L}{Z_L + Z_{in}} \tag{1.2.16}$$

The power received by the load Z_L can be expressed as

$$P_L = \frac{1}{2}\mathrm{Re}(VI^*) = \frac{1}{2}|V|^2 \frac{R_L}{|Z_L + Z_{in}|^2} \tag{1.2.17}$$

According to the equivalence principle, the aperture electric field can be replaced by an equivalent magnetic current defined as:

$$\mathbf{M} = -\hat{n} \times \mathbf{E}_a \tag{1.2.18}$$

Then the problem shown in Figure 1.2 can be reduced to two equivalent problems shown in Figure 1.4. It can been seen that the ground plane makes the derivation of Green's function in the upper half space, which has three layers, and the derivation of Green's function in the lower half space independent. The coupling occurs in the development of MFIE.

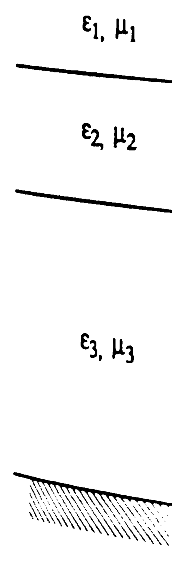

Figure 1.1 Image

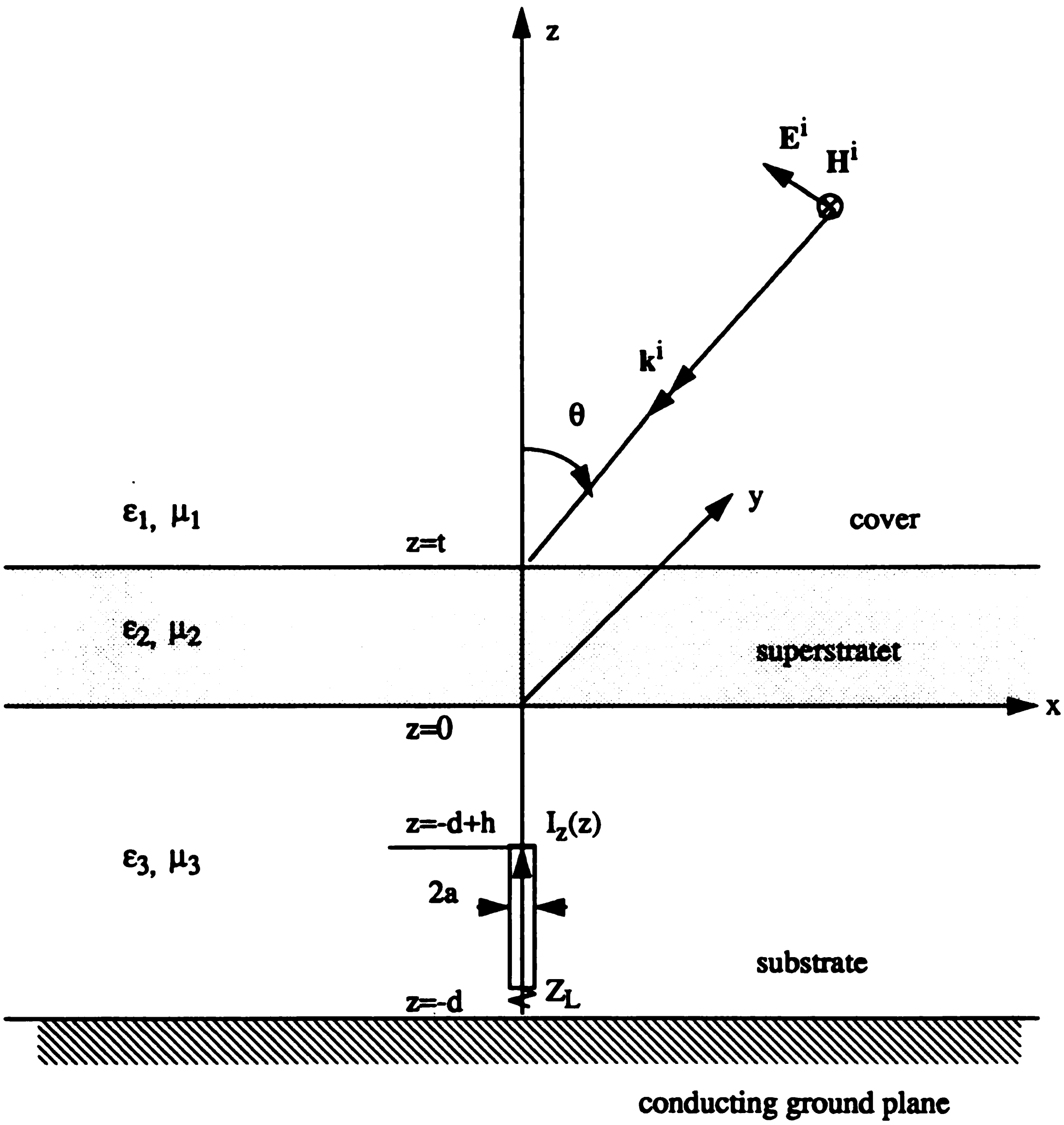

Figure 1.1 Imaged monopole in tri-layered media.

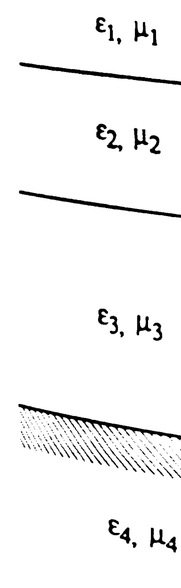

Figure 1.2 Sl

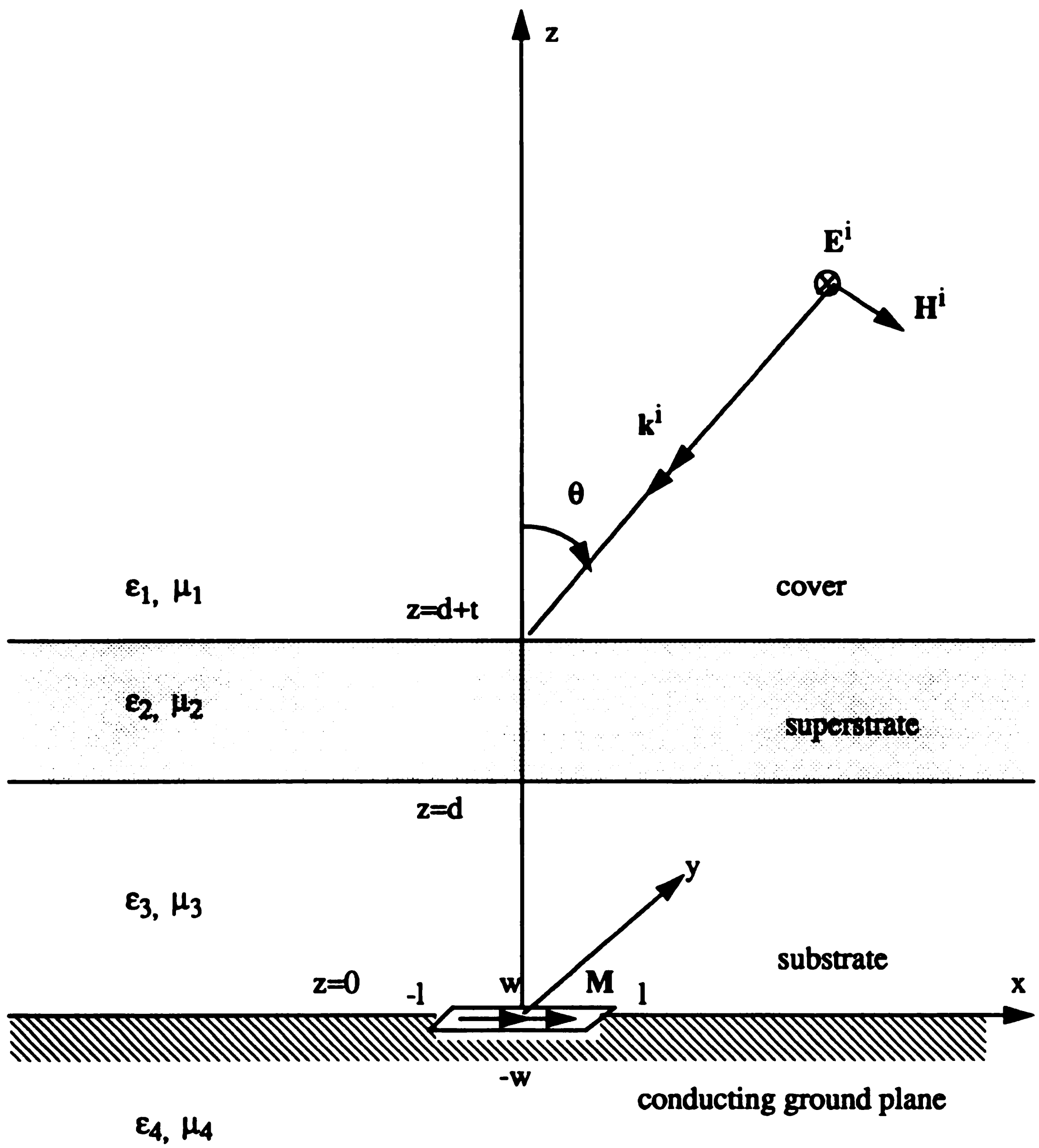

Figure 1.2 Slot in tri-layered media

Figure 1.3 Probl

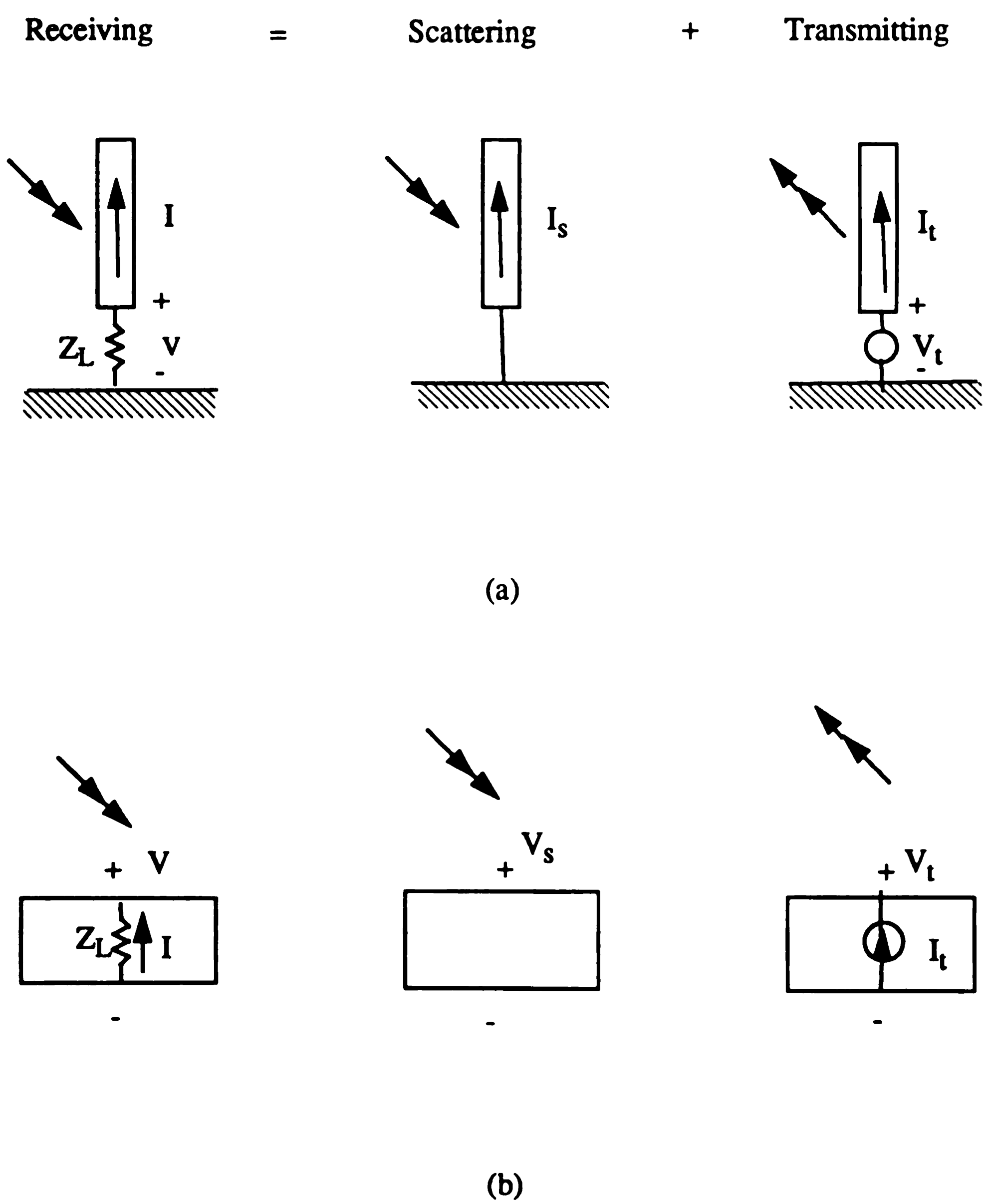

Figure 1.3 Problem decomposition for (a) imaged monopole. (b) slot.

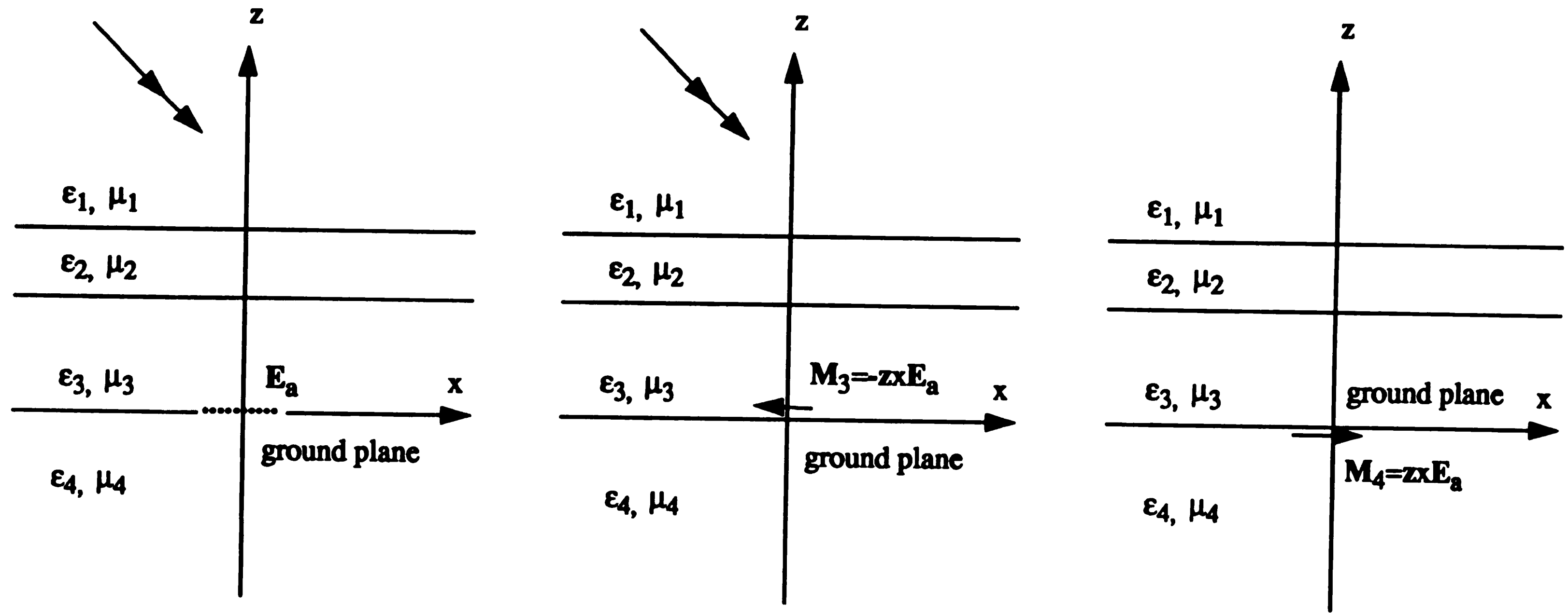

Original problem

Equivalent problem for z>0

Equivalent problem for z<0

Figure 1.4 Equivalent problems for slot in tri-layered media.

CHAPTER TWO

DERIVATION OF GREEN'S FUNCTIONS

2.1 Preliminaries

Consider the geometries shown in Figure 1.1 and 1.2, where a monopole and a slot in tri-layered media are illuminated by an incident electromagnetic (EM) plane wave. The existence of a perfectly conducting ground plane makes it possible to separate the upper and lower half spaces in the derivation of the Green's functions. The upper half space has three layers, while the lower half space is free space.

If an electric current **J** or a magnetic current **M** is placed in region 3, EM fields will be maintained in all three regions. EM fields produced by a vertical electric current $\hat{z}J_z$ in the case of an imaged monopole or a horizontal magnetic current $\hat{x}M_x$ in the case of a slot are of particular interest. The EM fields produced by an arbitrarily oriented current can be readily obtained following the same procedures outlined.

Because the layered media are invariant in the x-y plane, it is advantageous analytically to use a two dimensional Fourier transform. This is the famous Sommerfeld integral approach, by which the Green's function of an arbitrary source can be derived rigorously. The price paid for this analytical elegance is the computationally daunting task of the inverse transform. This chapter deals with the aspects of Green's function derivation, while the numerical implementation of the inverse Fourier transform will be handled in chapters 5 and 6.

One way to derive the Green's function is to express the EM fields in terms of Hertzian potentials. The EM fields can be expressed in terms of electric Hertzian potentials, which are produced by an electric current **J**, or in terms of magnetic Hertzian potentials, which are produced by a magnetic current **M**. In this dissertation, the source is either a

to represent either

there is a possibili

The represen

[55][56]

$$\mathbf{E} = k^2\Pi$$

$$\mathbf{H} = j\omega\varepsilon$$

where k is the wa

$$k^2 = \omega^2\varepsilon$$

and the electric H

$$\nabla^2\Pi + k$$

The representation

55][56]

$$\mathbf{E} = -j\omega$$

$$\mathbf{H} = k^2\Pi$$

and the magnetic H

$$\nabla^2\Pi + k$$

2.2 Boundary Co

To determine

ditions at the diele

the Hertzian potent

source is either a vertical electric current or a horizontal magnetic current. Π is used to represent either electric or magnetic Hertzian potentials, depending on the source. If there is a possibility of ambiguity, it will be mentioned explicitly what Π means.

The representation of EM fields by an electric Hertzian potential can be written as [55][56]

$$\mathbf{E} = k^2\Pi+\nabla(\nabla\cdot\Pi) \tag{2.1.1}$$

$$\mathbf{H} = j\omega\varepsilon\nabla\times\Pi \tag{2.1.2}$$

where k is the wavenumber of the medium,

$$k^2 = \omega^2\varepsilon\mu \tag{2.1.3}$$

and the electric Hertzian potential satisfies an inhomogeneous wave equation

$$\nabla^2\Pi + k^2\Pi = -\frac{\mathbf{J}}{j\omega\varepsilon} . \tag{2.1.4}$$

The representation of EM fields by a magnetic Hertzian potential can be written as [55][56]

$$\mathbf{E} = -j\omega\mu\nabla\times\Pi \tag{2.1.5}$$

$$\mathbf{H} = k^2\Pi + \nabla(\nabla\cdot\Pi) \tag{2.1.6}$$

and the magnetic Hertzian potential satisfies an inhomogeneous wave equation

$$\nabla^2\Pi + k^2\Pi = -\frac{\mathbf{M}}{j\omega\mu} . \tag{2.1.7}$$

2.2 Boundary Conditions for Hertzian Potentials

To determine the Hertzian potentials, it is necessary to invoke the boundary conditions at the dielectric interfaces and at the ground plane. The boundary conditions for the Hertzian potentials can be deduced from the boundary conditions for the EM fields.

Consider th

electric Hertzian

deduction of the

those for electric

Write equati

$E_x = -j$

$E_y = -j$

$E_z = -j$

$H_x = k^2\Gamma$

$H_y = k^2\Gamma$

$H_z = k^2\Gamma$

Boundary con

$E_x(y=0^-)$

$E_y(y=0^-)$

$H_x(y=0^-)$

$H_y(y=0^-)$

If region 2 is

$E_x(y=0^-)$

$E_y(y=0^-)$

Consider the geometry shown in Figure 2.1. The boundary conditions for the electric Hertzian potentials have been derived in [10] and [11]. Therefore, only the deduction of the boundary conditions for magnetic Hertzian potentials are outlined and those for electric Hertzian potentials are quoted from [10][11][63].

Write equations (2.1.5) and (2.1.6) in component form:

$$E_x = -j\omega\mu\left(\frac{\partial\Pi_z}{\partial y} - \frac{\partial\Pi_y}{\partial z}\right) \tag{2.2.1}$$

$$E_y = -j\omega\mu\left(\frac{\partial\Pi_x}{\partial z} - \frac{\partial\Pi_z}{\partial x}\right) \tag{2.2.2}$$

$$E_z = -j\omega\mu\left(\frac{\partial\Pi_y}{\partial x} - \frac{\partial\Pi_x}{\partial y}\right) \tag{2.2.3}$$

$$H_x = k^2\Pi_x + \frac{\partial}{\partial x}(\nabla\cdot\Pi) \tag{2.2.4}$$

$$H_y = k^2\Pi_y + \frac{\partial}{\partial y}(\nabla\cdot\Pi) \tag{2.2.5}$$

$$H_z = k^2\Pi_z + \frac{\partial}{\partial z}(\nabla\cdot\Pi)\ . \tag{2.2.6}$$

Boundary conditions for the EM fields at the interface between region 1 and 2 are

$$E_x(y=0^-) = E_x(y=0^+) \tag{2.2.7}$$

$$E_y(y=0^-) = E_y(y=0^+) \tag{2.2.8}$$

$$H_x(y=0^-) = H_x(y=0^+) \tag{2.2.9}$$

$$H_y(y=0^-) = H_y(y=0^+)\ . \tag{2.2.10}$$

If region 2 is perfectly conducting, the boundary conditions become

$$E_x(y=0^-) = 0 \tag{2.2.11}$$

$$E_y(y=0^-) = 0\ . \tag{2.2.12}$$

It is advantageous to study the cases of three orthogonal components of **M** separately and then combine the results to arrive at the general boundary conditions.

1. Vertical current $\mathbf{M} = \hat{z}M_z$

Vertical current M_z produces a Hertzian potential with only z component.

$$\Pi = \hat{z}\Pi_z \tag{2.2.13}$$

This **Π** can describe the EM fields completely.

Substituting (2.2.1-6) into (2.2.7-10) gives

$$\mu_1 \frac{\partial \Pi_{1z}}{\partial x} = \mu_2 \frac{\partial \Pi_{2z}}{\partial x} \tag{2.2.14}$$

$$\mu_1 \frac{\partial \Pi_{1z}}{\partial y} = \mu_2 \frac{\partial \Pi_{2z}}{\partial y} \tag{2.2.15}$$

$$\frac{\partial^2 \Pi_{1z}}{\partial x \partial z} = \frac{\partial^2 \Pi_{2z}}{\partial x \partial z} \tag{2.2.16}$$

$$\frac{\partial^2 \Pi_{1z}}{\partial y \partial z} = \frac{\partial^2 \Pi_{2z}}{\partial y \partial z} \; . \tag{2.2.17}$$

In order to satisfy equations (2.2.14-17) simultaneously, the following boundary conditions on **Π** must hold.

$$\mu_1 \Pi_{1z} = \mu_2 \Pi_{2z} \tag{2.2.18}$$

$$\frac{\partial \Pi_{1z}}{\partial z} = \frac{\partial \Pi_{1z}}{\partial z} \tag{2.2.19}$$

It is understood that the boundary conditions are valid at the interface, which is the z=0 plane.

If region 2 is a perfect conductor, (2.2.1-6) and (2.2.11-12) can be used to arrive at

$$\mu_1 \frac{\partial \Pi_{1z}}{\partial x} = 0 \tag{2.2.20}$$

$$\mu_1 \frac{\partial \Pi_{1z}}{\partial y}$$

The followin

$$\Pi_{1z} = 0$$

2. Horizontal cu

It can be sh

Π must have both

$$\Pi = \hat{x}\Pi$$

In other words, c

the case of horizo

Substituting

$$\mu_1 \frac{\partial \Pi_{1z}}{\partial y}$$

$$\mu_1(\frac{\partial \Pi_{1z}}{\partial x}$$

$$k_1^2 \Pi_{1x} -$$

$$\frac{\partial}{\partial y}(\frac{\partial \Pi_1}{\partial x}$$

Solving equations

$$\varepsilon_1 \mu_1 \Pi_{1x}$$

$$\mu_1 \frac{\partial \Pi_{1x}}{\partial z}$$

$$\mu_1 \Pi_{1z} =$$

$$\mu_1 \frac{\partial \Pi_{1z}}{\partial y} = 0 \ . \tag{2.2.21}$$

The following boundary condition on $\mathbf{\Pi}$ can be deduced from (2.2.20-21).

$$\Pi_{1z} = 0 \tag{2.2.22}$$

2. Horizontal current $\mathbf{M} = \hat{x} M_x$

It can be shown that in order to describe the EM fields completely for this case, $\mathbf{\Pi}$ must have both a horizontal component and a vertical one [10][11][63].

$$\mathbf{\Pi} = \hat{x}\Pi_x + \hat{z}\Pi_z \tag{2.2.23}$$

In other words, coupling between a horizontal component and a vertical one occurs in the case of horizontal current excitation.

Substituting (2.2.1-6) into (2.2.7-10) gives

$$\mu_1 \frac{\partial \Pi_{1z}}{\partial y} = \mu_1 \frac{\partial \Pi_{2z}}{\partial y} \tag{2.2.24}$$

$$\mu_1 \left(\frac{\partial \Pi_{1z}}{\partial x} - \frac{\partial \Pi_{1x}}{\partial z}\right) = \mu_2 \left(\frac{\partial \Pi_{2z}}{\partial x} - \frac{\partial \Pi_{2x}}{\partial z}\right) \tag{2.2.25}$$

$$k_1^2 \Pi_{1x} + \frac{\partial}{\partial x}\left(\frac{\partial \Pi_{1x}}{\partial x} + \frac{\partial \Pi_{1z}}{\partial z}\right) = k_2^2 \Pi_{2x} + \frac{\partial}{\partial x}\left(\frac{\partial \Pi_{2x}}{\partial x} + \frac{\partial \Pi_{2z}}{\partial z}\right) \tag{2.2.26}$$

$$\frac{\partial}{\partial y}\left(\frac{\partial \Pi_{1x}}{\partial x} + \frac{\partial \Pi_{1z}}{\partial z}\right) = \frac{\partial}{\partial y}\left(\frac{\partial \Pi_{2x}}{\partial x} + \frac{\partial \Pi_{2z}}{\partial z}\right) . \tag{2.2.27}$$

Solving equations (2.2.24-27) leads to the following boundary conditions

$$\varepsilon_1 \mu_1 \Pi_{1x} = \varepsilon_2 \mu_2 \Pi_{2x} \tag{2.2.28}$$

$$\mu_1 \frac{\partial \Pi_{1x}}{\partial z} = \mu_2 \frac{\partial \Pi_{2x}}{\partial z} \tag{2.2.29}$$

$$\mu_1 \Pi_{1z} = \mu_2 \Pi_{2z} \tag{2.2.30}$$

$$\frac{\partial}{\partial z}(\Pi_{1z}$$

The followin

12) in the case th

$$\frac{\partial \Pi_{1z}}{\partial y} =$$

$$(\frac{\partial \Pi_{1z}}{\partial x} -$$

Equations (2.

$$\Pi_{1z} = 0$$

$$\frac{\partial \Pi_{1x}}{\partial z} =$$

3. Horizontal cur

This case is

conditions can be

$$\varepsilon_1 \mu_1 \Pi_{1y}$$

$$\mu_1 \frac{\partial \Pi_{1y}}{\partial z}$$

$$\mu_1 \Pi_{1z} =$$

$$\frac{\partial}{\partial z}(\Pi_{1z} -$$

If region 2 is a per

$$\Pi_{1z} = 0$$

$$\frac{\partial \Pi_{1y}}{\partial z} =$$

$$\frac{\partial}{\partial z}(\Pi_{1z}-\Pi_{2z}) = -\frac{\partial}{\partial x}(\Pi_{1x}-\Pi_{2x}) \ . \tag{2.2.31}$$

The following equations can be written by using equations (2.2.1-6) and (2.2.11-12) in the case that region 2 is a perfect conductor

$$\frac{\partial \Pi_{1z}}{\partial y} = 0 \tag{2.2.32}$$

$$(\frac{\partial \Pi_{1z}}{\partial x} - \frac{\partial \Pi_{1x}}{\partial z}) = 0 \ . \tag{2.2.33}$$

Equations (2.2.32-33) can be solved to obtain the boundary conditions

$$\Pi_{1z} = 0 \tag{2.2.34}$$

$$\frac{\partial \Pi_{1x}}{\partial z} = 0 \ . \tag{2.2.35}$$

3. Horizontal current M $= \hat{y}M_y$

This case is the same as the previous one if y and x are exchanged. Boundary conditions can be written from equations (2.2.28-31)

$$\varepsilon_1\mu_1\Pi_{1y} = \varepsilon_2\mu_2\Pi_{2y} \tag{2.2.36}$$

$$\mu_1\frac{\partial \Pi_{1y}}{\partial z} = \mu_2\frac{\partial \Pi_{2y}}{\partial z} \tag{2.2.37}$$

$$\mu_1\Pi_{1z} = \mu_2\Pi_{2z} \tag{2.2.38}$$

$$\frac{\partial}{\partial z}(\Pi_{1z}-\Pi_{2z}) = -\frac{\partial}{\partial y}(\Pi_{1y}-\Pi_{2y}) \ . \tag{2.2.39}$$

If region 2 is a perfect conductor, the boundary conditions become

$$\Pi_{1z} = 0 \tag{2.2.40}$$

$$\frac{\partial \Pi_{1y}}{\partial z} = 0 \ . \tag{2.2.41}$$

4. General Boun

Combining t

tions on magnetic

can be expressed

$$\Pi_{1a} = \frac{\varepsilon}{\varepsilon}$$

$$\frac{\partial}{\partial z}\Pi_{1a}$$

$$\Pi_{1z} = \frac{\mu}{\mu}$$

$$\frac{\partial \Pi_{1z}}{\partial z}$$

where $a = x, y$.

If region 2 is

$$\Pi_{1z} = 0$$

$$\frac{\partial \Pi_{1x}}{\partial z} =$$

$$\frac{\partial \Pi_{1y}}{\partial z} =$$

5. General Bounc

The general

from [10][11][

$$\Pi_{1a} = \frac{\varepsilon}{\varepsilon}$$

$$\frac{\partial}{\partial z}\Pi_{1a} =$$

4. General Boundary Conditions on Magnetic Hertzian Potentials

Combining the results of the above three subsections, the general boundary conditions on magnetic Hertzian potentials produced by an arbitrary magnetic current source can be expressed as

$$\Pi_{1a} = \frac{\varepsilon_2\mu_2}{\varepsilon_1\mu_1}\Pi_{2a} \tag{2.2.42}$$

$$\frac{\partial}{\partial z}\Pi_{1a} = \frac{\mu_2}{\mu_1}\frac{\partial}{\partial z}\Pi_{2a} \tag{2.2.43}$$

$$\Pi_{1z} = \frac{\mu_2}{\mu_1}\Pi_{2z} \tag{2.2.44}$$

$$\frac{\partial \Pi_{1z}}{\partial z} - \frac{\partial \Pi_{2z}}{\partial z} = -\left(\frac{\varepsilon_2\mu_2}{\varepsilon_1\mu_1} - 1\right)\left(\frac{\partial \Pi_{2x}}{\partial x} + \frac{\partial \Pi_{2y}}{\partial y}\right) \tag{2.2.45}$$

where $a = x, y$.

If region 2 is a perfect conductor, the boundary conditions become

$$\Pi_{1z} = 0 \tag{2.2.46}$$

$$\frac{\partial \Pi_{1x}}{\partial z} = 0 \tag{2.2.47}$$

$$\frac{\partial \Pi_{1y}}{\partial z} = 0\,. \tag{2.2.48}$$

5. General Boundary Conditions on Electric Hertzian Potentials

The general boundary conditions for the electric Hertzian potentials are quoted from [10][11][63].

$$\Pi_{1a} = \frac{\varepsilon_2\mu_2}{\varepsilon_1\mu_1}\Pi_{2a} \tag{2.2.49}$$

$$\frac{\partial}{\partial z}\Pi_{1a} = \frac{\varepsilon_2}{\varepsilon_1}\frac{\partial}{\partial z}\Pi_{2a} \tag{2.2.50}$$

$$\Pi_{1z} = \frac{\varepsilon_2}{\varepsilon_1}\Pi_{2z} \tag{2.2.51}$$

$$\frac{\partial\Pi_{1z}}{\partial z} - \frac{\partial\Pi_{2z}}{\partial z} = -(\frac{\varepsilon_2\mu_2}{\varepsilon_1\mu_1} - 1)(\frac{\partial\Pi_{2x}}{\partial x} + \frac{\partial\Pi_{2y}}{\partial y}) \tag{2.2.52}$$

In the case that region 2 is a perfect conductor, the boundary conditions can be expressed as

$$\Pi_{1x} = 0 \tag{2.2.53}$$

$$\Pi_{1y} = 0 \tag{2.2.54}$$

$$\frac{\partial\Pi_{1z}}{\partial z} = 0 \tag{2.2.55}$$

2.3 Integral Representations of Hertzian Potentials

The Fourier transform is a very powerful tool for solving differential equations. The vector Fourier transform, i.e. two dimensional Fourier transform, is an extension of the commonly used one dimensional Fourier transform [49][50]. It is advantageous to use the two dimensional Fourier transform because the planarly layered media are invariant in the x-y plane.

The transform pair can be written as

$$\tilde{\Pi}(k_x,k_y,z) = \int\int_{-\infty}^{\infty} \Pi(x,y,z)e^{-j(k_x x+k_y y)}dxdy \tag{2.3.1}$$

$$\Pi(x,y,z) = \frac{1}{(2\pi)^2}\int\int_{-\infty}^{\infty} \tilde{\Pi}(k_x,k_y,z)e^{j(k_x x+k_y y)}dk_x dk_y \ . \tag{2.3.2}$$

Equation (2.3.2) means that any wave can be expressed as a superposition of plane waves with proper weighting. Equation (2.3.1) gives the weighting function or the spatial frequency spectrum.

Use the following notation for brevity

$$\mathbf{r} = x\hat{x}+y\hat{y}+z\hat{z} \quad ; \quad d^2r = dx\ dy \tag{2.3.3}$$

$$\mathbf{k} = k_x\hat{x}+k_y\hat{y} \quad ; \quad d^2k = dk_x\ dk_y\ . \tag{2.3.4}$$

Equations (2.3.1-2) can be rewritten as

$$\tilde{\Pi}(\mathbf{k},z) = \int\!\!\int_{-\infty}^{\infty} \Pi(\mathbf{r})e^{-j\mathbf{k}\cdot\mathbf{r}}d^2r \tag{2.3.5}$$

$$\Pi(\mathbf{r}) = \frac{1}{(2\pi)^2}\int\!\!\int_{-\infty}^{\infty} \tilde{\Pi}(\mathbf{k},z)e^{j\mathbf{k}\cdot\mathbf{r}}d^2k \quad . \tag{2.3.6}$$

Hertzian potentials can be categorized into two groups. The primary Hertzian potentials are produced by primary sources in an unbounded homogeneous space. They satisfy the inhomogeneous Helmholtz wave equation, which, in the rectangular coordinates, can be written as

$$(\nabla^2+k^2)\Pi^p(\mathbf{r}) = -\mathbf{F}(\mathbf{r}) \tag{2.3.7}$$

where

$$\mathbf{F}(\mathbf{r}) = \frac{\mathbf{J}(\mathbf{r})}{j\omega\varepsilon} \tag{2.3.8}$$

in the case of electric Hertzian potentials produced by a electric current and

$$\mathbf{F}(\mathbf{r}) = \frac{\mathbf{M}(\mathbf{r})}{j\omega\mu} \tag{2.3.9}$$

in the case of magnetic Hertzian potentials produced by a magnetic current.

The scattered potentials are generated by secondary sources caused by the primary potentials in an inhomogeneous region. The scattered potentials satisfy the homogeneous Helmholtz wave equation

$$(\nabla^2+k^2)\Pi^s(\mathbf{r}) = 0\ . \tag{2.3.10}$$

Equations (2.3.7) and (2.3.10) can be solved by the Fourier transform technique. The step-by-step procedures have been given in [10][11]. The final results from [10][11][63] are used.

The scattered Hertzian potentials can be expressed as

$$\Pi_a^s = \int\!\!\int_{-\infty}^{\infty} \frac{W_a^s(\mathbf{k})}{(2\pi)^2} e^{j\mathbf{k}\cdot\mathbf{r}} e^{\pm p(\mathbf{k})z} d^2k \qquad a = x, y, z \ . \tag{2.3.11}$$

The primary Hertzian potentials can be written as

$$\Pi^p(\mathbf{r}) = \int_v \mathbf{F}(\mathbf{r}') \int\!\!\int_{-\infty}^{\infty} \frac{e^{j\mathbf{k}\cdot(\mathbf{r}-\mathbf{r}')} e^{-p(\mathbf{k})|z-z'|}}{2(2\pi)^2 p(\mathbf{k})} d^2k \ dv' \tag{2.3.12}$$

where Π^p represents electric Hertzian potential if

$$\mathbf{F} = \frac{\mathbf{J}}{j\omega\varepsilon} \tag{2.2.13}$$

and Π^p represents magnetic Hertzian potential if

$$\mathbf{F} = \frac{\mathbf{M}}{j\omega\mu} \ . \tag{2.3.14}$$

In addition, wavenumber parameters are defined as

$$p(\mathbf{k}) = \sqrt{k_x^2 + k_y^2 - k^2} \tag{2.3.15}$$

$$k^2 = \omega^2 \varepsilon\mu \ . \tag{2.3.16}$$

In order to properly ensure that waves decay as they propagate in a lossy medium, the appropriate branch of $p(\mathbf{k})$ used must satisfy

$$\mathrm{Re}(p) > 0 \ ; \quad \mathrm{Im}(p) > 0 \ . \tag{2.3.17}$$

2.4 G

T

electri

2.4.1

C

placed

potent

potent

In reg

$\pm z$ di

In reg

comp

2.4 Green's Functions for Electric Hertzian Potentials

The Green's functions for electric Hertzian potentials maintained by a vertical electric current in tri-layered media are derived in this section.

2.4.1 Boundary Conditions

Consider the geometry shown in Figure 2.2. A vertical electric current source placed in region 3 will maintain electric Hertzian potentials in all three regions. The potentials have only vertical components for reasons explained in 2.2. In region 1, the potential will be entirely the scattered potential Π_z^t

$$\Pi_{1z} = \Pi_z^t \quad z>t \ . \tag{2.4.1.1}$$

In region 2 the potential will be composed of scattered terms propagating in both the $\pm z$ directions.

$$\Pi_{2z} = \Pi_z^+ + \Pi_z^- \quad 0<z<t \ . \tag{2.4.1.2}$$

In region 3 the potential will be made up of a primary component plus two scattered components propagating in the $\pm z$ directions.

$$\Pi_{3z} = \Pi_z^p + \Pi_z^r + \Pi_z^i \quad -d<z<0 \ . \tag{2.4.1.3}$$

The explicit representations of these terms can be obtained from (2.3.11-12).

$$\Pi_z^r(\mathbf{r}) = \iint_{-\infty}^{\infty} \frac{W_z^r(\mathbf{k})}{(2\pi)^2} e^{j\mathbf{k}\cdot\mathbf{r}} e^{-p_3 z} \, d^2k \tag{2.4.1.4}$$

$$\Pi_z^i(\mathbf{r}) = \iint_{-\infty}^{\infty} \frac{W_z^i(\mathbf{k})}{(2\pi)^2} e^{j\mathbf{k}\cdot\mathbf{r}} e^{+p_3 z} \, d^2k \tag{2.4.1.5}$$

$$\Pi_z^+(\mathbf{r}) = \iint_{-\infty}^{\infty} \frac{W_z^+(\mathbf{k})}{(2\pi)^2} e^{j\mathbf{k}\cdot\mathbf{r}} e^{-p_2 z} \, d^2k \tag{2.4.1.6}$$

$$\Pi_z^-(\mathbf{r}) = \iint_{-\infty}^{\infty} \frac{W_z^-(\mathbf{k})}{(2\pi)^2} e^{j\mathbf{k}\cdot\mathbf{r}} e^{+p_2 z} \, d^2k \tag{2.4.1.7}$$

where

App

leads to

The scat

unknown

from the

2.4.2 Sca

a) E

$$\Pi_z^t(\mathbf{r}) = \int\!\!\int_{-\infty}^{\infty} \frac{W_z^t(\mathbf{k})}{(2\pi)^2} e^{j\mathbf{k}\cdot\mathbf{r}} e^{-p_1 z} d^2k \tag{2.4.1.8}$$

where

$$p_m^2 = k_x^2 + k_y^2 - k_m^2 \qquad m=1,2,3 \tag{2.4.1.9)}$$

$$k_m^2 = \omega^2 \mu_m \varepsilon_m \tag{2.4.1.10}$$

$$\Pi_z^p(\mathbf{r}) = \int_V \frac{J_z(\mathbf{r}')}{j\omega\varepsilon_3} \int\!\!\int_{-\infty}^{\infty} \frac{e^{j\mathbf{k}\cdot(\mathbf{r}-\mathbf{r}')} e^{-p_3|z-z'|}}{2(2\pi)^2 p_3} d^2k \, dv' \, . \tag{2.4.1.11}$$

Application of equations (2.2.49-55) at the three interfaces z=t, z=0, and z=-d leads to the following five boundary conditions

$$\frac{\partial \Pi_{1z}}{\partial z} = \frac{\partial \Pi_{2z}}{\partial z} \qquad z=t \tag{2.4.1.12}$$

$$\varepsilon_1 \Pi_{1z} = \varepsilon_2 \Pi_{2z} \qquad z=t \tag{2.4.1.13}$$

$$\frac{\partial \Pi_{2z}}{\partial z} = \frac{\partial \Pi_{3z}}{\partial z} \qquad z=0 \tag{2.4.1.14}$$

$$\varepsilon_2 \Pi_{2z} = \varepsilon_3 \Pi_{3z} \qquad z=0 \tag{2.4.1.15}$$

$$\frac{\partial \Pi_{3z}}{\partial z} = 0 \qquad z=-d \, . \tag{2.4.1.16}$$

The scattered potential amplitudes W_z^r, W_z^i, W_z^+, W_z^-, and W_z^t are unknown. These five unknowns may be determined by applying the five equations (2.4.1.11-16) derived from the boundary conditions.

2.4.2 Scattered Potential Amplitudes

a) Employing (2.4.1.1-2) and (2.4.1.12) gives

$$\frac{\partial}{\partial z}\Pi_z^t = \frac{\partial}{\partial z}[\Pi_z^+ + \Pi_z^-] \qquad at \quad z=t \, . \tag{2.4.2.1}$$

Substituti

Taking t

equation

for all x

b) S

Proceedi

c)

Proceed

d)

Proceedi

Substituting (2.4.1.6-8) into (2.4.2.1) gives

$$\frac{\partial}{\partial z}\left\{ \frac{1}{(2\pi)^2}\int\int_{-\infty}^{\infty}[W_z^t e^{-p_1 z} - W_z^+ e^{-p_2 z} - W_z^- e^{+p_2 z}]e^{j\mathbf{k}\cdot\mathbf{r}}d^2k \right\} \quad = 0 \quad at \quad z=t \ .$$

Taking the derivative inside the integral and performing the differentiation gives an equation in which the inverse Fourier transform of a function is identically zero (ie. for all x and y). This is possible only if the function is identically zero

$$p_1 W_z^t e^{-p_1 t} - p_2 W_z^+ e^{-p_2 t} + p_2 W_z^- e^{+p_2 t} = 0 \ . \tag{2.4.2.2}$$

b) Substituting (2.4.1-2) into (2.4.1.13) leads to

$$\varepsilon_1 \Pi_z^t = \varepsilon_2[\Pi_z^+ + \Pi_z^-] \quad at \quad z=t \ . \tag{2.4.2.3}$$

Proceeding as in a) gives

$$\varepsilon_1 W_z^t e^{-p_1 t} - \varepsilon_2 W_z^+ e^{-p_2 t} - \varepsilon_2 W_z^- e^{+p_2 t} = 0 \ . \tag{2.4.2.4}$$

c) Substituting (2.4.2-3) into (2.4.1.14) gives

$$\frac{\partial}{\partial z}[\Pi_z^+ + \Pi_z^-] = \frac{\partial}{\partial z}[\Pi_z^p + \Pi_z^r + \Pi_z^i] \quad at \quad z=0 \ . \tag{2.4.2.5}$$

Proceeding as in (a), and using $|z-z'| = z-z'$ for $z>z'$ gives

$$p_2 W_z^+ - p_2 W_z^- - p_3 W_z^r + p_3 W_z^i = p_3 \int_V \frac{J_z(\mathbf{r}')}{j\omega\varepsilon_3}\frac{e^{-j\mathbf{k}\cdot\mathbf{r}'}}{2p_3}e^{p_3 z'}dv' \ . \tag{2.4.2.6}$$

d) Substituting (2.4.2-3) into (2.4.1.15) leads to

$$\varepsilon_2[\Pi_z^r + \Pi_z^-] = \varepsilon_3[\Pi_z^p + \Pi_z^r + \Pi_z^i] \quad at \quad z=0 \ . \tag{2.4.2.7}$$

Proceeding as in (c) gives

$$\varepsilon_2 W_z^+ + \varepsilon_2 W_z^- - \varepsilon_3 W_z^r - \varepsilon_3 W_z^i = \varepsilon_3 \int_V \frac{J_z(\mathbf{r}')}{j\omega\varepsilon_3}\frac{e^{-j\mathbf{k}\cdot\mathbf{r}'}}{2p_3}e^{p_3 z'}dv' \ . \tag{2.4.2.8}$$

e) S

Proceedi

Su

where

To

calculate

tude func

the above

Solvi

V

e) Substituting (2.4.3) into (2.4.1.16) gives

$$\frac{\partial}{\partial z}[\Pi_z^p+\Pi_z^r+\Pi_z^i] = 0 \quad at \quad z=-d \ . \tag{2.4.2.9}$$

Proceeding as in (a) and using $|z-z'| = z'-z$ for $z'>z$ gives

$$p_3W_z^r e^{p_3d}-p_3W_z^i e^{-p_3d} = p_3e^{-p_3d}\int_V \frac{J_z(\mathbf{r}')}{j\omega\varepsilon_3}\frac{e^{-j\mathbf{k}\cdot\mathbf{r}'}}{2p_3}e^{-p_3z'}dv' \ . \tag{2.4.2.10}$$

Summary:

$$(a)\ \frac{p_1}{p_2}W_z^t e^{-p_1t}-W_z^+e^{-p_2t}+W_z^-e^{+p_2t} = 0 \tag{2.4.2.2}$$

$$(b)\ \frac{\varepsilon_1}{\varepsilon_2}W_z^t e^{-p_1t}-W_z^+e^{-p_2t}-W_z^-e^{+p_2t} = 0 \tag{2.4.2.4}$$

$$(c)\ \frac{p_2}{p_3}W_z^+-\frac{p_2}{p_3}W_z^--W_z^r+W_z^i = V_z^+ \tag{2.4.2.6}$$

$$(d)\ \frac{\varepsilon_2}{\varepsilon_3}W_z^++\frac{\varepsilon_2}{\varepsilon_3}W_z^--W_z^r-W_z^i = V_z^+ \tag{2.4.2.8}$$

$$(e)\ W_z^r e^{p_3d}-W_z^i e^{-p_3d} = e^{-p_3d}V_z^- \tag{2.4.2.10}$$

where

$$V_z^\pm \equiv \int_V \frac{J_z(\mathbf{r}')}{j\omega\varepsilon_3}\frac{e^{-j\mathbf{k}\cdot\mathbf{r}'}}{2p_3}e^{\pm p_3z'}dv' \ . \tag{2.4.2.11}$$

To formulate the integral equation, the total potential in region 3 is needed. To calculate the back scattered field, the potential in region 1 is needed. Thus, the amplitude functions W_z^r, W_z^i and W_z^t must be determined. This is accomplished by reducing the above five equations (2.4.2.2)-(2.4.2.10) in the following sections.

Solving (2.4.2.2) for W_z^t and substituting this into (2.4.2.4) yields

$$W_z^- = \frac{\alpha-1}{\alpha+1}e^{-2p_2t}W_z^+ \tag{2.4.2.12}$$

where

Substitu

Solving

where

Next, (2

Lastly, (

Here (2.4

To c

in region

Π_2', and

The most

where

$$\alpha \equiv \frac{\varepsilon_1 p_2}{\varepsilon_2 p_1} \, . \tag{2.4.2.13}$$

Substituting (2.4.2.12) into (2.4.2.6) and (2.4.2.8) gives, respectively

$$\frac{p_2}{p_3}[1-\frac{\alpha-1}{\alpha+1}e^{-2p_2t}]W_z^+ - W_z^r + W_z^i = V_z^+ \tag{2.4.2.14}$$

$$\frac{\varepsilon_2}{\varepsilon_3}[1+\frac{\alpha-1}{\alpha+1}e^{-2p_2t}]W_z^+ - W_z^r - W_z^i = V_z^+ \, . \tag{2.4.2.15}$$

Solving (2.4.2.14) for W_z^+ and substituting this into (2.4.2.15) then gives

$$W_z^r[\gamma-1] - W_z^i[\gamma+1] = V_z^+[1-\gamma] \tag{2.4.2.16}$$

where

$$\gamma \equiv \frac{\varepsilon_2 p_3}{\varepsilon_3 p_2} \frac{1+\frac{\alpha-1}{\alpha+1}e^{-2p_2t}}{1-\frac{\alpha-1}{\alpha+1}e^{-2p_2t}} \, . \tag{2.4.2.17}$$

Next, (2.4.2.16) is solved for W_z^r and this is substituted into (2.4.2.10) to give

$$W_z^i = [\gamma-1]\frac{e^{-p_3d}V_z^- + e^{p_3d}V_z^+}{[\gamma+1]e^{p_3d} - [\gamma-1]e^{-p_3d}} \tag{2.4.2.18}$$

Lastly, (2.4.2.16) is solved for W_z^i and this is substituted into (2.4.2.10) to give

$$W_z^r = e^{-p_3d}\frac{[\gamma+1]V_z^- + [\gamma-1]V_z^+}{[\gamma+1]e^{p_3d} - [\gamma-1]e^{-p_3d}} \, . \tag{2.4.2.19}$$

Here (2.4.2.18) and (2.4.2.19) are the desired scattered potential amplitudes.

To calculate the scattered field in region 1 it is necessary to calculate the potential in region 1 due to a vertical current in region 3. The total potential in region 1 is just Π_z^t, and thus it is only necessary to determine W_z^t to use (2.4.1.8) to calculate Π_z^t. The most straightforward method for calculating W_z^t is to solve (2.4.2.2-10) from the start. Solving (2.4.2.10) for W_z^r and substituting it into (2.4.2.6) and (2.4.2.8) gives, respectively

$$\frac{p_2}{p_3}W_z^+ - \frac{p_2}{p_3}W_z^- + W_z^i[1-e^{-2p_3d}] = V_z^+ + e^{-2p_3d}V_z^- \tag{2.4.2.20}$$

$$\frac{\varepsilon_2}{\varepsilon_3}W_z^+ - \frac{\varepsilon_2}{\varepsilon_3}W_z^- + W_z^i[1-e^{-2p_3d}] = V_z^+ + e^{-2p_3d}V_z^- \ . \tag{2.4.2.21}$$

Solving (2.4.2.20) for W_z^i and substituting into (2.4.2.21) then gives

$$PW_z^+ + MW_z^- = \bar{V}_z \tag{2.4.2.22}$$

where

$$\bar{V}_z = V_z^+ e^{p_3 d} + V_z^- e^{-p_3 d} \tag{2.4.2.23}$$

$$P = \frac{\varepsilon_1}{\varepsilon_3}\sinh p_3 d + \frac{p_2}{p_3}\cosh p_3 d \tag{2.4.2.24}$$

$$M = \frac{\varepsilon_2}{\varepsilon_3}\sinh p_3 d - \frac{p_2}{p_3}\cosh p_3 d \ . \tag{2.4.2.25}$$

Note, (2.4.2.22) is solved for W_z^+ , which is substituted into (2.4.2.2) and (2.4.2.4) to give, respectively

$$\frac{p_1}{p_2}W_z^t e^{-p_1 t} + W_z^-[\frac{M}{P}e^{-p_2 t} + e^{p_2 t}] = \frac{\bar{V}_z}{P}e^{-p_2 t} \tag{2.4.2.26}$$

$$\frac{\varepsilon_1}{\varepsilon_2}W_z^t e^{-p_1 t} + W_z^-[\frac{M}{P}e^{-p_2 t} - e^{p_2 t}] = \frac{\bar{V}_z}{P}e^{-p_2 t} \ . \tag{2.4.2.27}$$

Finally, solving (2.4.2.26) for W_z^- and substituting into (2.4.2.27) gives an equation for W_z^t

$$W_z^t e^{-p_1 t}\left\{\frac{\varepsilon_1}{\varepsilon_2}[Me^{-p_2 t} + Pe^{p_2 t}] - \frac{p_1}{p_2}[Me^{-p_2 t} - Pe^{p_2 t}]\right\} = 2\bar{V}_z \ . \tag{2.4.2.28}$$

The terms in brackets in (2.4.2.28) may be evaluated with the help of (2.4.2.24) and

(2.4.2.25) as

$$Me^{-p_2t}+Pe^{p_2t} = 2\frac{\varepsilon_2}{\varepsilon_3}\sinh p_3d\ \cosh p_2t+2\frac{p_2}{p_3}\cosh p_3d\ \sinh p_2t \tag{2.4.2.29}$$

$$Me^{-p_2t}-Pe^{p_2t} = -2\frac{\varepsilon_2}{\varepsilon_3}\sinh p_3d\ \sinh p_2t-2\frac{p_2}{p_3}\cosh p_3d\ \cosh p_2t\ . \tag{2.4.2.30}$$

With these, (2.4.2.28) can be solved to yield

$$W_z^t = e^{p_1t}\frac{\bar{V}_z}{\chi} \tag{2.4.2.31}$$

where

$$\chi = \frac{\varepsilon_1}{\varepsilon_3}\sinh p_3d\ \cosh p_2t+\frac{\varepsilon_1 p_2}{\varepsilon_2 p_3}\cosh p_3d\ \sinh p_2t$$

$$+\frac{\varepsilon_2 p_1}{\varepsilon_3 p_2}\sinh p_3d\ \sinh p_2t+\frac{p_1}{p_3}\cosh p_3d\ \cosh p_2t\ . \tag{2.4.2.32}$$

The potential in region 1 can now be calculated. Substituting (2.4.2.31) into (2.4.1.8) gives

$$\Pi_z^t(\mathbf{r}) = \frac{1}{(2\pi)^2}\int\int_{-\infty}^{\infty}\frac{\bar{V}_z(\mathbf{k})}{\chi(\mathbf{k})}e^{j\mathbf{k}\cdot\mathbf{r}}e^{-p_1(z-t)}d^2k\ . \tag{2.4.2.33}$$

Here $\bar{V}_z$ can be calculated using (2.4.2.23) with (2.4.2.11), giving

$$\bar{V}_z = \int_V\frac{J_z^3(\mathbf{r}')}{j\omega\varepsilon_3}\frac{e^{-j\mathbf{k}\cdot\mathbf{r}'}}{p_3}\cosh p_3(d+z')dv'\ . \tag{2.4.2.34}$$

Substituting (2.4.2.34) into (2.4.2.33) then gives

$$\Pi_z^t = \int_V J_z^3(\mathbf{r}')\ \{\ \frac{1}{(2\pi)^2}\int\int_{-\infty}^{\infty}[\frac{e^{-p_1(z-t)}}{\chi}\frac{\cosh p_3(d+z')}{j\omega\varepsilon_3 p_3}e^{-j\mathbf{k}\cdot\mathbf{r}'}]$$

$$e^{j\mathbf{k}\cdot\mathbf{r}}d^2k\ \}\ dv'\ . \tag{2.4.2.35}$$

2.4.3 Green's Functions

The Green's function $G_{zz}^{3,3}$ describes the vertical component of Hertzian potential in region 3 produced by a vertically directed elementary current source in region 3. By superposition, the total potential in region 3 can be expressed in terms of the Green's function as

$$\Pi_{3z} = \Pi_z^p + \Pi_z^r + \Pi_z^i = \int_V G_{zz}^{3,3}(\mathbf{r},\mathbf{r}')J_z^3(\mathbf{r}')dv' \tag{2.4.3.1}$$

Thus, $G_{zz}^{3,3}$ can be determined by summing up the potentials for region 3. Using (2.4.2.18-19) in (2.4.1.8) and using (2.4.1.11) allows the total potential in region 3 to be written as

$$\Pi_{3z}(\mathbf{r}) = \int_V J_z^3(\mathbf{r}')dv' \int\int_{-\infty}^{\infty} \frac{1}{(2\pi)^2}[w_z^r e^{-p_3 z} + w_z^i e^{p_3 z} + \frac{e^{-j\mathbf{k}\cdot\mathbf{r}'}}{j\omega\varepsilon_3 2p_3} e^{-p_3|z-z'|}]$$

$$e^{j\mathbf{k}\cdot\mathbf{r}} d^2k \tag{2.4.3.2}$$

where the lower case w_z^r and w_z^i are defined through

$$W_z^{r,i}(\mathbf{r},\mathbf{k}) = \int_V J_z^3(\mathbf{r}')w_z^{r,i}(\mathbf{r},\mathbf{r}',\mathbf{k})dv' \tag{2.4.3.3}$$

so that from (2.4.2.18) and (2.4.2.19)

$$w_z^i = [\gamma-1]\frac{e^{-p_3 d}v_z^- + e^{p_3 d}v_z^+}{[\gamma+1]e^{p_3 d} - [\gamma-1]e^{-p_3 d}} \tag{2.4.3.4}$$

$$w_z^r = e^{-p_3 d}\frac{[\gamma+1]v_z^- + [\gamma-1]v_z^+}{[\gamma+1]e^{p_3 d} - [\gamma-1]e^{-p_3 d}} \; . \tag{2.4.3.5}$$

Here

$$v_z^{\pm} = \frac{e^{-j\mathbf{k}\cdot\mathbf{r}'}}{j\omega\varepsilon_3 2p_3} e^{\pm p_3 z'} \tag{2.4.3.6}$$

so that

E

N

n

or

wh

Us

Be

(2.

whe

$$V_z^{\pm} = \int_V J_z^3(\mathbf{r}')v_z^{\pm}dv' \ . \tag{2.4.3.7}$$

By comparing (2.4.3.2) with (2.4.3.1), the Green's function is seen to be

$$G_{zz}^{3,3} = \frac{1}{(2\pi)^2}\iint_{-\infty}^{\infty}[w_z^r e^{-p_3 z}+w_z^i e^{p_3 z}+\frac{e^{-j\mathbf{k}\cdot\mathbf{r}'}}{j\omega\varepsilon_3 2p_3}e^{-p_3|z-z'|}]e^{j\mathbf{k}\cdot\mathbf{r}}d^2k \ . \tag{2.4.3.8}$$

Note that this Green's function is the inverse Fourier transform of a spectral domain representation of the Green's function. Symbolically

$$G_{zz}^{3,3} = F^{-1}\{\tilde{G}_{zz}^{3,3}\} \tag{2.4.3.9}$$

or

$$G_{zz}^{3,3} = \frac{1}{(2\pi)^2}\iint_{-\infty}^{\infty}\tilde{G}_{zz}^{3,3}e^{j\mathbf{k}\cdot\mathbf{r}}d^2k \tag{2.4.3.10}$$

where

$$\tilde{G}_{zz}^{3,3} = w_z^r e^{-p_3 z}+w_z^i e^{p_3 z}+\frac{e^{-j\mathbf{k}\cdot\mathbf{r}'}}{j\omega\varepsilon_3 2p_3}e^{\pm p_3 z'}e^{\mp p_3 z} \quad \begin{cases} z>z' \\ z<z' \end{cases} . \tag{2.4.3.11}$$

Using (2.4.3.6), this can also be written as

$$\tilde{G}_{zz}^{3,3} = w_z^r e^{-p_3 z}+w_z^i e^{p_3 z}+v_z^{\pm}e^{\mp p_2 z} \tag{2.4.3.12}$$

Before substituting the expression for w_z^r and w_z^i into (2.4.3.12), the quantity γ in (2.4.2.17) can be written as

$$\gamma = B\frac{N}{\Delta} \tag{2.4.3.13}$$

where

$$B \equiv \frac{\varepsilon_2 p_3}{\varepsilon_3 p_2} \tag{2.4.3.14}$$

$$N \equiv \alpha\cosh p_2 t+\sinh p_2 t \tag{2.4.3.15}$$

I
c
S
Th
wh

$$\Delta \equiv \alpha \sinh p_2 t + \cosh p_2 t \ . \tag{2.4.3.16}$$

Then, substituting (2.4.3.4) and (2.4.3.5) into (2.4.3.12) gives

$$D\tilde{G}_{zz}^{3,3} = (BN-\Delta)e^{-p_3 d}e^{p_3 z}v_z^{-} + (BN-\Delta)e^{p_3 d}e^{p_3 z}v_z^{+} + (BN+\Delta)e^{-p_3 d}e^{-p_3 z}v_z^{-}$$

$$+ (BN-\Delta)e^{-p_3 d}e^{-p_3 z}v_z^{+} + (BN+\Delta)e^{p_3 d}e^{\mp p_3 z}v_z^{\pm} - (BN-\Delta)e^{-p_3 d}e^{\mp p_3 z}v_z^{\pm} \tag{2.4.3.17}$$

where

$$D \equiv 2BN sinh p_3 d + 2\Delta \cosh p_3 d \ . \tag{2.4.3.18}$$

Equation (2.4.3.17) can be simplified most easily by considering the following two cases.

Case I) $z > z'$ (upper sign)

Grouping terms gives

$$D\tilde{G}_{zz}^{3,3} = v_z^{+}[(BN-\Delta)e^{-p_3 d}e^{p_2 z} + (BN-\Delta)e^{-p_3 d}e^{-p_3 z} + (BN+\Delta)e^{p_3 d}e^{-p_3 z}$$

$$-(BN-\Delta)e^{-p_3 d}e^{-p_3 z}] + v_z^{-}[(BN-\Delta)e^{-p_3 d}e^{p_3 z} + (BN+\Delta)e^{-p_3 d}e^{-p_3 z}] \ . \tag{2.4.3.19}$$

Substituting (2.4.3.6) and simplifying then yields

$$D\tilde{G}_{zz}^{3,3} = 2\frac{e^{-j\mathbf{k}\cdot\mathbf{r}'}}{j\omega\varepsilon_3 2p_3} 2\cosh p_3(d+z')[BN\cosh p_3 z - \Delta\sinh p_3 z] \tag{2.4.3.20}$$

Case II) $z < z'$ (lower sign)

Proceeding exactly as above gives

$$D\tilde{G}_{zz}^{3,3} = 2\frac{e^{-j\mathbf{k}\cdot\mathbf{r}'}}{j\omega\varepsilon_3 2p_3} 2\cosh p_3(d+z)[BN\cosh p_3 z' - \Delta\sinh p_3 z'] \tag{2.4.3.21}$$

The above results can be combined into a single expression by using the notation

$$D\tilde{G}_{zz}^{3,3} = 2\frac{e^{-j\mathbf{k}\cdot\mathbf{r}'}}{j\omega\varepsilon_3 2p_3} 2\cosh p_3(d+z^{<})[BN\cosh p_3 z^{>} - \Delta\sinh p_3 z^{>}] \tag{2.4.3.22}$$

where

Th

thr

wh

U

A

th

s

T

$$z^{>} \equiv \max(z,z') \quad z^{<} \equiv min(z,z') . \tag{2.4.3.23}$$

The Green's function transform embedded in (2.4.3.22) can be isolated by dividing through by D. Using (2.4.3.14-16) then gives

$$\tilde{G}_{zz}^{3,3} = \frac{e^{-j\mathbf{k}\cdot\mathbf{r}'}}{j\omega\varepsilon_3 p_3}\cosh p_3(z^{<}+d)F(z^{>}) \tag{2.4.3.24}$$

where

$$F(z) = \frac{Q cosh p_3 z - Z sinh p_3 z}{Q \sinh p_3 d + Z cosh p_3 d} \tag{2.4.3.25}$$

$$Q = p_3\varepsilon_2[\varepsilon_1 p_2 \cosh p_2 t + \varepsilon_2 p_1 \sinh p_2 t] \tag{2.4.3.26}$$

$$Z = p_2\varepsilon_3[\varepsilon_1 p_2 \sinh p_2 t + \varepsilon_2 p_1 \cosh p_2 t] . \tag{2.4.3.27}$$

Using (2.4.3.10) gives the final form of the Green's function

$$G_{zz}^{3,3} = \frac{1}{(2\pi)^2}\int\int_{-\infty}^{\infty} \frac{e^{j\mathbf{k}\cdot(\mathbf{r}-\mathbf{r}')}}{j\omega\varepsilon_3 p_3}\cosh p_3(z^{<}+d)F(z^{>})d^2k . \tag{2.4.3.28}$$

A check on this Green's function can be performed by letting $\mu_2 = \mu_1$ and $\varepsilon_1 = \varepsilon_2$ so that the three-layer dielectric system reduces to a two-layer system. In this case

$$Q = p_3\varepsilon_2^2 p_2[\cosh p_2 t + \sinh p_2 t] \tag{2.4.3.29}$$

$$Z = \varepsilon_3 p_2^2 \varepsilon_2[\cosh p_2 t + \sinh p_2 t] \tag{2.4.3.30}$$

so that

$$F(x) = \frac{p_3\varepsilon_2 \cosh p_3 x - p_2\varepsilon_3 \sinh p_3 x}{p_3\varepsilon_2 \sinh p_3 d + p_2\varepsilon_3 \cosh p_3 d} . \tag{2.4.3.31}$$

Thus, the Green's function is

$$G_{zz}^{3,3} = \frac{1}{(2\pi)^2}\int\int_{-\infty}^{\infty} \frac{e^{j\mathbf{k}\cdot(\mathbf{r}-\mathbf{r}')}}{j\omega\varepsilon_3 p_3}\frac{\cosh p_3(z^{<}+d)}{T_m}[\frac{p_3}{p_2}\cosh p_2 z^{>} - \frac{\varepsilon_3}{\varepsilon_2}\sinh p_3 z^{>}] \tag{2.4.3.32}$$

where

$$T_m = \frac{\varepsilon_3}{\varepsilon_2}\cosh p_3 d + \frac{p_3}{p_2}\sinh p_3 d \ . \tag{2.4.3.33}$$

Equation (2.4.3.32) is identical to the two-layer expression (7.9.51) from [10].

The total potential in region 3 is found by substituting (2.4.3.10) into (2.4.3.1)

$$\Pi_{3z} = \frac{1}{(2\pi)^2}\int_{-\infty}^{\infty}\int [\int_{x'}\int_{y'}\{\int_{z'=-d}^{0} \tilde{G}_{zz}^{3,3} J_z^3(\mathbf{r}')dz'\}dx'dy']e^{j\mathbf{k}\cdot\mathbf{r}}d^2k \tag{2.4.3.34}$$

For the special case of a sheath current (an axially directed current on the surface $\rho = a$), the current density function becomes

$$J_z^3(\mathbf{r}') = \frac{I_z^3(z')}{2\pi a}\delta(\rho'-a) \tag{2.4.3.35}$$

so that

$$\Pi_{3z} = \frac{1}{(2\pi)^2}\int_{-\infty}^{\infty}\int [\int_{\phi'=0}^{2\pi}\int_{z'=-d}^{0} \frac{I_z^3(z')}{2\pi a}\tilde{G}_{zz}^{3,3}(z,a,\phi',z',\mathbf{k})dz'ad\phi']e^{j\mathbf{k}\cdot\mathbf{r}}d^2k \tag{2.4.3.36}$$

where (ρ,ϕ,z) are the cylindrical coordinate variables.

Because of the symmetry of the problem, it is most convenient to evaluate the integrals in (2.4.3.36) using cylindrical coordinates. Let

$$x = \rho\cos\phi \qquad y = \rho\sin\phi \tag{2.4.3.37}$$

$$k_x = \lambda\cos\Phi \qquad k_y = \lambda\sin\Phi \ . \tag{2.4.3.38}$$

Then

$$p^2 = k_x^2+k_y^2-k^2 = \lambda^2-k^2 \tag{2.4.3.39}$$

$$\mathbf{k}\cdot\mathbf{r} = \lambda\rho\cos\Phi\cos\phi+\lambda\rho\sin\Phi\sin\phi$$

$$= \lambda\rho\cos(\phi-\Phi) \ . \tag{2.4.3.40}$$

Also, let

$$\tilde{G}_{zz}^{3,3}(z,\rho',\phi',z',\mathbf{k}) = \tilde{\Gamma}_{zz}^{3,3}(z,z',\lambda)e^{-j\mathbf{k}\cdot\mathbf{r}'} \ . \tag{2.4.3.41}$$

S

N

a

in

w

w

No

tia

Substituting these into (2.4.3.36) gives

$$\Pi_{3z}(\rho,z) = \frac{1}{(2\pi)^2}\int_{\lambda=0}^{\infty}[\int_{z'=-d}^{0}\frac{I_z^3(z')}{2\pi}\tilde{\Gamma}_{zz}^{3,3}(z,z',\lambda)dz'\int_{\phi'=0}^{2\pi}e^{-j\lambda a\cos(\phi'-\Phi)}d\phi' \times$$

$$\int_{\Phi=0}^{2\pi}e^{j\lambda\rho\cos(\phi-\Phi)}d\Phi]\lambda d\lambda\ . \qquad (2.4.3.42)$$

Now use

$$\int_0^{2\pi}e^{j\rho\lambda\cos(\Phi-\phi)}d\Phi = \int_0^{2\pi}e^{j\rho\lambda\cos x}dx = 2\pi J_0(\lambda\rho) \qquad (2.4.3.43)$$

and

$$J_0(-x) = J_0(x) \qquad (2.4.3.44)$$

in (2.4.3.42) to give

$$\Pi_{3z}(\rho,z) = \frac{1}{2\pi}\int_0^{\infty}[\int_{-d}^{0}I_z^3(z')\tilde{\Gamma}_{zz}^{3,3}(z,z',\lambda)dz']J_0(\lambda a)J_0(\lambda\rho)\lambda d\lambda \qquad (2.4.3.45)$$

where

$$\tilde{\Gamma}_{zz}^{3,3}(z,z',\lambda) = \frac{1}{j\omega\varepsilon_3 p_3}\cosh p_3(z^{<}+d)F(z^{>})\ . \qquad (2.4.3.46)$$

Equation (2.4.3.45) can also be written as

$$\Pi_{3z}(\rho,z) = \int_{-d}^{0}G_{zz}^{3,3}(z,\rho,z')I_z^3(z')dz' \qquad (2.4.3.47)$$

where $G_{zz}^{3,3}$ is the Green's function

$$G_{zz}^{3,3}(z,\rho,z') = \frac{1}{2\pi}\int_0^{\infty}\tilde{\Gamma}_{zz}^{3,3}(z,z',\lambda)J_0(\lambda a)J_0(\lambda\rho)\lambda d\lambda\ . \qquad (2.4.3.48)$$

Now, letting $G_{zz}^{1,3}$ be the Green's function describing the vertical component of potential in region 1 produced by a vertical component of current in region 3, the total potential in region 1 can be written as

$$\Pi_{1z} = \Pi_z^t = \int_V G_{zz}^{1,3}(\mathbf{r},\mathbf{r}')J_z^3(\mathbf{r}')dv' \tag{2.4.3.49}$$

where

$$G_{zz}^{1,3} = \frac{1}{(2\pi)^2}\iint_{-\infty}^{\infty} \frac{e^{-p_1(z-t)}}{\chi}\frac{\cosh p_3(d+z')}{j\omega\varepsilon_3 p_3}e^{j\mathbf{k}\cdot(\mathbf{r}-\mathbf{r}')}d^2k \ . \tag{2.4.3.50}$$

This can also be written as

$$G_{zz}^{1,3} = \frac{1}{(2\pi)^2}\iint_{-\infty}^{\infty} \tilde{G}_{zz}^{1,3}e^{j\mathbf{k}\cdot\mathbf{r}}d^2k \tag{2.4.3.51}$$

where

$$\tilde{G}_{zz}^{1,3}(\mathbf{r}',k) = \frac{e^{-p_1(z-t)}}{\chi}\frac{\cosh p_3(d+z')}{j\omega\varepsilon_3 p_3}e^{-j\mathbf{k}\cdot\mathbf{r}'} \tag{2.4.3.52}$$

is the Fourier transform of the Green's function.

2.5 Green's Functions for Magnetic Hertzian Potentials

The Green's functions for magnetic Hertzian potentials maintained by a horizontal magnetic current in tri-layered media are derived in this section.

2.5.1 Scattered Potential Amplitudes

Consider the upper half space (z>0) shown in Figure 2.3 first. A horizontal magnetic current in region 3, $\mathbf{M}_3 = \hat{x}M_{3x}$, generates the following Hertzian potentials in the three regions above the ground plane. Attention should be paid to the coupling between the horizontal and vertical components. The potentials in each of the three layers can be expressed as

$$\Pi_3^p = \hat{x}\Pi_{3x}^p \tag{2.5.1.1}$$

$$\Pi_i^{\gamma} = \hat{x}\,\Pi_{ix}^{\gamma} + \hat{z}\,\Pi_{iz}^{\gamma} \quad ; \; i=1,2,3 \; ; \; \gamma=+,- \tag{2.5.1.2}$$

where

Π_3^p: Primary potential generated by magnetic source in region 3.

Π_i^+: Scattered potential in region i traveling in +z direction.

Π_i^-: Scattered potential in region i traveling in -z direction.

The superscript m of magnetic Hertzian potential Π^m has been dropped for brevity. This should not cause any ambiguity because in most cases in this dissertation it is quite clear from the context that Π means either electric Hertzian potential or magnetic Hertzian potential. The superscript m will be added, or explicit explanation will be provided, whenever there is a possibility of confusion.

In region 1, the scattered potential wave can travel to infinity without reflection. Therefore

$$\Pi_{1x}^- = \Pi_{1z}^- = 0 \tag{2.5.1.3}$$

By using (2.3.11-12), primary and scattered potential can be written as

$$\Pi_{3x}^p(\mathbf{r}) = \int_{V_3} \frac{M_{3x}(\mathbf{r}')}{j\omega\mu_3} [\iint_{-\infty}^{\infty} \frac{e^{j\mathbf{k}\cdot(\mathbf{r}-\mathbf{r}')} e^{-p_3|z-z'|}}{(2\pi)^2 2p_3} d^2k]\, dv' \tag{2.5.1.4}$$

$$\Pi_{i\beta}^{\gamma} = \iint_{-\infty}^{\infty} \frac{W_{i\beta}^{\gamma}(\mathbf{k})}{(2\pi)^2} e^{-\gamma p_i z} e^{j\mathbf{k}\cdot\mathbf{r}} d^2k \tag{2.5.1.5}$$

where

$$\beta = x,z \; ; \quad \gamma = +,- \; ; \quad i = 1,2,3$$

$$\mathbf{r} = \hat{x}x+\hat{y}y+\hat{z}z \quad ; \quad k_i^2 = \omega^2\varepsilon_i\mu_i \tag{2.5.1.6}$$

$$\mathbf{k} \equiv \hat{x}k_x+\hat{y}k_y \quad ; \quad d^2k \equiv dk_x dk_y \tag{2.5.1.7}$$

$$p_i^2 \equiv k_x^2+k_y^2-k_i^2 \quad ; \quad \mathrm{Re}\{p_i\}>0 \text{ and } \mathrm{Im}\{p_i\}>0 \,. \tag{2.5.1.8}$$

The Hertzian potential in each region can be written as

$$\Pi_1 = \hat{x}\Pi_{1x}^{+} + \hat{z}\Pi_{1z}^{+} \tag{2.5.1.9}$$

$$\Pi_2 = \hat{x}(\Pi_{2x}^{+} + \Pi_{2x}^{-}) + \hat{z}(\Pi_{2z}^{+} + \Pi_{2z}^{-}) \tag{2.5.1.10}$$

$$\Pi_3 = \hat{x}(\Pi_{3x}^{p} + \Pi_{3x}^{+} + \Pi_{3x}^{-}) + \hat{z}(\Pi_{3z}^{+} + \Pi_{3z}^{-}) \tag{2.5.1.11}$$

Using the boundary conditions (2.2.42-48) at the three interfaces, ten equations result, which will be solved analytically to obtain the ten unknowns W_{1x}^{+}, W_{1z}^{+}, W_{2x}^{-}, W_{2x}^{+}, W_{2z}^{-}, W_{2z}^{+}, W_{3x}^{-}, W_{3x}^{+}, W_{3z}^{-}, and W_{3z}^{+}. The ten boundary conditions are listed as follows:

At interface z=d+t,

$$\Pi_{1x} = \varepsilon_{21}\mu_{21}\Pi_{2x} \tag{2.5.1.12}$$

$$\frac{\partial}{\partial z}\Pi_{1x} = \mu_{21}\frac{\partial}{\partial z}\Pi_{2x} \tag{2.5.1.13}$$

$$\Pi_{1z} = \mu_{21}\Pi_{2z} \tag{2.5.1.14}$$

$$\frac{\partial}{\partial z}(\Pi_{1z} - \Pi_{2z}) = -(\varepsilon_{21}\mu_{21} - 1)\frac{\partial}{\partial x}\Pi_{2x} \tag{2.5.1.15}$$

At interface z=d,

$$\Pi_{2x} = \varepsilon_{32}\mu_{32}\Pi_{3x} \tag{2.5.1.16}$$

$$\frac{\partial}{\partial z}\Pi_{2x} = \mu_{32}\frac{\partial}{\partial z}\Pi_{3x} \tag{2.5.1.17}$$

$$\Pi_{2z} = \mu_{32}\Pi_{3z} \tag{2.5.1.18}$$

$$\frac{\partial}{\partial z}(\Pi_{2z} - \Pi_{3z}) = -(\varepsilon_{32}\mu_{32} - 1)\frac{\partial}{\partial x}\Pi_{3x} \tag{2.4.19}$$

At interface z=0,

$$\Pi_{3z} = 0 \tag{2.5.1.20}$$

$$\frac{\partial}{\partial z}\Pi_{3x} = 0 \tag{2.5.1.21}$$

where

$$\varepsilon_{ij} \equiv \frac{\varepsilon_i}{\varepsilon_j} \quad ; \quad \mu_{ij} \equiv \frac{\mu_i}{\mu_j} \quad ; \quad i,j=1,2,3 \tag{2.5.1.22}$$

Substituting (2.5.1.5), (2.5.1.9), and (2.5.1.10) into (2.5.1.12) gives

$$\iint_{-\infty}^{\infty} \frac{W_{1x}^{+}(\mathbf{k})}{(2\pi)^2} e^{-p_1(d+t)} e^{j\mathbf{k}\cdot\mathbf{r}} d^2k$$

$$= \varepsilon_{21}\mu_{21}[\iint_{-\infty}^{\infty} \frac{W_{2x}^{+}(\mathbf{k})}{(2\pi)^2} e^{-p_2(d+t)} e^{j\mathbf{k}\cdot\mathbf{r}} d^2k +$$

$$\iint_{-\infty}^{\infty} \frac{W_{2x}^{-}(\mathbf{k})}{(2\pi)^2} e^{p_2(d+t)} e^{j\mathbf{k}\cdot\mathbf{r}} d^2k \;] \tag{2.5.1.23}$$

For equation (2.5.1.23) to be valid for arbitrary $\mathbf{r}$, the following relationship must be true.

$$W_{1x}^{+} e^{-p_1(d+t)} = \varepsilon_{21}\mu_{21}[W_{2x}^{+} e^{-p_2(d+t)} + W_{2x}^{-} e^{p_2(d+t)}] \tag{2.5.1.24}$$

Using equations (2.5.1.13)-(2.5.1.15), following the above procedure, and interchanging the order of integration and differentiation when $\frac{\partial}{\partial z}$ or $\frac{\partial}{\partial x}$ is encountered, give the following equations.

$$p_1 W_{1x}^{+} e^{-p_1(d+t)} = \mu_{21} p_2 [W_{2x}^{+} e^{-p_2(d+t)} - W_{2x}^{-} e^{p_2(d+t)}] \tag{2.5.1.25}$$

$$W_{1z}^{+} e^{-p_1(d+t)} = \mu_{21}[W_{2z}^{+} e^{-p_2(d+t)} + W_{2z}^{-} e^{p_2(d+t)}] \tag{2.5.1.26}$$

$$p_1 W_{1z}^{+} e^{-p_1(d+t)} - p_2 W_{2z}^{+} e^{-p_2(d+t)} + p_2 W_{2z}^{-} e^{p_2(d+t)}$$

$$= (\varepsilon_{21}\mu_{21} - 1) jk_x [W_{2x}^{+} e^{-p_2(d+t)} + W_{2x}^{-} e^{p_2(d+t)}] \; . \tag{2.5.1.27}$$

Equation (2.5.1.4) can be rewritten as

$$\Pi^p_{3x} = \int\!\!\int_{-\infty}^{\infty} \frac{W^p_{3x}(\mathbf{k})}{(2\pi)^2} e^{j\mathbf{k}\cdot\mathbf{r}} d^2k \tag{2.5.1.28}$$

where

$$W^p_{3x}(\mathbf{k},z) = \int_{V_3} \frac{M_{3x}(\mathbf{r}')}{2j\omega\mu_3 p_3} e^{-j\mathbf{k}\cdot\mathbf{r}'} e^{-p_3|z-z'|} dv' . \tag{2.5.1.29}$$

Substituting (2.5.1.5), (2.5.1.10), (2.5.1.11), and (2.5.1.28) into (2.5.1.16) gives

$$\int\!\!\int_{-\infty}^{\infty} \frac{W^+_{2x}(\mathbf{k})}{(2\pi)^2} e^{-p_2 d} e^{j\mathbf{k}\cdot\mathbf{r}} d^2k + \int\!\!\int_{-\infty}^{\infty} \frac{W^-_{2x}(\mathbf{k})}{(2\pi)^2} e^{p_2 d} e^{j\mathbf{k}\cdot\mathbf{r}} d^2k$$

$$= \varepsilon_{32}\mu_{32}[\int\!\!\int_{-\infty}^{\infty} \frac{W^p_{3x}(\mathbf{k},d)}{(2\pi)^2} e^{j\mathbf{k}\cdot\mathbf{r}} d^2k +$$

$$\int\!\!\int_{-\infty}^{\infty} \frac{W^+_{3x}(\mathbf{k})}{(2\pi)^2} e^{-p_3 d} e^{j\mathbf{k}\cdot\mathbf{r}} d^2k + \int\!\!\int_{-\infty}^{\infty} \frac{W^-_{3x}(\mathbf{k})}{(2\pi)^2} e^{p_3 d} e^{j\mathbf{k}\cdot\mathbf{r}} d^2k \ ] . \tag{2.5.1.30}$$

The following equation can be obtained because equation (2.5.1.30) must be valid for arbitrary **r**

$$W^+_{2x} e^{-p_2 d} + W^-_{2x} e^{p_2 d} = \varepsilon_{32}\mu_{32}[W^p_{3x}(d) + W^+_{3x} e^{-p_3 d} + W^-_{3x} e^{p_3 d}] \tag{2.5.1.31}$$

Using equations (2.5.1.17-21) and (2.5.1.4-11), following the procedure outlined above, and interchanging the order of integration and differentiation when $\frac{\partial}{\partial x}$ or $\frac{\partial}{\partial z}$ is involved give

$$p_2(W^+_{2x} e^{-p_2 d} - W^-_{2x} e^{p_2 d}) = \mu_{32} p_3(W^p_{3x}(d) + W^+_{3x} e^{-p_3 d} - W^-_{3x} e^{p_3 d}) \tag{2.5.1.32}$$

$$W^+_{2z} e^{-p_2 d} + W^-_{2z} e^{p_2 d} = \mu_{32}(W^+_{3z} e^{-p_3 d} + W^-_{3z} e^{p_3 d}) \tag{2.5.1.33}$$

$$p_2(W^+_{2z} e^{-p_2 d} - W^-_{2z} e^{p_2 d}) - p_3(W^+_{3z} e^{-p_3 d} - W^-_{3z} e^{p_3 d})$$

$$= (\varepsilon_{32}\mu_{32} - 1) jk_x (W^p_{3x}(d) + W^+_{3x} e^{-p_3 d} + W^-_{3x} e^{p_3 d}) \tag{2.5.1.34}$$

$$W_{3z}^{+}+W_{3z}^{-} = 0 \tag{2.5.1.35}$$

$$-W_{3x}^{p}(0)+W_{3x}^{+}-W_{3x}^{-} = 0 \tag{2.5.1.36}$$

$$W_{3x}^{p}(d) = \int_{V_3} \frac{M_{3x}(\mathbf{r}')}{2j\omega\mu_3 p_3} e^{-j\mathbf{k}\cdot\mathbf{r}'} e^{-p_3(d-z')} dv' = V_{3x}^{+}(\mathbf{k}) e^{-p_3 d} \tag{2.5.1.37}$$

$$W_{3x}^{p}(0) = \int_{V_3} \frac{M_{3x}(\mathbf{r}')}{2j\omega\mu_3 p_3} e^{-j\mathbf{k}\cdot\mathbf{r}'} e^{-p_3 z'} dv' = V_{3x}^{-}(\mathbf{k}) \tag{2.5.1.38}$$

$$V_{3x}^{\pm} = \int_{V_3} \frac{M_{3x}(\mathbf{r}')}{2j\omega\mu_3 p_3} e^{-j\mathbf{k}\cdot\mathbf{r}'} e^{\pm p_3 z'} dv' \, . \tag{2.5.1.39}$$

There are ten independent equations (2.5.1.24-27) and (2.5.1.31-36). These equations can be solved to obtain the ten unknown Hertzian potential components. Equations (2.5.1.24), (2.5.1.25), (2.5.1.31), (2.5.1.32), and (2.5.1.36) can be solved first to get the five x components. The other five equations can be solved to obtain the five z components. Notice that equations (2.5.1.27) and (2.5.1.34) describe the coupling between x and z components.

To simplify the derivation, the following notation is introduced:

$$d_i \equiv e^{-p_i d} \quad ; \quad t_i \equiv e^{-p_i t} \quad ; \quad i=1,2,3 \tag{2.5.1.40}$$

$$p_{ij} \equiv \frac{p_i}{p_j} \quad ; \quad d_{ij} \equiv \frac{d_i}{d_j} \quad ; \quad t_{ij} \equiv \frac{t_i}{t_j} \quad ; \quad i,j=1,2,3 \, . \tag{2.5.1.41}$$

Now, $p_2\times$ (2.5.1.24) plus $\varepsilon_{21}\times$ (2.5.1.25) results in

$$W_{2x}^{+} = \frac{1}{2}\mu_{12}(\varepsilon_{12}+p_{12}) t_{12} d_{12} W_{1x}^{+} \, . \tag{2.5.1.42}$$

While, $p_2\times$ (2.5.1.24) minus $\varepsilon_{21}\times$ (2.5.1.25) gives

$$W_{2x}^{-} = \frac{1}{2}\mu_{12}(\varepsilon_{12}-p_{12}) t_1 t_2 d_1 d_2 W_{1x}^{+} \tag{2.5.1.43}$$

and $p_3\times$ (2.5.1.31) plus $\varepsilon_{32}\times$ (2.5.1.32) results in

$$p_3(W^+_{2x}d_2+W^-_{2x}d_2^{-1})+\varepsilon_{32}p_2(W^+_{2x}d_2+W^-_{2x}d_2^{-1}) \tag{2.5.1.44}$$

$$= 2\varepsilon_{32}\mu_{32}p_3(V^+_{3x}d_3+W^+_{3x}d_3) \tag{2.5.1.44}$$

Some algebraic manipulation then gives

$$W^+_{3x} = -V^+_{3x}+\frac{1}{4}\mu_{13}d_3^{-1}\,[(\varepsilon_{12}+p_{12})(\varepsilon_{23}+p_{23})t_{12}d_1+$$

$$(\varepsilon_{12}-p_{12})(\varepsilon_{23}-p_{23})t_1t_2d_1]W^+_{1x}\ . \tag{2.5.1.45}$$

Next, $p_3\times$ (2.5.1.31) minus $\varepsilon_{32}\times$ (2.5.1.32) produces

$$W^-_{3x} = \frac{1}{4}\mu_{13}d_3[(\varepsilon_{12}+p_{12})(\varepsilon_{23}-p_{23})t_{12}d_1+$$

$$(\varepsilon_{12}-p_{12})(\varepsilon_{23}+p_{23})t_1t_2d_1]W^+_{1x}\ . \tag{2.5.1.46}$$

Substituting (2.5.1.45) and (2.5.1.46) into (2.5.1.36) gives the solution for W^+_{1x}.

$$W^+_{1x} = 4\varepsilon_2\varepsilon_3\mu_{31}p_2p_3t_{21}d_{31}\frac{V^+_{3x}+V^-_{3x}}{D_x} \tag{2.5.1.47}$$

where

$$D_x(\mathbf{k}) = (\varepsilon_1p_2+\varepsilon_2p_1)(\varepsilon_2p_3+\varepsilon_3p_2)+(\varepsilon_1p_2-\varepsilon_2p_1)(\varepsilon_2p_3-\varepsilon_3p_2)t_2^2$$

$$-(\varepsilon_1p_2+\varepsilon_2p_1)(\varepsilon_2p_3-\varepsilon_3p_2)d_3^2-(\varepsilon_1p_2-\varepsilon_2p_1)(\varepsilon_2p_3+\varepsilon_3p_2)t_2^2d_3^2 \tag{2.5.1.48}$$

$$N^+_{1x}(\mathbf{k}) = 4\varepsilon_2\varepsilon_3\mu_{31}p_2p_3t_{21}d_{31}(V^+_{3x}+V^-_{3x})\ . \tag{2.5.1.49}$$

Now, rewrite equation (2.5.1.46) as

$$W^+_{1x} = \frac{N^+_{1x}}{D_x} \tag{2.5.1.50}$$

while, substituting (2.5.1.50) into (2.5.1.42) gives

$$W^+_{2x} = \frac{N^+_{2x}}{D_x} \tag{2.5.1.51}$$

where

$$N^+_{2x}(\mathbf{k}) = 2\varepsilon_3 p_3(\varepsilon_1 p_2+\varepsilon_2 p_1)\mu_{12}\mu_{31}d_{32}(V^+_{3x}+V^-_{3x}) \ . \qquad (2.5.1.52)$$

Next, substituting (2.5.1.50) into (2.5.1.43), (2.5.1.45), and (2.5.1.46) respectively gives

$$W^-_{2x} = \frac{N^-_{2x}}{D_x} \qquad (2.5.1.53)$$

where

$$N^-_{2x}(\mathbf{k}) = 2\varepsilon_3 p_3(\varepsilon_1 p_2-\varepsilon_2 p_1)\mu_{12}\mu_{31}t_2^2 d_2 d_3(V^+_{3x}+V^-_{3x}) \qquad (2.5.1.54)$$

$$W^+_{3x} = \frac{N^+_{3x}}{D_x} \qquad (2.5.1.55)$$

with

$$N^+_{3x} = [(\varepsilon_1 p_2+\varepsilon_2 p_1)(\varepsilon_2 p_3-\varepsilon_3 p_2)d_3^2+(\varepsilon_1 p_2-\varepsilon_2 p_1)(\varepsilon_2 p_3+\varepsilon_3 p_2)t_2^2 d_3^2]V^+_{3x}$$

$$+ [(\varepsilon_1 p_2+\varepsilon_2 p_1)(\varepsilon_2 p_3+\varepsilon_3 p_2)+(\varepsilon_1 p_2-\varepsilon_2 p_1)(\varepsilon_2 p_3-\varepsilon_3 p_2)t_2^2]V^-_{3x} \qquad (2.5.1.56)$$

$$W^-_{3x} = \frac{N^-_{3x}}{D_x} \qquad (2.5.1.57)$$

and

$$N^-_{3x} = [(\varepsilon_1 p_2+\varepsilon_2 p_1)(\varepsilon_2 p_3-\varepsilon_3 p_2)d_3^2+$$

$$(\varepsilon_1 p_2-\varepsilon_2 p_1)(\varepsilon_2 p_3+\varepsilon_3 p_2)t_2^2 d_3^2](V^+_{3x}+V^-_{3x}) \ . \qquad (2.5.1.58)$$

Next, $\mu_{21}^{-1}t_2^{-1} \times$ (2.5.1.26) minus (2.5.1.33) and then using (2.5.1.35) result in

$$W^-_{2z} = \frac{d_2}{(1-t_2^2)d_3}[\mu_{12}t_1 t_2 d_1 d_3 W^+_{1z}+\mu_{32}t_2^2(1-d_3^2)W^+_{3z}] \qquad (2.5.1.59)$$

hile, $-\mu_{21}^{-1}t_2\times$ (2.5.1.26) plus (2.5.1.33) gives

$$W^+_{2z} = \frac{-1}{(1-t_2^2)d_2 d_3}[\mu_{12}t_1 t_2 d_1 d_3 W^+_{1z}+\mu_{32}(1-d_3^2)W^+_{3z}] \ . \qquad (2.5.1.60)$$

Substituting (2.5.1.59) and (2.5.1.60) into (2.5.1.27) and (2.5.1.34) gives the following matrix equation.

$$\begin{bmatrix} a_{11} & a_{12} \\ a_{21} & a_{22} \end{bmatrix} \begin{bmatrix} W_{1z}^{+} \\ W_{3z}^{+} \end{bmatrix} = \begin{bmatrix} b_1 \\ b_2 \end{bmatrix} \tag{2.5.1.61}$$

where

$$a_{11} = t_1 d_1 (1-t_2^2) p_1 + \mu_{12} t_1 d_1 (1+t_2^2) p_2 \tag{2.5.1.62}$$

$$a_{12} = 2\mu_{32} t_2 (1-d_3^2) d_3^{-1} p_2 \tag{2.5.1.63}$$

$$a_{21} = 2\mu_{12} t_1 t_2 d_1 p_2 \tag{2.5.1.64}$$

$$a_{22} = \mu_{32}(1-d_3^2)(1+t_2^2) d_3^{-1} p_2 + (1+d_3^2)(1-t_2^2) d_3^{-1} p_3 \tag{2.5.1.65}$$

$$b_1 = jk_x(\varepsilon_{21}\mu_{21}-1)(1-t_2^2)(t_2 d_2 W_{2x}^{+} + t_2^{-1} d_2^{-1} W_{2x}^{-}) \tag{2.5.1.66}$$

$$b_2 = -jk_x(\varepsilon_{32}\mu_{32}-1)(1-t_2^2)(d_3 V_{3x}^{+} + d_3 W_{3x}^{+} + d_3^{-1} W_{3x}^{-}) \ . \tag{2.5.1.67}$$

Equation (2.5.1.61) can be solved readily:

$$\Delta = a_{11}a_{22} - a_{12}a_{21} \tag{2.5.1.68}$$

$$\Delta_{1z}^{+} = b_1 a_{22} - b_2 a_{12} \tag{2.5.1.69}$$

$$\Delta_{3z}^{+} = a_{11} b_2 - a_{21} b_1 \tag{2.5.1.70}$$

$$W_{1z}^{+} = \frac{\Delta_{1z}^{+}}{\Delta} \tag{2.5.1.71}$$

$$W_{3z}^{+} = \frac{\Delta_{3z}^{+}}{\Delta} \ . \tag{2.5.1.72}$$

The next task is to express W_{1z}^{+} W_{3z}^{+} in terms of known parameters and expressions. Substituting (2.5.1.62-65) into (2.5.1.68) gives

$$\Delta = [t_1 d_1 (1-t_2^2) p_1 + \mu_{12} t_1 d_1 (1+t_2^2) p_2][\mu_{32}(1-d_3^2)(1+t_2^2) d_3^{-1} p_2 + (1+d_3^2)$$

$$(1-t_2^2) d_3^{-1} p_3] - [2\mu_{32} t_2 (1-d_3^2) d_3^{-1} p_2](2\mu_{12} t_1 t_2 d_1 p_2) \tag{2.5.1.73}$$

$$= t_1 d_1 d_3^{-1} \mu_2^{-1} \{ [(1-t_2^2) p_1 \mu_2 + (1+t_2^2) \mu_1 p_2][(1-d_3^2)(1+t_2^2) p_2 \mu_3 +$$

$$(1+d_3^2)(1-t_2^2) \mu_2 p_3] - 4 \mu_1 p_2^2 \mu_3 t_2^2 (1-d_3^2) \}$$

$$= \frac{(1-t_2^2) t_1 d_1}{\mu_2^2 d_3} D_z$$

where

$$D_z(\mathbf{k}) = [\mu_1 \mu_2 p_2 p_3 (1+t_2^2)(1+d_3^2) + \mu_1 p_2^2 \mu_3 (1-t_2^2)(1-d_3^2) +$$

$$p_1 \mu_2^2 p_3 (1-t_2^2)(1+d_3^2) + p_1 p_2 \mu_2 \mu_3 (1+t_2^2)(1-d_3^2)] \qquad (2.5.1.74)$$

Substituting (2.5.1.51-58) into (2.5.1.66) and (2.5.1.67) results in

$$b_1 = jk_x (\varepsilon_{21} \mu_{21} - 1)(1-t_2^2)(t_2 d_2 \frac{N_{2x}^+}{D_x} + t_2^{-1} d_2^{-1} \frac{N_{2x}^-}{D_x}) \qquad (2.5.1.75)$$

$$= jk_x (\varepsilon_{21} \mu_{21} - 1)(1-t_2^2) 4 \mu_{32} \varepsilon_1 p_2 p_3 \varepsilon_3 t_2 d_3 \frac{V_{3x}^+ + V_{3x}^-}{D_x}$$

$$b_2 = -jk_x (\varepsilon_{32} \mu_{32} - 1)(1-t_2^2)(d_3 V_{3x}^+ + d_3 \frac{N_{3x}^+}{D_x} + d_3^{-1} \frac{N_{3x}^-}{D_x}) \qquad (2.5.1.76)$$

$$= -jk_x (\varepsilon_{32} \mu_{32} - 1)(1-t_2^2) 2 \varepsilon_2 p_3 d_3 [\varepsilon_1 p_2 (1+t_2^2) + \varepsilon_2 p_1 (1-t_2^2)] \frac{V_{3x}^+ + V_{3x}^-}{D_x} \ .$$

Next, substituting (2.5.1.62-65), (2.5.1.75), and (2.5.1.76) into (2.5.1.69) and (2.5.1.70) gives

$$\Delta_{1z}^+ = jk_x \frac{V_{3x}^+ + V_{3x}^-}{D_x} 4 \mu_{31} p_2 p_3 t_2 (1-t_2^2) \mu_2^{-2} [(1+t_2^2)(1-d_3^2)(\varepsilon_3 \mu_3 - \varepsilon_1 \mu_1) \varepsilon_2 \mu_2 p_2$$

$$+ (1-t_2^2)(1+d_3^2)(\varepsilon_2 \mu_2 - \varepsilon_1 \mu_1) \mu_2 \varepsilon_3 p_3 +$$

$$(1-t_2^2)(1-d_3^2)(\varepsilon_3 \mu_3 - \varepsilon_2 \mu_2) \varepsilon_2 \mu_1 p_1] \qquad (2.5.1.77)$$

$$\Delta_{3z}^+ = -jk_x \frac{V_{3x}^+ + V_{3x}^-}{D_x} 2 t_1 d_1 d_3 p_3 (1-t_2^2) \mu_2^{-2} \{ (\varepsilon_3 \mu_3 - \varepsilon_2 \mu_2)[\mu_1 p_2 (1+t_2^2) +$$

$$\mu_2 p_1(1-t_2^2)][\varepsilon_1 p_2(1+t_2^2)+\varepsilon_2 p_1(1-t_2^2)]+4(\varepsilon_2\mu_2-\varepsilon_1\mu_1)\varepsilon_3\mu_3 t_2^2 p_2^2\} \ . \quad (2.5.1.78)$$

Then, substituting (2.5.1.73), (2.5.1.77), and (2.5.1.78) into (2.5.1.71) and (2.5.1.72) results in

$$W_{1z}^{+} = jk_x \frac{N_{1z}^{+}}{D_x D_z} \quad (2.5.1.79)$$

where

$$N_{1z}^{+} = 4\mu_{31} t_{21} d_{31} p_2 p_3[(1+t_2^2)(1-d_3^2)(\varepsilon_3\mu_3-\varepsilon_1\mu_1)\varepsilon_2\mu_2 p_2$$

$$+ (1-t_2^2)(1+d_3^2)(\varepsilon_2\mu_2-\varepsilon_1\mu_1)\varepsilon_3\mu_2 p_3$$

$$+ (1-t_2^2)(1-d_3^2)(\varepsilon_3\mu_3-\varepsilon_2\mu_2)\varepsilon_2\mu_1 p_1](V_{3x}^{+}+V_{3x}^{-}) \quad (2.5.1.80)$$

and

$$W_{3z}^{+} = jk_x \frac{N_{3z}^{+}}{D_x D_z} \quad (2.5.1.81)$$

where

$$N_{3z}^{+} = -2d_3^2 p_3\{(\varepsilon_3\mu_3-\varepsilon_2\mu_2)[\mu_1 p_2(1+t_2^2)+\mu_2 p_1(1-t_2^2)]$$

$$[\varepsilon_1 p_2(1+t_2^2)+\varepsilon_2 p_1(1-t_2^2)]+4(\varepsilon_2\mu_2-\varepsilon_1\mu_1)\varepsilon_3\mu_3 t_2^2 p_2^2\}(V_{3x}^{+}+V_{3x}^{-}) \ . \quad (2.5.1.82)$$

Next, substituting (2.5.1.81) and (2.5.1.82) into (2.5.1.35) gives

$$W_{3z}^{-} = jk_x \frac{N_{3z}^{-}}{D_x D_z} \quad (2.5.1.83)$$

where

$$N_{3z}^{-} = -N_{3z}^{+} \quad (2.5.1.84)$$

Finally, substituting (2.5.1.79-82) into (2.5.1.59) and (2.5.1.60) results in

$$W_{2z}^{-} = jk_x \frac{N_{2z}^{-}}{D_x D_z} \quad (2.5.1.85)$$

where

$$N_{2z}^{-} = \frac{2\mu_{32}t_2^2 d_2 d_3}{(1-t_2^2)} p_3\{2[(1+t_2^2)(1-d_3^2)(\varepsilon_3\mu_3-\varepsilon_1\mu_1)\varepsilon_2\mu_2 p_2^2$$

$$+ (1-t_2^2)(1+d_3^2)(\varepsilon_2\mu_2-\varepsilon_1\mu_1)\varepsilon_3\mu_2 p_2 p_3 + (1-t_2^2)(1-d_3^2)(\varepsilon_3\mu_3-\varepsilon_2\mu_2)\varepsilon_2\mu_1 p_1 p_2]$$

$$- (1-d_3^2)\{(\varepsilon_3\mu_3-\varepsilon_2\mu_2)[\mu_1 p_2(1+t_2^2)+\mu_2 p_1(1-t_2^2)][\varepsilon_1 p_2(1+t_2^2)+\varepsilon_2 p_1(1-t_2^2)]$$

$$+4(\varepsilon_2\mu_2-\varepsilon_1\mu_1)\varepsilon_3\mu_3 t_2^2 p_2^2\}\}(V_{3x}^{+}+V_{3x}^{-}) \tag{2.5.1.86}$$

and

$$W_{2z}^{+} = jk_x \frac{N_{2z}^{+}}{D_x D_z} \tag{2.5.1.87}$$

where

$$N_{2z}^{+} = \frac{2\mu_{32}d_{32}}{(1-t_2^2)} p_3\{2t_2^2[(1+t_2^2)(1-d_3^2)(\varepsilon_3\mu_3-\varepsilon_1\mu_1)\varepsilon_2\mu_2 p_2^2$$

$$+ (1-t_2^2)(1+d_3^2)(\varepsilon_2\mu_2-\varepsilon_1\mu_1)\varepsilon_3\mu_2 p_2 p_3 + (1-t_2^2)(1-d_3^2)(\varepsilon_3\mu_3-\varepsilon_2\mu_2)\varepsilon_2\mu_1 p_1 p_2]$$

$$- (1-d_3^2)\{(\varepsilon_3\mu_3-\varepsilon_2\mu_2)[\mu_1 p_2(1+t_2^2)+\mu_2 p_1(1-t_2^2)][\varepsilon_1 p_2(1+t_2^2)+\varepsilon_2 p_1(1-t_2^2)]$$

$$+4(\varepsilon_2\mu_2-\varepsilon_1\mu_1)\varepsilon_3\mu_3 t_2^2 p_2^2\}\}(V_{3x}^{+}+V_{3x}^{-})\ . \tag{2.5.1.88}$$

The following summary will be convenient for later use:

$$W_{1x}^{+} = \frac{N_{1x}^{+}}{D_x} \tag{2.5.1.89}$$

$$W_{2x}^{+} = \frac{N_{2x}^{+}}{D_x} \tag{2.5.1.90}$$

$$W_{2x}^{-} = \frac{N_{2x}^{-}}{D_x} \tag{2.5.1.91}$$

$$W_{3x}^{+} = \frac{N_{3x}^{-}}{D_x} \tag{2.5.1.92}$$

$$W_{3x}^{-} = \frac{N_{3x}^{-}}{D_x} \tag{2.5.1.93}$$

$$W_{1z}^{+} = jk_x \frac{N_{1z}^{+}}{D_x D_z} \tag{2.5.1.94}$$

$$W_{2z}^{+} = jk_x \frac{N_{2z}^{+}}{D_x D_z} \tag{2.5.1.95}$$

$$W_{2z}^{-} = jk_x \frac{N_{2z}^{-}}{D_x D_z} \tag{2.5.1.96}$$

$$W_{3z}^{+} = jk_x \frac{N_{3z}^{+}}{D_x D_z} \tag{2.5.1.97}$$

$$W_{3z}^{-} = jk_x \frac{N_{3z}^{-}}{D_x D_z} \tag{2.5.1.98}$$

$$D_x(\mathbf{k}) = [\varepsilon_1\varepsilon_2 p_2 p_3(1+e^{-2p_2 t})(1-e^{-2p_3 d})+\varepsilon_1 p_2^2 \varepsilon_3(1-e^{-2p_2 t})(1+e^{-2p_3 d})$$

$$+ p_1\varepsilon_2^2 p_3(1-e^{-2p_2 t})(1-e^{-2p_3 d})+p_1 p_2\varepsilon_2\varepsilon_3(1+e^{-2p_2 t})(1+e^{-2p_3 d})] \tag{2.5.1.99}$$

$$D_z(\mathbf{k}) = [\mu_1\mu_2 p_2 p_3(1+e^{-2p_2 t})(1+e^{-2p_3 d})+\mu_1 p_2^2 \mu_3(1-e^{-2p_2 t})(1-e^{-2p_3 d})$$

$$+ p_1\mu_2^2 p_3(1-e^{-2p_2 t})(1+e^{-2p_3 d})+p_1 p_2\mu_2\mu_3(1+e^{-2p_2 t})(1-e^{-2p_3 d})] \tag{2.5.1.100}$$

$$N_{1x}^{+}(\mathbf{k}) = 4\varepsilon_2\varepsilon_3\mu_{31} p_2 p_3 e^{-(p_2-p_1)t} e^{-(p_3-p_1)d}(V_{3x}^{+}+V_{3x}^{-}) \tag{2.5.1.101}$$

$$N_{2x}^{+}(\mathbf{k}) = 2\varepsilon_3 p_3(\varepsilon_1 p_2+\varepsilon_2 p_1)\mu_{32} e^{-(p_3-p_2)d}(V_{3x}^{+}+V_{3x}^{-}) \tag{2.5.1.102}$$

$$N_{2x}^{-}(\mathbf{k}) = 2\varepsilon_3 p_3(\varepsilon_1 p_2-\varepsilon_2 p_1)\mu_{32} e^{-2p_2 t} e^{-(p_2+p_3)d}(V_{3x}^{+}+V_{3x}^{-}) \tag{2.5.1.103}$$

$$N_{3x}^{+}(\mathbf{k}) = [(\varepsilon_1 p_2+\varepsilon_2 p_1)(\varepsilon_2 p_3-\varepsilon_3 p_2)e^{-2p_3 d}+(\varepsilon_1 p_2-\varepsilon_2 p_1)(\varepsilon_2 p_3+\varepsilon_3 p_2)e^{-2p_2 t} e^{-2p_3 d}]$$

$$V_{3x}^{+} + [(\varepsilon_1 p_2+\varepsilon_2 p_1)(\varepsilon_2 p_3+\varepsilon_3 p_2)+(\varepsilon_1 p_2-\varepsilon_2 p_1)(\varepsilon_2 p_3-\varepsilon_3 p_2)e^{-2p_2 t}]V_{3x}^{-} \tag{2.5.1.104}$$

$$N_{3x}^{-}(\mathbf{k}) = [(\varepsilon_1 p_2+\varepsilon_2 p_1)(\varepsilon_2 p_3-\varepsilon_3 p_2)e^{-2p_3 d}$$

$$+ (\varepsilon_1 p_2-\varepsilon_2 p_1)(\varepsilon_2 p_3+\varepsilon_3 p_2)e^{-2p_2 t} e^{-2p_3 d}](V_{3x}^{+}+V_{3x}^{-}) \tag{2.5.1.105}$$

$$N_{1z}^{+}(\mathbf{k}) = 4\mu_{31}p_2p_3e^{-(p_2-p_1)t}e^{-(p_3-p_1)d}[(1+e^{-2p_2t})(1-e^{-2p_3d})(\varepsilon_3\mu_3-\varepsilon_1\mu_1)\varepsilon_2\mu_2p_2$$

$$+ (1-e^{-2p_2t})(1+e^{-2p_3d})(\varepsilon_2\mu_2-\varepsilon_1\mu_1)\varepsilon_3\mu_2p_3$$

$$+ (1-e^{-2p_2t})(1-e^{-2p_3d})(\varepsilon_3\mu_3-\varepsilon_2\mu_2)\varepsilon_2\mu_1p_1](V_{3x}^{+}+V_{3x}^{-}) \qquad (2.5.1.106)$$

$$N_{2z}^{-}(\mathbf{k}) = \frac{2\mu_{32}e^{-2p_2t}e^{-(p_2+p_3)d}}{(1-e^{-2p_2t})}p_3\{2[(1+e^{-2p_2t})(1-e^{-2p_3d})(\varepsilon_3\mu_3-\varepsilon_1\mu_1)\varepsilon_2\mu_2p_2^2$$

$$+ (1-e^{-2p_2t})(1+e^{-2p_3d})(\varepsilon_2\mu_2-\varepsilon_1\mu_1)\varepsilon_3\mu_2p_2p_3$$

$$+ (1-e^{-2p_2t})(1-e^{-2p_3d})(\varepsilon_3\mu_3-\varepsilon_2\mu_2)\varepsilon_2\mu_1p_1p_2]$$

$$- (1-e^{-2p_3d})\{(\varepsilon_3\mu_3-\varepsilon_2\mu_2)[\mu_1p_2(1+e^{-2p_2t})+\mu_2p_1(1-e^{-2p_2t})]$$

$$[\varepsilon_1p_2(1+e^{-2p_2t})+\varepsilon_2p_1(1-e^{-2p_2t})]$$

$$+ 4(\varepsilon_2\mu_2-\varepsilon_1\mu_1)\varepsilon_3\mu_3t_2^2p_2^2\}\}(V_{3x}^{+}+V_{3x}^{-}) \qquad (2.5.1.107)$$

$$N_{2z}^{+}(\mathbf{k}) = \frac{-2\mu_{32}e^{-(-p_2+p_3)d}}{(1-e^{-2p_2t})}p_3\{2e^{-2p_2t}[(1+e^{-2p_2t})(1-e^{-2p_3d})(\varepsilon_3\mu_3-\varepsilon_1\mu_1)\varepsilon_2\mu_2p_2^2$$

$$+ (1-e^{-2p_2t})(1+e^{-2p_3d})(\varepsilon_2\mu_2-\varepsilon_1\mu_1)\varepsilon_3\mu_2p_2p_3$$

$$+ (1-e^{-2p_2t})(1-e^{-2p_3d})(\varepsilon_3\mu_3-\varepsilon_2\mu_2)\varepsilon_2\mu_1p_1p_2]$$

$$- (1-e^{-2p_3d})\{(\varepsilon_3\mu_3-\varepsilon_2\mu_2)[\mu_1p_2(1+e^{-2p_2t})+\mu_2p_1(1-e^{-2p_2t})]$$

$$[\varepsilon_1p_2(1+e^{-2p_2t})+\varepsilon_2p_1(1-e^{-2p_2t})]$$

$$+ 4(\varepsilon_2\mu_2-\varepsilon_1\mu_1)\varepsilon_3\mu_3t_2^2p_2^2\}\}(V_{3x}^{+}+V_{3x}^{-}) \qquad (2.5.1.108)$$

$$N_{3z}^{+}(\mathbf{k}) = -2e^{-2p_3d}p_3\{(\varepsilon_3\mu_3-\varepsilon_2\mu_2)[\mu_1p_2(1+e^{-2p_2t})+\mu_2p_1(1-e^{-2p_2t})]$$

$$[\varepsilon_1p_2(1+e^{-2p_2t})+\varepsilon_2p_1(1-e^{-2p_2t})]$$

$$+ 4(\varepsilon_2\mu_2-\varepsilon_1\mu_1)\varepsilon_3\mu_3e^{-2p_2t}p_2^2\}(V_{3x}^{+}+V_{3x}^{-}) \qquad (2.5.1.109)$$

$$N_{3z}^{-}(\mathbf{k}) = -N_{3z}^{+}(\mathbf{k}) \qquad (2.5.1.110)$$

$$V_{3x}^{\pm}(\mathbf{k}) = \int_{V_3} \frac{M_{3x}(\mathbf{r}')}{2j\omega\mu_3 p_3} e^{-j\mathbf{k}\cdot\mathbf{r}'} e^{\pm p_3 z'} dv' . \tag{2.5.1.111}$$

Notice that D_x, D_z, N_{1x}^{+}, N_{2x}^{+}, N_{2x}^{-}, N_{3x}^{+}, N_{3x}^{-}, N_{1z}^{+}, N_{2z}^{+}, N_{2z}^{-}, N_{3z}^{+}, and N_{3z}^{-} are functions of $|\mathbf{k}| = \sqrt{k_x^2+k_y^2}$ only.

The lower half space shown in Figure 2.3 is a much simpler structure to analyze. A horizontal magnetic current in region 4, $\mathbf{M}_4 = \hat{x}M_{4x}$, generates the Hertzian potentials

$$\Pi_4 = \hat{x}(\Pi_{4x}^{p}+\Pi_{4x}^{-}) \tag{2.5.1.112}$$

Because there is no interface except the ground plane in region 4, there is no coupling between the horizontal component and vertical component. In other words, the horizontal component of Hertzian potential can describe the electromagnetic field in region 4 completely. Using the integral representation of primary and scattered potential (2.5.1.4-5) gives

$$\Pi_{4x}^{p}(\mathbf{r}) = \int_{V_3} \frac{M_{4x}(\mathbf{r}')}{j\omega\mu_4} \left[\int\int_{-\infty}^{\infty} \frac{e^{j\mathbf{k}\cdot(\mathbf{r}-\mathbf{r}')} e^{-p_4|z-z'|}}{(2\pi)^2 2p_4} d^2k\right] dv' \tag{2.5.1.113}$$

$$\Pi_{4x}^{-} = \int\int_{-\infty}^{\infty} \frac{W_{4x}^{-}}{(2\pi)^2} e^{p_4 z} e^{j\mathbf{k}\cdot\mathbf{r}} d^2k . \tag{2.5.1.114}$$

The boundary condition at the interface z=0 is

$$\frac{\partial \Pi_{4x}}{\partial z} = 0 . \tag{2.5.1.115}$$

Substituting (2.5.1.113-114) into (2.5.1.115) gives

$$W_{4x}^{-} = \int_{V_4} \frac{M_{4x}(\mathbf{r}')}{j2\omega\mu_4 p_4} e^{-j\mathbf{k}\cdot\mathbf{r}'} e^{-p_4 z'} dv' . \tag{2.5.1.116}$$

Now, assume that

$$\mathbf{M}_4(\mathbf{r}) = \hat{x}M_{4x}(\mathbf{r}_t)\delta(z) \ . \tag{2.5.1.117}$$

Then, equation (2.5.1.116) can be rewritten as

$$W_{4x}^{-} = \iint_S \frac{M_{4x}(\mathbf{r}')}{j2\omega\mu_4 p_4} e^{-j\mathbf{k}\cdot\mathbf{r}'} ds' \ . \tag{2.5.1.118}$$

2.5.2 Green's Functions

After solving for the scattered magnetic Hertzian potentials in the three regions produced by the three orthogonal components of an arbitrary magnetic current source in region 3, the dyadic Green's function for Hertzian potentials can be determined. The following notation will be used:

$$\Pi_i^m(\mathbf{r}) = \int_{V_j} \overleftrightarrow{G}^{i,j}(\mathbf{r}|\mathbf{r}')\cdot\mathbf{M}_j(\mathbf{r}')dv' \quad ; \quad i,j = 1,2,3 \ . \tag{2.5.2.1}$$

Here $\Pi_i^m(\mathbf{r})$ is the magnetic Hertzian potential in region i maintained by a magnetic current source in region j.

In this dissertation, the case of interest is the one when i=1,3 and j=3. Also, the source is assumed to be on the $z' = 0$ plane and has only an x-directed component. Thus

$$\mathbf{M}_3(\mathbf{r}) = \hat{x}M_{3x}(\mathbf{r}_t)\delta(z)$$

In this case (2.5.1.111) can be written as

$$V_{3x}^{+}(\mathbf{k}) = V_{3x}^{-}(\mathbf{k}) = \int_{S_3} \frac{M_{3x}(\mathbf{r}'_t)}{2j\omega\mu_3 p_3} e^{-j\mathbf{k}\cdot\mathbf{r}'} ds' \tag{2.5.2.2}$$

where

$$\mathbf{r}'_t = \hat{x}x' + \hat{y}y' \ .$$

Now, using (2.5.1.5), (2.5.1.9), (2.5.1.89), (2.5.1.101), and (2.5.2.1) gives

$$\Pi_{1x} = \int_{V_3} G_{xx}^{1,3}(\mathbf{r}|\mathbf{r}')M_{3x}(\mathbf{r}_t')\delta(z')dv'$$

$$= \int\int_{-\infty}^{\infty} d^2k \{\frac{1}{(2\pi)^2}\frac{N_{1x}^{+}}{D_x}e^{-p_1 z}e^{j\mathbf{k}\cdot\mathbf{r}}[\int_{S_3}\frac{M_{3x}(\mathbf{r}_t')}{2j\omega\mu_3 p_3}2e^{-j\mathbf{k}\cdot\mathbf{r}'}ds']\}$$

$$= \int_{S_3}[\frac{1}{(2\pi)^2}\int\int_{-\infty}^{\infty} d^2k\frac{e^{j\mathbf{k}\cdot(\mathbf{r}-\mathbf{r}')}}{j\omega\mu_3 p_3}(\frac{N_{1x}^{+}}{D_x}e^{-p_1 z})]M_{3x}(\mathbf{r}_t')ds' .$$

So

$$G_{xx}^{1,3}(\mathbf{r}|\mathbf{r}') = \frac{1}{(2\pi)^2}\int\int_{-\infty}^{\infty} d^2k\frac{e^{j\mathbf{k}\cdot(\mathbf{r}-\mathbf{r}')}}{j\omega\mu_3 p_3}(\frac{N_{1x}}{D_x}) \tag{2.5.2.3}$$

where

$$N_{1x}(z,\mathbf{k}) = 4\varepsilon_2\varepsilon_3\mu_{31}p_2p_3e^{-(p_2-p_1)t}e^{-(p_3-p_1)d}e^{-p_1 z} \tag{2.5.2.4}$$

and

$$\mathbf{r}_t = \hat{x}x + \hat{y}y .$$

Other components of the dyadic Green's function can be obtained by following the same procedure and using (2.5.1.4), (2.5.1.5), (2.5.1.9), (2.5.1.11), (2.5.1.89-110), (2.5.2.1), and (2.5.2.2). Some algebraic manipulation gives

$$G_{yx}^{1,3}(\mathbf{r}|\mathbf{r}') = 0 \tag{2.5.2.5}$$

$$G_{zx}^{1,3}(\mathbf{r}|\mathbf{r}') = \frac{1}{(2\pi)^2}\int\int_{-\infty}^{\infty} d^2k\frac{e^{j\mathbf{k}\cdot(\mathbf{r}-\mathbf{r}')}}{j\omega\mu_3 p_3}(jk_x\frac{N_{1z}}{D_xD_z}) \tag{2.5.2.6}$$

$$G_{xx}^{3,3}(\mathbf{r}|\mathbf{r}') = \frac{1}{(2\pi)^2}\int\int_{-\infty}^{\infty} d^2k\frac{e^{j\mathbf{k}\cdot(\mathbf{r}-\mathbf{r}')}}{j\omega\mu_3 p_3}(\frac{N_{3x}}{D_x}) \tag{2.5.2.7}$$

$$G_{yx}^{3,3}(\mathbf{r}|\mathbf{r}') = 0 \tag{2.5.2.8}$$

$$G_{zx}^{3,3}(\mathbf{r}|\mathbf{r}') = \frac{1}{(2\pi)^2}\int\int_{-\infty}^{\infty} d^2k\frac{e^{j\mathbf{k}\cdot(\mathbf{r}-\mathbf{r}')}}{j\omega\mu_3 p_3}(jk_x\frac{N_{3z}}{D_xD_z}) \tag{2.5.2.9}$$

where

$$N_{1z}(z,\mathbf{k}) = 4\mu_{31}p_2p_3e^{-(p_2-p_1)t}e^{-(p_3-p_1)d}[(1+e^{-2p_2t})(1-e^{-2p_3d})(\varepsilon_3\mu_3-\varepsilon_1\mu_1)\varepsilon_2\mu_2p_2$$

$$+ (1-e^{-2p_2t})(1+e^{-2p_3d})(\varepsilon_2\mu_2-\varepsilon_1\mu_1)\varepsilon_3\mu_2p_3$$

$$+ (1-e^{-2p_2t})(1-e^{-2p_3d})(\varepsilon_3\mu_3-\varepsilon_2\mu_2)\varepsilon_2\mu_1p_1]e^{-p_1z} \qquad (2.5.2.10)$$

$$N_{3x}(z,\mathbf{k}) = [(\varepsilon_1p_2+\varepsilon_2p_1)(\varepsilon_2p_3+\varepsilon_3p_2)+(\varepsilon_1p_2-\varepsilon_2p_1)(\varepsilon_2p_3-\varepsilon_3p_2)e^{-2p_2t}]e^{-p_3z}$$

$$+ [(\varepsilon_1p_2+\varepsilon_2p_1)(\varepsilon_2p_3-\varepsilon_3p_2)+(\varepsilon_1p_2-\varepsilon_2p_1)(\varepsilon_2p_3+\varepsilon_3p_2)e^{-2p_2t}]e^{-2p_3d}e^{p_3z} \qquad (2.5.2.11)$$

$$N_{3z} = 2e^{-2p_3d}p_3\{(\varepsilon_3\mu_3-\varepsilon_2\mu_2)[\mu_1p_2(1+e^{-2p_2t})+\mu_2p_1(1-e^{-2p_2t})][\varepsilon_1p_2(1+e^{-2p_2t})$$

$$+\varepsilon_2p_1(1-e^{-2p_2t})]+4(\varepsilon_2\mu_2-\varepsilon_1\mu_1)\varepsilon_3\mu_3e^{-2p_2t}p_2^2\}(e^{p_3z}-e^{-p_3z}) \, . \qquad (2.5.2.12)$$

Again using (2.5.1.112), (2.5.1.114), (2.5.1.118), and (2.5.2.1) gives $G_{xx}^{4,4}$ as

$$G_{xx}^{4,4}(\mathbf{r}|\mathbf{r}') = \frac{1}{(2\pi)^2}\int\int_{-\infty}^{\infty} d^2k \frac{e^{j\mathbf{k}\cdot(\mathbf{r}-\mathbf{r}')}}{j\omega\mu_4p_4}e^{p_4z} \qquad z<0 \, . \qquad (2.5.2.13)$$

2.6 Green's Functions for Fields

After the Green's functions for the Hertzian potentials have been obtained, the Green's functions for EM fields can be derived by using the relationship between the fields and the potentials. The dyadic Green's function for the fields due to an electric current is derived in section 2.6.1 and the dyadic Green's function for the fields due to a magnetic current is derived in section 2.6.2.

2.6.1 Green's Function for the Fields due to an Electric Current

The electric field maintained by an electric current can be written in terms of dyadic Green's function

$$\mathbf{E}_i(\mathbf{r}) = \int_V \overleftrightarrow{g}^{i,j}(\mathbf{r}|\mathbf{r}')\cdot\mathbf{J}_j(\mathbf{r}')dv' \quad ; \quad i,j = 1,2,3\ . \tag{2.6.1.1}$$

The electric field is represented by electric Hertzian potentials (2.1.1) via

$$\mathbf{E}_i = (k_i^2+\nabla\nabla\cdot)\Pi_i \tag{2.6.1.2}$$

$$\Pi_i = \int_V \overleftrightarrow{G}^{i,j}(\mathbf{r}|\mathbf{r}')\cdot\mathbf{J}_j(\mathbf{r}')dv'\ . \tag{2.6.1.3}$$

Substituting (2.6.1.3) into (2.6.1.2) gives the dyadic electric Green's function

$$\overleftrightarrow{g}^{i,j}(\mathbf{r}|\mathbf{r}') = (k_i^2+\nabla\nabla\cdot)\overleftrightarrow{G}^{i,j}(\mathbf{r}|\mathbf{r}')\ . \tag{2.6.1.4}$$

Assume the current distribution in region 3 is a sheath current along the z-axis. Then (2.4.3.35) holds, and (2.4.2.33) becomes

$$\Pi_z^t = \Pi_{1z} = \frac{1}{2\pi}\int_0^\infty \frac{\bar{V}_z(\lambda)}{\chi(\lambda)} e^{-p_1(z-t)} J_0(\lambda\rho)\lambda d\lambda \tag{2.6.1.5}$$

in analogy with (2.4.3.44), where

$$\bar{V}_z(\lambda) = \int_z \frac{I_z^3(z')}{j\omega\epsilon_3}\frac{\cosh p_3(d+z')}{p_3} J_0(\lambda a)dz'\ . \tag{2.6.1.6}$$

The electric field in region 1 can be found using (2.6.1.2). For a vertically directed potential this reduces to the relations

$$E_{1z} = k_1^2\Pi_{1z}+\frac{\partial^2\Pi_{1z}}{\partial z^2} \tag{2.6.1.7}$$

$$E_{1\rho} = \frac{\partial^2\Pi_{1z}}{\partial\rho\partial z} \tag{2.6.1.8}$$

where ρ is the radial variable in polar coordinates. The necessary derivatives for using (2.6.1.5) in (2.6.1.7) are

$$\frac{\partial\Pi_{1z}}{\partial z} = -\frac{1}{2\pi}\int_0^\infty \frac{\bar{V}_z(\lambda)}{\chi(\lambda)} p_1 e^{-p_1(z-t)} J_0(\lambda\rho)\lambda d\lambda \tag{2.6.1.9}$$

$$\frac{\partial^2\Pi_{1z}}{\partial z^2} = \frac{1}{2\pi}\int_0^\infty \frac{\bar{V}_z(\lambda)}{\chi(\lambda)} p_1^2 e^{-p_1(z-t)} J_0(\lambda\rho)\lambda d\lambda \tag{2.6.1.10}$$

$$\frac{\partial^2\Pi_{1z}}{\partial z\partial\rho} = \frac{1}{2\pi}\int_0^\infty \frac{\bar{V}_z(\lambda)}{\chi(\lambda)} p_1\lambda e^{-p_1(z-t)} J_1(\lambda\rho)\lambda d\lambda\ . \tag{2.6.1.11}$$

Substituting (2.6.1.10) and (2.6.1.5) into (2.6.1.7) gives

$$E_{1z} = \frac{1}{2\pi}\int_0^\infty \frac{\bar{V}_z(\lambda)}{\chi(\lambda)}[p_1^2+k_1^2]J_0(\lambda\rho)e^{-p_1(z-t)}\lambda d\lambda \tag{2.6.1.12}$$

or, using (2.4.3.39)

$$E_{1z} = \frac{1}{2\pi}\int_o^\infty \frac{\bar{V}_z(\lambda)}{\chi(\lambda)} J_0(\lambda\rho)e^{-p_1(z-t)}\lambda^3 d\lambda\ . \tag{2.6.1.13}$$

Finally, substituting (2.6.1.11) into (2.6.1.8) gives

$$E_{1\rho} = \frac{1}{2\pi}\int_o^\infty \frac{\bar{V}_z(\lambda)}{\chi(\lambda)} J_1(\lambda\rho)e^{-p_1(z-t)}p_1\lambda^2 d\lambda\ . \tag{2.6.1.14}$$

To derive an electric field integral equation for an imaged monopole, it is necessary to know the z component of the scattered field in region 3. From (2.6.1.2), the electric field in region 3 maintained by a vertical electric current in region 3 can be written as

$$E_{3z} = k_3^2\Pi_{3z} + \frac{\partial^2\Pi_{3z}}{\partial z^2} \tag{2.6.1.15}$$

$$E_{1\rho} = \frac{\partial^2\Pi_{3z}}{\partial\rho\partial z} \tag{2.6.1.16}$$

Then, substituting (2.4.3.47) into (2.6.1.15-16) gives

$$E_{3z} = (k_3^2+\frac{\partial^2}{\partial z^2})\int_{-d}^{0} G_{zz}^{3,3}(z,\rho,zp)I_z^3(z')dz' \tag{2.6.1.17}$$

2.6.2 Green's Function for the Fields due to a Magnetic Current

The relationship between the magnetic Hertzian potential and EM field is used to construct the dyadic Green's function for the EM field. The magnetic field Green's function can be written as

$$\mathbf{H}_i(\mathbf{r}) = \int_V \overleftrightarrow{\mathcal{G}}^{i,j}(\mathbf{r}|\mathbf{r}')\cdot\mathbf{M}_j(\mathbf{r}')dv' \quad ; \quad i,j = 1,2,3,4\ . \tag{2.6.2.1}$$

Expressing $\mathbf{H}_i$ in terms of magnetic Hertzian potential Π_i^m gives

$$\begin{aligned}\mathbf{H}_i &= k_i^2\Pi_i^m+\nabla(\nabla\cdot\Pi_i^m)\\ &= (k_i^2+\nabla\nabla\cdot)\int_{V_3} \overleftrightarrow{G}^{i,j}(\mathbf{r}|\mathbf{r}')\cdot\mathbf{M}_j(\mathbf{r}')dv'\ .\end{aligned} \tag{2.6.2.2}$$

Exchanging the order of integration and differentiation and using (2.6.1), the magnetic field Green's function can be expressed as

$$\overleftrightarrow{\mathcal{G}}^{i,j}(\mathbf{r}|\mathbf{r}') = P.V.\,(k_i^2+\nabla\nabla\cdot)\overleftrightarrow{G}^{i,j}(\mathbf{r}|\mathbf{r}') - \frac{\overleftrightarrow{L}\delta(\mathbf{r}-\mathbf{r}')}{k_i^2} \tag{2.6.2.3}$$

where $P.V.$ stands for principal value and

$$\overleftrightarrow{L} = L_{xx}\hat{x}\hat{x}+L_{yy}\hat{y}\hat{y}+L_{zz}\hat{z}\hat{z}$$

is the source dyad. Each term on the right hand side of (2.6.2.3) is dependent on the shape of principal volume, but the combination of the two terms is independent on the principal volume [6][12]. The explicit expression of $\overleftrightarrow{L}$ is not given because magnetic field Green's function in (2.6.2.3) is not used directly.

Carrying out $\nabla\nabla\cdot\overleftrightarrow{G}$ results in

$$\begin{aligned}\nabla\cdot\overleftrightarrow{G} &= \frac{\partial}{\partial x}[G_{xx}\hat{x}+G_{xy}\hat{y}+G_{xz}\hat{z}]+\frac{\partial}{\partial y}[G_{yx}\hat{x}+G_{yy}\hat{y}+G_{yz}\hat{z}]\\ &+\frac{\partial}{\partial z}[G_{zx}\hat{x}+G_{zy}\hat{y}+G_{zz}\hat{z}]\end{aligned} \tag{2.6.2.4}$$

and

$$\nabla\nabla\cdot\overleftrightarrow{G} = \hat{x}\frac{\partial}{\partial x}(\nabla\cdot\overleftrightarrow{G})+\hat{y}\frac{\partial}{\partial y}(\nabla\cdot\overleftrightarrow{G})+\hat{z}\frac{\partial}{\partial z}(\nabla\cdot\overleftrightarrow{G})$$

$$= \hat{x}\hat{x}\,(\frac{\partial^2 G_{xx}}{\partial x^2}+\frac{\partial^2 G_{yx}}{\partial x\,\partial y}+\frac{\partial^2 G_{zx}}{\partial x\,\partial z})+\hat{x}\hat{y}\,(\frac{\partial^2 G_{xy}}{\partial x^2}+\frac{\partial^2 G_{yy}}{\partial x\,\partial y}+\frac{\partial^2 G_{zy}}{\partial x\,\partial z})+$$

$$\hat{x}\hat{z}\,(\frac{\partial^2 G_{xz}}{\partial x^2}+\frac{\partial^2 G_{yz}}{\partial x\,\partial y}+\frac{\partial^2 G_{zz}}{\partial x\,\partial z})+\hat{y}\hat{x}\,(\frac{\partial^2 G_{xx}}{\partial x\,\partial y}+\frac{\partial^2 G_{yx}}{\partial y^2}+\frac{\partial^2 G_{zx}}{\partial y\,\partial z})+$$

$$\hat{y}\hat{y}\,(\frac{\partial^2 G_{xy}}{\partial x\,\partial y}+\frac{\partial^2 G_{yy}}{\partial y^2}+\frac{\partial^2 G_{zy}}{\partial y\,\partial z})+\hat{y}\hat{z}\,(\frac{\partial^2 G_{xz}}{\partial x\,\partial y}+\frac{\partial^2 G_{yz}}{\partial y^2}+\frac{\partial^2 G_{zz}}{\partial y\,\partial z})+$$

$$\hat{z}\hat{x}\,(\frac{\partial^2 G_{xx}}{\partial x\,\partial z}+\frac{\partial^2 G_{yx}}{\partial y\,\partial z}+\frac{\partial^2 G_{zx}}{\partial z^2})+\hat{z}\hat{y}\,(\frac{\partial^2 G_{xy}}{\partial x\,\partial z}+\frac{\partial^2 G_{yy}}{\partial y\,\partial z}+\frac{\partial^2 G_{zy}}{\partial z^2})+$$

$$\hat{z}\hat{z}\,(\frac{\partial^2 G_{xz}}{\partial x\,\partial z}+\frac{\partial^2 G_{yz}}{\partial y\,\partial z}+\frac{\partial^2 G_{zz}}{\partial z^2}) \tag{2.6.2.5}$$

Throughout the dissertation, the magnetic current is assumed to have only a x-component

$$\mathbf{M}_3 = \hat{x}M_{3x} \tag{2.6.2.6}$$

$$\mathbf{M}_4 = \hat{x}M_{4x}\ . \tag{2.6.2.7}$$

The components of $\overleftrightarrow{g}^{i,j}$ can be expressed in terms of the components of $\overleftrightarrow{G}^{i,j}$ by using (2.5.2.3), (2.5.2.5-9), (2.6.2.3), and (2.6.2.5) and they are summarized as

$$g_{xx}^{3,3} = P.V.[\frac{\partial^2}{\partial x^2}G_{xx}^{3,3}+\frac{\partial^2}{\partial x\,\partial z}G_{zx}^{3,3}+k_3^2G_{xx}^{3,3}]-\frac{L_{xx}\,\delta(\mathbf{r}-\mathbf{r}')}{k_3^2}$$

$$= P.V.(\frac{1}{(2\pi)^2}\int\int_{-\infty}^{\infty} d^2k\frac{e^{j\mathbf{k}\cdot(\mathbf{r}-\mathbf{r}')}}{j\omega\mu_3 p_3}[(k_3^2-k_x^2)(\frac{N_{3x}}{D_x})-k_x^2p_3(\frac{N_{3z}^d}{D_xD_z})])$$

$$-\frac{L_{xx}\,\delta(\mathbf{r}-\mathbf{r}')}{k_3^2}$$

$$= P.V.\frac{1}{(2\pi)^2}\int\int_{-\infty}^{\infty}\tilde{g}_{xx}^{3,3}e^{j\mathbf{k}\cdot\mathbf{r}}d^2k-\frac{L_{xx}\,\delta(\mathbf{r}-\mathbf{r}')}{k_3^2} \tag{2.6.2.8}$$

$$g_{yx}^{3,3} = \frac{\partial^2}{\partial y\,\partial x}G_{xx}^{3,3}+\frac{\partial^2}{\partial y\,\partial z}G_{zx}^{3,3}$$

$$= \frac{1}{(2\pi)^2}\int\int_{-\infty}^{\infty} d^2k\frac{e^{j\mathbf{k}\cdot(\mathbf{r}-\mathbf{r}')}}{j\omega\mu_3 p_3}[-k_x k_y(\frac{N_{3x}}{D_x})-k_x k_y p_3(\frac{N_{3z}^d}{D_x D_z})]$$

$$= \frac{1}{(2\pi)^2}\int\int_{-\infty}^{\infty} \tilde{g}_{yx}^{3,3}e^{j\mathbf{k}\cdot\mathbf{r}}d^2k \tag{2.6.2.9}$$

$$g_{zx}^{3,3} = \frac{\partial^2}{\partial z\,\partial x}G_{xx}^{3,3}+\frac{\partial^2}{\partial z^2}G_{zx}^{3,3}$$

$$= \frac{1}{(2\pi)^2}\int\int_{-\infty}^{\infty} d^2k\frac{e^{j\mathbf{k}\cdot(\mathbf{r}-\mathbf{r}')}}{j\omega\mu_3 p_3}[jk_x p_3\frac{N_{3x}^d}{D_x}+p_3^2\frac{N_{3z}}{D_x D_z}]$$

$$= \frac{1}{(2\pi)^2}\int\int_{-\infty}^{\infty} \tilde{g}_{zx}^{3,3}e^{j\mathbf{k}\cdot\mathbf{r}}d^2k \tag{2.6.2.10}$$

$$g_{xx}^{1,3} = (k_1^2+\frac{\partial^2}{\partial x^2})G_{xx}^{1,3}+\frac{\partial^2}{\partial x\,\partial z}G_{zx}^{1,3}$$

$$= \frac{1}{(2\pi)^2}\int\int_{-\infty}^{\infty} d^2k\frac{e^{j\mathbf{k}\cdot(\mathbf{r}-\mathbf{r}')}}{j\omega\mu_3 p_3}[(k_3^2-k_x^2)(\frac{N_{1x}}{D_x})-k_x^2 p_3(\frac{N_{1z}^d}{D_x D_z})]$$

$$= \frac{1}{(2\pi)^2}\int\int_{-\infty}^{\infty} \tilde{g}_{xx}^{1,3}e^{j\mathbf{k}\cdot\mathbf{r}}d^2k \tag{2.6.2.11}$$

$$g_{yx}^{1,3} = \frac{\partial^2}{\partial y\,\partial x}G_{xx}^{1,3}+\frac{\partial^2}{\partial y\,\partial z}G_{zx}^{1,3}$$

$$= \frac{1}{(2\pi)^2}\int\int_{-\infty}^{\infty} d^2k\frac{e^{j\mathbf{k}\cdot(\mathbf{r}-\mathbf{r}')}}{j\omega\mu_3 p_3}[-k_x k_y(\frac{N_{1x}}{D_x})-k_x k_y p_3(\frac{N_{1z}^d}{D_x D_z})]$$

$$= \frac{1}{(2\pi)^2}\int\int_{-\infty}^{\infty} \tilde{g}_{yx}^{1,3}e^{j\mathbf{k}\cdot\mathbf{r}}d^2k \tag{2.6.2.12}$$

$$g_{zx}^{1,3} = \frac{\partial^2}{\partial z\,\partial x}G_{xx}^{1,3}+\frac{\partial^2}{\partial z^2}G_{zx}^{1,3}$$

$$= \frac{1}{(2\pi)^2}\int\int_{-\infty}^{\infty} d^2k\frac{e^{j\mathbf{k}\cdot(\mathbf{r}-\mathbf{r}')}}{j\omega\mu_3 p_3}[jk_x p_3\frac{N_{1x}^d}{D_x}+p_3^2\frac{N_{1z}}{D_x D_z}]$$

$$= \frac{1}{(2\pi)^2}\int\int_{-\infty}^{\infty} \tilde{g}_{zx}^{1,3} e^{j\mathbf{k}\cdot\mathbf{r}} d^2k \tag{2.6.2.13}$$

$$g_{xx}^{4,4} = P.V.(k_4^2 + \frac{\partial^2}{\partial x^2})G_{xx}^{4,4} - \frac{L_{xx}\delta(\mathbf{r}-\mathbf{r}')}{k_4^2}$$

$$= P.V.\frac{1}{(2\pi)^2}\int\int_{-\infty}^{\infty} d^2k \frac{e^{j\mathbf{k}\cdot(\mathbf{r}-\mathbf{r}')}}{j\omega\mu_4 p_4}(k_3^2 - k_x^2) - \frac{L_{xx}\delta(\mathbf{r}-\mathbf{r}')}{k_4^2}$$

$$= \frac{1}{(2\pi)^2}\int\int_{-\infty}^{\infty} \tilde{g}_{xx}^{4,4} e^{j\mathbf{k}\cdot\mathbf{r}} d^2k - \frac{L_{xx}\delta(\mathbf{r}-\mathbf{r}')}{k_4^2} \tag{2.6.2.14}$$

$$g_{yx}^{4,4} = \frac{\partial^2}{\partial y\,\partial x}G_{xx}^{4,4}$$

$$= \frac{1}{(2\pi)^2}\int\int_{-\infty}^{\infty} d^2k \frac{e^{j\mathbf{k}\cdot(\mathbf{r}-\mathbf{r}')}}{j\omega\mu_4 p_4}(-k_x k_y)$$

$$= \frac{1}{(2\pi)^2}\int\int_{-\infty}^{\infty} \tilde{g}_{yx}^{4,4} e^{j\mathbf{k}\cdot\mathbf{r}} d^2k \tag{2.6.2.15}$$

$$g_{zx}^{4,4} = \frac{\partial^2}{\partial z\,\partial x}G_{xx}^{4,4}$$

$$= \frac{1}{(2\pi)^2}\int\int_{-\infty}^{\infty} d^2k \frac{e^{j\mathbf{k}\cdot(\mathbf{r}-\mathbf{r}')}}{j\omega\mu_4 p_4}(jk_x p_3)$$

$$= \frac{1}{(2\pi)^2}\int\int_{-\infty}^{\infty} \tilde{g}_{zx}^{4,4} e^{j\mathbf{k}\cdot\mathbf{r}} d^2k \tag{2.6.2.16}$$

where

$$\tilde{g}_{xx}^{3,3}(\mathbf{r}',\mathbf{k}) = \frac{1}{j\omega\mu_3 p_3}[(k_3^2 - k_x^2)(\frac{N_{3x}}{D_x}) - k_x^2 p_3(\frac{N_{3z}^d}{D_x D_z})]e^{-j\mathbf{k}\cdot\mathbf{r}'} \tag{2.6.2.17}$$

$$\tilde{g}_{yx}^{3,3}(\mathbf{r}',\mathbf{k}) = \frac{1}{j\omega\mu_3 p_3}[-k_x k_y(\frac{N_{3x}}{D_x}) - k_x k_y p_3(\frac{N_{3z}^d}{D_x D_z})]e^{-j\mathbf{k}\cdot\mathbf{r}'} \tag{2.6.2.18}$$

$$\tilde{g}_{zx}^{3,3}(\mathbf{r}',\mathbf{k}) = \frac{1}{j\omega\mu_3 p_3}[jk_x p_3(\frac{N_{3x}^d}{D_x}) + p_3^2(\frac{N_{3z}}{D_x D_z})]e^{-j\mathbf{k}\cdot\mathbf{r}'} \tag{2.6.2.19}$$

$$\tilde{g}_{xx}^{1,3}(\mathbf{r}',\mathbf{k}) = \frac{1}{j\omega\mu_3 p_3}[(k_1^2-k_x^2)(\frac{N_{1x}}{D_x})-k_x^2 p_3(\frac{N_{1z}^d}{D_x D_z})]e^{-j\mathbf{k}\cdot\mathbf{r}'} \tag{2.6.2.20}$$

$$\tilde{g}_{yx}^{1,3}(\mathbf{r}',\mathbf{k}) = \frac{1}{j\omega\mu_3 p_3}[-k_x k_y(\frac{N_{1x}}{D_x})-k_x k_y p_3(\frac{N_{1z}^d}{D_x D_z})]e^{-j\mathbf{k}\cdot\mathbf{r}'} \tag{2.6.2.21}$$

$$\tilde{g}_{zx}^{1,3}(\mathbf{r}',\mathbf{k}) = \frac{1}{j\omega\mu_3 p_3}[jk_x p_3(\frac{N_{1x}^d}{D_x})+p_3^2(\frac{N_{1z}}{D_x D_z})]e^{-j\mathbf{k}\cdot\mathbf{r}'} \tag{2.6.2.22}$$

$$\tilde{g}_{xx}^{4,4}(\mathbf{r}',\mathbf{k}) = \frac{1}{j\omega\mu_4 p_4}(k_4^2-k_x^2)e^{-j\mathbf{k}\cdot\mathbf{r}'} \tag{2.6.2.23}$$

$$\tilde{g}_{yx}^{4,4}(\mathbf{r}',\mathbf{k}) = \frac{1}{j\omega\mu_4 p_4}(-k_x k_y)e^{-j\mathbf{k}\cdot\mathbf{r}'} \tag{2.6.2.24}$$

$$\tilde{g}_{zx}^{4,4}(\mathbf{r}',\mathbf{k}) = \frac{1}{j\omega\mu_4 p_4}(jk_x p_4)e^{-j\mathbf{k}\cdot\mathbf{r}'} \tag{2.6.2.25}$$

$$N_{3x}^d(z,\mathbf{k}) \equiv \frac{\partial}{\partial z}N_{3x}(z,\mathbf{k}) \tag{2.6.2.26}$$

$$= p_3\{-[(\varepsilon_1 p_2+\varepsilon_2 p_1)(\varepsilon_2 p_3+\varepsilon_3 p_2)+(\varepsilon_1 p_2-\varepsilon_2 p_1)(\varepsilon_2 p_3-\varepsilon_3 p_2)e^{-2p_2 t}]e^{-p_3 z}$$

$$+ [(\varepsilon_1 p_2+\varepsilon_2 p_1)(\varepsilon_2 p_3-\varepsilon_3 p_2)+(\varepsilon_1 p_2-\varepsilon_2 p_1)(\varepsilon_2 p_3+\varepsilon_3 p_2)e^{-2p_2 t}]e^{-2p_3 d}e^{p_3 z}\}$$

$$N_{3z}^d(z,\mathbf{k}) \equiv \frac{\partial}{\partial z}N_{3z}(z,\mathbf{k}) \tag{2.6.2.27}$$

$$= 2e^{-2p_3 d}p_3^2\{(\varepsilon_3\mu_3-\varepsilon_2\mu_2)[\mu_1 p_2(1+e^{-2p_2 t})+\mu_2 p_1(1-e^{-2p_2 t})]$$

$$[\varepsilon_1 p_2(1+e^{-2p_2 t})+\varepsilon_2 p_1(1-e^{-2p_2 t})]+4(\varepsilon_2\mu_2-\varepsilon_1\mu_1)\varepsilon_3\mu_3 e^{-2p_2 t}p_2^2\}(e^{p_3 z}+e^{-p_3 z})$$

$$N_{1x}^d(z,\mathbf{k}) \equiv \frac{\partial}{\partial z}N_{1x}(z,\mathbf{k}) \tag{2.6.2.28}$$

$$= -4\varepsilon_2\varepsilon_3\mu_{31}p_1 p_2 p_3 e^{-(p_2-p_1)t}e^{-(p_3-p_1)d}e^{-p_1 z}$$

$$N^{d}_{1z}(z,\mathbf{k}) \equiv \frac{\partial}{\partial z} N_{1z}(z,\mathbf{k}) \tag{2.6.2.29}$$

$$= -4\mu_{31}p_1p_2p_3e^{-(p_2-p_1)t}e^{-(p_3-p_1)d}[(1+e^{-2p_2t})(1-e^{-2p_3d})(\varepsilon_3\mu_3-\varepsilon_1\mu_1)\varepsilon_2\mu_2p_2$$

$$+ (1-e^{-2p_2t})(1+e^{-2p_3d})(\varepsilon_2\mu_2-\varepsilon_1\mu_1)\varepsilon_3\mu_2p_3$$

$$+ (1-e^{-2p_2t})(1-e^{-2p_3d})(\varepsilon_3\mu_3-\varepsilon_2\mu_2)\varepsilon_2\mu_1p_1]e^{-p_1z}$$

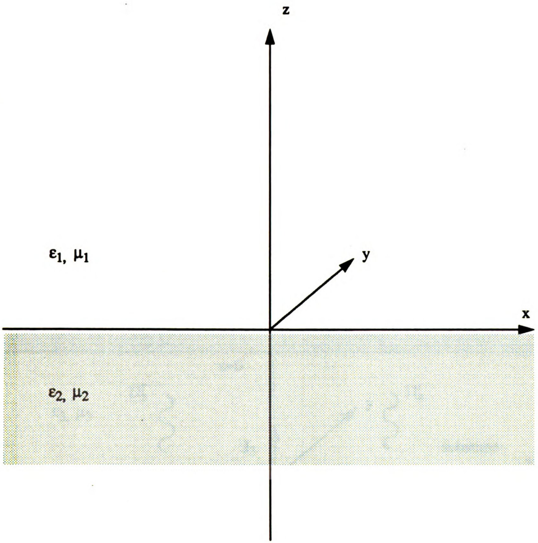

Figure 2.1 Hertzian potential boundary conditions at interface

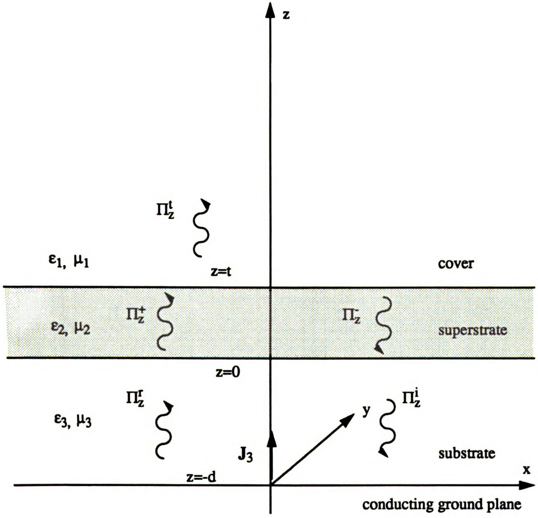

Figure 2.2 Hertzian potentials generated by vertical electric current.

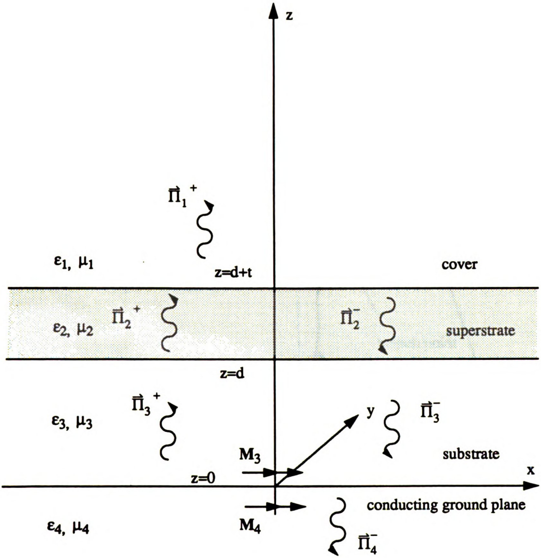

Figure 2.3 Hertzian potentials generated by horizontal magnetic current.

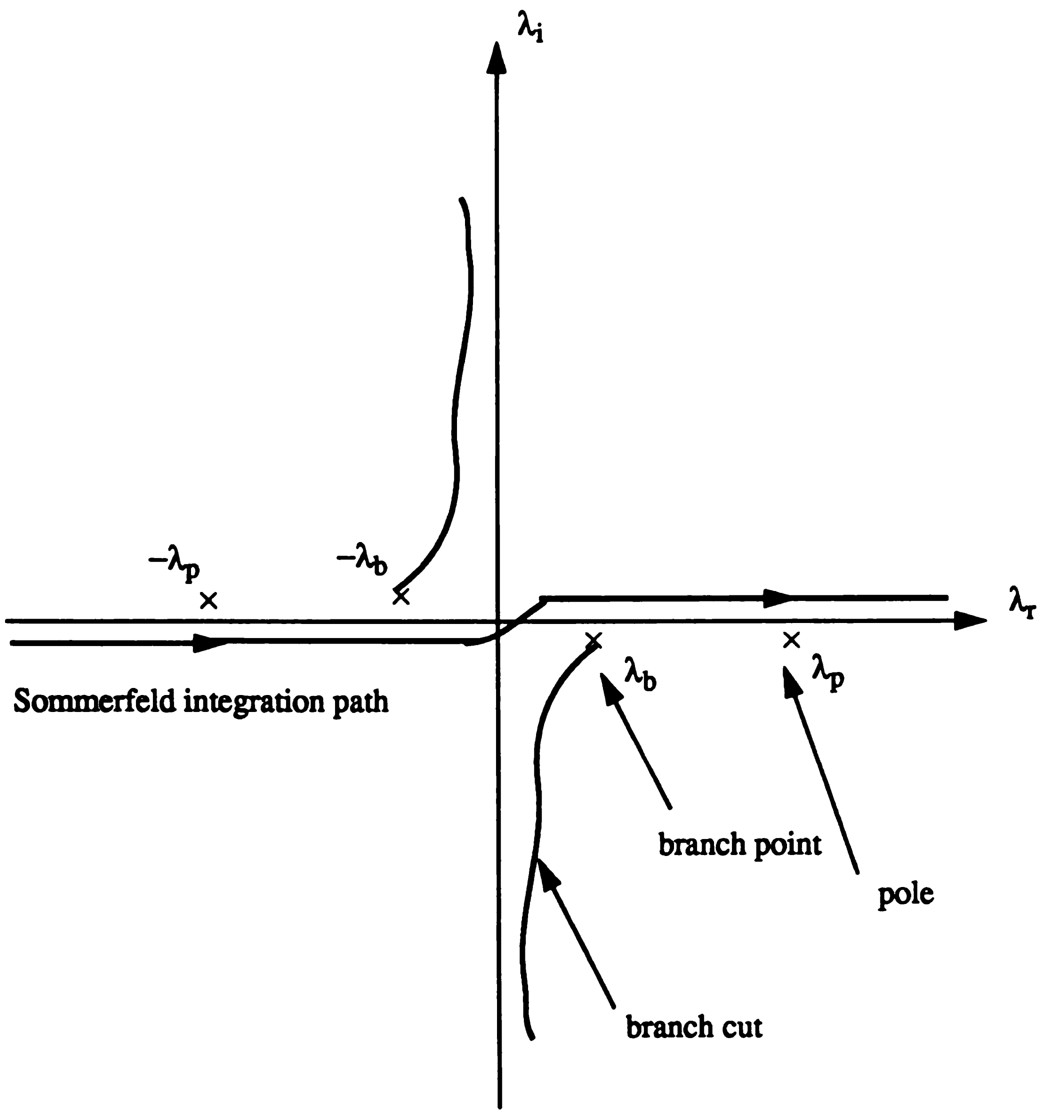

Figure 2.4 Sommerfeld integration path in the complex λ plane

CHAPTER THREE
PLANE WAVE PROPAGATION IN TRI-LAYERED MEDIA

Plane wave propagation in layered media is very different from that in free space. In order to know the excitation field on a antenna in tri-layered media due to a plane wave illumination, it is necessary to study the transmission and reflection of a plane wave in the tri-layered media.

Consider a plane wave illuminating a lossy layer above a ground plane with the wave vector making an angle θ_0 with the z-axis, as shown in Figure 3.1. A general incident plane wave can be decomposed into a TE wave and a TM wave. A TE wave is defined as a wave with the electric field normal to the plane of incidence, which is taken to be the y-z plane without loss of generality. A TM wave is defined as a wave with the electric field lying in the plane of incidence. The cases of TE wave and TM waves will be treated separately.

3.1 TM Plane Wave Propagation in Tri-layered Media

The incident magnetic field is given by

$$\mathbf{H}_1^i = \hat{x} H_{1x}^i e^{-j\mathbf{k}_1^i \cdot \mathbf{r}} \tag{3.1.1}$$

where

$$\mathbf{k}_1^i = (-\hat{y}\sin\theta_0 - \hat{z}\cos\theta_0)k_1 \tag{3.1.2}$$

The magnetic fields in each of the regions 1-3 can be written in terms of plane wave terms similar to (3.1) representing waves traveling in either the +z or -z direction. The total field in region 1 is composed of the incident wave $\mathbf{H}_1^i$ plus a reflected wave $\mathbf{H}_1^+$, while the field in region 2 is made up of a transmitted wave $\mathbf{H}_2^-$ and a reflected wave $\mathbf{H}_2^+$, and the field in region 3 is composed of a transmitted wave $\mathbf{H}_3^-$

$$\mathbf{H}_i^{\gamma} = \hat{x}H_{ix}^{\gamma}e^{-j\mathbf{k}_i^{\gamma}\cdot\mathbf{r}} \qquad i = 1,2,3; \;\; \gamma = +,- \tag{3.1.3}$$

where

$$k^2 = k_y^2 + k_z^2$$

$$\begin{aligned}(k_1^i)^2 &= (k_1^+)^2 = \omega^2\mu_1\varepsilon_1 = k_1^2 \\ (k_2^+)^2 &= (k_2^-)^2 = \omega^2\mu_2\varepsilon_2 = k_2^2 \\ (k_3^-)^2 &= (k_3^+)^2 = \omega^2\mu_3\varepsilon_3 = k_3^2\end{aligned} \tag{3.1.4}$$

It is understood that $\mathbf{H}_1^i = \mathbf{H}_1^-$ and $\mathbf{k}_1^i = \mathbf{k}_1^-$.

$\mathbf{H}_1^i$ is assumed to be a known quantity, while $\mathbf{H}_1^+, \mathbf{H}_2^+, \mathbf{H}_2^-, \mathbf{H}_3^+$, and $\mathbf{H}_3^-$ are to be determined by applying appropriate boundary conditions on $\mathbf{E}$ and $\mathbf{H}$ at each of the interfaces. The electric field in each region can be obtained via using the Maxwell's equation:

$$\mathbf{E} = \frac{1}{j\omega\varepsilon}\nabla\times\mathbf{H} \tag{3.1.5}$$

The electromagnetic fields in the three regions can be expressed as:

Region 1

$$\mathbf{H}_1 = \mathbf{H}_1^i + \mathbf{H}_1^+ = \hat{x}[H_{1x}^i e^{-j\mathbf{k}_1^i\cdot\mathbf{r}} + H_{1x}^+ e^{-j\mathbf{k}_1^+\cdot\mathbf{r}}] \tag{3.1.6}$$

$$\mathbf{E}_1 = \frac{1}{\omega\varepsilon_1}[(\hat{z}k_{1y}^i - \hat{y}k_{1z}^i)H_{1x}^i e^{-j\mathbf{k}_1^i\cdot\mathbf{r}} + (\hat{z}k_{1y}^+ - \hat{y}k_{1z}^+)H_{1x}^+ e^{-j\mathbf{k}_1^+\cdot\mathbf{r}}] \tag{3.1.7}$$

Region 2

$$\mathbf{H}_2 = \mathbf{H}_2^+ + \mathbf{H}_2^- = \hat{x}[H_{2x}^+ e^{-j\mathbf{k}_2^+\cdot\mathbf{r}} + H_{2x}^- e^{-j\mathbf{k}_2^-\cdot\mathbf{r}}] \tag{3.1.8}$$

$$\mathbf{E}_2 = \frac{1}{\omega\varepsilon_2}[(\hat{z}k_{2y}^+ - \hat{y}k_{2z}^+)H_{2x}^+ e^{-j\mathbf{k}_2^+\cdot\mathbf{r}} + (\hat{z}k_{2y}^- - \hat{y}k_{2z}^-)H_{2x}^- e^{-j\mathbf{k}_2^-\cdot\mathbf{r}}] \tag{3.1.9}$$

Region 3

$$\mathbf{H}_3 = \mathbf{H}_3^- + \mathbf{H}_3^+ = \hat{x}[H_{3x}^- e^{-j\mathbf{k}_3^-\cdot\mathbf{r}} + H_{3x}^+ e^{-j\mathbf{k}_3^+\cdot\mathbf{r}}] \tag{3.1.10}$$

$$\mathbf{E}_3 = \frac{1}{\omega\varepsilon_3}[(\hat{z}k_{3y}^- - \hat{y}k_{3z}^-)H_{3x}^- e^{-j\mathbf{k}_3^-\cdot\mathbf{r}} + (\hat{z}k_{3y}^+ - \hat{y}k_{3z}^+)H_{3x}^+ e^{-j\mathbf{k}_3^+\cdot\mathbf{r}}] \tag{3.1.11}$$

Applying the boundary conditions on the tangential **E** and **H** at each of the three interfaces requires immediately

$$k_y = k_{1y}^i = k_{1y}^+ = k_{2y}^+ = k_{2y}^- = k_{3y}^- = k_{3y}^+ = -k_1\sin\theta_0 \tag{3.1.12}$$

for continuity of the phase terms. With this relationship established, the boundary conditions can be written as:

B.C. 1: $\mathbf{H}_{tan}$ continuous at $z=z_1$. ($H_{1x} = H_{2x}$).

$$H_{1x}^i e^{-jk_{1z}^i z_1} + H_{1x}^+ e^{-jk_{1z}^+ z_1} = H_{2x}^+ e^{-jk_{2z}^+ z_1} + H_{2x}^- e^{-jk_{2z}^- z_1} \tag{3.1.13}$$

B.C. 2: $\mathbf{E}_{tan}$ continuous at $z=z_1$. ($E_{1y} = E_{2y}$).

$$\frac{k_{1z}^i}{\varepsilon_1}H_{1x}^i e^{-jk_{1z}^i z_1} + \frac{k_{1z}^+}{\varepsilon_1}H_{1x}^+ e^{-jk_{1z}^+ z_1} = \frac{k_{2z}^-}{\varepsilon_2}H_{2x}^- e^{-jk_{2z}^- z_1} + \frac{k_{2z}^+}{\varepsilon_2}H_{2x}^+ e^{-jk_{2z}^+ z_1} \tag{3.1.14}$$

B.C. 3: $\mathbf{H}_{tan}$ continuous at $z=z_2$. ($H_{2x} = H_{3x}$).

$$H_{2x}^- e^{-jk_{2z}^- z_2} + H_{2x}^+ e^{-jk_{2z}^+ z_2} = H_{3x}^- e^{-jk_{3z}^- z_2} + H_{3x}^+ e^{-jk_{3z}^+ z_2} \tag{3.1.15}$$

B.C. 4: $\mathbf{E}_{tan}$ continuous at $z=z_2$. ($E_{2y} = E_{3y}$).

$$\frac{k_{2z}^-}{\varepsilon_2}H_{2x}^- e^{-jk_{2z}^- z_2} + \frac{k_{2z}^+}{\varepsilon_2}H_{2x}^+ e^{-jk_{2z}^+ z_2} = \frac{k_{3z}^-}{\varepsilon_3}H_{3x}^- e^{-jk_{3z}^- z_2} + \frac{k_{3z}^+}{\varepsilon_3}H_{3x}^+ e^{-jk_{3z}^+ z_2} \tag{3.1.16}$$

B.C. 5: $E_{tan} = 0$ at $z=z_3$. ($E_{3y} = 0$)

$$k_{3z}^- H_{3x}^- e^{-jk_{3z}^- z_3} + k_{3z}^+ H_{3x}^+ e^{-jk_{3z}^+ z_3} = 0 \tag{3.1.17}$$

Note that through (3.1.4) and (3.1.12) there exists a relationship between k_z and k_y in each region. However, care must be taken to choose the sign on the square root terms to make each wave decay as it propagates. In general

$$k_z = \pm\sqrt{k^2 - k_y^2} \tag{3.1.18}$$

Thus, assuming region 1 to be lossless, the sign on the square root must be chosen such that

$$\begin{aligned}
&\mathrm{Re}\{k_{1z}^{+}\} > 0 \\
&\mathrm{Re}\{k_{2z}^{-}\} < 0 \quad \mathrm{Im}\{k_{2z}^{-}\} > 0 \\
&\mathrm{Re}\{k_{2z}^{+}\} > 0 \quad \mathrm{Im}\{k_{2z}^{+}\} < 0 \\
&\mathrm{Re}\{k_{3z}^{-}\} < 0 \quad \mathrm{Im}\{k_{3z}^{-}\} > 0 \\
&\mathrm{Re}\{k_{3z}^{+}\} > 0 \quad \mathrm{Im}\{k_{3z}^{+}\} < 0
\end{aligned} \tag{3.1.19}$$

giving

$$\begin{aligned}
k_{1z}^{+} &= -k_{1z}^{i} = \sqrt{k_1^2 - k_1^2 \sin^2\theta_0} \\
k_{2z}^{+} &= -k_{2z}^{-} = \sqrt{k_2^2 - k_1^2 \sin^2\theta_0} \\
k_{3z}^{+} &= -k_{3z}^{-} = \sqrt{k_3^2 - k_1^2 \sin^2\theta_0}
\end{aligned} \tag{3.1.20}$$

Remember that in a lossy region, the wave number k is complex, due to the complex permittivity and permeability,

$$\varepsilon = \varepsilon' - j\varepsilon'' = \varepsilon_0[\varepsilon_r - j\frac{\sigma}{\omega\varepsilon_0}] \tag{3.1.21}$$

$$\mu = \mu' - j\mu'' \tag{3.1.22}$$

To formulate the integral equation for the monopole current or the slot current, the incident fields in region 3 need to be determined. Thus, equations (3.1.13)-(3.1.17) must be solved for H_{3x}^{+} and H_{3x}^{-} in terms of the known quantity H_{1x}^{i} . Using (3.1.20), these can be solved as follows. From equation (3.1.17)

$$H_{3x}^{+} = H_{3x}^{-} e^{-j2k_{3z}^{-}z_3} \tag{3.1.23}$$

Substituting (3.1.23) into (3.1.16) gives

$$H_{2x}^{+} e^{jk_{2z}^{-}z_2} - H_{2x}^{-} e^{-jk_{2z}^{-}z_2} + AH_{3x}^{-}[e^{-jk_{3z}^{-}z_2} - e^{-j2k_{3z}^{-}z_3} e^{jk_{3z}^{-}z_2}] = 0 \tag{3.1.24}$$

where

$$A \equiv \frac{\varepsilon_2 k^-_{3z}}{\varepsilon_3 k^-_{2z}} . \tag{3.1.25}$$

Next, substituting (3.1.23) into (3.1.15) gives

$$H^+_{2x} e^{jk^-_{2z} z_2} + H^-_{2x} e^{-jk^-_{2z} z_2} - H^-_{3x} [e^{-jk^-_{3z} z_2} + e^{-j2k^-_{3z} z_3} e^{jk^-_{3z} z_2}] = 0 . \tag{3.1.26}$$

For simplicity, (3.1.24) and (3.1.26) can be rewritten as

$$H^+_{2x} e^{jk^-_{2z} z_2} - H^-_{2x} e^{-jk^-_{2z} z_2} - H^-_{3x} P = 0 \tag{3.1.27}$$

$$H^+_{2x} e^{jk^-_{2z} z_2} + H^-_{2x} e^{-jk^-_{2z} z_2} - H^-_{3x} Q = 0 \tag{3.1.28}$$

where

$$P \equiv A [e^{-j2k^-_{3z} z_3} e^{jk^-_{3z} z_2} - e^{-jk^-_{3z} z_2}] \tag{3.1.29}$$

$$Q \equiv [e^{-j2k^-_{3z} z_3} e^{jk^-_{3z} z_2} + e^{-jk^-_{3z} z_2}] . \tag{3.1.30}$$

Now, adding (3.1.27) and (3.1.28) gives

$$2H^+_{2x} e^{jk^-_{2z} z_2} = (P+Q) H^-_{3x} \tag{3.1.31}$$

or

$$H^+_{2x} = Z H^-_{3x} \tag{3.1.32}$$

where

$$Z \equiv \frac{Q+P}{2e^{jk^-_{2z} z_2}} . \tag{3.1.33}$$

Also, subtracting (3.1.28) from (3.1.27) gives

$$H^-_{2x} = Y H^-_{3x} \tag{3.1.34}$$

where

$$Y \equiv \frac{Q-P}{2e^{-jk^-_{2z} z_2}} . \tag{3.1.35}$$

Next, rewrite (3.1.13) as

$$-e^{2jk_{1z}^i z_1} H_{1x}^+ + e^+ H_{2x}^+ + e^- H_{2x}^- = H_{1x}^i \tag{3.1.36}$$

and (3.1.14) as

$$e^{2jk_{1z}^i z_1} H_{1x}^+ - Be^+ H_{2x}^+ + Be^- H_{2x}^- = H_{1x}^i \tag{3.1.37}$$

where

$$e^{\pm} \equiv e^{j(k_{1z}^i \pm k_{2z}^-)z_1} \tag{3.1.38}$$

$$B \equiv \frac{\varepsilon_1 k_{2z}^-}{\varepsilon_2 k_{1z}^i} \ . \tag{3.1.39}$$

Now, substituting (3.1.32) and (3.1.34) into (3.1.36) gives

$$-H_{1x}^+ e^{2jk_{1z}^i z_1} + e^+ Z H_{3x}^- + e^- Y H_{3x}^- = H_{1x}^i \tag{3.1.40}$$

and into (3.1.37) gives

$$H_{1x}^+ e^{2jk_{1z}^i z_1} - Be^+ Z H_{3x}^- + Be^- Y H_{3x}^- = H_{1x}^i \tag{3.1.41}$$

Adding (3.1.40) and (3.1.41) gives

$$H_{3x}^- [Ze^+(1-B) + Ye^-(1+B)] = 2H_{1x}^i \tag{3.1.42}$$

Equations (3.1.23) and (3.1.42) give the transmission coefficients.

$$T^- \equiv \frac{H_{3x}^-}{H_{1x}^i} = \frac{2}{Ze^+(1-B) + Ye^-(1+B)} \tag{3.1.43}$$

$$T^+ \equiv \frac{H_{3x}^+}{H_{1x}^i} = T^- e^{-j2k_{3z}^- z_3} \tag{3.1.44}$$

Knowing transmission coefficients T^+ and T^- , it is possible to calculate the electric field in region 3. From (3.1.11), the z component of the electric field can be expressed as

$$E_{3z} = \frac{k_{3y}^{-}}{\omega\epsilon_3}[H_{3x}^{-}e^{-j\mathbf{k}_3^{-}\cdot\mathbf{r}}+H_{3x}^{+}e^{-j\mathbf{k}_3^{+}\cdot\mathbf{r}}] . \tag{3.1.45}$$

Substituting (3.1.43) and (3.1.44) into (3.1.45) gives

$$E_{3z} = \frac{k_{3y}^{-}}{\omega\epsilon_3}[T^{-}H_{1x}^{i}e^{-j\mathbf{k}_3^{-}\cdot\mathbf{r}}+T^{+}H_{1x}^{i}e^{-j\mathbf{k}_3^{+}\cdot\mathbf{r}}] . \tag{3.1.46}$$

The field along the z axis becomes

$$E_{3z}(\mathbf{r}=\hat{z}z) = \frac{k_{3y}^{-}}{\omega\epsilon_3}T^{-}H_{1x}^{i}[e^{-jk_{3z}^{-}z}+e^{-j2k_{3z}^{-}z_3}e^{+jk_{3z}^{-}z}] . \tag{3.1.47}$$

Finally, from (3.1.2), (3.1.12) and using $\omega\epsilon_3 = \frac{k_3}{\eta_3}$ and $\eta_3 = \sqrt{\frac{\mu_3}{\epsilon_3}}$

$$E_{3z} = -\frac{k_1}{k_3}\eta_3 H_{1x}^{i}T^{-}\sin\theta_0 2e^{-jk_{3z}^{-}z_3}\cos[k_{3z}^{-}(z-z_3)]$$

$$= W\cos[\sqrt{k_3^2-k_1^2\sin^2\theta_0}\,(z-z_3)] \tag{3.1.48}$$

where

$$W = -2\,\frac{k_1}{k_3}\eta_3 H_{1x}^{i}T^{-}\sin\theta_0 e^{-jk_{3z}^{-}z_3} .$$

Also from (3.1.11) and (3.1.20)

$$E_{3y} = -\frac{k_{3z}^{-}}{\omega\epsilon_3}[H_{3x}^{-}e^{-j\mathbf{k}_3^{-}\cdot\mathbf{r}}-H_{3x}^{+}e^{-j\mathbf{k}_3^{+}\cdot\mathbf{r}}] \tag{3.1.49}$$

Substituting (3.1.43-44) into (3.1.49) gives

$$E_{3y} = -\frac{k_{3z}^{-}}{\omega\epsilon_3}H_{1x}^{i}[T^{-}e^{-j\mathbf{k}_3^{-}\cdot\mathbf{r}}-T^{+}e^{-j\mathbf{k}_3^{+}\cdot\mathbf{r}}] . \tag{3.1.50}$$

Then, substituting (3.1.20) and (3.1.43-44) into (3.1.10) gives the horizontal magnetic field in region 3.

$$H_{3x} = H^i_{1x} e^{-jk_y y} T^- (e^{-jk^-_{3z} z} + e^{-j2k^-_{3z} z_3} e^{jk^-_{3z} z}) \,. \tag{3.1.51}$$

On the ground plane $z=z_3$, the magnetic field can be written as

$$H_{3x}(z=z_3) = 2H^i_{1x} e^{-jk_y y} T^- e^{-jk^-_{3z} z_3} \tag{3.1.52}$$

The important results are summarized and renumbered for convenient use later.

$$E_{3z}(\mathbf{r}) = W cos\,[\sqrt{k_3^2 - k_1^2 \sin^2\theta_0}\,(z - z_3)] \;\;;\;\; x=0 \,,\, y=0 \tag{3.1.53}$$

$$W = -2\,\frac{k_1}{k_3}\sqrt{\frac{\mu_3}{\varepsilon_3}} H^i_{1x} T^- \sin\theta_0 e^{-jk^-_{3z} z_3} \tag{3.1.54}$$

$$H_{3x}(\mathbf{r}) = 2H^i_{1x} e^{-jk_y y} T^- e^{-jk^-_{3z} z_3} \;\;;\;\; z=z_3 \tag{3.1.55}$$

$$T^- \equiv \frac{H^-_{3x}}{H^i_{1x}} = \frac{2}{Ze^+(1-B) + Ye^-(1+B)} \tag{3.1.56}$$

$$Z = \frac{Q+P}{2e^{jk^-_{2z} z_2}} \tag{3.1.57}$$

$$Y = \frac{Q-P}{2e^{-jk^-_{2z} z_2}} \tag{3.1.58}$$

$$P = A\,[e^{-j2k^-_{3z} z_3} e^{jk^-_{3z} z_2} - e^{-jk^-_{3z} z_2}] \tag{3.1.59}$$

$$Q = [e^{-j2k^-_{3z} z_3} e^{jk^-_{3z} z_2} + e^{-jk^-_{3z} z_2}] \tag{3.1.60}$$

$$e^\pm \equiv e^{j(k^i_{1z} \pm k^-_{2z}) z_1} \tag{3.1.61}$$

$$A = \frac{\varepsilon_2 k^-_{3z}}{\varepsilon_3 k^-_{2z}} \tag{3.1.62}$$

$$B = \frac{\varepsilon_1 k^-_{2z}}{\varepsilon_2 k^i_{1z}} \tag{3.1.63}$$

$$k_y = k^i_{1y} = k^+_{1y} = k^+_{2y} = k^-_{2y} = k^-_{3y} = k^+_{3y} = -k_1 \sin\theta_0 \tag{3.1.64}$$

$$k^i_{1z} = -\sqrt{k_1^2 - k_1^2 \sin^2\theta_0} \tag{3.1.65}$$

$$k_{2z}^{-} = -\sqrt{k_2^2 - k_1^2 \sin^2\theta_0} \tag{3.1.66}$$

$$k_{3z}^{-} = -\sqrt{k_3^2 - k_1^2 \sin^2\theta_0} \tag{3.1.67}$$

3.2 TE Plane Wave Propagation in Tri-layered Media

The incident electric field is given by

$$\mathbf{E}_1^i = \hat{x} E_{1x}^i e^{-j\mathbf{k}_1^i \cdot \mathbf{r}} \tag{3.2.1}$$

where

$$\mathbf{k}_1^i = (-\hat{y}\sin\theta_0 - \hat{z}\cos\theta_0) k_1 \tag{3.2.2}$$

The electric fields in each of the regions 1-3 can be written in terms of plane wave terms similar to (3.2.1) representing waves traveling in either +z or -z direction. The total field in region 1 is composed of the incident wave $\mathbf{E}_1^i$ plus a reflected wave $\mathbf{E}_1^+$, while the field in region 2 is made up of a transmitted wave $\mathbf{E}_2^-$ and a reflected wave $\mathbf{E}_2^+$, and the field in region 3 is composed of a transmitted wave $\mathbf{E}_3^-$ and a reflected wave $\mathbf{E}_3^+$. All of these terms can be written in generic form as

$$\mathbf{E}_i^{\gamma} = \hat{x} E_{ix}^{\gamma} e^{-j\mathbf{k}_i^{\gamma} \cdot \mathbf{r}} \qquad i = 1,2,3; \;\; \gamma = +,- \tag{3.2.3}$$

where

$$k^2 = k_y^2 + k_z^2$$

$$\begin{aligned} (k_1^i)^2 &= (k_1^+)^2 = \omega^2 \mu_1 \varepsilon_1 = k_1^2 \\ (k_2^+)^2 &= (k_2^-)^2 = \omega^2 \mu_2 \varepsilon_2 = k_2^2 \\ (k_3^-)^2 &= (k_3^+)^2 = \omega^2 \mu_3 \varepsilon_3 = k_3^2 \; . \end{aligned} \tag{3.2.4}$$

It is understood that $\mathbf{E}_1^i = \mathbf{E}_1^-$ and $\mathbf{k}_1^i = \mathbf{k}_1^-$.

$\mathbf{E}_1^i$ is a known quantity, while $\mathbf{E}_1^+, \mathbf{E}_2^+, \mathbf{E}_2^-, \mathbf{E}_3^+$, and $\mathbf{E}_3^-$ are to be determined by applying appropriate boundary conditions on $\mathbf{E}$ and $\mathbf{H}$ at each of the interfaces. The magnetic field in each region can be obtained by using the Maxwell's equation:

$$\mathbf{H} = \frac{1}{-j\omega\mu}\nabla\times\mathbf{E} \ . \tag{3.2.5}$$

The electromagnetic fields in the three regions can be expressed as:

Region 1

$$\mathbf{E}_1 = \mathbf{E}_1^i+\mathbf{E}_1^+ = \hat{x}\,[E_{1x}^i e^{-j\mathbf{k}_1^i\cdot\mathbf{r}}+E_{1x}^+ e^{-j\mathbf{k}_1^+\cdot\mathbf{r}}] \tag{3.2.6}$$

$$\mathbf{H}_1 = \frac{1}{-\omega\mu_1}[(\hat{z}k_{1y}^i-\hat{y}k_{1z}^i)E_{1x}^i e^{-j\mathbf{k}_1^i\cdot\mathbf{r}}+(\hat{z}k_{1y}^+-\hat{y}k_{1z}^+)E_{1x}^+ e^{-j\mathbf{k}_1^+\cdot\mathbf{r}}] \tag{3.2.7}$$

Region 2

$$\mathbf{E}_2 = \mathbf{E}_2^++\mathbf{E}_2^- = \hat{x}\,[E_{2x}^+ e^{-j\mathbf{k}_2^+\cdot\mathbf{r}}+E_{2x}^- e^{-j\mathbf{k}_2^-\cdot\mathbf{r}}] \tag{3.2.8}$$

$$\mathbf{H}_2 = \frac{1}{-\omega\mu_2}[(\hat{z}k_{2y}^+-\hat{y}k_{2z}^+)E_{2x}^+ e^{-j\mathbf{k}_2^+\cdot\mathbf{r}}+(\hat{z}k_{2y}^--\hat{y}k_{2z}^-)E_{2x}^- e^{-j\mathbf{k}_2^-\cdot\mathbf{r}}] \tag{3.2.9}$$

Region 3

$$\mathbf{E}_3 = \mathbf{E}_3^-+\mathbf{E}_3^+ = \hat{x}\,[E_{3x}^- e^{-j\mathbf{k}_3^-\cdot\mathbf{r}}+E_{3x}^+ e^{-j\mathbf{k}_3^+\cdot\mathbf{r}}] \tag{3.2.10}$$

$$\mathbf{H}_3 = \frac{1}{-\omega\mu_3}[(\hat{z}k_{3y}^--\hat{y}k_{3z}^-)E_{3x}^- e^{-j\mathbf{k}_3^-\cdot\mathbf{r}}+(\hat{z}k_{3y}^+-\hat{y}k_{3z}^+)E_{3x}^+ e^{-j\mathbf{k}_3^+\cdot\mathbf{r}}] \tag{3.2.11}$$

Applying the boundary conditions on the tangential $\mathbf{E}$ and $\mathbf{H}$ at each of the three interfaces requires immediately

$$k_{1y}^i = k_{1y}^+ = k_{2y}^+ = k_{2y}^- = k_{3y}^- = k_{3y}^+ = -k_1\sin\theta_0 \tag{3.2.12}$$

for continuity of the phase terms. With this relationship established, the boundary conditions can be written as

B.C. 1: $\mathbf{E}_{tan}$ continuous at $z=z_1$. ($E_{1x} = E_{2x}$).

$$E^i_{1x}e^{-jk^i_{1z}z_1}+E^+_{1x}e^{-jk^+_{1z}z_1} = E^+_{2x}e^{-jk^+_{2z}z_1}+E^-_{2x}e^{-jk^-_{2z}z_1} \tag{3.2.13}$$

B.C. 2: $\mathbf{H}_{tan}$ continuous at $z=z_1$. ($H_{1y} = H_{2y}$).

$$\frac{k^i_{1z}}{\mu_1}E^i_{1x}e^{-jk^i_{1z}z_1}+\frac{k^+_{1z}}{\mu_1}E^+_{1x}e^{-jk^+_{1z}z_1} = \frac{k^-_{2z}}{\mu_2}E^-_{2x}e^{-jk^-_{2z}z_1}+\frac{k^+_{2z}}{\mu_2}E^+_{2x}e^{-jk^+_{2z}z_1} \tag{3.2.14}$$

B.C. 3: $\mathbf{E}_{tan}$ continuous at $z=z_2$. ($E_{2x} = E_{3x}$).

$$E^-_{2x}e^{-jk^-_{2z}z_2}+E^+_{2x}e^{-jk^+_{2z}z_2} = E^-_{3x}e^{-jk^-_{3z}z_2}+E^+_{3x}e^{-jk^+_{3z}z_2} \tag{3.2.15}$$

B.C. 4: $\mathbf{H}_{tan}$ continuous at $z=z_2$. ($H_{2y} = H_{3y}$).

$$\frac{k^-_{2z}}{\mu_2}E^-_{2x}e^{-jk^-_{2z}z_2}+\frac{k^+_{2z}}{\mu_2}E^+_{2x}e^{-jk^+_{2z}z_2} = \frac{k^-_{3z}}{\mu_3}E^-_{3x}e^{-jk^-_{3z}z_2}+\frac{k^+_{3z}}{\mu_3}E^+_{3x}e^{-jk^+_{3z}z_2} \tag{3.2.16}$$

B.C. 5: $\mathbf{E}_{tan} = 0$ at $z=z_3$. ($E_{3x} = 0$)

$$E^-_{3x}e^{-jk^-_{3z}z_3}+E^+_{3x}e^{-jk^+_{3z}z_3} = 0 \tag{3.2.17}$$

Note that through (3.2.4) and (3.2.12) there exists a relationship between k_z and k_y in each region. However, care must be taken to choose the sign on the square root terms to make each wave decay as it propagates. In general

$$k_z = \pm\sqrt{k^2-k_y^2} \tag{3.2.18}$$

Thus, assuming region 1 to be lossless, the sign on the square root must be chosen such that

$$\begin{aligned}
&\mathrm{Re}\{k^+_{1z}\} > 0 \\
&\mathrm{Re}\{k^-_{2z}\} < 0 \quad \mathrm{Im}\{k^-_{2z}\} > 0 \\
&\mathrm{Re}\{k^+_{2z}\} > 0 \quad \mathrm{Im}\{k^+_{2z}\} < 0 \\
&\mathrm{Re}\{k^-_{3z}\} < 0 \quad \mathrm{Im}\{k^-_{3z}\} > 0
\end{aligned} \tag{3.2.19}$$

$$\mathrm{Re}\{k_{3z}^{+}\} > 0 \quad \mathrm{Im}\{k_{3z}^{+}\} < 0$$

giving

$$\begin{aligned} k_{1z}^{+} &= -k_{1z}^{i} = \sqrt{k_1^2 - k_1^2 \sin^2\theta_0} \\ k_{2z}^{+} &= -k_{2z}^{-} = \sqrt{k_2^2 - k_1^2 \sin^2\theta_0} \\ k_{3z}^{+} &= -k_{3z}^{-} = \sqrt{k_3^2 - k_1^2 \sin^2\theta_0} \end{aligned} \tag{3.2.20}$$

Remember that in a lossy region, the wave number k is complex, due to the complex permittivity and permeability:

$$\varepsilon = \varepsilon' - j\varepsilon'' = \varepsilon_0[\varepsilon_r - j\frac{\sigma}{\omega\varepsilon_0}] \tag{3.2.21}$$

$$\mu = \mu' - j\mu'' \tag{3.2.22}$$

To formulate the integral equation for the monopole current or slot current, the incident fields in region 3 need to be determined. Thus, equations (3.2.13)-(3.2.17) must be solved for E_{3x}^{+} and E_{3x}^{-} in terms of the known quantity E_{1x}^{i} . Using (3.2.20), these can be solved as follows. From equation (3.2.17)

$$E_{3x}^{+} = -E_{3x}^{-} e^{-j2k_{3z}^{-} z_3} \tag{3.2.23}$$

Substituting (3.2.23) into (3.2.16) gives

$$E_{2x}^{+} e^{jk_{2z}^{-} z_2} - E_{2x}^{-} e^{-jk_{2z}^{-} z_2} + A' E_{3x}^{-} [e^{-jk_{3z}^{-} z_2} + e^{-j2k_{3z}^{-} z_3} e^{jk_{3z}^{-} z_2}] = 0 \tag{3.2.24}$$

where

$$A' \equiv \frac{\mu_2 k_{3z}^{-}}{\mu_3 k_{2z}^{-}} . \tag{3.2.25}$$

Next, substituting (3.2.23) into (3.2.15) gives

$$E_{2x}^{+} e^{jk_{2z}^{-} z_2} + E_{2x}^{-} e^{-jk_{2z}^{-} z_2} - E_{3x}^{-} [e^{-jk_{3z}^{-} z_2} - e^{-j2k_{3z}^{-} z_3} e^{jk_{3z}^{-} z_2}] = 0 . \tag{3.2.26}$$

For brevity and convenience, (3.1.24) and (3.1.26) can be rewritten as

$$E_{2x}^{+}e^{jk_{\bar{2}z}z_2}-E_{2x}^{-}e^{-jk_{\bar{2}z}z_2}-E_{3x}^{-}P' = 0 \tag{3.2.27}$$

$$E_{2x}^{+}e^{jk_{\bar{2}z}z_2}+E_{2x}^{-}e^{-jk_{\bar{2}z}z_2}-E_{3x}^{-}Q' = 0 \tag{3.2.28}$$

where

$$P' \equiv A'[e^{-j2k_{\bar{3}z}z_3}e^{jk_{\bar{3}z}z_2}+e^{-jk_{\bar{3}z}z_2}] \tag{3.1.29}$$

$$Q' \equiv [-e^{-j2k_{\bar{3}z}z_3}e^{jk_{\bar{3}z}z_2}+e^{-jk_{\bar{3}z}z_2}]\ . \tag{3.1.30}$$

Now, adding (3.2.27) and (3.2.28) gives

$$2E_{2x}^{+}e^{jk_{\bar{2}z}z_2} = (P'+Q')E_{3x}^{-} \tag{3.2.31}$$

or

$$E_{2x}^{+} = Z'E_{3x}^{-} \tag{3.2.32}$$

where

$$Z' \equiv \frac{Q'+P'}{2e^{jk_{\bar{2}z}z_2}}\ . \tag{3.2.33}$$

Also, subtracting (3.2.28) from (3.2.27) gives

$$E_{2x}^{-} = Y'E_{3x}^{-} \tag{3.2.34}$$

where

$$Y' \equiv \frac{Q'-P'}{2e^{-jk_{\bar{2}z}z_2}}\ . \tag{3.2.35}$$

Next, rewrite (3.2.13) and (3.2.14) as

$$-e^{2jk_{1z}^{i}z_1}E_{1x}^{+}+e^{+}E_{2x}^{+}+e^{-}E_{2x}^{-} = E_{1x}^{i} \tag{3.2.36}$$

$$e^{2jk_{1z}^{i}z_1}E_{1x}^{+}-B'e^{+}E_{2x}^{+}+B'e^{-}E_{2x}^{-} = E_{1x}^{i} \tag{3.2.37}$$

where

$$e^{\pm} \equiv e^{j(k^i_{1z} \pm k^-_{2z})z_1} \tag{3.2.38}$$

$$B' \equiv \frac{\mu_1 k^-_{2z}}{\mu_2 k^i_{1z}} \, . \tag{3.2.39}$$

Now, substituting (3.2.32) and (3.2.34) into (3.2.36) gives

$$-E^+_{1x} e^{2jk^i_{1z}z_1} + e^+ Z' E^-_{3x} + e^- Y' E^-_{3x} = E^i_{1x} \tag{3.2.40}$$

and into (3.2.37) gives

$$E^+_{1x} e^{2jk^i_{1z}z_1} - B' e^+ Z' E^-_{3x} + B' e^- Y' E^-_{3x} = E^i_{1x} \, . \tag{3.2.41}$$

Adding (3.2.40) and (3.2.41) gives

$$E^-_{3x}[Z' e^+(1-B') + Y' e^-(1+B')] = 2E^i_{1x} \, . \tag{3.1.42}$$

The transmission coefficients can be obtained from (3.2.23) and (3.2.42).

$$T^-_e \equiv \frac{E^-_{3x}}{E^i_{1x}} = \frac{2}{Z' e^+(1-B') + Y' e^-(1+B')} \tag{3.2.43}$$

$$T^+_e \equiv \frac{E^+_{3x}}{E^i_{1x}} = -T^-_e e^{-j2k^-_{3z}z_3} \tag{3.2.44}$$

Knowing transmission coefficients T^+_e and T^-_e, it is possible to calculate the EM fields in region 3. Substituting (3.2.20) and (3.2.43-44) into (3.2.10) gives the electric field in region 3.

$$E_{3x}(\mathbf{r}) = E^i_{1x} e^{-jk_y y} T^-_e (e^{-jk^-_{3z}z} - e^{-j2k^-_{3z}z_3} e^{jk^-_{3z}z}) \, . \tag{3.2.45}$$

Substituting (3.2.43) and (3.2.44) into (3.2.11) gives

$$H_{3z}(\mathbf{r}) = -\frac{k^-_{3y}}{\omega\mu_3}[T^-_e E^i_{1x} e^{-j\mathbf{k}^-_3\cdot\mathbf{r}} + T^+_e E^i_{1x} e^{-j\mathbf{k}^+_3\cdot\mathbf{r}}] \tag{3.2.46}$$

$$H_{3y}(\mathbf{r}) = \frac{k^-_{3z}}{\omega\mu_3} E^i_{1x}[T^-_e e^{-j\mathbf{k}^-_3\cdot\mathbf{r}} - T^+_e e^{-j\mathbf{k}^+_3\cdot\mathbf{r}}] \, . \tag{3.2.47}$$

Of particular interest is the tangential magnetic field on the ground plane, which can be written as

$$H_{3y}(z=z_3) = 2\frac{k_{3z}^{-}}{\omega\mu_3} E_{1x}^{i} T_e^{-} e^{-jk_y y} e^{-jk_{3z}^{-} z_3} \ . \tag{3.2.48}$$

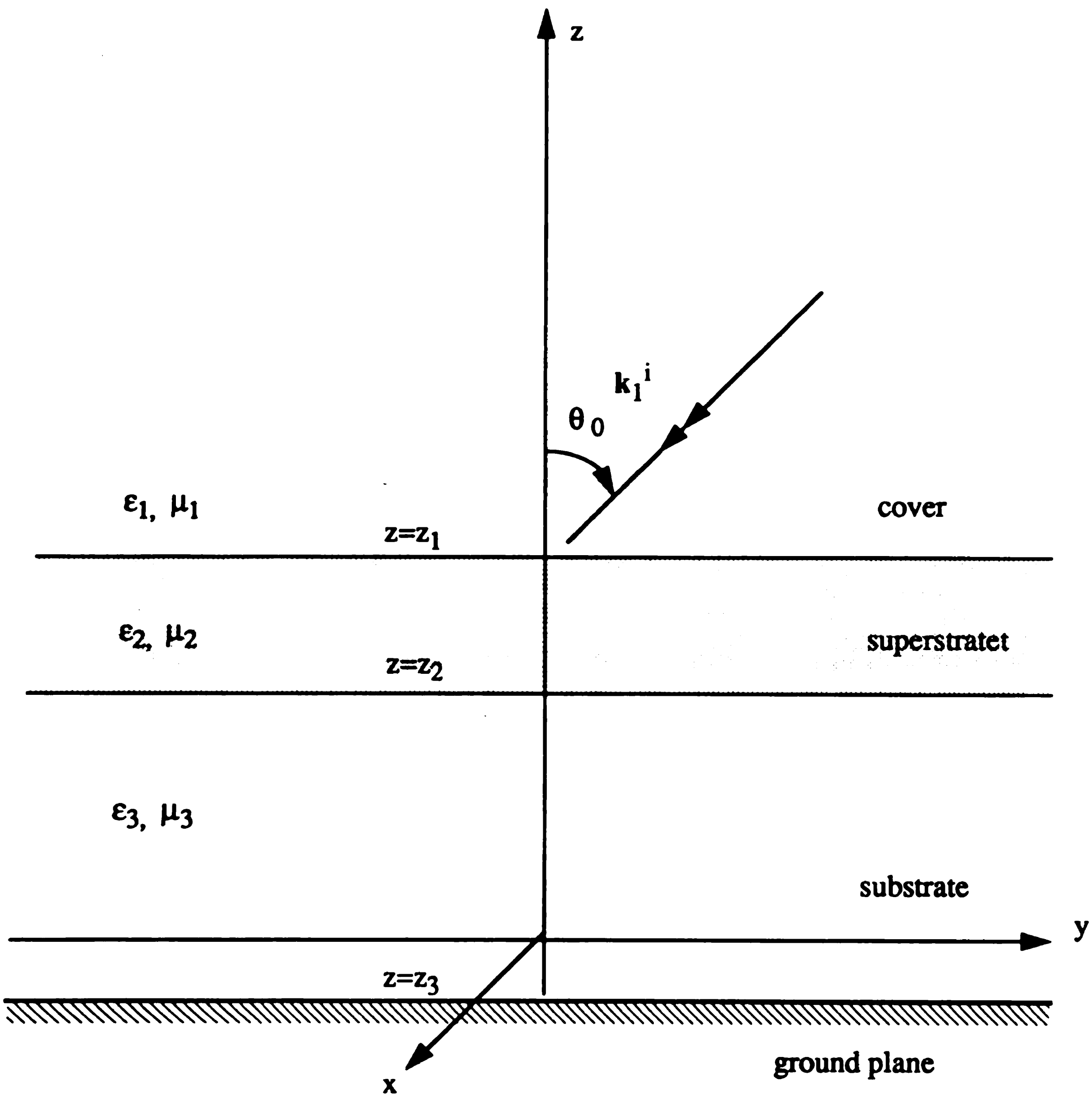

Figure 3.1 Plane wave propagation in tri-layered media

CHAPTER FOUR

FORMULATION OF INTEGRAL EQUATIONS

The dyadic Green's functions for the EM fields have been derived in chapter 2. Integral equations are obtained in this chapter by enforcing appropriate boundary conditions. The case of a monopole and that of a slot will be considered separately.

4.1 Integral Equations for a Monopole

Consider the imaged monopole beneath a lossy sheet as shown in Figure 1.1. When illuminated by a plane wave, a current will be induced on the monopole surface causing a voltage drop across the load resistance, and thus deliver power to the load. The current induced on the monopole surface will be solved by using superposition; the scattering mode current and transmitting mode current are found independently and then they are combined to get receiving mode current.

Throughout this dissertation the monopole is assumed to be a thin wire. That is, the radius is much smaller than a wavelength. Then, the monopole surface current distribution, I_z^3, can be assumed angularly invariant.

Electric field integral equations (EFIE) for the monopole current distribution when the antenna is acting as a scatterer and as a transmitter can be formulated by applying the boundary condition that the total electric field tangential to the surface must be zero:

$$E_z = E_z^s + E_z^i = 0 \qquad at\ \rho{=}a\,,\ -d \le z \le -d+h \tag{4.1.1}$$

or

$$E_z^s = -E_z^i \qquad at\ \rho{=}a\,,\ -d \le z \le -d+h\ .$$

Here E_z^s represents the scattered field maintained by the induced current, and E_z^i the impressed field due to either the incident wave in the scattering case, or the load voltage in the transmitting case.

In the scattering case, the impressed field is the incident electric field in the substrate. A TM incident plane wave is considered explicitly. A TE incident plane wave can be solved in a similar way. Comparing the coordinate system in Figure 3.1 with that in Figure 1.1 gives

$$z_1 = t \;;\; z_2 = 0 \;;\; z_3 = -d \;.$$

Substituting the above into (3.1.48) leads to

$$E_z^i = W\cos\left[k_{3z}^-(z+d)\right] \quad -d \le z \le -d+h \tag{4.1.2}$$

where

$$k_{3z}^- = \sqrt{k_3^2 - k_1^2 \sin^2\theta_0} \;.$$

This expression is derived in detail in section 1 of Chapter 3. Note that the quantity W depends on the incidence angle and incident field strength, as well as the thickness and the parameters (electric or magnetic) of the lossy layer. Also note that in (4.1.1), the impressed field on the surface of the thin wire is approximated to be the same as the field on the wire axis. This is a good approximation when the wire radius is much smaller than a wavelength.

In the transmitting case, the impressed field will be modeled using a delta function (slice-gap) generator

$$E_z^i = V_0 \delta(z+d) \tag{4.1.3}$$

where V_0 represents a voltage applied to the terminal region at z=-d.

The scattered field produced by the induced current on the monopole can be represented in terms of a scattered Hertzian potential Π_z^s . The axial component of the

Hertzian potential produced by an axial current is found using (2.6.1.7) as

$$E_z^s = k_3^2 \Pi_{3z} + \frac{\partial^2 \Pi_{3z}}{\partial z^2} \tag{4.1.4}$$

Substituting (4.1.4) into (4.1.1) yields an inhomogeneous ordinary differential equation (ODE)

$$\left(\frac{\partial^2}{\partial z^2} + k_3^2\right)\Pi_{3z}(z) = -E_z^i(z) \quad -d \le z \le -d+h \ . \tag{4.1.5}$$

The solution to the ODE takes on a slightly different form in the scattering and transmitting cases, so each case will be considered separately.

A) Transmitting case

Using (4.1.3) in (4.1.5), the ODE becomes

$$\left(\frac{\partial^2}{\partial z^2} + k_3^2\right)\Pi_{3z}(z) = -V_0 \delta(z+d) \tag{4.1.6}$$

which has the general solution [11],

$$\Pi_{3z}(z) = C_1 \sin k_3(z+d) + C_2 \cos k_3(z+d) - \frac{V_0}{2k_3}\sin k_3 |z+d| \tag{4.1.7}$$

where C_1 and C_2 are arbitrary constants. Now, because of the ground plane, currents on the monopole must image in the same direction. Therefore the current on the monopole is an even function about z=-d. Thus, the vertical electric field must be even, and because of the relationship (4.1.4) the potential $\Pi_{3z}(z)$ must be even. Thus, the first term in (4.1.7) is not implicated and the expression reduces to

$$\Pi_{3z}(z) = C_2 \cos k_3(z+d) - \frac{V_0}{2k_3}\sin k_3(z+d) \quad -d \le z \le -d+h \tag{4.1.8}$$

B) Scattering case

Substituting (4.1.2) into (4.1.5) leads to

$$\left(\frac{\partial^2}{\partial z^2} + k_3^2\right)\Pi_{3_z}(z) = -W\cos\left[k_{\bar{3_z}}(z+d)\right] \tag{4.1.9}$$

which has the solution [11]

$$\Pi_{3_z}(z) = C_1 \sin k_3(z+d) + C_2 \cos k_3(z+d) -$$

$$\frac{1}{k_3}\int_{-d}^{z} W\cos\left[k_{\bar{3_z}}(u+d)\right]\sin k_3(z-u)\,du \tag{4.1.10}$$

where C_1 and C_2 are constants. The integral term in (4.1.10) can be evaluated as follows. Let

$$U(z) = \int_{-d}^{z} \cos\left[k_{\bar{3_z}}(u+d)\right]\sin k_3(z-u)\,du \tag{4.1.11}$$

and use the change of variables

$$v = u+d\ . \tag{4.1.12}$$

Then

$$U(z) = \int_{0}^{z+d} \cos\left[k_{\bar{3_z}}v\right]\sin k_3(z+d-v)\,dv \tag{4.1.13}$$

Expanding the sine function gives

$$U(z) = \sin k_3(z+d)\int_{0}^{z+d} \cos\left[k_{\bar{3_z}}v\right]\cos k_3 v\,dv$$

$$+ \cos k_3(z+d)\int_{0}^{z+d} \cos\left[k_{\bar{3_z}}v\right]\sin k_3 v\,dv\ . \tag{4.1.14}$$

The integrals in (4.1.14) can be evaluated in a straight-forward manner. After a little algebraic manipulation the result becomes

$$U(z) = \frac{k_3(cos\,[\bar{k}_{3_z}(z+d)] - cos k_3(z+d))}{k_3^2 - \bar{k}_{3_z}^2} \tag{4.1.15}$$

Substituting (4.1.15) into (4.1.10), and again eliminating the first term due to symmetry, gives the solution to the ODE as

$$\Pi_{3_z}(z) = C_2 \cos k_3(z+d) - \frac{W}{k_3}\left[\frac{k_3(cos\,[\bar{k}_{3_z}(z+d)] - cos k_3(z+d))}{k_3^2 - \bar{k}_{3_z}^2}\right] \tag{4.1.16}$$

Upon substitution of (2.4.3.47) into (4.1.8) and (4.1.16), the integral equations for the monopole current $I_z^3(z)$ for the transmitting and scattering cases, respectively, are obtained.

a) transmitting case

$$\int_{-d}^{-d+h} G_{zz}^{3,3}(z,a,z')I_z^3(z')dz' = C cos k_3(z+d) - \frac{V_0}{2k_3}\sin k_3(z+d)$$

$$-d \le z \le -d+h \tag{4.1.17}$$

b) scattering case

$$\int_{-d}^{-d+h} G_{zz}^{3,3}(z,a,z')I_z^3(z')dz' = C cos k_3(z+d)$$

$$- \frac{W}{k_3}\left[\frac{k_3(cos\,[\bar{k}_{3_z}(z+d)] - cos k_3(z+d))}{k_3^2 - \bar{k}_{3_z}^2}\right] \quad -d \le z \le -d+h \tag{4.1.18}$$

Here, from (2.4.3.48)

$$G_{zz}^{3,3}(z,a,z') = \frac{1}{2\pi}\int_0^{\infty} \tilde{\Gamma}_{zz}^{3,3}(z,z',\lambda) J_0^2(\lambda a)\lambda d\lambda \tag{4.1.19}$$

where $\tilde{\Gamma}_{zz}^{3,3}(z,z',\lambda)$ is given in (2.4.3.46).

Equations (4.1.17) and (4.1.18) are Hallen-Type Integral Equations (HTIE). The EFIE is applicable to an arbitrary source and a wire of arbitrary shape while the HTIE is applicable to the special case of a one dimensional current and a straight thin wire. The advantage of the HTIE over EFIE is that its kernel is less singular than that of EFIE. This makes it numerically easier to solve.

4.2 Magnetic Field Integral Equation for a Slot

Consider a slot antenna in tri-layered media shown in figure 2.3. The receiving characteristics are determined by the receiving mode equivalent magnetic current on the slot. This receiving mode induced current can be solved by superposition. The scattering and transmitting modes are found independently and the results are combined to yield the receiving mode result.

Throughout the dissertation the slot is assumed to be a narrow one. That is, $l \gg w$ and $\lambda_0 \gg w$. A good approximation in the case of a narrow slot is $E_y \gg E_x$. In other words, the longitudinal aperture field component E_x can be ignored. To incorporate the well-known edge behavior of electric field, the aperture field E_y can be written as

$$E_y(x,y,z=0) = \frac{f(x)}{\sqrt{1-(\frac{y}{w})^2}} . \tag{4.2.1}$$

The equivalent magnetic currents on the slot in regions 3 and 4 can be written as

$$\mathbf{M}_3(x,y) = -\hat{z}\times\hat{y}E_y = \hat{x}\frac{f(x)}{\sqrt{1-(\frac{y}{w})^2}} = \mathbf{M}(x,y) \tag{4.2.2}$$

$$\mathbf{M}_4(x,y) = -(-\hat{z})\times\hat{y}E_y = -\mathbf{M}(x,y) \tag{4.2.3}$$

where

$$\mathbf{M}(x,y) = \hat{x} f(x) W(y) \tag{4.2.3}$$

$$W(y) = \frac{1}{\sqrt{1-(\frac{y}{w})^2}} \tag{4.2.4}$$

and f(x) is the unknown function to be determined.

With the help of dyadic Green's functions derived in chapter 2, the magnetic field in region i generated by a source in region j can be written as

$$\mathbf{H}_i(\mathbf{M}_j) = \int_{V_j} \overline{\overline{G}}^{i,j}(\mathbf{r}|\mathbf{r}')\cdot\mathbf{M}_j(\mathbf{r}')dv' \quad ; \quad i,j=1,2,3,4 \tag{4.2.5}$$

The boundary condition on tangential magnetic field is used to obtain the magnetic field integral equation (MFIE)

$$\hat{z}\times(\ \mathbf{H}_3^{tot}(\mathbf{M}_3)-\mathbf{H}_4^{tot}(\mathbf{M}_4)\ ) = \mathbf{K} \tag{4.2.6}$$

where $\mathbf{H}_3^{tot}(\mathbf{M}_3)$ and $\mathbf{H}_4^{tot}(\mathbf{M}_4)$ are the total magnetic fields in regions 3 and 4 respectively and **K** is surface electric current density in the aperture. In region 3, the total magnetic field is composed of a scattered field and an incident field. In region 4, the total magnetic field is just the scattered field. Using the results in chapter 2, the scattered field can be expressed in terms of Green's function and magnetic current.

Scattering case:

$$H_{3x}(\mathbf{M}) + H_{4x}(\mathbf{M}) = -H_x^{in} \tag{4.2.7}$$

Transmitting case:

$$H_{3x}(\mathbf{M}) + H_{4x}(\mathbf{M}) = K_y^e \tag{4.2.8}$$

The generic form of the MFIE can thus be written as

$$L(\mathbf{M}) = F \tag{4.2.9}$$

where L is the proper linear operator and F is the excitation term.

In this dissertation L is defined as

$$L(\hat{x}M_x) = \iint_{slot} [g_{xx}^{3,3}(\mathbf{r}|\mathbf{r}')+g_{xx}^{4,4}(\mathbf{r}|\mathbf{r}')]M_x(\rho')d^2\rho'$$

$$= \iint_{slot} \{\frac{1}{(2\pi)^2}\int_{\infty}^{-\infty}\int [\tilde{g}_{xx}^{3,3}(z\,|\mathbf{r}',\mathbf{k})+\tilde{g}_{xx}^{4,4}(z\,|\mathbf{r}',\mathbf{k})]e^{j\mathbf{k}\cdot\rho}d^2k\,\}M_x(\rho')d^2\rho' \tag{4.2.10}$$

where

$$\rho = \hat{x}x+\hat{y}y \tag{4.2.11}$$

$$d^2\rho = dxdy\ . \tag{4.2.12}$$

4.3 Hallen-Type Integral Equation for a Slot

The MFIE (4.2.9) has a highly singular kernel, which manifests as a slowly converging integral in the spectral domain. A magnetic dyadic Green's function in the magnetic source region is the dual of an electric dyadic Green's function in electric source region. It is well known that when the source point and the observation point coincide, special care must be taken to treat the singularity of the the dyadic Green's function. There have been extensive discussions on this subject [12]. One way to circumvent the singularity problem is to convert the MFIE into a Hallen-Type Integral Equation (HTIE). This conversion is possible if the source is one dimensional.

Substituting (2.6.2.2), (2.6.2.3-4) into (4.2.9) gives

$$(k_3^2+\frac{\partial^2}{\partial x^2})\iint_S G_{xx}^{3,3}(\mathbf{r}|\mathbf{r}')\mathbf{M}(\mathbf{r}')d^2r'+\frac{\partial^2}{\partial x\partial z}\iint_S G_{zx}^{3,3}(\mathbf{r}|\mathbf{r}')\mathbf{M}(\mathbf{r}')d^2r'$$

$$+(k_4^2+\frac{\partial^2}{\partial x^2})\iint_S G_{xx}^{4,4}(\mathbf{r}|\mathbf{r}')\mathbf{M}(\mathbf{r}')d^2r' = F(\mathbf{r}) \tag{4.3.1}$$

This is essentially a different form of MFIE. A discussion on the singularities of the Green's function can be found in [6]. The terms on the left hand side of (4.3.1) converge as improper integrals if $\mathbf{M}(\mathbf{r})$ satisfies the Holder's condition at $\mathbf{r}$, i.e., there exist positive constants c, A, and α such that

$$|\mathbf{M}(\mathbf{r})-\mathbf{M}(\mathbf{r}')| \le A\,|\mathbf{r}-\mathbf{r}'|^{\alpha} \quad \text{for} \quad |\mathbf{r}'-\mathbf{r}|<c \ . \tag{4.3.2}$$

$G_{xx}^{3,3}, G_{zx}^{3,3}, G_{xx}^{4,4}$ are given in (2.5.2.7), (2.5.2.9), and (2.5.2.13).

Define

$$\bar{G}_{zx}^{3,3} \equiv \frac{1}{(2\pi)^2}\int\int_{-\infty}^{\infty} d^2k \frac{e^{j\mathbf{k}\cdot(\mathbf{r}-\mathbf{r}')}}{j\omega\mu_3 p_3}\left(\frac{N_{3z}}{D_x D_z}\right) . \tag{4.3.3}$$

It can be seen by comparing (2.5.2.9) with (4.3.3) that

$$G_{zx}^{3,3} = \frac{\partial}{\partial x}\bar{G}_{zx}^{3,3} \ . \tag{4.3.4}$$

After adding a few terms and exchanging the order of integration and differentiation, (4.3.1) can be rewritten as

$$\left(k_s^2+\frac{\partial^2}{\partial x^2}\right)\iint_S G_L(\mathbf{r}|\mathbf{r}')M_x(\mathbf{r}')d^2r' = F(\mathbf{r})+\iint_S k_s^2 G_R(\mathbf{r}|\mathbf{r}')M_x(\mathbf{r}')d^2r' \tag{4.3.5}$$

where

$$k_s^2 \equiv k_3^2+k_4^2 \tag{4.3.6}$$

$$G_L = G_{xx}^{3,3}+G_{xx}^{4,4}+\frac{\partial \bar{G}_{zx}^{3,3}}{\partial z} \tag{4.3.7}$$

$$G_R = \frac{k_3^2}{k_s^2}G_{xx}^{4,4}+\frac{k_4^2}{k_s^2}G_{xx}^{3,3}+\frac{\partial \bar{G}_{zx}^{3,3}}{\partial z} \ . \tag{4.3.8}$$

Equation (4.3.5) is a differential-integral equation. Solving the ordinary differential equation first produces a Hallen-Type Integral Equation (HTIE). The steps are outlined in [48] and the result is

$$\iint_S G_L(\mathbf{r}|\mathbf{r}')M_x(\mathbf{r}')d^2r' = C_1\sin k_s x+C_2\cos k_s x+$$

$$\frac{1}{k_s}\int_{-\infty}^{\infty}\left[F(\mathbf{r})+\iint_S k_s^2 G_R(\mathbf{r}|\mathbf{r}')M_x(\mathbf{r}')d^2r'\right]\Big|_{x=x'}\sin k_s|x-x'|dx' \ . \tag{4.3.9}$$

Generally speaking C_1 and C_2 are two unknown functions of y. How to handle them will be discussed later. Define the operators

$$L_L(M_x) \equiv \iint_S G_L(\mathbf{r}|\mathbf{r}')M_x(\mathbf{r}')d^2r' \tag{4.3.10}$$

$$L_R(M_x) \equiv \iint_S G_R(\mathbf{r}|\mathbf{r}')M_x(\mathbf{r}')d^2r' \tag{4.3.11}$$

The HTIE (4.3.9) can then be rewritten as

$$L_L(M_x)-\frac{1}{k_s}\int_{-\infty}^{\infty} L_R(M_x)|_{x=x'}\sin k_s|x-x'|dx'$$

$$= C_1\sin k_s x + C_2\cos k_s x + \frac{1}{k_s}\int_{-\infty}^{\infty} F(\mathbf{r}')|_{x=x'}\sin k_s|x-x'|dx' . \tag{4.3.12}$$

Substituting (2.5.2.7), (2.5.2.13), and (4.3.3) into (4.3.7-8) gives

$$G_L = \frac{1}{(2\pi)^2}\iint_{-\infty}^{\infty} d^2k e^{j\mathbf{k}\cdot(\mathbf{r}-\mathbf{r}')}\Psi_L(\mathbf{k}) \tag{4.3.13}$$

$$G_R = \frac{1}{(2\pi)^2}\iint_{-\infty}^{\infty} d^2k e^{j\mathbf{k}\cdot(\mathbf{r}-\mathbf{r}')}\Psi_R(\mathbf{k}) \tag{4.3.14}$$

where

$$\Psi_L(\mathbf{k}) = \frac{N_{3x}}{j\omega\mu_3 p_3 D_x} + \frac{N_{3z}^d}{j\omega\mu_3 p_3 D_x D_z} + \frac{1}{j\omega\mu_4 p_4} \tag{4.3.15}$$

$$\Psi_R(\mathbf{k}) = \left(\frac{k_4}{k_s}\right)^2\frac{N_{3x}}{j\omega\mu_3 p_3 D_x} + \frac{N_{3z}^d}{j\omega\mu_3 p_3 D_x D_z} + \left(\frac{k_3}{k_s}\right)^2\frac{1}{j\omega\mu_4 p_4} \tag{4.3.16}$$

$$N_{3z}^d(\mathbf{k}) \equiv \frac{\partial}{\partial z}N_{3z}(z,\mathbf{k})|_{z=0} . \tag{4.3.17}$$

The right hand side of (4.3.12) can be written in a different form, which is more convenient to use [48]

$$L_L(M_x)-\frac{1}{k_s}\int_0^x L_R(M_x)|_{x=x'}\sin k_s(x-x')dx'$$

$$= C_1 \sin k_s x + C_2 \cos k_s x + \frac{1}{k_s} \int_0^x F(\mathbf{r}')|_{x=x'} \sin k_s (x - x') dx' . \qquad (4.3.18)$$

The kernel of HTIE (4.3.18) is less singular than that of MFIE (4.3.1), which means that it is easier to solve numerically. The price paid for the numerical stability is that the kernel of HTIE is more complicated than that of MFIE.

CHAPTER FIVE

SOLUTIONS OF INTEGRAL EQUATIONS

5.1 Method of Moments

Method of Moments is a general procedure to solve linear inhomogeneous functional equations [7]. The basic idea is to convert a functional equation to a matrix equation, and then to solve the matrix equation by known techniques. Consider the inhomogeneous equation

$$L(f) = g \tag{5.1.1}$$

where L is a linear operator, g is the source (known function), and f is the response (unknown function to be determined). Let f be expanded in a series of basis functions in the domain of L.

$$f = \sum_n a_n f_n \tag{5.1.2}$$

where a_n are expansion coefficients to be determined. Substituting (5.1.2) in (5.1.1) and using the linearity of L gives

$$\sum_n a_n L(f_n) = g \ . \tag{5.1.3}$$

Assume that a suitable inner product <f,g> has been determined for the problem. Define a set of testing functions w_m in the range of L. The functional equation (5.1.1) can be reduced to a matrix equation (5.1.4) by taking the inner product of (5.1.3) with w_m

$$[l_{mn}][a_n] = [g_m] \tag{5.1.4}$$

where

$$l_{mn} = <w_m, L(f_n)> \qquad (5.1.5)$$

$$g_m = <w_m, g> . \qquad (5.1.6)$$

The matrix equation (5.1.4) can be solved by known techniques to determine a_n. The particular choice $w_n = f_n$ is known as Galerkin's method.

5.2 Impedance Matrix for a Monopole

The integral equations (4.1.17) and (4.1.18) for the transmitting and scattering mode current distributions can be solved using the method of moments (MoM) with pulse function expansion and point matching.

Expand the current as

$$I_z^3(z) = \sum_{n=1}^{N} a_n P_n(z) \qquad -d \le z \le -d+h \qquad (5.2.1)$$

where

$$P_n(z) = \begin{cases} 1 & -d+(n-1)\Delta \le z \le -d+n\Delta \\ 0 & elsewhere \end{cases} \qquad (5.2.2)$$

is a rectangular pulse basis function, a_n is the set of unknown complex expansion coefficients, and

$$\Delta = \frac{h}{N} . \qquad (5.2.3)$$

Substituting (5.2.1) into (4.1.17) and (4.1.18) gives

$$\sum_{n=1}^{N} a_n \int_{-d+(n-1)\Delta}^{-d+n\Delta} G_{zz}^{3,3}(z,a,z')dz' = C\cos k_3(z+d) + u(z) \qquad -d \le z \le -d+h \qquad (5.2.4)$$

where

$$u(z) = \begin{cases} -\dfrac{V_0}{2k_3}\sin k_3(z+d) & \textit{transmitting case} \\[2ex] -\dfrac{W}{k_3}\left[\dfrac{k_3\,(\cos[\bar{k}_{3z}(z+d)] - \cos k_3(z+d))}{k_3^2 - \bar{k}_{3z}^2}\right] & \textit{scattering case} \end{cases} \tag{5.2.5}$$

A system of N equations for the N+1 unknowns a_n and C can be obtained by matching (4.1.4) at the N discrete points

$$z_m = -d + (m - \frac{1}{2})\Delta \quad m=1,2,\ldots,N \tag{5.2.6}$$

representing the centers of the pulse functions P_n. This gives

$$\sum_{n=1}^{N} a_n \int_{-d+(n-1)\Delta}^{-d+n\Delta} G_{zz}^{3,3}(z_m, a, z')dz' = C\cos k_3(z_m + d) + u(z_m) \quad m=1,2,..,N \tag{5.2.7}$$

An additional equation can be obtained by applying continuity of current at the tip of the monopole. Assuming that the monopole is a thin wire, the current should go to zero at the tip. Using (5.2.1), this implies

$$a_N = 0 \,. \tag{5.2.8}$$

With condition (5.2.8), (5.2.7) represent a system of N equations in the N unknowns $a_1, \ldots, a_{N-1}, C$. In terms of a matrix equation, (5.2.7) can be written as

$$\begin{bmatrix} A_{11} & A_{12} & \ldots & A_{1,N-1} & -\cos k_3\delta_1 \\ A_{21} & A_{22} & \ldots & A_{2,N-1} & -\cos k_3\delta_2 \\ \cdot & \cdot & \ldots & \cdot & \cdot \\ \cdot & \cdot & \ldots & \cdot & \cdot \\ \cdot & \cdot & \ldots & \cdot & \cdot \\ A_{N1} & A_{N2} & \cdots & A_{N,N-1} & -\cos k_3\delta_N \end{bmatrix} \begin{bmatrix} a_1 \\ a_2 \\ \cdot \\ \cdot \\ a_{N-1} \\ C \end{bmatrix} = \begin{bmatrix} u(z_1) \\ u(z_2) \\ \cdot \\ \cdot \\ \cdot \\ u(z_n) \end{bmatrix} \tag{5.2.9}$$

where

$$\delta_m = (m - \frac{1}{2})\Delta \tag{5.2.10}$$

with

$$A_{mn} = \int_{-d+(n-1)\Delta}^{-d+n\Delta} G_{zz}^{3,3}(z_m,a,z')dz' \quad n=1,2,\ldots,N-1, \;\; m=1,2,..,N \tag{5.2.11}$$

and

$$u(z_m) = \begin{cases} -\dfrac{V_0}{2k_3}\sin k_3\delta_m & \textit{transmitting case} \\ \quad\quad . & \\ -\dfrac{W}{k_3}\left[\dfrac{k_3\,(cos\,[k_{\bar{3}z}(\delta_m+d)]-\cos k_3(\delta_m+d))}{k_3^2-k_{\bar{3}z}^{\;2}}\right] & \textit{scattering case} \end{cases} \tag{5.2.12}$$

5.3 Calculation of Impedance Matrix Elements

Because of the simple dependence of the Green's function on z', the integral in the matrix entries (5.2.11) can be calculated in closed form. Substituting (2.4.3.48) into (5.2.11) allows the matrix entries to be written as

$$A_{mn} = \frac{1}{2\pi j\omega\varepsilon_3}\int_0^\infty I_{mn}(\lambda)J_0^2(a\lambda)\lambda d\lambda \tag{5.3.1}$$

where

$$I_{mn}(\lambda) = j\omega\varepsilon_3 \int_{-d+(n-1)\Delta}^{-d+n\Delta} \tilde{\Gamma}_{zz}^{3,3}(z_m,z',\lambda)dz' \,. \tag{5.3.2}$$

The integrals I_{mn} will be calculated based on the values of m and n.

A) m>n

In this case, $z>z'$ holds. Substituting (2.4.3.46) into (5.3.2) and using $z^>=z_m$ and $z^<=z'$ from (2.4.3.23), the integrals become

$$I_{mn}(\lambda) = \frac{1}{p_3}F(z_m)\int_{-d+(n-1)\Delta}^{-d+n\Delta} \cosh p_3(z'+d)dz' \,. \tag{5.3.3}$$

Evaluating the integral yields

$$I_{mn}(\lambda) = \frac{F(z_m)}{p_3^2}[\sinh p_3 n\Delta - \sinh p_3 (n-1)\Delta] \tag{5.3.4}$$

Using [53]

$$\sinh x - \sinh y = 2\cosh\frac{1}{2}(x+y)\,\sinh\frac{1}{2}(x-y) \tag{5.3.5}$$

then gives

$$I_{mn}(\lambda) = 2\frac{F(z_m)}{p_3^2}\cosh p_3 (n-\frac{1}{2})\Delta \sinh p_3 \frac{\Delta}{2}\ . \tag{5.3.6}$$

B) m<n

In this case $z<z'$ holds. Substituting (2.4.3.46) into (4.2.2), and using $z^> = z'$ and $z^< = z_m$ from (2.4.3.23), the integrals become

$$I_{mn}(\lambda) = \frac{\cosh p_3 (z_m+d)}{p_3}\int_{-d+(n-1)\Delta}^{-d+n\Delta} F(z')dz'\ . \tag{5.3.7}$$

Substituting (2.4.3.25-27) in (5.3.7) gives

$$I_{mn}(\lambda) = \frac{1}{p_3}\frac{\cosh p_3 (z_m+d)}{Q\sinh p_3 d + Z\cosh p_3 d}\int_{-d+(n-1)\Delta}^{-d+n\Delta} [Q\cosh p_3 z' - Z\sinh p_3 z']dz'\ . \tag{5.3.8}$$

Carrying out the integral in (5.3.8) and using (5.3.5) eventually leads to

$$I_{mn}(\lambda) = 2\frac{F(z_n)}{p_3^2}\cosh p_3 (m-\frac{1}{2})\Delta \sinh p_3 \frac{\Delta}{2}\ . \tag{5.3.9}$$

Comparing (5.3.6) and (5.3.9) shows

$$I_{mn} = I_{nm}\ . \tag{5.3.10}$$

C) m=n

In this case $z>z'$ for the lower half of the domain of integration, and $z<z'$ for the upper half. Thus it is necessary to split the integrals into two pieces. Using (2.4.3.46) in (5.3.2) gives

$$I_{nn} = \frac{1}{p_3}\{F(z_n) \int_{-d+(n-1)\Delta}^{-d+(n-\frac{1}{2})\Delta} \cosh p_3(z'+d)dz' +$$

$$\frac{\cosh p_3(z_n+d)}{Q\sinh p_3 d+Z\cosh p_3 d} \int_{-d+(n-\frac{1}{2})\Delta}^{-d+n\Delta} [Q\cosh p_3 z'-Z\sinh p_3 z']dz'\} . \qquad (5.3.11)$$

Evaluating these integrals yields

$$I_{nn} = \frac{1}{p_3^2}\{2F(z_n)\cosh p_3(n-\frac{3}{4})\Delta\sinh p_3\frac{\Delta}{4} +$$

$$2F(z_n+\frac{\Delta}{4})\cosh p_3(n-\frac{1}{2})\Delta\sinh p_3\frac{\Delta}{4}\} . \qquad (5.3.12)$$

Substitution of (5.3.9) and (5.3.12) in (5.3.1) gives the impedance matrix entries. In their present form, however, involving hyperbolic sine and cosine functions, these entries are prone to numerical difficulty. As the integration variable in (5.3.1) increases toward infinity, both the sinh and cosh functions overflow. In addition, it is very difficult to ascertain the convergence properties of the integral. Both of these problems can be overcome if the integrand is written in terms of exponentials. This is done as follows.

A) m>n

Equation (5.3.6) can be written in terms of exponentials as follows. From (2.4.3.25-27) and (5.2.10)

$$F(z_m) = \frac{\frac{Q}{Z}\cosh p_3(-d+\delta_m)-\sinh p_3(-d+\delta_m)}{\frac{Q}{Z}\sinh p_3 d+\cosh p_3 d} . \qquad (5.3.13)$$

By the definition of hyperbolic sine and cosine functions in terms of exponentials, this becomes

$$F(z_m) = e^{-p_3\delta_m} \frac{\frac{Q}{Z}[1+e^{-2p_3(d-\delta_m)}]+[1-e^{-2p_3(d-\delta_m)}]}{\frac{Q}{Z}[1-e^{-2p_3d}]+[1+e^{-2p_3d}]} \ . \tag{5.3.14}$$

Here the quantity $\frac{Q}{Z}$ can be written using (2.4.3.26) and (2.4.3.27) as

$$\frac{Q}{Z} = \left(\frac{p_3\varepsilon_2}{p_2\varepsilon_3}\right) \frac{\varepsilon_1 p_2[1+e^{-2p_2t}]+\varepsilon_2 p_1[1-e^{-2p_2t}]}{\varepsilon_1 p_2[1-e^{-2p_2t}]+\varepsilon_2 p_1[1+e^{-2p_2t}]} \tag{5.3.15}$$

Also needed in (5.3.6) is the quantity

$$\cosh p_3\delta_n \sinh p_3\frac{\Delta}{2} = \frac{1}{4}e^{p_3\delta_n}e^{p_3\frac{\Delta}{2}}[1+e^{-2p_3\delta_n}][1-e^{-p_3\Delta}] \ . \tag{5.3.16}$$

Substituting (5.3.14) and (5.3.16) into (5.3.6) gives

$$I_{mn} = \frac{1}{2p_3^2}[1+e^{-2p_3\delta_n}][1-e^{-p_3\Delta}]e^{-p_3(\delta_m-\delta_n-\frac{\Delta}{2})}$$

$$\times \frac{\frac{Q}{Z}[1+e^{-2p_3(d-\delta_m)}]+[1-e^{-2p_3(d-\delta_m)}]}{D} \tag{5.3.17}$$

where

$$D = \frac{Q}{Z}[1-e^{-2p_3d}] + [1+e^{-2p_3d}] \ . \tag{5.3.18}$$

Multiplying the exponentials together and using (5.2.10) gives

$$I_{mn} = \frac{1}{2p_3^2D}[1-e^{-p_3\Delta}]\{[e^{-p_3[(m-n)\Delta-\frac{\Delta}{2}]}+e^{-p_3[(m+n)\Delta-\frac{3\Delta}{2}]}$$

$$-e^{-p_3[2d-(m-n)\Delta-\frac{\Delta}{2}]}-e^{-p_3[2d-(m+n)\Delta-\frac{3\Delta}{2}]}]+\frac{Q}{Z}[e^{-p_3[(m-n)\Delta-\frac{\Delta}{2}]}$$

$$+e^{-p_3[(m+n)\Delta-\frac{3\Delta}{2}]}+e^{-p_3[2d-(m-n)\Delta-\frac{\Delta}{2}]}+e^{-p_3[2d-(m+n)\Delta-\frac{3\Delta}{2}]}]\} \ . \tag{5.3.19}$$

This expression can be written more compactly by letting

$$e_1(k) = e^{-p_3(k\Delta-\frac{\Delta}{2})} \tag{5.3.20}$$

$$e_2(k) = e^{-p_3(2d-k\Delta-\frac{\Delta}{2})} \tag{5.3.21}$$

Then

$$I_{mn} = \frac{1}{2p_3^2D}\{\frac{Q}{Z}[e_1(m-n)+e_2(m-n)]+[e_1(m-n)-e_2(m-n)] +$$

$$\frac{Q}{Z}[e_1(m+n-1)+e_2(m+n-1)]+[e_1(m+n-1)-e_2(m+n-1)]\} \ . \tag{5.3.22}$$

Thus, letting

$$f(k) = \frac{Q}{Z}[e_1(k)+e_2(k)]+[e_1(k)-e_2(k)] \tag{5.3.23}$$

gives

$$I_{mn} = \frac{1}{2p_3^2D}[1-e^{-p_3\Delta}][f(m+n-1)+f(m-n)] \ . \tag{5.3.24}$$

Using the form of the integrand given in (5.3.24) allows a dramatic reduction in the amount of effort needed to fill the moment method matrix. Letting

$$A(k) = \frac{1}{2\pi j\omega\varepsilon_3}\int_o^\infty \frac{1}{2p_3^2D}[1-e^{-p_3\Delta}]f(k)J_0^2(\lambda a)\lambda d\lambda \qquad 2\le k\le 2N-1 \tag{5.3.25}$$

allows the matrix entries (5.3.1) to be written as

$$A_{mn} = A(m+n-1) + A(m-n) \qquad m>n \ . \tag{5.3.26}$$

Thus, only 2N-2 integral evaluations are needed for $m\neq n$, as opposed to the N(N-1)/2 which would be required if (5.3.6) were used. This is a reduction in computational effort by a factor of N/4.

Note that each of the exponential terms involved in calculating the integrand of (5.3.25) go to zero as the integration variable $\lambda \rightarrow \infty$, since $\mathrm{Re}\{p_3\} \rightarrow \infty$ from (2.3.17). Thus, each of the integrals converge exponentially for $m \neq n$, and little difficulty is anticipated in their numerical computation.

B) m<n

In this case, equation (5.3.10) still holds.

C) m=n

Equation (5.3.12) can be written in terms of exponentials as follows.

$$I_{nn} = \frac{1}{p_3^2}[U+V] \tag{5.3.27}$$

where

$$U = 2F(z_n)\cosh p_3(n-\frac{\Delta}{4})\sinh p_3\frac{\Delta}{4} \tag{5.3.28}$$

$$V = 2F(z_n+\frac{\Delta}{4})\cosh p_3\delta_n \sinh p_3\frac{\Delta}{4} \ . \tag{5.3.29}$$

Substituting the definitions of sinh and cosh, and using (5.3.14) gives

$$U = \frac{1}{2}[1+e^{-2p_3(\delta_n-\frac{\Delta}{4})}][1-e^{-p_3\frac{\Delta}{2}}]\frac{\frac{Q}{Z}[1+e^{-2p_3(d-\delta_n)}]+[1-e^{-2p_3(d-\delta_n)}]}{\frac{Q}{Z}[1-e^{-2p_3d}]+[1+e^{-2p_3d}]} \ . \tag{5.3.30}$$

Similarly, (5.3.29) becomes

$$V = \frac{1}{2}[1+e^{-2p_3\delta_n}][1-e^{-p_3\frac{\Delta}{2}}]\frac{\frac{Q}{Z}[1+e^{-2p_3(d-\delta_n-\frac{\Delta}{4})}]+[1-e^{-2p_3(d-\delta_n-\frac{\Delta}{4})}]}{\frac{Q}{Z}[1-e^{-2p_3d}]+[1+e^{-2p_3d}]} \ . \tag{5.3.31}$$

The entries in the MoM matrix determined in this section are summaried and renumbered below for convenience.

A) m>n

$$A_{mn} = A(m+n-1) + A(m-n) \tag{5.3.32}$$

$$A(k) = \frac{1}{2\pi j\omega\varepsilon_3}\int_0^\infty \frac{1}{2p_3^2}\frac{1-e^{-p_3\Delta}}{D}f(k)J_0^2(a\lambda)\lambda d\lambda \tag{5.3.33}$$

$$f(k) = \frac{Q}{Z}[e_1(k)+e_2(k)]+[e_1(k)-e_2(k)] \tag{5.3.34}$$

$$e_1(k) = e^{-p_3(k\Delta-\frac{\Delta}{2})} \tag{5.3.35}$$

$$e_2(k) = e^{-p_3(2d-k\Delta-\frac{\Delta}{2})} \tag{5.3.36}$$

B) m<n

$$I_{nm} = I_{mn} \tag{5.3.37}$$

C) m=n

$$A_{nn} = \frac{1}{2\pi j\omega\varepsilon_3}\int_0^\infty I_{nn}J_0^2(a\lambda)\lambda d\lambda \tag{5.3.38}$$

$$I_{nn} = \frac{1}{2p_3^2}[1+e^{-2p_3(\delta_n-\frac{\Delta}{4})}][1-e^{-p_3\frac{\Delta}{2}}]\frac{\frac{Q}{Z}[1+e^{-2p_3(d-\delta_n)}]+[1-e^{-2p_3(d-\delta_n)}]}{D}+$$
$$\frac{1}{2p_3^2}[1+e^{-2p_3\delta_n}][1-e^{-p_3\frac{\Delta}{2}}]\frac{\frac{Q}{Z}[1+e^{-2p_3(d-\delta_n-\frac{\Delta}{4})}]+[1-e^{-2p_3(d-\delta_n-\frac{\Delta}{4})}]}{D} \tag{5.3.39}$$

In the above

$$\delta_n = (n-\frac{1}{2})\Delta \tag{5.3.40}$$

$$D = \frac{Q}{Z}[1-e^{-2p_3d}]+[1+e^{-2p_3d}] \tag{5.3.41}$$

$$\frac{Q}{Z} = \frac{p_3\varepsilon_2}{p_2\varepsilon_3}\frac{\varepsilon_1 p_2[1+e^{-2p_2t}]+\varepsilon_2 p_1[1-e^{-2p_2t}]}{\varepsilon_1 p_2[1-e^{-2p_2t}]+\varepsilon_2 p_1[1+e^{-2p_2t}]} \tag{5.3.42}$$

5.4 Comments on the Calculation of Impedance Matrix Entries

Each of the impedance matrix entries takes the form of an infinite real line integral (5.3.1). These integrals have all been done by numerical techniques and several issues have arisen during their computation. These are discussed below.

5.4.1 Integration through Surface-wave Pole Singularities

In many Sommerfeld-integral type solutions, surface-wave pole singularities of the integrand appear along the real axis, and are thus within the domain of integration. In the cases considered in this dissertation, the presence of the loss in region 2 makes p_2 a complex number, causing all the surface-wave poles of the integrand of (5.3.1) to shift off the real axis. Thus, surface-wave pole singularities are not encountered while calculating (5.3.1).

5.4.2 Integration through Branch Point Pole Singularities

There are three branch points involved in the calculation of (5.3.32). They are at

$$p_2 = 0 \tag{5.4.2.1}$$

$$p_3 = 0 \;\; ; \;\; p_1 = 0 \tag{5.4.2.2}$$

Because of the lossy layer, $p_2 = 0$ is not located along the integration path. In contrast, $p_3 = 0$ is located along the integration contour, and results in a singularity of the integrand in (5.3.1). Symbolically, each of the matrix entries (5.3.1) may be written as

$$A_{mn} = \frac{1}{2\pi j\omega\varepsilon_3}\int_0^{\infty} G_{mn}(\lambda)\frac{1-e^{-\sqrt{\lambda^2-k_3^2}\,\zeta}}{\lambda^2-k_3^2}J_0^2(a\lambda)\lambda d\lambda \tag{5.4.2.3}$$

Where

$$\zeta = \begin{cases} \Delta & n \neq m \\ \dfrac{\Delta}{2} & n = m \end{cases} \tag{5.4.2.4}$$

Thus there is a first order pole of the integrand at $\lambda = k_3$. Remember , however, that because of the square root in the exponential, this is also a branch point, and care must be exercised to ensure (2.3.17) is satisfied. This implies that contributions to the integral are not symmetric about $\lambda = k_3$.

Calculation of (5.4.2.3) is done in a purely numerical fashion, by splitting the integral into two parts at $\lambda = k_3$, and using a routine which does not evaluate the integrand at the limits of the integration [54].

It is also instructive to show how the integral in the vicinity of $\lambda = k_3$ can be done analytically. Isolate the singularity within an interval $[k_3-\gamma, k_3+\gamma]$ and examine the integral

$$I = \int_{k_3-\gamma}^{k_3+\gamma} \frac{1}{2\pi} G_{mn}(\lambda) \frac{1-e^{-\sqrt{\lambda^2-k_3^2}\,\zeta}}{\lambda^2-k_3^2} J_0^2(a\lambda)\lambda d\lambda \,. \tag{5.4.2.5}$$

Assuming γ is chosen small enough such that

$$\gamma\Delta \ll 1 \quad \text{and} \quad \gamma \ll k_3 \tag{5.4.2.6}$$

Then the exponential in (5.4.2.5) can be approximated using the first two terms of its Taylor series expansion, giving

$$I \approx \frac{\zeta}{2\pi} G_{mn}(k_3) J_0^2(k_3 a) \int_{k_3-\gamma}^{k_3+\gamma} \frac{\sqrt{\lambda^2-k_3^2}}{\lambda^2-k_3^2} \lambda d\lambda \,. \tag{5.4.2.7}$$

Now, using (2.3.17) to determined the sign on the square root, the integral (5.4.2.7) can be split into two portions

$$I \simeq \frac{\zeta}{2\pi} G_{mn}(k_3) J_0^2(k_3 a) \left[\int_{k_3}^{k_3+\gamma} \frac{\lambda d\lambda}{(\lambda^2-k_3^2)^{\frac{1}{2}}} - j \int_{k_3-\gamma}^{k_3} \frac{\lambda d\lambda}{(k_3^2-\lambda^2)^{\frac{1}{2}}} \cdot \right] \tag{5.4.2.8}$$

Carrying out the integrals, substituting the limits, and using (5.4.2.6) gives

$$I \simeq \frac{\zeta}{2\pi} G_{mn}(k_3) J_0^2(k_3 a) \sqrt{2k_3\gamma}(1-j) \ . \tag{5.4.2.9}$$

5.4.3 Convergence of the MoM Matrix Entry Integrals

Before undertaking the numerical integration of (5.3.1), it is quite helpful to anticipate the rate of convergence of the integrals. Of interest is the behavior of the integrand as $\lambda \to \infty$.

For $n \neq m$ the integrand has, from (5.3.17), an exponential decay factor

$$e^{-p_3(\delta_m - \delta_n - \frac{\Delta}{2})} \to 0 \quad as\ \lambda \to \infty \tag{5.4.3.1}$$

and thus the integrals converge quite rapidly.

For $m = n$ the integral has no exponential decay. Since each bracketed term converges to 1 as $\lambda \to \infty$, it is easy to show that, from (5.3.39)

$$I_{nn} \sim \frac{1}{\lambda^2 - k_3^2} \quad as\ \lambda \to \infty \tag{5.4.3.2}$$

Thus, the asymptotic form of the integrand in (5.3.1) is, for m=n

$$\frac{J_0^2(a\lambda)}{\lambda^2 - k_3^2}\lambda \sim \frac{J_0^2(a\lambda)}{\lambda} \ . \tag{5.4.3.3}$$

Numerical integration of a term with the above asymptotic behavior is quite time consuming. The integral must be computed by summing over periods of the Bessel function. If the Bessel function is not aided by a strong decay factor, many periods must be summed; more periods are necessary with a thick antenna than with a thinner one. The additional decay factor of $\frac{1}{\lambda}$ in (5.4.3.3) is sufficient for convergence, but the convergence is slow.

To help improve convergence, a term which has the same asymptotic behavior as the integrand, but can be integrated in closed form, can be added and subtracted as follows. Let

$$A_{nn} = \frac{1}{2\pi j \omega \varepsilon_3} \int_0^{\infty} \bar{I}_{nn}(\lambda) J_0^2(a\lambda) \lambda d\lambda + \bar{A} \tag{5.4.3.4}$$

where

$$\bar{I}_{nn} = I_{nn}(\lambda) - I_{nn}^a(\lambda) \tag{5.4.3.5}$$

and

$$\bar{A} = \frac{1}{2\pi j \omega \varepsilon_3} \int_0^{\infty} I_{nn}^a(\lambda) J_0^2(a\lambda) \lambda d\lambda \,. \tag{5.4.3.6}$$

Here $I_{nn}^a(\lambda)$ is any function which has roughly the same asymptotic behavior as $I_{nn}(\lambda)$, but also allows (5.4.3.6) to be integrated in closed form. It is easily seen that as $\lambda \rightarrow \infty$, the two terms in (5.4.3.5) subtract, and the integral in (5.4.3.4) converges at a more rapid rate than (5.3.1).

A convenient choice for $I_{nn}^a(\lambda)$ is

$$I_{nn}^a(\lambda) = \frac{1}{\lambda^2 + k_3^2} \,. \tag{5.4.3.7}$$

Then,

$$\bar{A} = \frac{1}{2\pi j \omega \varepsilon_3} \int_0^{\infty} \frac{J_0^2(a\lambda)}{\lambda^2 + k_3^2} \lambda d\lambda \tag{5.4.3.8}$$

which can be integrated in closed form [51] to give

$$\bar{A} = \frac{1}{2\pi j\,\omega\epsilon_3} K_0(k_3 a) I_0(k_3 a) \tag{5.4.3.9}$$

where I_0 is the modified Bessel function of the first kind and K_0 is the modified Bessel function of the second kind.

Note that as the radius of the antenna is decreased, the contribution to the total integral by (5.4.3.9) is increased, and thus the importance of the integral contribution in (5.4.3.4) is reduced.

Using (5.4.3.7), the integrand in (5.4.3.4) varies as

$$\lambda J_0^2(a\lambda)\left[\frac{1}{\lambda^2-k_3^2} - \frac{1}{\lambda^2+k_3^2}\right]$$

$$\sim \frac{\lambda J_0^2(a\lambda)}{\lambda^4-k_3^4} \sim \frac{J_0^2(a\lambda)}{\lambda^3} \tag{5.4.3.10}$$

which decays much faster than the original integrand (5.4.3.3).

5.5 Admittance Matrix for a Slot

The integral equation (4.3.12) can be solved by Galerkin's method with pulse basis and testing functions. With the narrow slot approximation, the magnetic current has a known lateral distribution and an unknown longitudinal distribution. Expand the magnetic current as

$$M_x(\mathbf{r}) = \sum_{n=1}^{2N} a_n P_n(x) W(y) \quad ; \quad x \in [-l, l] \; ; \; y \in [-w, w] \tag{5.5.1}$$

Here, the weighting function W(y) is assumed to be

$$W(y) = \frac{1}{\sqrt{1-(\frac{y}{w})^2}} \tag{5.5.2}$$

to account for the edge behavior of the current. A pulse basis function is chosen:

$$P_n(x) = \begin{cases} 1 \; ; \; x_{n-1} \le x \le x_n \\ \\ 0 \; ; \; elsewhere \end{cases} \tag{5.5.3}$$

where

$$x_{n-1} = (\frac{n-1}{N}-1)l \quad ; \quad x_n = (\frac{n}{N}-1)l \; . \tag{5.5.4}$$

Now, define the inner product as

$$<f(x,y),g(x,y)> \equiv \iint f(x,y) \; g(x,y) dx \; dy \tag{5.5.5}$$

and use Galerkin's method to reduce the integral equation (4.3.18) to the set of linear algebraic equations

$$\sum_{n=1}^{2N} <L(P_n W),P_m W> = <F_H,P_m W> \; ; \quad m=1,2,...,2N \; . \tag{5.5.6}$$

Using (4.3.10-11) and (4.3.13-16) then gives

$$L(M_x) = L_L(M_x) - L_R^g(M_x) \tag{5.5.7}$$

$$L_R^g(M_x) \equiv \int_0^x L_R(M_x)|_{x=x'} (\frac{1}{k_s}) sink_s(x-x')dx' \tag{5.5.8}$$

$$F_H(\mathbf{r}) = C_1 \sin k_s x + C_2 \cos k_s x + \frac{1}{k_s}\int_0^x F(\mathbf{r})|_{x=x'} \sin k_s(x-x')dx' \; . \tag{5.5.9}$$

Notice that there are 2N equations and 2N+2 unknowns, { a_n }, C_1, and C_2. The boundary condition that the magnetic current is zero at the two ends of the slot gives two more equations. For pulse basis functions, the two equations can be written as

$$a_1 = 0 \tag{5.5.10}$$

$$a_{2N} = 0 \tag{5.5.11}$$

Substituting (5.5.10) and (5.5.11) in (5.5.6) gives the matrix equation

$$[y_{mn}][v_n] = [i_m] \tag{5.5.12}$$

where $[y_{mn}]$ is a 2N by 2N complex matrix and $[v_n]$ and $[i_m]$ are 2N by 1 complex vectors

$$y_{mn} = \begin{cases} <L(P_n W), P_m W> \ ; \ \text{if } n=2,\ldots,2N-1 \\ <-sin k_s x, P_m W> \ ; \ \text{if } n=1 \\ <-cos k_s x, P_m W> \ ; \ \text{if } n=2N \end{cases} \tag{5.5.13}$$

$$[v_n] = [C_1 \; a_2 \; \cdots \; a_{2N-1} \; C_2]^T \tag{5.5.14}$$

$$[i_m] = [i_1 \; \cdots \; i_{2N}]^T \tag{5.5.15}$$

As stated in section 3 of chapter 4, C_1 and C_2 are unknown functions of y. Because of the expansion (5.5.1) and the fact that the weighting functions are known, the explicit forms of C_1 and C_2 will not affect the solution of the matrix equation. Therefore C_1 and C_2 can be assumed to be unknown constants.

The calculation of an admittance matrix entry $<L(P_n W), P_m W>$ requires a six-fold integration, four finite spatial integrations and two infinite spectral integrations. This calculation is very demanding numerically because the integrand is highly oscillatory.

In this dissertation, the matrix entries are calculated by the approach described below. First, the four spatial integrations are carried out analytically with simple basis functions. Then, the two spectral integrations are computed numerically. From (4.3.10-11), (4.3.13-16), and (5.5.5), the admittance matrix entries and the excitation vector can be written as

$$<L(P_n W), P_m W> = y_{mn}^L - y_{mn}^R \tag{5.5.16}$$

$$y_{mn}^L = <L_L(P_n W), P_m W>$$

$$= \frac{1}{(2\pi)^2}\iint_{-\infty}^{\infty} d^2k\,\Psi_L(\mathbf{k})\Gamma_y^-(k_y)\Gamma_y^+(k_y)\Gamma_{nx}^-(k_x)\Gamma_{mx}^+(k_x) \tag{5.5.17}$$

$$y_{mn}^R = <L_R^g(P_n W), P_m W>$$

$$= \frac{1}{(2\pi)^2}\iint_{-\infty}^{\infty} d^2k\,\Psi_R(\mathbf{k})\Gamma_y^-(k_y)\Gamma_y^+(k_y)\Gamma_{nx}^-(k_x)T_{mx}(k_x) \tag{5.5.18}$$

where

$$\Gamma_{nx}^{\pm}(k_x) = \int_{-l}^{l} P_n(x)e^{\pm jk_x x}\,dx \tag{5.5.19}$$

$$\Gamma_y^{\pm}(k_y) = \int_{-w}^{w} W(y)e^{\pm jk_y y}\,dy \tag{5.5.20}$$

$$T_{mx}(k_x) = \int_{-l}^{l} P_m(x)\Lambda(k_x, x)dx \tag{5.5.21}$$

$$\Lambda(k_x, x) = \int_0^x e^{jk_x x'}\left(\frac{1}{k_s}\right)\sin k_s(x-x')dx' \tag{5.5.22}$$

$$= \frac{1}{2k_s}\left(\frac{e^{jk_x x}-e^{-jk_s x}}{k_x+k_s} - \frac{e^{jk_x x}-e^{jk_s x}}{k_x-k_s}\right). \tag{5.5.22}$$

Substituting (5.5.2) into (5.5.20) and using a known integral identity [51] give

$$\Gamma_y^{\pm}(k_y) = 2\int_0^w \frac{cos(k_y y)}{\sqrt{1-(\frac{y}{w})^2}}dy = \pi w J_0(k_y w) = \Gamma_y(k_y)\,. \tag{5.5.23}$$

Substituting (5.5.3) and (5.5.4) into (5.5.19) results

$$\Gamma_{nx}^{+} = \frac{e^{jk_x x_n} - e^{jk_x x_{n-1}}}{jk_x} \tag{5.5.24}$$

$$\Gamma_{nx}^{-} = \frac{e^{-jk_x x_n} - e^{-jk_x x_{n-1}}}{-jk_x} \tag{5.5.25}$$

while substituting (5.5.3) into (5.5.21) leads to

$$T_{mx}(k_x) = \frac{-1}{(k_x+k_s)(k_x-k_s)}\Gamma^{+}_{mx}(k_x)+\frac{1}{2k_s(k_x-k_s)}\Gamma^{+}_{mx}(k_s)-$$

$$\frac{1}{2k_s(k_x+k_s)}\Gamma^{-}_{mx}(k_s)\ . \tag{5.5.26}$$

Then, substituting (5.5.2-5) into (5.5.13) gives

$$y_{m,1} = -A_y A^s_m \tag{5.5.27}$$

$$y_{m,2N} = -A_y A^c_m \tag{5.5.28}$$

where

$$A_y = \int_{-w}^{w} \frac{1}{\sqrt{1-(\frac{y}{w})^2}}dy = \pi w \tag{5.5.29}$$

$$A^c_m = \int_{x_{m-1}}^{x_m} cos(k_s x)dx = \frac{sin(k_s x_m)-sin(k_s x_{m-1})}{k_s} \tag{5.5.30}$$

$$A^s_m = \int_{x_{m-1}}^{x_m} sin(k_s x)dx = \frac{cos(k_s x_m)-cos(k_s x_{m-1})}{-k_s}\ . \tag{5.5.31}$$

The excitation vector can be written as

$$i_m = <\int_0^x F(\mathbf{r})|_{x=x'}(\frac{1}{k_s})\sin k_s(x-x')dx', P_m W> \tag{5.5.32}$$

The admittance matrix is independent on the form of excitation while the excitation vector takes different forms for different sources of the slot. In the transmitting case, a delta gap generator is placed at the center of the slot

$$K_y(\mathbf{r}) = I_y\delta(x) = F(\mathbf{r}) \tag{5.5.33}$$

Substituting (5.5.2-5) and (5.5.33) into (5.5.32) gives

$$i_m = \frac{I_y}{2k_s} A_y A_m^s \tag{5.5.34}$$

It is worth noting that because $\delta(x)$ is an even function of x, the following result is obtained:

$$\int_0^x I_y \delta(x')(\frac{1}{k_s})\sin k_s(x-x')dx' = \frac{I_y}{2k_s}\sin(k_s x) \ . \tag{5.5.35}$$

In the scattering case, the source is the tangential incident magnetic field $\mathbf{H}_{3t}^{in}$ on the slot. Plane wave propagation in layered media is studied in chapter 3. Results in chapter 3 are used to express $\mathbf{H}_{3t}^{in}$ in terms of the known incident plane wave field $\mathbf{H}_3^{in}$.

Because the antenna problem is 3D in nature and has no angular symmetry, it is necessary to specify an incident plane and the polarization for the incident plane wave before the scattering case can be solved. In this dissertation, a TM plane wave in the E-plane (y-z plane) is considered explicitly. Any other orientation and polarization of the incident wave can be handled by the same procedure.

Comparing Figure 1.2 and Figure 3.1 gives

$$z_1 = d+t \ ; \quad z_2 = d \ ; \quad z_3 = 0 \tag{5.5.36}$$

Substituting (5.5.36) into (3.1.55) gives

$$H_{3x}^{in}(\mathbf{r}) = 2H_{1x}^{in} e^{jk_1 \sin\theta_0 y} T^- = -F(\mathbf{r}) \ ; \ x \in [-l,l] \ ; y \in [-w,w] \ ; z=0 \tag{5.5.37}$$

while substituting (5.5.5) and (5.5.37) into (5.5.32) results in

$$i_m = \frac{2H_{1x}^{in} T^-}{k_s^2} A_y (\frac{l}{N} - A_m^c) \tag{5.5.38}$$

where the following approximation is used

$$|y| \le w \ll \lambda_1 \rightarrow |k_1 y| \ll 1 \rightarrow e^{jk_1 \sin\theta_0 y} \simeq 1 \ . \tag{5.5.39}$$

5.6 Calculation of Admittance Matrix Entries

It is a daunting task to carry out the numerical integrations of (5.5.17) and (5.5.18) because the integrands are highly oscillatory. The 2D infinite spectral integrations can be carried out in either rectangular coordinates or in cylindrical coordinates.

In this dissertation, the 2D spectral integrations are computed in cylindrical coordinates. A generic form of the spectral integrals can be written as

$$\begin{cases} k_x = \lambda\cos\alpha \\ k_y = \lambda\sin\alpha \end{cases} \tag{5.6.1}$$

$$\int\int_{-\infty}^{\infty} f(k_x,k_y)dk_x\, dk_y = \int_0^{\infty}\left[\int_0^{2\pi} f(\lambda,\alpha)\lambda d\alpha\right]d\lambda \tag{5.6.2}$$

where α is a real variable and λ is a complex variable. This representation provides valuable physical insight into the problem. Note that from the results of section 5 of chapter 2, the branch points and poles of the integrands are independent of the angular variable. To compute (5.6.2), first the angular integration is carried out numerically. Then the radial integration is computed. The semi-infinite integral can be converted to an infinite integral. A generic form of the radial integration can be written as

$$\int_0^{\infty} g(\lambda)d\lambda = \int_{-\infty}^{\infty} g'(\lambda)d\lambda \tag{5.6.3}$$

There are two methods to do the radial integration. In the complex λ plane, the infinite integral can be computed by real line integration or contour integration.

It is necessary to define all the branch cuts and to find all the poles of the integrand before contour integration can be used. The advantage of the contour integration method is that the integration is stable and rapidly converging, while the disadvantage is that a lot of analytical work is involved. The existence of three layers above the ground plane makes the eigen-value equations very complicated. It is very difficult to find all the eigenvalues (the poles), especially when the layers are lossy.

The real line integration involves little analytical effort. But because the integrand is highly oscillatory, the integration is numerically unstable and converges slowly. If there are poles on the real axis and their positions are unknown, the real line integration method might fail. The existence of a lossy superstrate shifts all the poles off the real axis. Thus real line integration can be used successfully. One drawback of the real line integration is that it requires extensive computation power.

It is advantageous to explore the symmetry of the integrands to reduce numerical computation. From (5.5.24-26), the functions can be decomposed into even and parts

$$\Gamma_{nx}^{\pm}(k_x) = \Gamma_n^e(k_x) \pm \Gamma_n^o(k_x) \tag{5.6.4}$$

$$\Gamma_n^e(k_x) = \frac{\sin(k_x x_n) - \sin(k_x x_{n-1})}{k_x} \tag{5.6.5}$$

$$\Gamma_n^o(k_x) = \frac{\cos(k_x x_n) - \cos(k_x x_{n-1})}{jk_x} \tag{5.6.6}$$

$$T_{mx}(k_x) = T_m^e(k_x) + T_m^o(kx) \tag{5.6.7}$$

$$T_m^e(k_x) = \frac{k_s}{k_x^2 - k_s^2}[\Gamma_m^e(k_s) - \Gamma_m^e(k_x)] \tag{5.6.8}$$

$$T_m^o(k_x) = \frac{1}{k_x^2 - k_s^2}[k_x \Gamma_m^o(k_s) - k_s \Gamma_m^o(k_x)] \tag{5.6.9}$$

Obviously Γ_n^e andT_m^e are even functions of k_x and Γ_n^o and T_m^o are odd functions of k_x. Substituting (5.6.4-9) into (5.5.17-18) gives

$$y_{mn}^L = \frac{4}{(2\pi)^2} \iint_0^\infty d^2k \Psi_L(\mathbf{k}) \Gamma_y^2(k_y) P_{mn}(k_x) \tag{5.6.10}$$

$$y_{mn}^R = \frac{4}{(2\pi)^2} \iint_0^\infty \Psi_R(\mathbf{k}) \Gamma_y^2(k_y) Q_{mn}(k_x) \tag{5.6.11}$$

where

$$P_{mn}(k_x) = \Gamma_m^e(k_x)\Gamma_n^e(k_x) - \Gamma_m^o(k_x)\Gamma_n^o(k_x) \tag{5.6.12}$$

$$Q_{mn}(k_x) = T_m^e(k_x)\Gamma_n^e(k_x) - T_m^o(k_x)\Gamma_n^o(k_x)\ . \tag{5.6.13}$$

The computer can not handle indeterminate forms reliably. All the indeterminate forms have to be carried out analytically.

When $k_x \to 0$, (5.6.5-6) can be approximated as

$$\Gamma_n^e(k_x) \approx \frac{l}{N} \tag{5.6.14}$$

$$\Gamma_n^o(k_x) \approx j\left(\frac{2n-1}{N^2} - \frac{2}{N}\right)k_x l^2 \tag{5.6.15}$$

When $|k_x - k_s| \to 0$, (5.6.8-9) can be approximated as

$$T_m^e(k_x) \approx -\frac{1}{2}\frac{d}{dk_x}\Gamma_m^e(k_s) \tag{5.6.16}$$

$$T_m^o(k_x) \approx \frac{1}{2k_s}\left[-k_s\frac{d}{dk_s}\Gamma_m^o(k_s) + \Gamma_m^o(k_s)\right] \tag{5.6.17}$$

where

$$\frac{d}{dk_x}\Gamma_n^e(k_x) = \frac{1}{k_x^2}[k_x(x_n\cos k_x x_n - x_{n-1}\cos k_x x_{n-1}) - (\sin k_x x_n - \sin k_x x_{n-1})] \tag{5.6.18}$$

$$\frac{d}{dk_x}\Gamma_n^o(k_x) = \frac{1}{jk_x^2}[k_x(-x_n\sin k_x x_n + x_{n-1}\sin k_x x_{n-1}) - (\cos k_x x_n - \cos k_x x_{n-1})] \tag{5.6.19}$$

Now express the spectral integrations in cylindrical coordinates. Substituting (5.6.1) into (5.6.10-13) gives

$$y_{mn}^L = \frac{4}{(2\pi)^2}\int_0^\infty d\lambda\ \lambda\Psi_L(\lambda)s_{mn}^L(\lambda) \tag{5.6.20}$$

$$y_{mn}^R = \frac{4}{(2\pi)^2}\int_0^\infty d\lambda\ \lambda\Psi_R(\lambda)s_{mn}^R(\lambda) \tag{5.6.21}$$

where

$$s_{mn}^{L}(\lambda) = \int_{0}^{\frac{\pi}{2}} \Gamma_y^2(\lambda \sin\alpha) P_{mn}(\lambda \cos\alpha) d\alpha \tag{5.6.22}$$

$$s_{mn}^{R}(\lambda) = \int_{0}^{\frac{\pi}{2}} \Gamma_y^2(\lambda \sin\alpha) Q_{mn}(\lambda \cos\alpha) d\alpha \ . \tag{5.6.23}$$

Integration around singularity points of the integrand needs special treatment. As mentioned before, integration through surface wave poles is avoided because of the lossy superstrate. Integration through branch point singularities must be carried out analytically. All the branch points are contained in $\Psi_L(\lambda)$ and $\Psi_R(\lambda)$. Rewrite (4.3.15) and (4.3.16)

$$\Psi_L(\lambda) = \Psi_a(\lambda) + \Psi_b(\lambda) + \Psi_c(\lambda) \tag{5.6.24}$$

$$\Psi_R(\lambda) = (\frac{k_4}{k_s})^2 \Psi_a(\lambda) + \Psi_b(\lambda) + (\frac{k_3}{k_s})^2 \Psi_c(\lambda) \tag{5.6.25}$$

where

$$\Psi_a(\lambda) \equiv \frac{N_{3x}(z=0)}{j\omega\mu_3 p_3 D_x} \tag{5.6.26}$$

$$\Psi_b(\lambda) \equiv \frac{N_{3z}^{d}(z=0)}{j\omega\mu_3 p_3 D_x D_z} \tag{5.6.27}$$

$$\Psi_c(\lambda) \equiv \frac{1}{j\omega\mu_4 p_4} \tag{5.6.28}$$

From (2.5.2.11-12) and (4.3.17)

$$\begin{aligned} N_{3x}(z=0) = {} & [(\varepsilon_1 p_2 + \varepsilon_2 p_1)(\varepsilon_2 p_3 + \varepsilon_3 p_2) + (\varepsilon_1 p_2 - \varepsilon_2 p_1)(\varepsilon_2 p_3 - \varepsilon_3 p_2) e^{-2p_2 t}] \\ & + [(\varepsilon_1 p_2 + \varepsilon_2 p_1)(\varepsilon_2 p_3 - \varepsilon_3 p_2) + (\varepsilon_1 p_2 - \varepsilon_2 p_1)(\varepsilon_2 p_3 + \varepsilon_3 p_2) e^{-2p_2 t}] e^{-2p_3 d} \end{aligned} \tag{5.6.29}$$

$$N_{3z}^{d}(z=0) = 4p_3^2 e^{-2p_3 d} \{(\varepsilon_3\mu_3 - \varepsilon_2 u_2)[u_1 p_2 (1+e^{-2p_2 t}) + u_2 p_1 (1-e^{-2p_2 t})]$$

$$[\varepsilon_1 p_2(1+e^{-2p_2 t})+\varepsilon_2 p_1(1-e^{-2p_2 t})]+4(\varepsilon_2 u_2-\varepsilon_1 u_1)\varepsilon_3\mu_3 e^{-2p_2 t} p_2^2\} \tag{5.6.30}$$

It can be seen that Ψ_a contains the singularity p_3=0 , Ψ_c has singularity p_4=0, and Ψ_b does not have a branch point singularity because the factor p_3^2 in N_{3z}^d cancels the p_3 in the denominator. The branch points can be written as

$$p_3 = 0 \rightarrow \lambda_3 = k_3 \tag{5.6.31}$$

$$p_4 = 0 \rightarrow \lambda_4 = k_4 . \tag{5.6.32}$$

If k_3 and k_4 are real, the branch points λ_3 and λ_4 will be on the integration path. The integration through them must be carried out analytically. The procedure is outlined below. Select a small γ such that

$$\gamma \ll k_i \quad \text{and} \quad \gamma \ll 1 \ ; \ i=3,4 \tag{5.6.33}$$

The semi-infinite integral can be split into three parts and one of them can be evaluated analytically.

$$\int_0^\infty \frac{f(\lambda)}{p_i} d\lambda = \left(\int_0^{k_i-\gamma} + \int_{k_i-\gamma}^{k_i+\gamma} + \int_{k_i+\gamma}^\infty \right) \frac{f(\lambda)}{\sqrt{\lambda^2-k_i^2}} d\lambda$$

$$\simeq \left(\int_0^{k_i-\gamma} + \int_{k_i+\gamma}^\infty \right) \frac{f(\lambda)}{p_i} + f(k_i) ln\left(\frac{k_i+\gamma+\sqrt{\gamma^2+2\gamma k_i}}{k_i-\gamma+\sqrt{\gamma^2-2\gamma k_i}} \right) \ ; \ i=3,4 \tag{5.6.34}$$

Semi-adaptive integration subprograms, based on extended Simpson's rule and Romberg integration [55], are used in numerical integration of matrix elements.

After the calculation of the matrix elements, the matrix equation (5.5.12) is solved to obtain magnetic current in slot. Then the aperture tangential electric field can be obtained via (4.2.2)

$$E_y(x,y) = M_x(x,y) \tag{5.6.35}$$

The voltage across a slot is obtained by integration of aperture electric field

$$V(x) = \int_{-w}^{w} E_y(x,y)dy \tag{5.6.36}$$

Substituting (5.6.35-36) into (5.5.1) then gives

$$V(x{=}0) = a_N \int_{-w}^{w} \frac{1}{\sqrt{1-(\frac{y}{w})^2}} dy = \pi w a_N \tag{5.6.37}$$

The input impedance of a slot depends on the location of the current source in the slot. In this dissertation, a current source is centered in a slot. The input impedance of a slot is defined as

$$Z_{in} = \frac{V(x{=}0)}{I} = \frac{\pi w a_N}{I} \tag{5.6.38}$$

CHAPTER SIX

SCATTERED FIELD

The induced electric current on an imaged monopole and induced equivalent magnetic current in a slot are obtained by solving matrix equations (5.2.9) and (5.5.12). In this chapter, the scattered electromagnetic fields, radar cross section, and radiation pattern are determined.

6.1. Scattered Field for a Monopole

Once the monopole current has been obtained, the field scattered into region 1 may be determined by using equations (2.6.1.13-14). The term $\bar{V}_z(\lambda)$ given by (2.6.1.6) is common to both expressions. Substituting (5.2.1) into (2.6.1.6) gives

$$\bar{V}_z(\lambda) = \sum_{n=1}^{N} a_n \int_{-d+(n-1)\Delta}^{-d+n\Delta} \frac{1}{j\omega\varepsilon_3} \frac{\cosh p_3(d+z')}{p_3} dz' . \tag{6.1.1}$$

Carrying out the integration in (6.1.1) analytically leads to

$$\bar{V}_z(\lambda) = \frac{1}{j\omega\varepsilon_3} \frac{2}{p_3^2} \sum_{n=1}^{N} a_n \cosh p_3\delta_n \sinh p_3\frac{\Delta}{2} . \tag{6.1.2}$$

Substituting (6.1.2) into (2.6.1.13-14) gives

$$E_{1z} = \sum_{n=1}^{N} a_n \int_0^{\infty} \frac{\cosh p_3\delta_n \sinh p_3\frac{\Delta}{2}}{2\pi j\omega\varepsilon_3\, \chi(\lambda)} e^{-p_1(z-t)} J_0(\lambda a) J_0(\lambda\rho) \frac{\lambda^3}{p_3^2} d\lambda \tag{6.1.3}$$

$$E_{1\rho} = \sum_{n=1}^{N} a_n \int_0^{\infty} \frac{\cosh p_3\delta_n \sinh p_3\frac{\Delta}{2}}{2\pi j\omega\varepsilon_3\, \chi(\lambda)} e^{-p_1(z-t)} J_0(\lambda a) J_1(\lambda\rho) \frac{p_1\lambda^2}{p_3^2} d\lambda \tag{6.1.4}$$

It is important to understand the asymptotic behavior of the integrands in (6.1.3-4). To write the integrands in terms of exponentials, use

$$\cosh p_3\delta_n \sinh p_3\frac{\Delta}{2} = \frac{1}{4} e^{p_3\delta_n} e^{p_3\frac{\Delta}{2}} [1+e^{-2p_3\delta_n}][1-e^{-2p_3\frac{\Delta}{2}}] \tag{6.1.5}$$

$$\chi(\lambda) = \frac{1}{4}e^{p_3 d}e^{p_2 t}\left\{\frac{\varepsilon_1}{\varepsilon_3}[1-e^{-2p_3 d}][1+e^{-2p_2 t}] + \frac{\varepsilon_1 p_2}{\varepsilon_2 p_3}[1+e^{-2p_3 d}][1-e^{-2p_2 t}] + \right.$$

$$\left.\frac{\varepsilon_2 p_1}{\varepsilon_3 p_2}[1-e^{-2p_3 d}][1-e^{-2p_2 t}] + \frac{p_1}{p_3}[1+e^{-2p_3 d}][1+e^{-2p_2 t}]\right\} \tag{6.1.6}$$

to give

$$E_{1z} = \sum_{n=1}^{N} a_n \int_0^\infty H(\lambda) e^{-p_3(d-\delta_n-\frac{\Delta}{2})} e^{-p_2 t} e^{-p_1(z-t)} J_0(\lambda a) J_0(\lambda\rho) \frac{\lambda^3}{p_3^2} d\lambda \tag{6.1.7}$$

$$E_{1\rho} = \sum_{n=1}^{N} a_n \int_0^\infty H(\lambda) e^{-p_3(d-\delta_n-\frac{\Delta}{2})} e^{-p_2 t} e^{-p_1(z-t)} J_0(\lambda a) J_1(\lambda\rho) \frac{p_1\lambda^2}{p_3^2} d\lambda \tag{6.1.8}$$

where

$$H(\lambda) = [1+e^{-2p_3\delta_n}][1-e^{-2p_3\frac{\Delta}{2}}]\left\{\frac{\varepsilon_1}{\varepsilon_3}[1-e^{-2p_3 d}][1+e^{-2p_2 t}] + \frac{\varepsilon_1 p_2}{\varepsilon_2 p_3}[1+e^{-2p_3 d}]\right.$$

$$\left.[1-e^{-2p_2 t}] + \frac{\varepsilon_2 p_1}{\varepsilon_3 p_2}[1-e^{-2p_3 d}][1-e^{-2p_2 t}] + \frac{p_1}{p_3}[1+e^{-2p_3 d}][1+e^{-2p_2 t}]\right\}^{-1} \tag{6.1.9}$$

Since each term in brackets in (6.1.9) converges to unity as $\lambda \to \infty$, the asymptotic form of $H(\lambda)$ is

$$H(\lambda) \sim \left\{\frac{\varepsilon_1}{\varepsilon_3} + \frac{\varepsilon_1 p_2}{\varepsilon_2 p_3} + \frac{\varepsilon_2 p_1}{\varepsilon_3 p_2} + \frac{p_1}{p_3}\right\}^{-1} = constant\ . \tag{6.1.10}$$

Thus, the decay of the integrands of (6.1.7) and (6.1.8) is controlled by the exponential terms. It is seen that the integrand has the slowest decay when n=N and z=t, causing two of the exponential terms to drop out. Then, the integrand behaves asymptotically as

$$\sim \lambda e^{-p_2 t}\begin{Bmatrix} J_0(\lambda a) J_0(\lambda\rho) \\ J_0(\lambda a) J_1(\lambda\rho) \end{Bmatrix}. \tag{6.1.11}$$

Since $\mathrm{Re}\{p_2\}>0$,(2.3.17), there is always an exponential decay factor, and the integrals will converge.

Even though the integrals converge, they are still difficult to calculate numerically. This is due to the oscillatory behavior of both the exponential term and the Bessel functions in (6.1.11) at large λ. Care must be taken to integrate over complete periods of the Bessel function.

6.2 Far Field Calculation

From (6.1.3-4), the scattered electric field in region 1 can be written as

$$E_{1z} = \sum_{n=1}^{N} a_n \int_0^{\infty} H_n(\lambda) e^{-p_1 z} J_0(\lambda\rho) \frac{\lambda^3}{p_3} d\lambda \tag{6.2.1}$$

$$E_{1\rho} = \sum_{n=1}^{N} a_n \int_0^{\infty} H_n(\lambda) e^{-p_1 z} J_1(\lambda\rho) \frac{p_1 \lambda^2}{p_3} d\lambda \tag{6.2.2}$$

where

$$H_n(\lambda) = \frac{1}{D(\lambda)} [1+e^{-2p_3\delta_n}] \frac{[1-e^{-2p_3\frac{\Delta}{2}}]}{p_3} e^{-p_3(d-\delta_n-\frac{\Delta}{2})} e^{-p_2 t} e^{p_1 t} J_0(\lambda a) \tag{6.2.3}$$

$$D(\lambda) = \{\frac{\varepsilon_1}{\varepsilon_2}[1-e^{-2p_3 d}][1+e^{-2p_2 t}]+\frac{\varepsilon_1 p_2}{\varepsilon_2 p_3}[1+e^{-2p_3 d}][1-e^{-2p_2 t}]+$$

$$\frac{\varepsilon_2 p_1}{\varepsilon_3 p_2}[1-e^{-2p_3 d}][1-e^{-2p_2 t}]+\frac{p_1}{p_3}[1+e^{-2p_3 d}][1+e^{-2p_2 t}]\} \tag{6.2.4}$$

$$\delta_n = (n-\frac{1}{2})\Delta \tag{6.2.5}$$

$$\Delta = \frac{h}{N} \tag{6.2.6}$$

$$k_1 = \omega\sqrt{\varepsilon_1\mu_1}\ ; \ \ k_2 = \omega\sqrt{\varepsilon_2\mu_2} \tag{6.2.7}$$

$$z \in (t,\infty)\ ; \quad \rho \in (0,\infty)$$

a_n — *current expansion coefficients*

N — *number of basis functions*

These fields can be calculated either exactly, through direct numerical integration, or approximately, using the stationary phase method. Both approaches are outlined below.

6.2.1 Numerical Integration Along the Real Axis

For a lossy superstrate, ε_2 and/or μ_2 can be complex. Because of this the zeros of $D(\lambda)$ are all complex numbers. In other words, the poles of the integrands of (6.2.1) and (6.2.2) are all off the real axis. Therefore, direct numerical integration can be used to compute the scattered far field. A real axis integration technique has the advantage of a wide range of validity in medium, frequency, and spatial parameters. The major limitation is computation time [36].

In the far field and radiation pattern calculations, the spatial parameters z and ρ have a very big dynamic range. Terms like $e^{-p_1(z-t)}$, $J_0(\lambda\rho)$, and $J_1(\lambda\rho)$ oscillate rapidly with large z and ρ. Highly oscillatory integrands make accurate and rapidly convergent numerical integration difficult to achieve.

The oscillations of the integrands of (6.2.1) and (6.2.2) in the interval $\lambda \in [0,k_1]$ are due to the terms $e^{-p_1(z-t)}$, $J_0(\lambda\rho)$, and $J_1(\lambda\rho)$. The oscillation of $e^{-p_1(z-t)}$ as a function of λ becomes more rapid near the branch point $\lambda = k_1$. Integration of these oscillatory functions is further complicated by the peak behavior of the integrands near the branch point. To make the densely packed oscillations more evenly spaced and to remove the peak behavior of the integrands at the branch point, the nonlinear transform [36]

$$\lambda = k_1 \sin\theta \qquad \theta \in [0,\frac{\pi}{2}] \tag{6.2.1.1}$$

is used over the interval $\lambda \in [0, k_1]$. Then let

$$I_{nz}^1 = \int_0^{k_1} H_n(\lambda) e^{-p_1 z} J_0(\lambda\rho) \frac{\lambda^3}{p_3} d\lambda$$

$$= \int_0^{\frac{\pi}{2}} H_n(k_1 \sin\theta) e^{-k_1 z \cos\theta} J_0(k_1 \rho \sin\theta)(k_1 \sin\theta)^3 d\theta \qquad (6.2.1.2)$$

and

$$I_{n\rho}^1 = \int_0^{k_1} H_n(\lambda) e^{-p_1 z} J_1(\lambda\rho) \frac{p_1 \lambda^2}{p_3} d\lambda$$

$$= \int_0^{\frac{\pi}{2}} H_n(k_1 \sin\theta) e^{-k_1 z \cos\theta} J_1(k_1 \rho \sin\theta)(k_1 \sin\theta)^2 k_1 \cos\theta d\theta \qquad (6.2.1.3)$$

After the transform, the branch point is removed and the integrands in (6.2.1.2-3) have an almost evenly distributed oscillation, and both approach zero at $\theta = \frac{\pi}{2}$.

A similar transform

$$\lambda = k_1 \sec\theta \quad \theta \in [0, cos^{-1}(\frac{1}{2})] \qquad (6.2.1.4)$$

may be used in the interval $\lambda \in [k_1, 2k_1]$ to even out the oscillation and remove the peak behavior of integrands at the branch point $\lambda = k_1$. Then

$$I_{nz}^2 = \int_{k_1}^{2k_1} H_n(\lambda) e^{-p_1 z} J_0(\lambda\rho) \frac{\lambda^3}{p_3} d\lambda$$

$$= \int_0^{\cos^{-1}(\frac{1}{2})} H_n(k_1 \sec\theta) e^{-k_1 z \tan\theta} J_0(k_1 \rho \sec\theta)(k_1 \sec\theta)^3 \sec^2\theta d\theta \qquad (6.2.1.5)$$

and

$$I_{n\rho}^2 = \int_{k_1}^{2k_1} H_n(\lambda) e^{-p_1 z} J_1(\lambda\rho) \frac{p_1 \lambda^2}{p_3} d\lambda$$

$$= \int_0^{\cos^{-1}(\frac{1}{2})} H_n(k_1\sec\theta)e^{-k_1 z\tan\theta}J_1(k_1\rho\sec\theta)(k_1\sec\theta)^3\tan\theta d\theta \quad (6.2.1.6)$$

In the interval $\lambda \in [2k_1,\infty)$, the exponentially decaying term $e^{-p_1 z}$ makes the numerical integration rapidly convergent, so no special transform is needed. Let

$$I_{nz}^3 = \int_{2k_1}^{\infty} H_n(\lambda)e^{-p_1 z}J_0(\lambda\rho)\frac{\lambda^3}{p_3}d\lambda \quad (6.2.1.7)$$

$$I_{n\rho}^3 = \int_{2k_1}^{\infty} H_n(\lambda)e^{-p_1 z}J_1(\lambda\rho)\frac{p_1\lambda^2}{p_3}d\lambda \quad (6.2.1.8)$$

Romberg integration is performed between the zeros of $J_0(\lambda\rho)$ and $J_1(\lambda\rho)$ and the results of subsections are summed up to get I_{nz}^1, I_{nz}^2, $I_{n\rho}^1$, and $I_{n\rho}^2$. A transform $\lambda = \frac{1}{x}$ is used to convert (6.2.1.7-8) into proper integrals and then the Romberg method is used [54]. The final results for the electric field are

$$E_{1z} = \sum_{n=1}^{N} a_n[I_{nz}^1+I_{nz}^2+I_{nz}^3] \quad (6.2.1.9)$$

$$E_{1\rho} = \sum_{n=1}^{N} a_n[I_{n\rho}^1+I_{n\rho}^2+I_{n\rho}^3] \quad (6.2.1.10)$$

Real axis integration can calculate both the near field and far field. But it is quite time-consuming. This method can be used to compute the scattered field at a specific point or to calibrate the results from more efficient approximate methods. It is not suited for radiation pattern calculation.

6.2.2 Stationary Phase Method

In order to calculate the far field more efficiently, some kind of asymptotic technique must be used. In this report, a simple and efficient stationary phase method originally proposed by Chew [38] has been used.

First the following generic integral is considered

$$I = \int_{-\infty}^{\infty} g(\alpha,\lambda) d\lambda \tag{6.2.2.1}$$

where α is a large parameter. If $g(\alpha,\lambda)$ becomes rapidly oscillating when α is large, and if there exists a stationary phase point of $g(\alpha,\lambda)$, a leading-order approximation can be obtained by the method of stationary phase. Several major steps of the method are highlighted.

The first step is to factor the integrand $g(\alpha,\lambda)$ into a slowly varying part $f(\lambda)$ and a rapidly varying part $p(\alpha,\lambda)$.

$$I = \int_{0}^{\infty} f(\lambda) p(\alpha,\lambda) d\lambda \, . \tag{6.2.2.2}$$

Assume $p(\alpha,\lambda)$ to be of the generic form

$$p(\alpha,\lambda) \sim e^{i\alpha s(\lambda)} \qquad \alpha \to \infty \tag{6.2.2.3}$$

The key in the factorization is to have a function $p(\alpha,\lambda)$ that can be integrated in closed form.

The second step is to find the stationary phase point λ_0 of $p(\alpha,\lambda)$, defined by

$$\frac{\partial s(\lambda)}{\partial \lambda}\bigg|_{\lambda=\lambda_0} = 0 \tag{6.2.2.4}$$

Most contribution to the integral in (6.2.2.2) will come from the vicinity of the stationary phase point $\lambda = \lambda_0$. A leading-order asymptotic approximation to (4.6.2.1) can be written as

$$I \sim f(\lambda_0) \int_{-\infty}^{\infty} p(\alpha,\lambda) d\lambda \qquad \alpha \to \infty \, . \tag{6.2.2.5}$$

The Sommerfeld identity [6][60] is needed in the stationary phase method.

$$\frac{e^{-jkr}}{r} = \int_{0}^{\infty} J_0(\lambda\rho) e^{-p|z|} \frac{\lambda}{p} d\lambda \tag{6.2.2.6}$$

where

$$p = \sqrt{\lambda^2 - k^2}$$

The physical interpretation of the Sommerfeld identity is that the spherical wave is expressed in terms of cylindrical waves.

Now, let

$$I_{nz} = \int_0^\infty H_n(\lambda) e^{-p_1 z} J_0(\lambda\rho) \frac{\lambda^3}{p_3} d\lambda$$

$$= \int_0^\infty [H_n(\lambda) \frac{p_1 \lambda^2}{p_3}][e^{-p_1 z} J_0(\lambda\rho) \frac{\lambda}{p_1}] d\lambda \, . \tag{6.2.2.7}$$

The term in the first bracket is slowly varying and the one in the second bracket is rapidly varying. The next step is to find the stationary phase point.

Express the Bessel functions in terms of Hankel functions [53]

$$J_n(\lambda\rho) = \frac{1}{2}[H_n^{(1)}(\lambda\rho) + H_n^{(2)}(\lambda\rho)] \, . \tag{6.2.2.8}$$

Then (6.2.2.7) can be rewritten as

$$I_{nz} = \frac{1}{2}\int_0^\infty f_{nz}(\lambda)[H_0^{(1)}(\lambda\rho) + H_0^{(2)}(\lambda\rho)] e^{-p_1 z} \frac{\lambda}{p_1} d\lambda$$

$$= \int_{-\infty}^\infty f_{nz}(\lambda) H_0^{(2)}(\lambda\rho) e^{-p_1 z} \frac{\lambda}{p_1} d\lambda \tag{6.2.2.9}$$

where

$$f_{nz}(\lambda) = H_n(\lambda) \frac{p_1 \lambda^2}{p_3} \tag{6.2.2.10}$$

Here the fact that $f_{nz}(\lambda)$ is an even function of λ and the following identity have been used [53]:

$$H_n^{(1)}(x) = -e^{-in\pi} H_n^{(2)}(xe^{-i\pi})$$

Note that

$$H_n^{(2)}(x) \sim \sqrt{\frac{2}{\pi x}}e^{-i(x-\frac{n\pi}{2}-\frac{\pi}{4})} \quad as \ |x| \to \infty \tag{6.2.2.11}$$

then

$$H_0^{(2)}(\lambda\rho)e^{-p_1 z} \sim e^{-p_1 z}\sqrt{\frac{2}{\pi\lambda\rho}}e^{-i(\lambda\rho-\frac{\pi}{4})} \quad as \ \lambda\rho\to\infty \tag{6.2.2.12}$$

The stationary phase point is given by

$$\frac{\partial}{\partial\lambda}[-(p_1 z+i\lambda\rho)] = 0 \,. \tag{6.2.2.13}$$

The solution to (6.2.2.13) is

$$\lambda_0 = \frac{\rho k_1}{(z^2+\rho^2)^{\frac{1}{2}}} = k_1\sin\theta \tag{6.2.2.14}$$

where

$$\theta = \sin^{-1}[\frac{\rho}{(z^2+\rho^2)^{\frac{1}{2}}}] \,.$$

The first order approximation to (6.2.2.7) can then be written using (6.2.2.6) as

$$I_{nz} = H_n(\lambda_0)\frac{p_1\lambda_0^2}{p_3}\int_0^\infty e^{-p_1 z}J_0(\lambda\rho)\frac{\lambda}{p_1}d\lambda$$

$$= H_n(\lambda_0)\frac{p_1\lambda_0^2}{p_3}\frac{e^{-jk_1 r}}{r} \tag{6.2.2.15}$$

So the far field asymptotic approximation of E_{1z} becomes

$$E_{1z} = \sum_{n=1}^{N} a_n f_{nz}(\lambda_0)\frac{e^{-jk_1 r}}{r} \tag{6.2.2.16}$$

where $r = \sqrt{\rho^2+z^2}$. The asymptotic approximation of $E_{1\rho}$ can be obtained in a similar way.

$$E_{1\rho} = \sum_{n=1}^{N} a_n f_{nr}(\lambda_0) \frac{e^{-jk_1 r}}{r} \tag{6.2.2.17}$$

where

$$f_{nr}(\lambda) = H_n(\lambda) \frac{p_1^2 \lambda}{p_3} \frac{J_1(\lambda\rho)}{J_0(\lambda\rho)} \ . \tag{6.2.2.18}$$

Equations (6.2.2.17) and (6.2.2.18) can be used to compute the scattered far field or to get the radiation pattern.

The radar cross section is defined as

$$RCS(\theta,\phi) = 4\pi r^2 \lim_{r\to\infty} \left| \frac{\mathbf{E}^s(\mathbf{r})}{\mathbf{E}^{in}(\mathbf{r})} \right|^2 \tag{6.2.8}$$

For a monopole illuminated by a TM plane wave, using (6.2.2.16-17), (3.1.1), and (6.2.8), the radar cross section can be expressed as

$$RCS(\theta,\phi) = \frac{4\pi}{(\eta_0 H_{1x}^i)^2} [(\sum_{n=1}^{N} a_n f_{nz}(\lambda_0))^2 + (\sum_{n=1}^{N} a_n f_{nr}(\lambda_0))^2] \tag{6.2.9}$$

where

$$\eta_0 = \left| \frac{\mathbf{E}_1^i}{\mathbf{H}_1^i} \right| = 120\pi(\Omega) \tag{6.2.10}$$

is the intrinsic impedance of free space.

6.3 Scattered Field for a Slot

After the magnetic current in the slot is obtained by solving the matrix equation (5.5.12), the scattered magnetic field can be computed from (2.6.2.1), (2.6.2.11-13), and (2.6.2.20-22).

$$H_{1a}(\mathbf{r}) = \iint_{slot} g_{ax}^{1,3}(\mathbf{r}|\mathbf{r}') M_{3x}(\mathbf{r}') dx' dy' \quad ; \quad a = x, y, z \tag{6.3.1}$$

where

$$g_{ax}^{1,3}(\mathbf{r}) = \frac{1}{(2\pi)^2}\iint_{-\infty}^{\infty} \tilde{g}_{ax}^{1,3}(\mathbf{r},\mathbf{k})e^{j\mathbf{k}\cdot\mathbf{r}}d^2k \tag{6.3.2}$$

and $\tilde{g}_{xx}^{1,3}$, $\tilde{g}_{yx}^{1,3}$, and $\tilde{g}_{zx}^{1,3}$ are given in (2.6.2.20-22).

Substituting (5.5.1) into (6.3.1) gives

$$H_{1a}(\mathbf{r}) = \sum_{n=1}^{2N} a_n \; [\,[\int_{x_{n-1}}^{x_n} dx' \int_{-w}^{w} dy' \; g_{ax}^{1,3}(\mathbf{r}|\mathbf{r}')W(y')] \tag{6.3.3}$$

where

$$W(y) = \frac{1}{\sqrt{1-(\frac{y}{w})^2}} \qquad y \in [-w,w] \tag{6.3.4}$$

$$\begin{cases} x_n = (\frac{n}{N}-1)l \\ x_{n-1} = (\frac{n-1}{N}-1)l \end{cases} \tag{6.3.5}$$

Now, define

$$\tilde{g}_{ax}^{1,3}(\mathbf{r},\mathbf{k}) = \tilde{S}_{ax}(\mathbf{k})e^{-j\mathbf{k}\cdot\mathbf{r}'}e^{-p_1 z} \tag{6.3.6}$$

Substituting (6.3.6) and (6.3.2) into (6.3.3) and carrying out the two spatial integrations analytically lead to

$$H_{1a}(\mathbf{r}) = \sum_{n=1}^{2N} \frac{a_n}{(2\pi)^2}\iint_{-\infty}^{\infty} \tilde{P}_{ax}^{n}(\mathbf{k})\frac{e^{j(k_x x+k_y y-k_z|z|)}}{k_z}dk_x dk_y \quad ; \quad z>0 \tag{6.3.7}$$

where

$$p_1 = jk_z \tag{6.3.8}$$

$$\tilde{P}_{ax}^{n}(\mathbf{k}) = \tilde{S}_{ax}(\mathbf{k})\Gamma_y(k_y)\Gamma_{nx}^{-}(k_x)(-jp_1) \tag{6.3.9}$$

$$\Gamma_y = \pi w J_0(k_y w) \tag{6.3.10}$$

$$\Gamma_{nx}^{-} = \frac{-1}{jk_x}(e^{-jk_x x_n} - e^{-jk_x x_{n-1}}) \tag{6.3.11}$$

Next, define

$$\bar{N} = Ne^{-p_1 z} \tag{6.3.12}$$

where N can be $N_{1x}, N_{1x}^d, N_{1z}, N_{1z}^d$ defined in (2.5.2.4), (2.5.2.10), (2.6.2.28), and (2.6.2.29). Substituting (6.3.6) into (2.6.2.20-22) gives

$$\tilde{S}_{xx} = \frac{1}{j\omega\mu_3 p_3}[(k_1^2 - k_x^2)(\frac{\bar{N}_{1x}}{D_x}) - k_x^2(\frac{\bar{N}_{1z}^d}{D_x D_z})] \tag{6.3.13}$$

$$\tilde{S}_{yx} = \frac{1}{j\omega\mu_3 p_3}[(-k_x k_y)(\frac{\bar{N}_{1x}}{D_x} + \frac{\bar{N}_{1z}^d}{D_x D_z})] \tag{6.3.14}$$

$$\tilde{S}_{zx} = \frac{1}{j\omega\mu_3 p_3}[jk_x(\frac{\bar{N}_{1x}^d}{D_x}) + jk_x(k_1^2 + p_1^2)\frac{\bar{N}_{1z}}{D_x D_z})] \tag{6.3.15}$$

The integrals in (6.3.7) can be carried out numerically to obtain the scattered magnetic field. But when the distance $r=\sqrt{x^2+y^2+z^2}$ becomes large, the integrand in (6.3.7) becomes highly oscillatory. This makes accurate and efficient numerical integration almost impossible. This is where asymptotic approximation comes in. A stationary phase method is used to arrive at the first order approximation to the scattered far field [6][38]. The general procedure of this stationary phase method is outlined in section 6.2.2.

The Weyl identity [60] makes the approximation of (6.3.7) possible. This identity is given by

$$\frac{e^{-jkr}}{r} = \frac{-j}{2\pi}\int\int_{-\infty}^{\infty} dk_x dk_y \frac{e^{jk_x x + jk_y y - jk_z |z|}}{k_z} \tag{6.3.16}$$

where

$$k_x^2 + k_y^2 + k_z^2 = k^2 \ or \ k_z = \sqrt{k^2 - k_x^2 - k_y^2} \tag{6.3.17}$$

To satisfy the radiation condition, the branch cut of k_z is defined by

$$\mathrm{Im}[k_z]<0 \text{ and } Re[k_z]>0 \tag{6.3.18}$$

The physical interpretation of (6.3.16) is that a spherical wave can be expressed as an integral summation of plane waves propagating in all directions, including evanescent waves.

From (6.2.2.3-4) the stationary phase point $\mathbf{k}_x^{sp}$ is given as

$$\mathbf{k}^{sp} = \hat{x}k_x^{sp}+\hat{y}k_y^{sp}+\hat{z}k_z^{sp} \tag{6.3.19}$$

$$k_x^{sp} = k_1\frac{x}{r} = k_1\sin\theta\cos\phi \tag{6.3.20}$$

$$k_y^{sp} = k_1\frac{y}{r} = k_1\sin\theta\cos\phi \tag{6.3.21}$$

$$k_z^{sp} = k_1\frac{z}{r} = k_1\cos\theta \tag{6.3.22}$$

$$r = \sqrt{x^2+y^2+z^2}\ ;\ \ \theta \in [0,\pi]\ ;\ \ \phi \in [0,2\pi]\ . \tag{6.3.23}$$

For $r \rightarrow \infty$, substituting (6.3.16) and (6.3.19-23) into (6.3.7) leads to the first order approximation of scattered far field

$$H_{1a} = 2j\frac{e^{-jk_1r}}{4\pi r}[\sum_{n=1}^{2N} a_n\ \tilde{P}_{ax}^n(\mathbf{k}^{sp})]\ ;\ \ a=x,y,z\ . \tag{6.3.24}$$

The second term in brackets on the right hand side of equation (6.3.24) determines the radiation pattern of a slot in tri-layered media.

The radar cross section is defined as

$$RCS(\theta,\phi) = 4\pi r^2 \lim_{r\rightarrow\infty} |\frac{\mathbf{H}^s(\mathbf{r})}{\mathbf{H}^{in}(\mathbf{r})}|^2 \tag{6.3.25}$$

For a slot illuminated by a TM plane wave, using (6.3.24-25) and (3.1.1), the radar cross section can be written as:

$$RCS(\theta,\phi) = \frac{1}{\pi(H_{1x}^{in})^2}[(\sum_{n=1}^{2N} a_n \tilde{P}_{xx}^n(\mathbf{k}^{sp}))^2 +$$

$$(\sum_{n=1}^{2N} a_n \tilde{P}_{yx}^n(\mathbf{k}^{sp}))^2 + (\sum_{n=1}^{2N} a_n \tilde{P}_{yx}^n(\mathbf{k}^{sp}))^2] \; . \qquad (6.3.26)$$

CHAPTER SEVEN

NUMERICAL RESULTS

7.1 Numerical Results for a Monopole

FORTRAN programs have been written to implement the MoM solution for the monopole current and the scattered field described in chapter 5 and 6. These programs have been run on both IBM PC microcomputers and the Sun workstations of College of Engineering. The programs are very efficient and it takes a few minutes to run a case with twenty impedance matrix fillings on a fast 486 PC.

7.1.1 Comparison with Existing Numerical Results

To establish the validity of this analysis it is desirable to make a comparison with previously published results. The simplest possible comparison is with a dipole in free space, which is equivalent to an imaged monopole in free space. The input impedance of a dipole in free space is twice that of an imaged monopole in free space. Free space is the simplest special case of tri-layered media with both substrate and superstrate having unit permittivity and permeability. Figure 7.1.1 compares the input impedance of a dipole in free space obtain by the theory developed in the dissertation with that of King's book [4]. The two results are in good agreement.

Tesche [46] analyzed a dipole sandwiched between two perfectly conducting parallel plates using a Pocklington-type integral equation, the kernel of which was determined using an infinite image sequence. This situation can be handled by the present analysis if the superstrate is allowed to become perfectly conducting.

Figure 7.1.2 shows the input impedance of a half-wavelength dipole oriented vertically and centered between two conducting plates, as a function of the plate separation. The lossy layer is assumed to have a conductivity which gives $\varepsilon_2 = (1-j\,1000)\varepsilon_0$ and thus is, for all practical purposes, perfectly conducting. Agreement with Tesche's results is seen to be good. The discrepancies may be due to Tesche's use of the less stable Pocklington-type integral equation.

Comparison have also been made with work done by Chi and Alexopoulos [45], who has studied the radiation of an imaged monopole through a perfect dielectric substrate. This case is handled by assuming the superstrate (region 2) to be nearly free space. It has been found that to insure the proper convergence of the moment method matrix entries, the lossy layer must have some small, non-zero conductivity. Best agreement with [45] was obtained by using sinusoidal basis function detailed in [47].

Figures 7.2.3 and 7.2.4 show the input resistance and reactance of an imaged monopole radiating through a perfect dielectric substrate, for two values of substrate permittivity, as a function of antenna length. Agreement with [47] is seen to be quite good for most antenna lengths.

7.1.2 Comparison with Experimental Results

The effect of resistive coverings on the backscattering from a monopole on a conducting surface are studied experimentally by the Boeing Company, the sponsor of the research project. This experimental work was performed as an aid in confirming the analytical work presented in this dissertation. Backscatter measurements were made on a vacuum kayak measurement platform. The experimental setup is shown in Figure 7.1.21. A monopole is short circuited to the aluminum surface of a kayak measurement platform, which means that the load impedance is set to zero

$$Z_L = 0\ (\Omega)\ .$$

A 0.23 inch thick foam support and three resistive coverings were used. The foam is estimated to have near unit relative permittivity and permeability. Throughout the dissertation, a foam substrate is assumed to have unit relative permittivity and permeability. The three resistive sheets are believed to have constant surface resistances in the frequency range from 8GHz to 18GHz. The resistance R and thickness t of the three resistive sheets are:

$$R = 75(\Omega/\square)\ ;\ \ t = 4.72(mil) = 0.120(mm) \tag{7.1.2.1}$$

$$R = 250(\Omega/\square)\ ;\ \ t = 1.58(mil) = 0.0401(mm) \tag{7.1.2.2}$$

$$R = 500(\Omega/\square)\ ;\ \ t = 0.57(mil) = 0.0145(mm) \tag{7.1.2.3}$$

With the assumption that the resistance is independent of frequency, the complex permittivity can be written as

$$\varepsilon_2 = (1-j\frac{1}{Rt\,2\pi f\,\varepsilon_0})\varepsilon_0 \tag{7.1.2.4}$$

where f is the operation frequency and ε_0 is the free space permittivity.

The relative complex permeability of the resistive sheets is assumed to be one

$$\mu_2 = \mu_0\ . \tag{7.1.2.5}$$

Throughout the dissertation, air film, as the name implies, is a superstrate with unit relative permittivity and permeability.

Theoretical prediction of radar cross section of a shorted monopole in tri-layered media with foam substrate and four different superstrates versus frequency is compared with experimental data in Figure 7.1.5. The relevant parameters are specified in the plot. The complementary incident angle ϕ is formed by the incident wave vector and the ground plane. There is qualitative agreement between the experimental and theoretical results. The biggest discrepancy is 3dB and occurs at the high frequency end. The relevant parameters are marked in the figure.

Radar cross section of a monopole versus complementary incident angle at two operating frequencies is presented in Figure 7.1.6 and 7 respectively. The trend of the theoretical data and experimental data are the same. The qualitative agreement between numerical results and experimental ones in Figure 7.1.6 and 7 is not as good as that in Figure 7.1.5.

Several factors can possibly cause the discrepancy between the theoretical result and experimental one. The major factor is that the experimental setup is finite while the theoretical model is of infinite extend. The contribution to the total radar cross section from edge scattering can not be ignored. The assumption that the resistance is independent of frequency and foam substrate has unit relative permittivity and permeability may not hold in the frequency range from 8GHz to 18GHz. Accurate parameter of the foam and resistive sheets are not available. In the measurement of radar cross section versus frequency, both the antennas and the kayak platform are fixed in position. In the measurement of radar cross section versus incident angle, the antennas are stationary and the kayak platform is rotated. This can be the reason that the former measurement is more stable and accurate than the later one.

7.1.3 Results for Lossy Superstrates

It is necessary to check the convergence of algorithms, at least numerically. Figure 7.1.8 shows the input impedance of a monopole in layered media versus number of basis functions per wavelength. Two configurations are considered, one with an air film superstrate and a foam substrate, the other with a resistive sheet of 250 ohm and a PTFE substrate. The relevant parameters are clearly marked in the plot. The Figure 7.1.9 and Figure 7.1.10 show the radar cross section and received power versus the number of basis functions per wavelength for the same two configurations. A load impedance of 50 ohms is located at the center of the slot and a TM plane is illuminating the entire structure. The angle between the incident wave vector and the ground plane is 20 degrees.

It is observed that the input impedance is quite sensitive to the number of basis functions used and the radar cross section and received power are less sensitive to the number of basis functions. In the analysis of monopoles, the density of basis functions is in the range from 70 to 100 basis functions per wavelength.

In this section, the magnetic coating denotes a fictitious electrically and magnetically lossy layer with the following parameters:

$$\varepsilon_2 = (10-j0.5)\varepsilon_0 \;;\; \mu_2 = (5-j4)\mu_0 \;;\; t = 4.72(mil) = 0.12(mm) \; . \qquad (7.1.3.1)$$

The next ten figures are for the following geometry. A monopole of length 0.216 inch and radius 0.0185 inch is immersed in a substrate of thickness 0.23 inch. The substrate can be a foam substrate or a PTFE one. The monopole is loaded with a 50 ohm resistor. Five superstrates defined previously are used. The system is illuminated by a TM plane wave with 20 degree complementary incident angle.

The input resistance and reactance of an imaged monopole in tri-layered media with foam substrate and five different superstrates are presented in Figure 7.1.11 and 12 respectively. Figure 7.1.13 and 14 show the input resistance and reactance of an imaged monopole in tri-layered media with four superstrates and a PTFE substrate. Notice the down-shift of the peak resistance because the the monopole is electrically longer in PTFE than in foam.

Figure 7.1.15 and 16 give the radar cross section and received power of an imaged monopole in tri-layered media with a foam substrate and five different superstrates respectively. The radar cross section and received power of the same monopole in tri-layered media with a PTFE substrate and four different lossy superstrates are shown in Figure 7.1.17 and 18 respectively. Tri-layered media with a foam substrate and an air film is actually a half free space. The case of a monopole in layered media with a foam substrate and an air film is used as a reference to determine the effects of lossy superstrate on the scattering and receiving characteristics of a monopole in tri-layered media. Figure 7.1.15-18 demonstrate that the existence of a lossy superstrate reduces both the received power and radar cross section of a monopole. But the reduction of radar cross section is more than that of received power.

E-plane (y-z plane) radiation pattern of a monopole in a foam substrate under five different superstrates is presented in Figure 7.1.19 and E-plane pattern of the same monopole in a PTFE substrate under four lossy superstrates is shown in Figure 7.1.20.

7.2. Numerical Results for a Slot

The numerical results for slots in tri-layered media based on the theory described in the dissertation are presented in this section.

7.2.1. Comparison with Published Results

The most convincing way to validate theory and computer code is to compare experimental results with theoretical ones. The Electromagnetic Laboratory at Michigan State University does not have the capability to do radar cross section measurement. The next best way is compare numerical results with published results.

The simplest case is a slot in free space. S.A. Long [32] did experimental study of impedance of an open slot and a slot backed by different cavities. Figure 7.2.1 compares the measured impedance of an open slot, which radiates freely into the upper and lower half of the free space separated by a ground plane, with that generated by the computer code. The slot has a total length of 25cm (2l=25cm) and width of 1cm (2w=1cm). In the measurement, the ground plane is a quarter inch thick and eight square foot.

To compare with Long's experimental results, the parameters are set as such

$$\begin{array}{l} \varepsilon_1=\varepsilon_2=\varepsilon_3=\varepsilon_4=\varepsilon_0\ ;\ \ \mu_1=\mu_2=\mu_3=\mu_4=\mu_0 \\ 2l=25(cm)\ ;\ \ 2w=1(cm)\ ;\ \ d=1.5(mm)\ ;\ \ w=0.268(mm) \end{array} \tag{7.2.1.1}$$

Figure 7.2.1 shows the input impedance of an open slot. The results from the theory described in the dissertation show good agreement with that of Long. The minor discrepancies are caused by the fact that in the dissertation the ground plane is assumed to be infinite and infinitesimally thin while in Long's experiment the ground plane is finite and thick.

M. Kominami et al. [29] investigated printed dipole or slot antenna on a semi-infinite substrate and infinite phased arrays of these elements. The results in [29] are compared with the numerical results in the next two figures. Figure 7.2.2 gives the input impedance of a slot on a PTFE (ε_r=2.55, tanδ=0.002; X*-band*) semi-infinite substrate. Figure 7.2.3 gives the input impedance of a slot on a semi-infinite GaAs substrate (ε_r=12.8, tanδ=0.002; X*-band*).

The rest of parameters are set as

$$\begin{aligned} &\varepsilon_1=\varepsilon_2=\varepsilon_3=\varepsilon_0\ ,\ \varepsilon_4=(2.55-j0.0051)\varepsilon_0\ (PTFE)\ or\ (12.8-j0.0256)\varepsilon_0\ (GaAs) \\ &\mu_1=\mu_2=\mu_3=\mu_4=\mu_0\ ;\ \ w/l=0.02 \end{aligned} \tag{7.2.1.2}$$

The numerical results agree with Kominami's published results very well.

7.2.2 Results for Lossy Superstrates

This section contains the numerical results of a slot in tri-layered media with different superstrates and substrates. Terms of interests are input impedance, radar cross section, received power, and radiation pattern.

Three kinds of superstrates are used. The first superstrate, denoted as air film, is a vacuum layer with permittivity $\varepsilon_2=\varepsilon_0$, permeability $\mu_2=\mu_0$, and thickness t=0.12mm. The second superstrate, denoted as resistive cover, is an electrically lossy sheet with resistance R=75($\Omega/\Box$), permeability $\mu_2=\mu_0$, and thickness t=0.12mm. The third superstrate, denoted as magnetic coating, is a fictitious electrically and magnetically lossy coating with permittivity $\varepsilon_2=(10-j0.5)\varepsilon_0$, permeability $\mu_2=(5-j4)\mu_0$, and thickness t=0.12mm.

The resistance of the resistive cover is assumed to be constant in the frequency range of interest and the real part of relative complex permittivity is assumed to be one. This assumption makes the relative permittivity a function of frequency, which is written as

$$\sigma = \frac{1}{Rt} \tag{7.2.2.1}$$

$$\varepsilon_2 = \varepsilon_0\left(1 - j\frac{\sigma}{\omega\varepsilon_0}\right) \tag{7.2.2.2}$$

In the frequency range of interest, the imaginary part of $\varepsilon_2/\varepsilon_0$ is in the order of one hundred while the real part is in the order of one. So the above assumption is a good approximation.

Three substrates are used. The first is a foam substrate with permittivity $\varepsilon_3=\varepsilon_0$ and permeability $\mu_3=\mu_0$. The second is a reinforced PTFE substrate with permittivity $\varepsilon_3=(2.20-j0.00198)\varepsilon_0$ and permeability $\mu_3=\mu_0$. The third is a GaAs substrate with permittivity $\varepsilon_3=(12.9-j0.0258)\varepsilon_0$ and permeability $\mu_3=\mu_0$. The last two are commonly used substrates in microwave and millimeter-wave frequency range [18]. Another way to present complex relative permittivity is to use dielectric constant ε_r and loss tangent $\tan\delta$

$$\varepsilon = \varepsilon_r\varepsilon_0(1 - j\tan\delta) \tag{7.2.2.3}$$

Figure 7.2.4 gives the input impedance of a slot in tri-layered media with an air film superstrate and a foam substrate. Figure 7.2.5 shows the input impedance of a slot in tri-layered media with a magnetic coating and a foam substrate and Figure 7.2.6 gives the input impedance of a slot in tri-layered media with a resistive sheet superstrate and a foam substrate. The parameters for the above three figures are set to be

$$\begin{gathered} \varepsilon_1=\varepsilon_3=\varepsilon_4=\varepsilon_0\ ;\ \ \mu_1=\mu_3=\mu_4=\mu_0 \\ t=0.12(mm),\ d=1.5(mm),\ l=5.26(mm),\ w=0.268(mm)\ . \end{gathered} \tag{7.2.2.4}$$

The length of the slot is chosen such that at 14GHz, the length of the slot equals to a quarter of free space wavelength.

Figure 7.2.7 shows the input impedance of a slot in tri-layered media with a resistive sheet superstrate and a PTFE substrate. The relevant parameters are

$$\begin{aligned}
&\varepsilon_1=\varepsilon_3=\varepsilon_4=\varepsilon_0, \;;\; \mu_1=\mu_2=\mu_3=\mu_4=\mu_0 \\
&\varepsilon_2=(2.20-j\,0.00198)\varepsilon_0 \\
&t=0.12(mm),\ d=1.5(mm),\ l=5.26(mm),\ w=0.268(mm)
\end{aligned} \qquad (7.2.2.5)$$

Figure 7.2.8 gives the input impedance of a slot in tri-layered media with a resistive sheet superstrate and a GaAs substrate. The relevant parameters are

$$\begin{aligned}
&\varepsilon_1=\varepsilon_3=\varepsilon_4=e\,0, \;;\; \mu_1=\mu_2=\mu_3=\mu_4=\mu_0 \\
&\varepsilon_2=(12.9-j\,0.0258)\varepsilon_0 \\
&t=0.12(mm),\ d=1.5(mm),\ l=5.26(mm),\ w=0.268(mm)
\end{aligned} \qquad (7.2.2.6)$$

Throughout this section, a load impedance Z_L is placed at the center of the slot and the slot is illuminated by a TM plane wave (E_y, E_z, H_x) with an incident angle θ_0

$$\begin{aligned}
&Z_L = 500\ \Omega \\
&\theta_0 = 60^\circ
\end{aligned} \qquad (7.2.2.7)$$

The radar cross section and received power of a slot in tri-layered media with a foam substrate and different superstrates, namely air film, resistive sheet, and magnetic coating, are given in Figure 7.2.9 and 10 respectively. It can be seen from Figure 7.2.9 and 10 that with a resistive sheet or a magnetic coating, the reduction of radar cross section is more than the reduction of received power. The case of a slot in tri-layered media with an air film and a foam substrate is used as reference. For example, at 14GHz the reduction of the radar cross section is 6.79dB for the case of a resistive sheet and 4.88dB for the case of a magnetic coating. At the same frequency, the reduction of the received power is 4.53dB for the case of a resistive sheet and 2.57dB for the case of a magnetic coating.

The radar cross section and received power of a slot in tri-layered media with a resistive sheet and different substrates, namely foam, PTFE, GaAs, are presented in Figure 7.2.11 and 12 respectively. The relevant parameters are given in (7.2.2.6-7). An observation can be made from Figure 7.2.11 and 12. The higher the dielectric constant of the substrate, the more the reduction of both radar cross section and received power. In other words, a substrate with high dielectric constant will decrease the radiation capability of a slot.

The E-plane (y-z plane) radiation patterns of a slot in layered media with a foam substrate and different superstrate are presented in Figure 7.2.13. Figure 7.2.14 shows the H-plane (x-z plane) radiation pattern. Figure 7.2.15 and 16 present the radiation pattern of a slot in tri-layered media with a resistive sheet and three different substrates in E-plane and H-plane respectively. For all the radiation patterns, the operating frequency is 14GHz. There are significant changes of E-plane pattern for various superstrates and substrates. The change of superstrate and substrate does not alter the H-plane pattern very much.

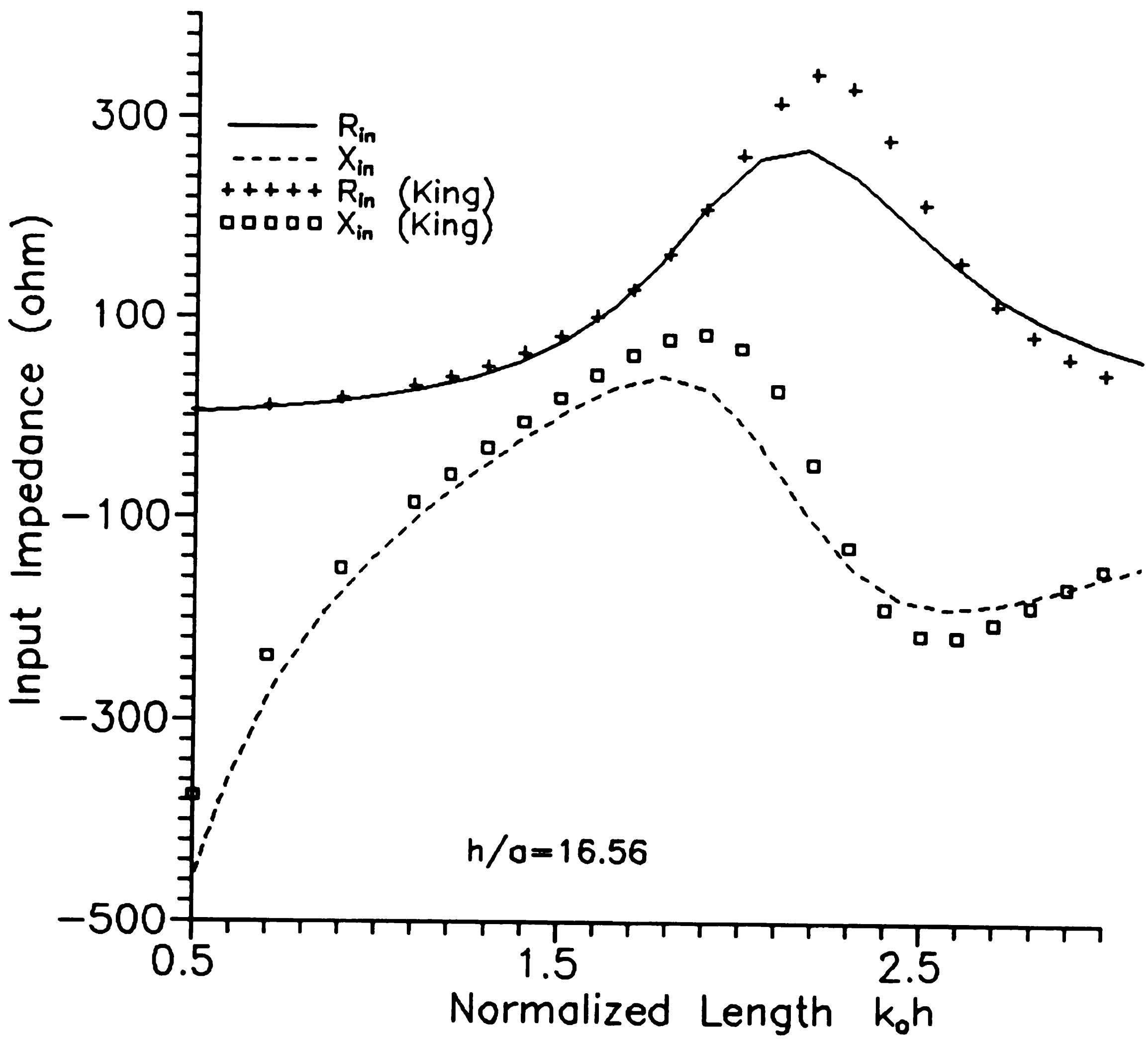

Figure 7.1.1 Input impedance of dipole in free space.

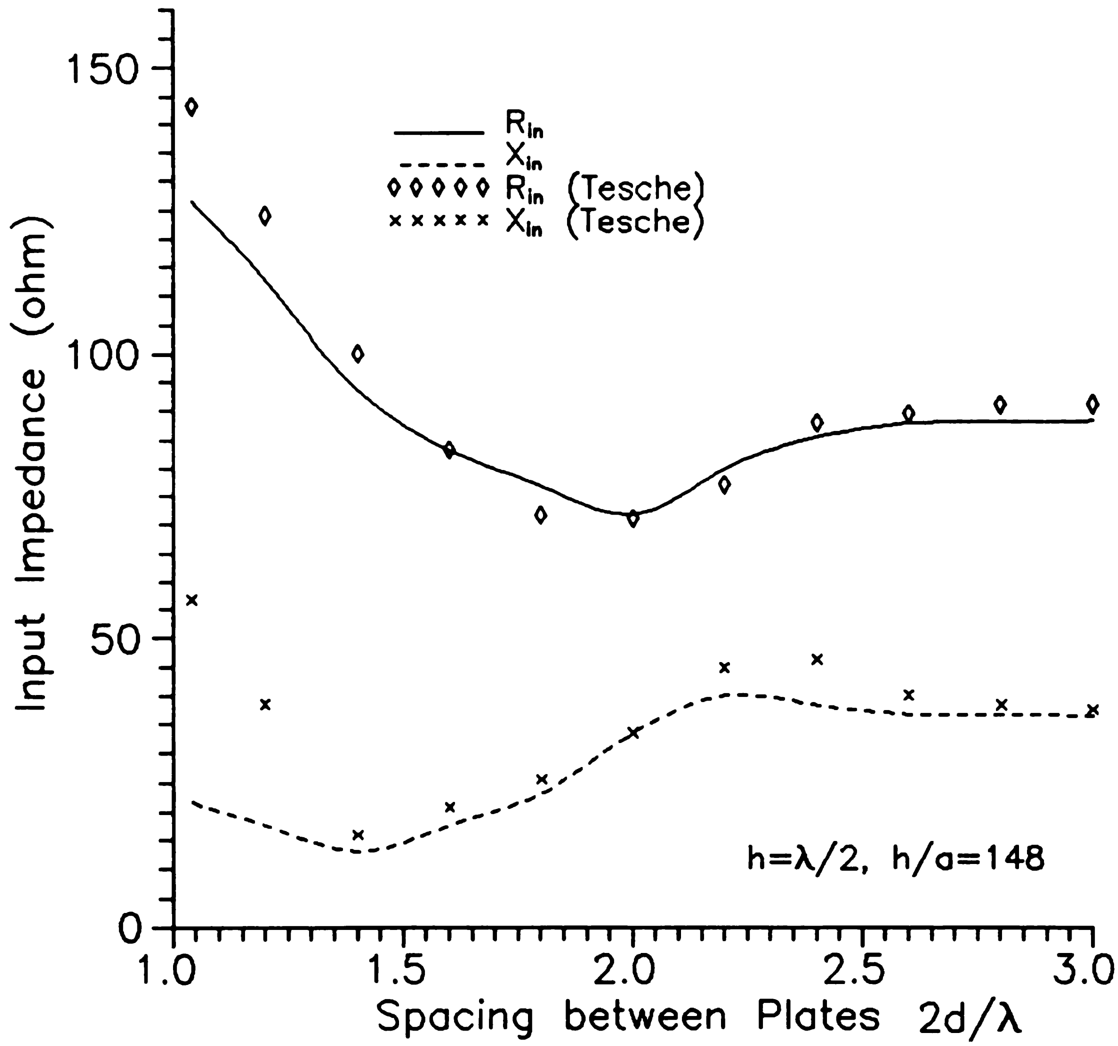

Figure 7.1.2 Input impedance of dipole between two parallel conducting plates.

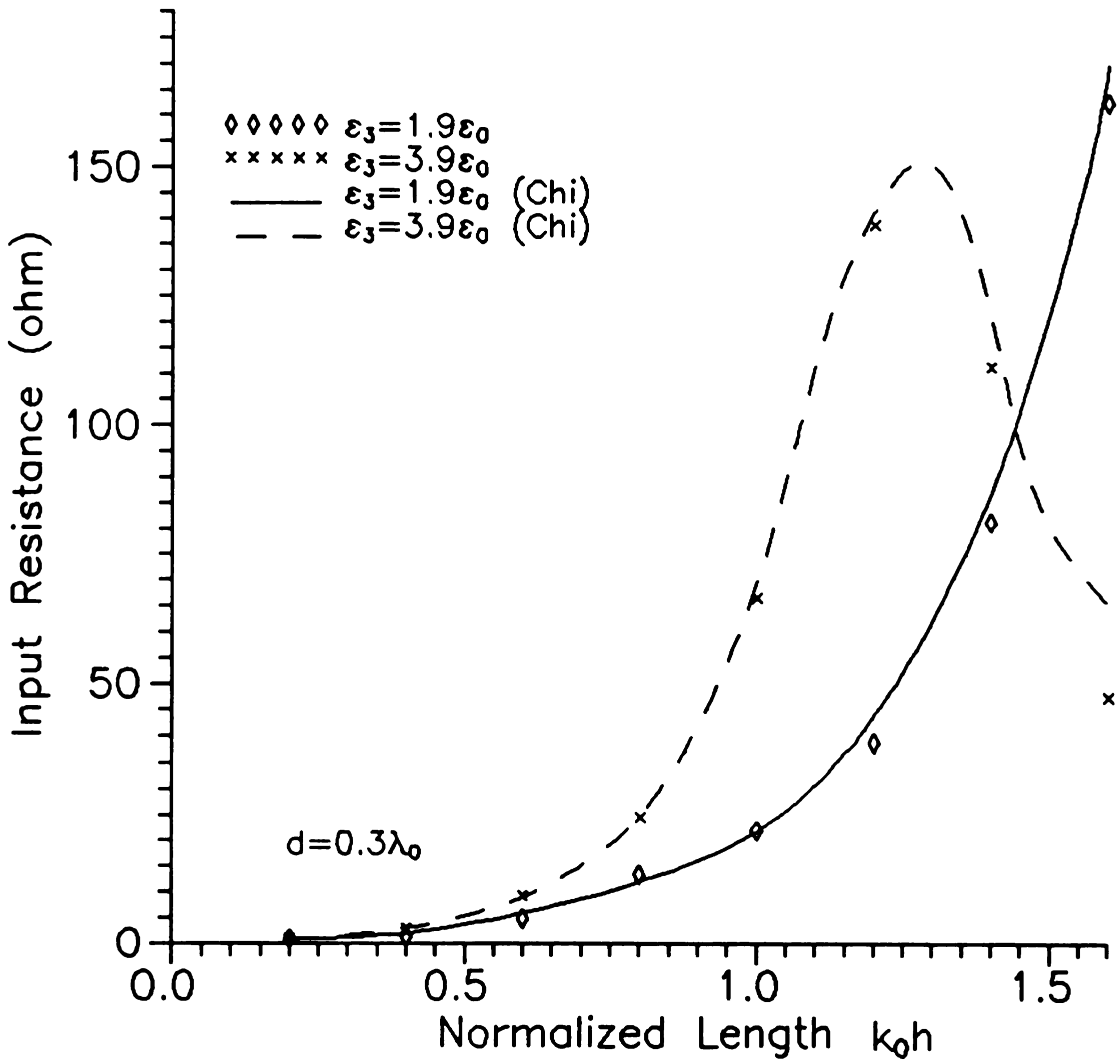

Figure 7.1.3 Input resistance of probe through substrate.

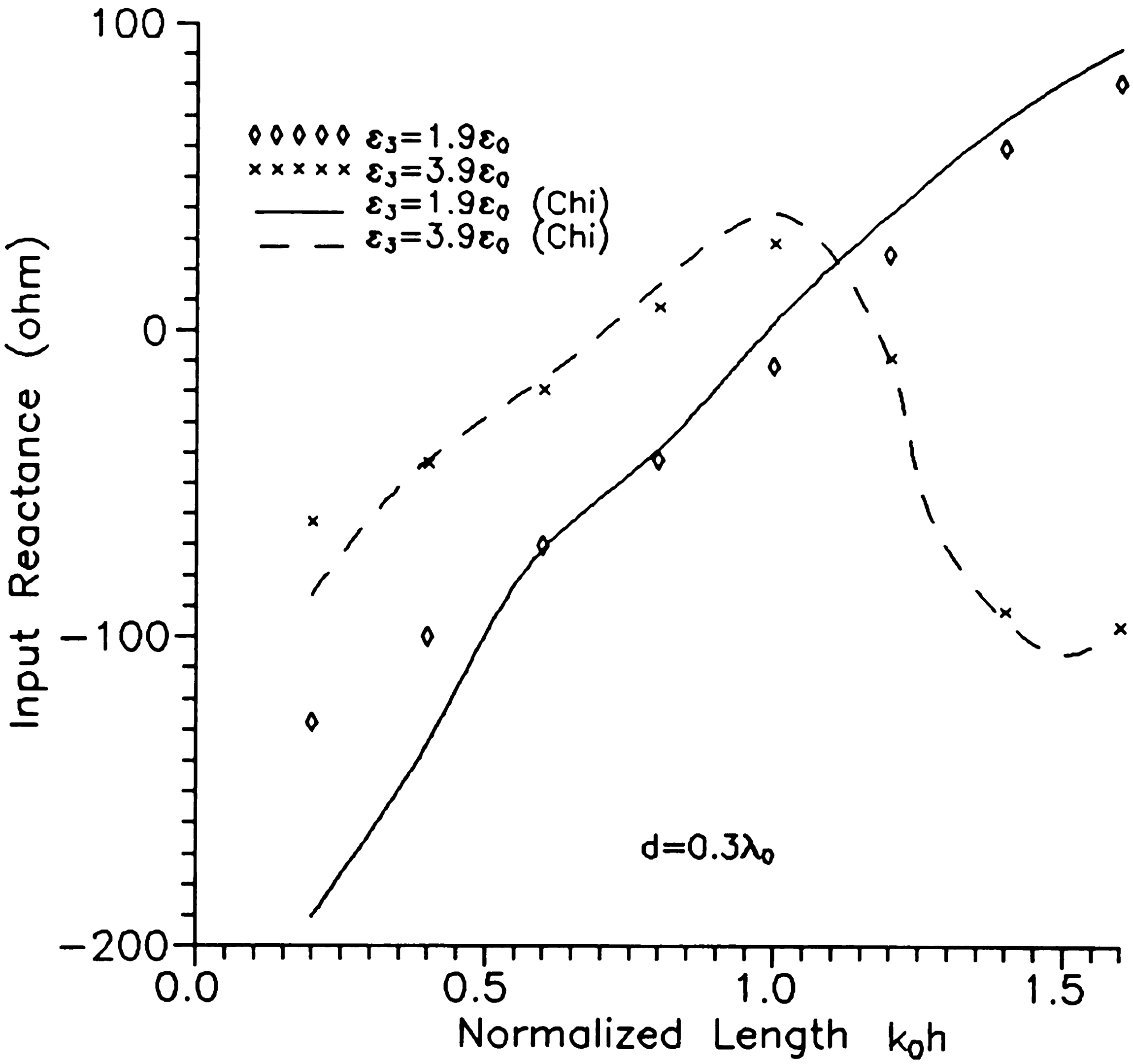

Figure 7.1.4 Input reactance of probe through substrate.

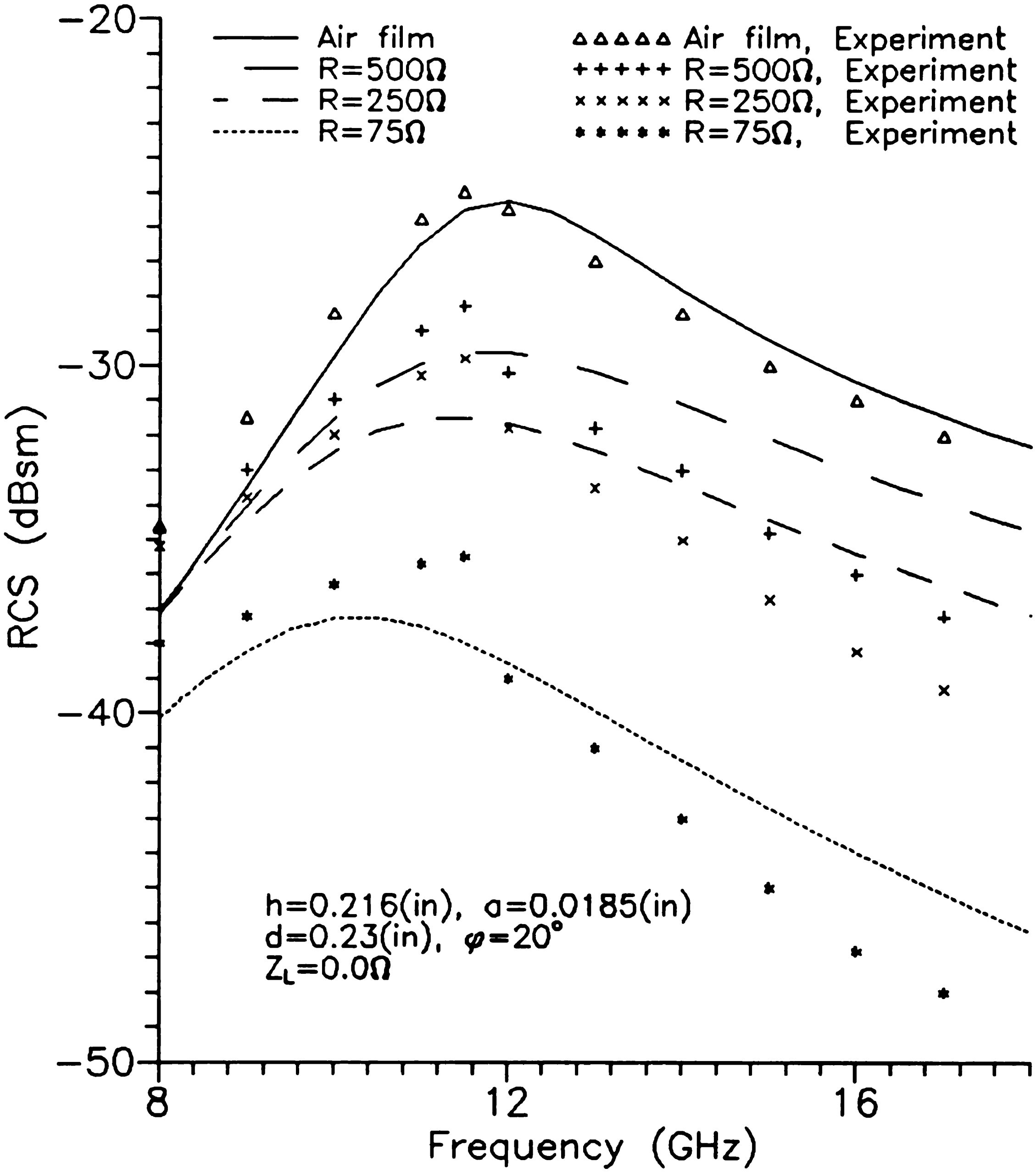

Figure 7.1.5 Radar cross section of monopole in tri-layered media with foam substrate and various superstrates versus frequency.

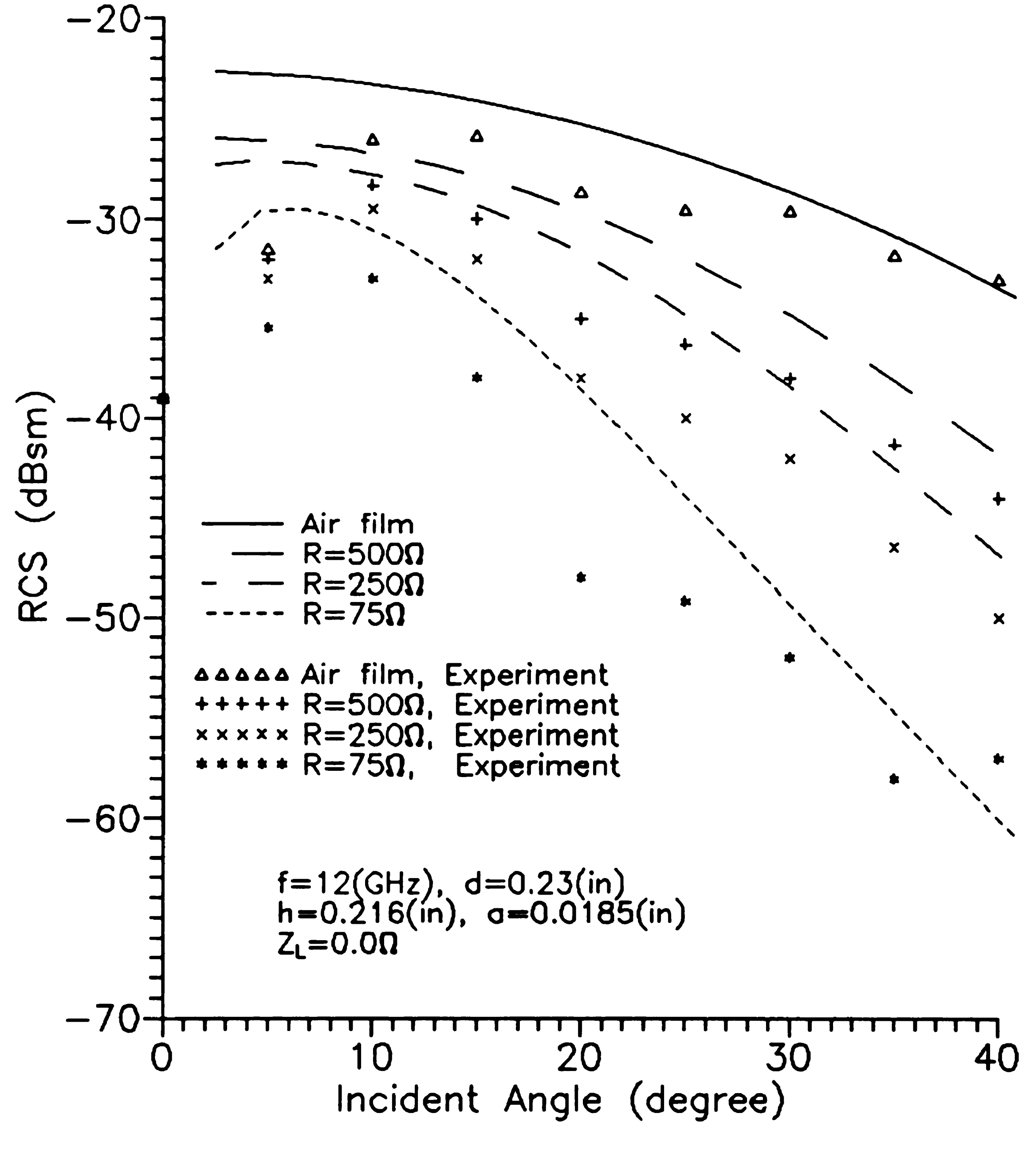

Figure 7.1.6 Radar cross section of monopole in tri-layered media with foam substrate and various superstrates versus incident angle at 12GHz.

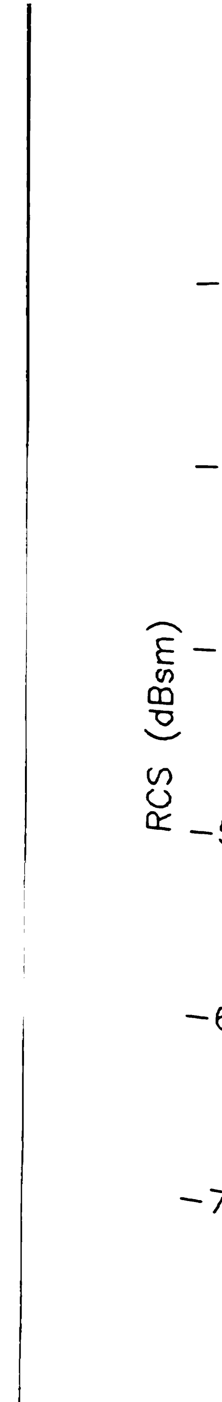

Figure 7.1.

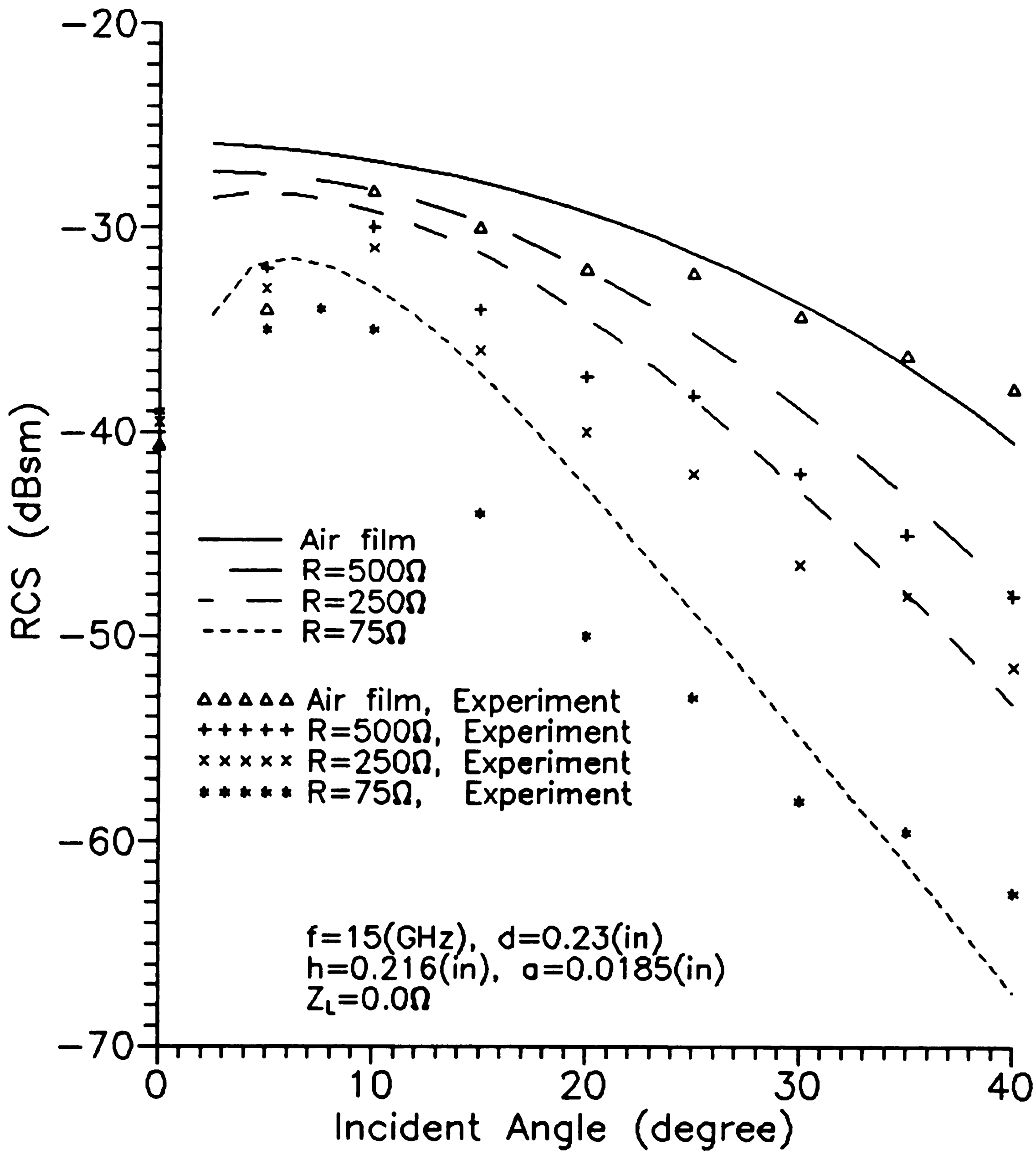

Figure 7.1.7 Radar cross section of in tri-layered media with foam substrate and various superstrates versus incident angle at 15GHz.

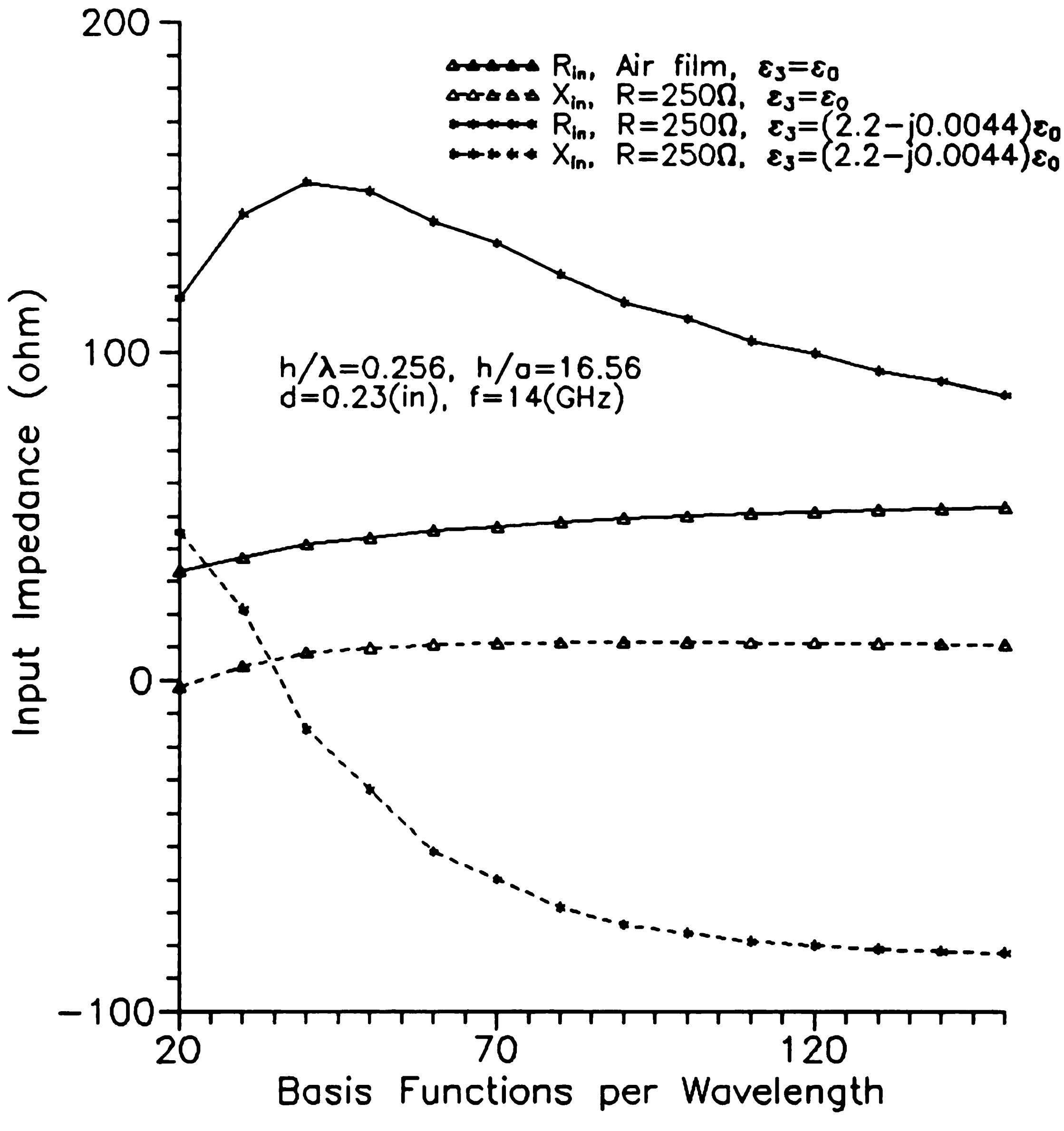

Figure 7.1.8 Input impedance of imaged monopole in tri-layered media versus number of basis functions.

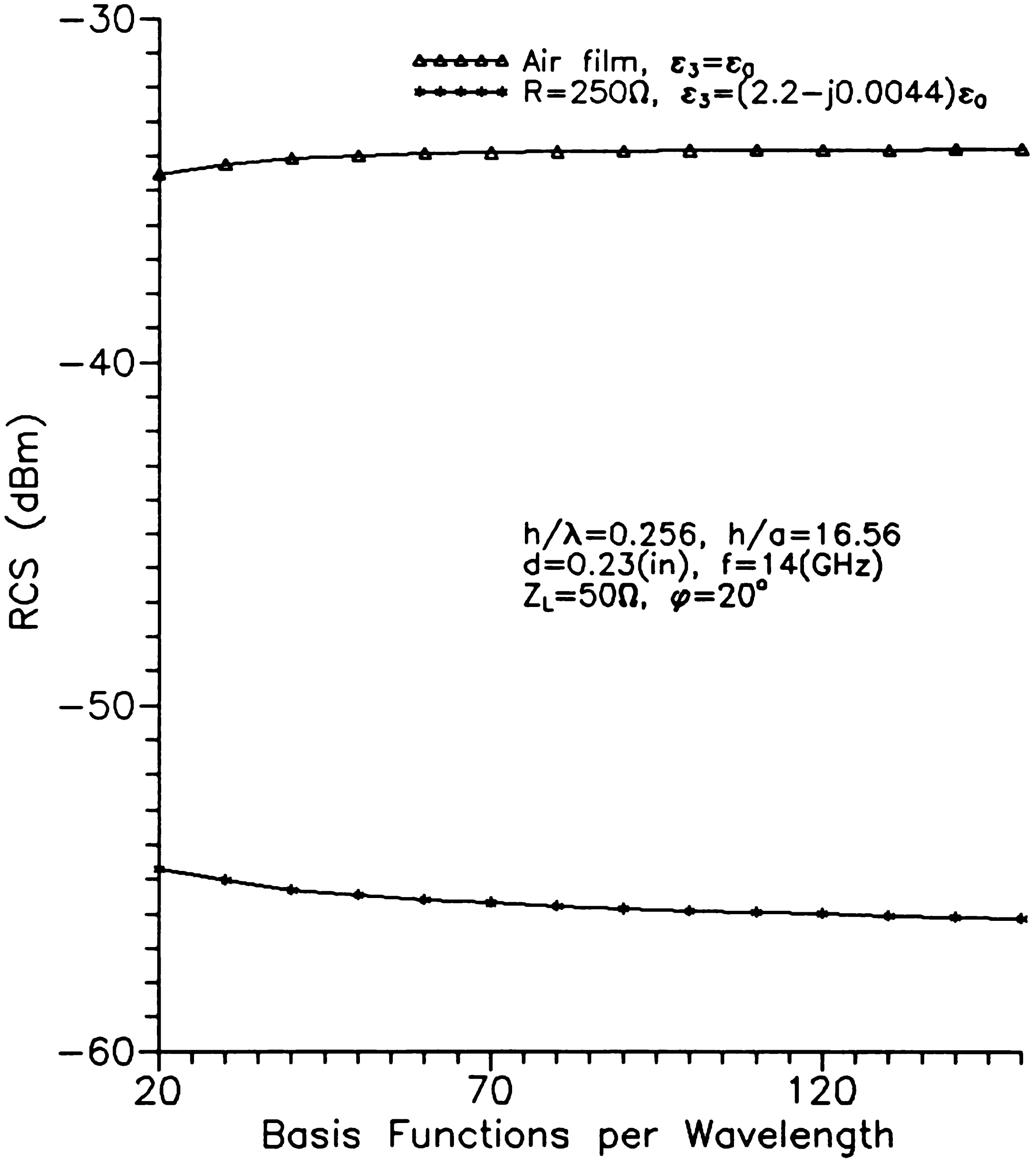

Figure 7.1.9 Radar cross section of imaged monopole in tri-layered media versus number of basis functions.

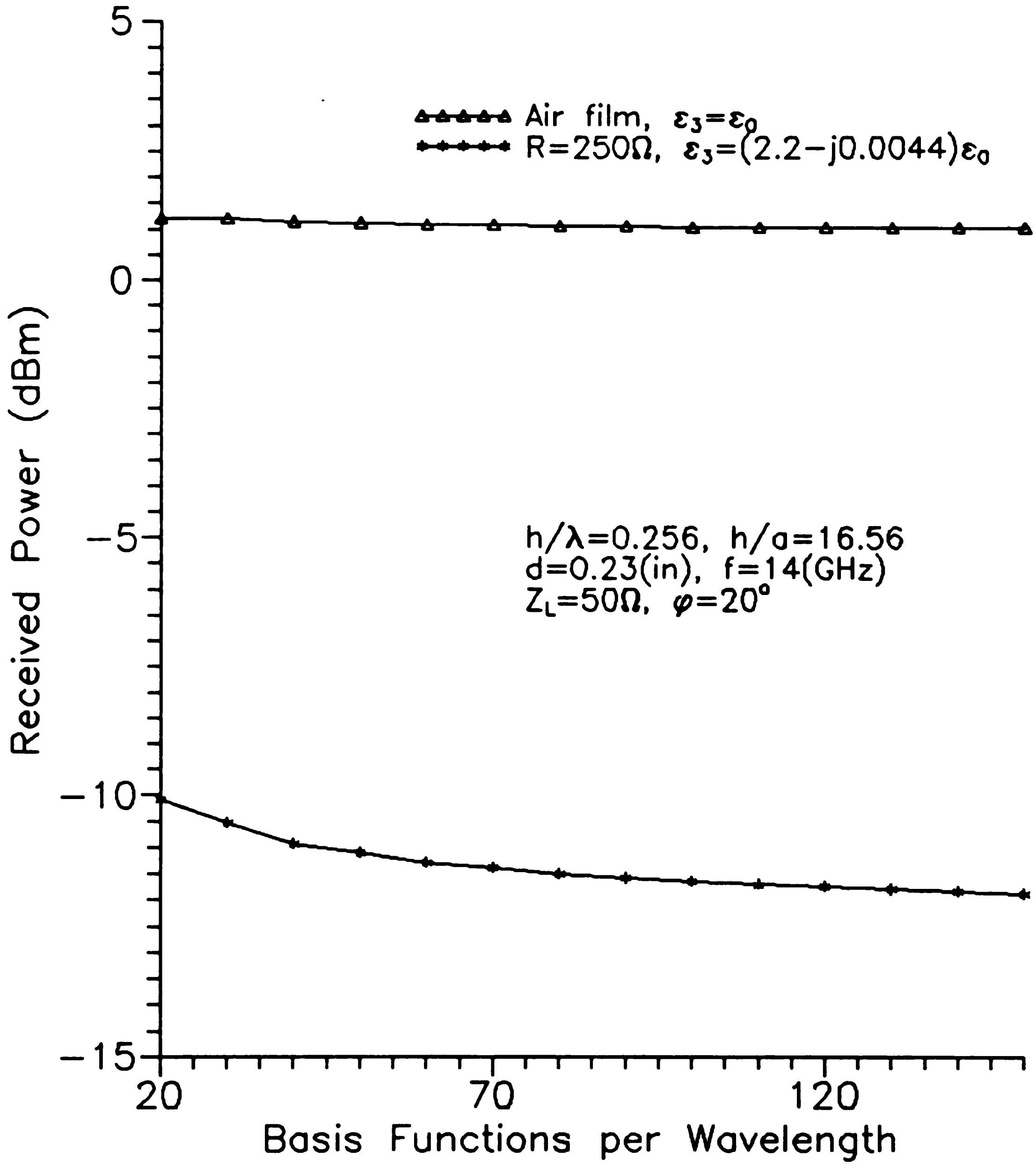

Figure 7.1.10 Received power of imaged monopole in tri-layered media versus number of basis functions.

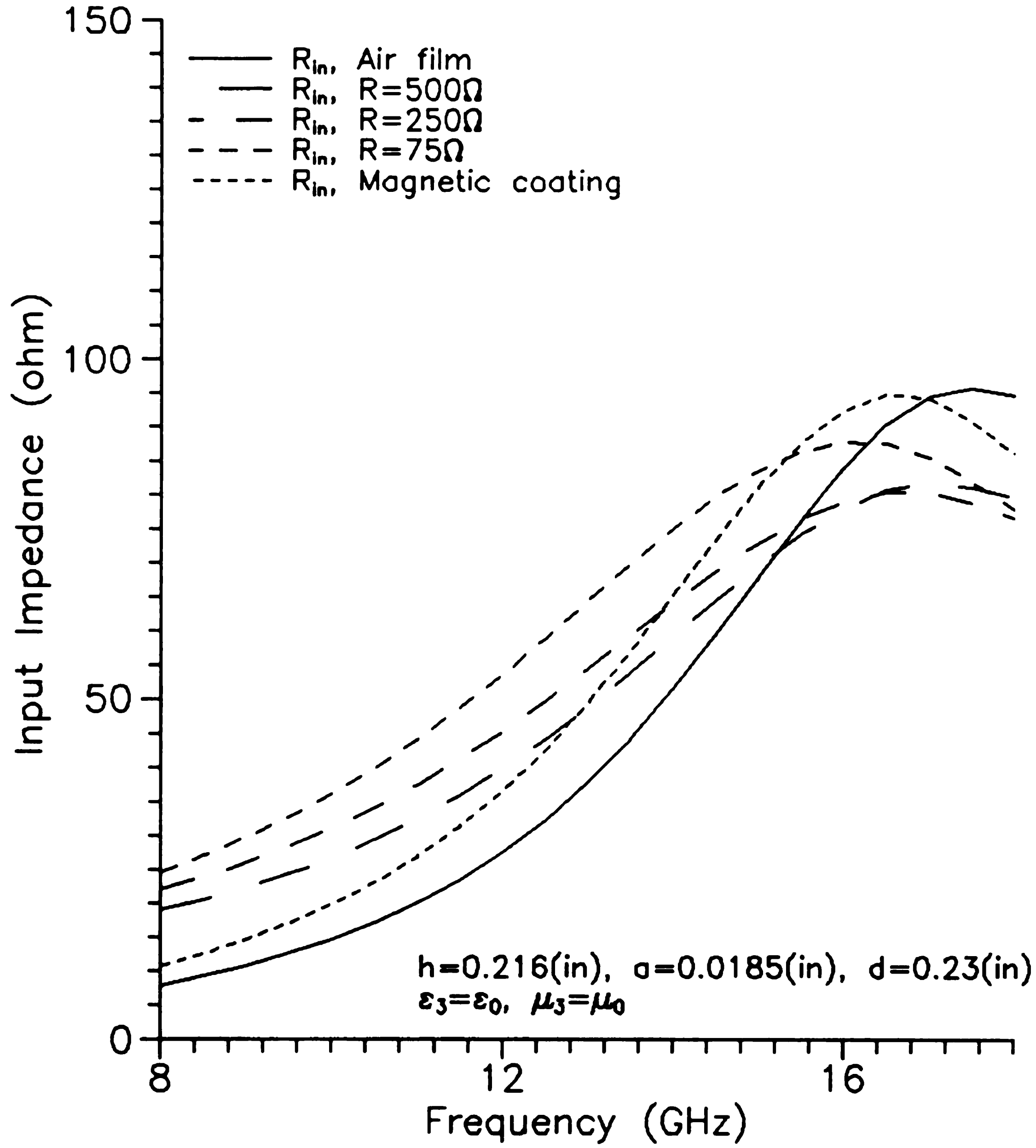

Figure 7.1.11 Input resistance of imaged monopole in tri-layered media with foam substrate and different superstrates.

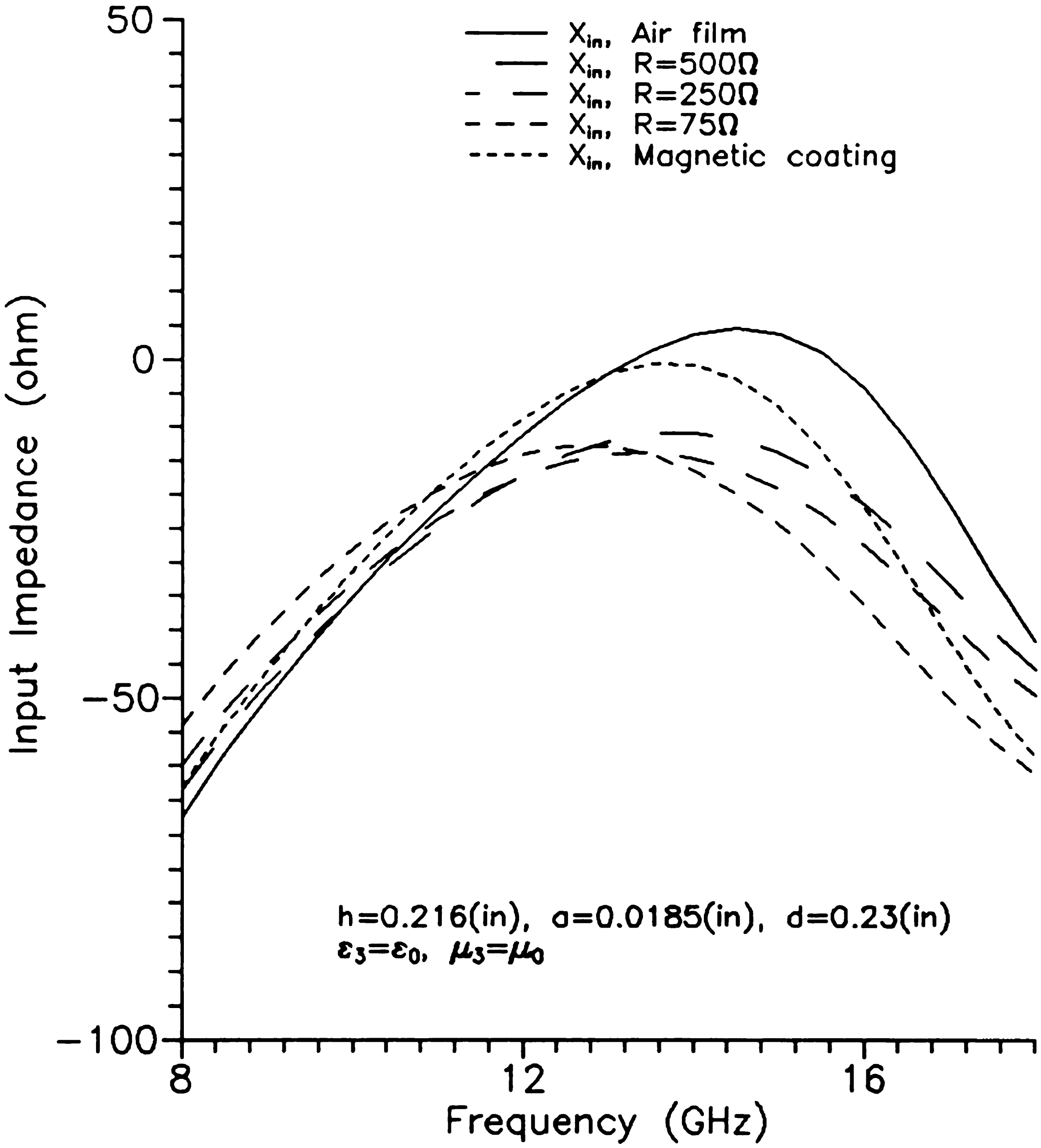

Figure 7.1.12 Input reactance of imaged monopole in tri-layered media with foam substrate and different superstrates.

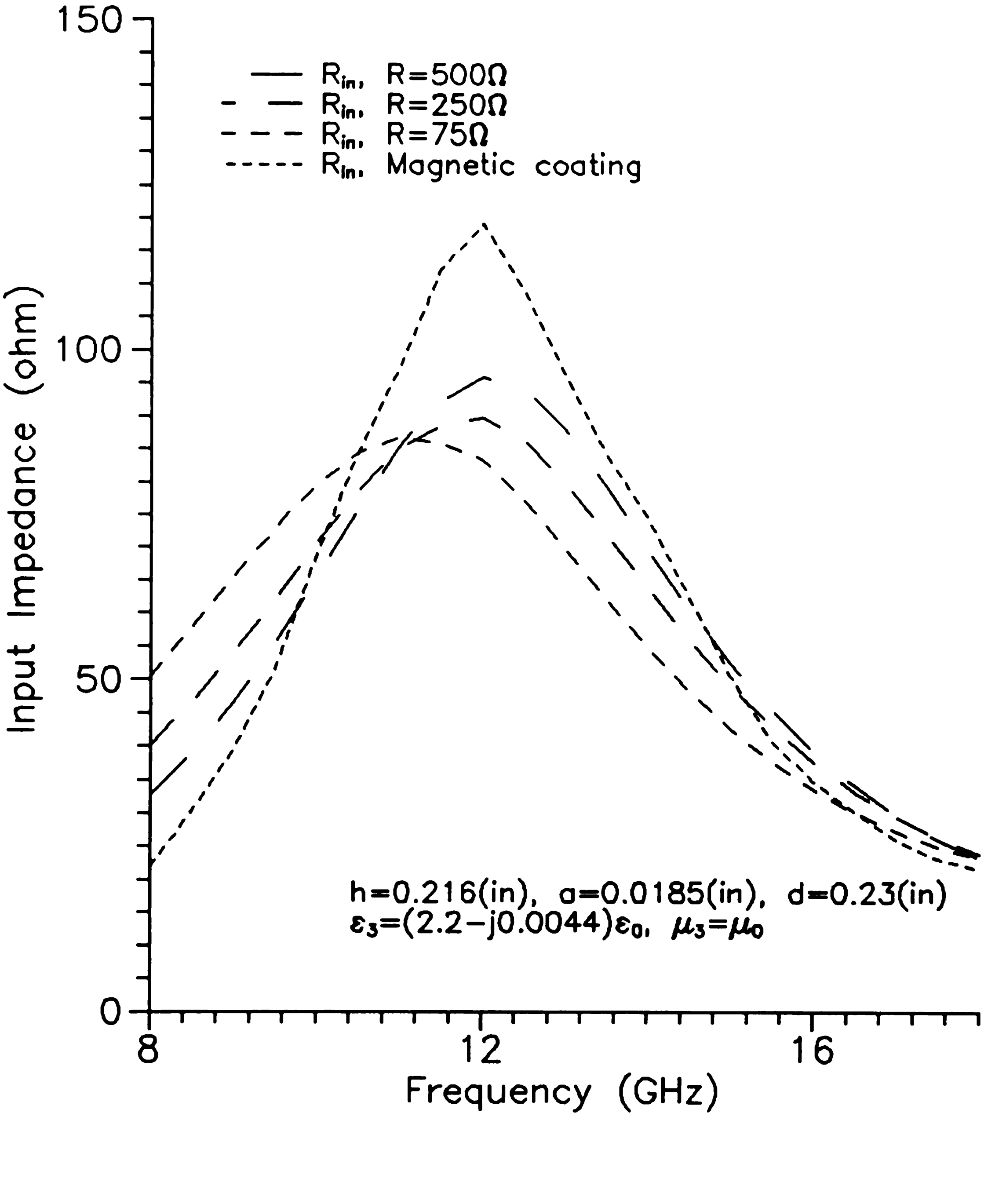

Figure 7.1.13 Input resistance of imaged monopole in tri-layered media with PTFE substrate and different superstrates.

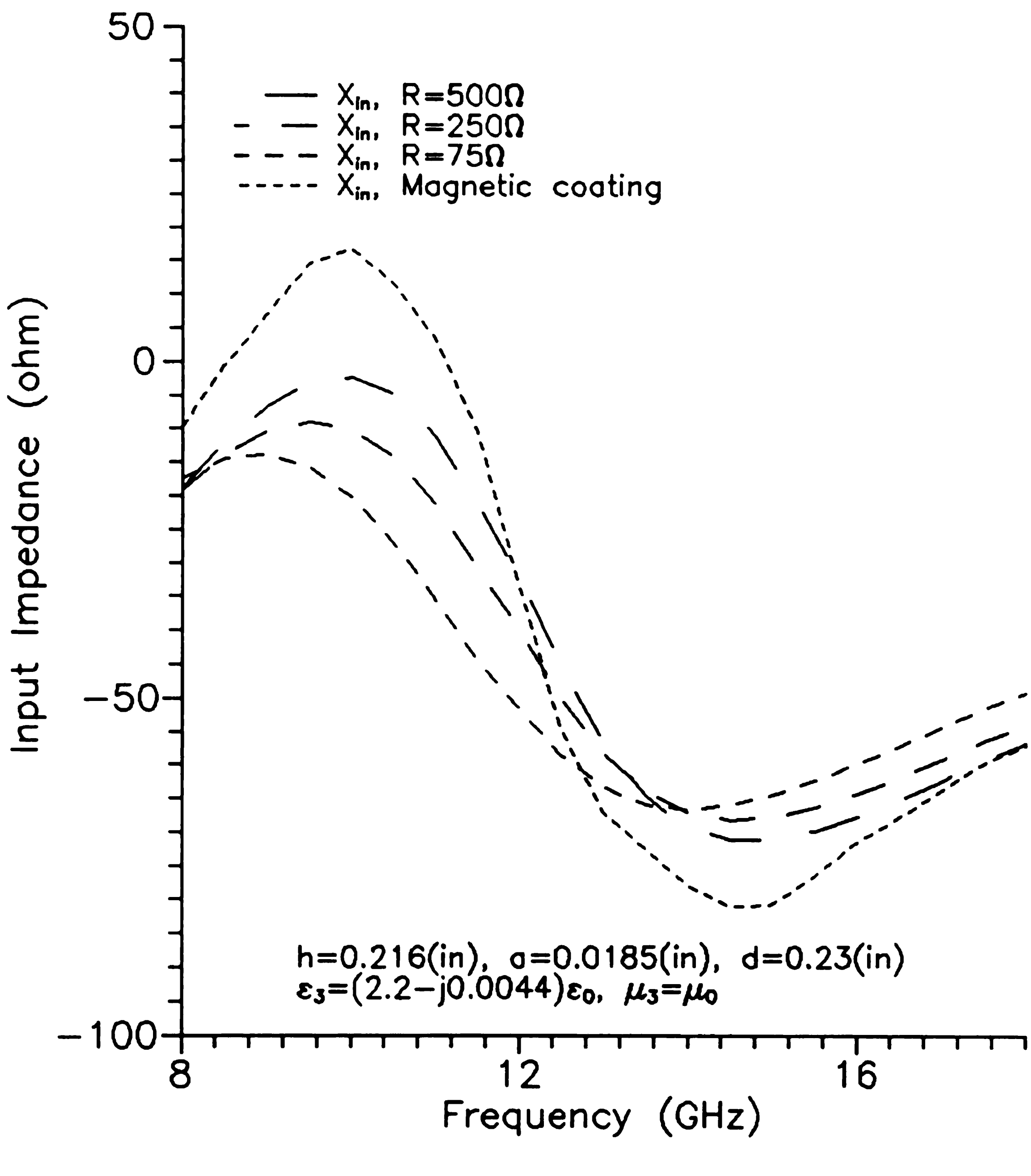

Figure 7.1.14 Input reactance of imaged monopole in tri-layered media with PTFE substrate and different superstrates.

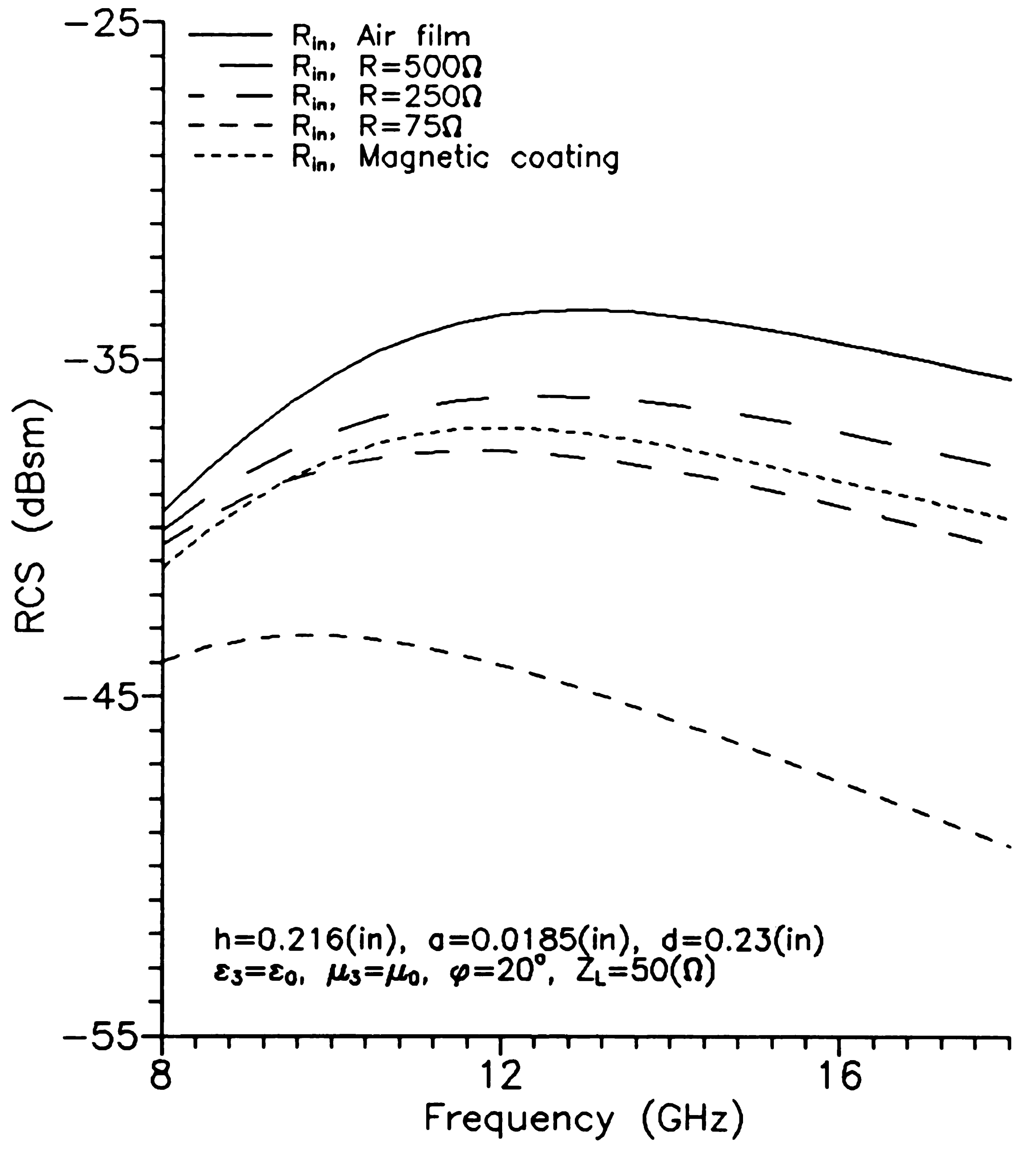

Figure 7.1.15 Radar cross section of imaged monopole in tri-layered media with foam substrate and different superstrates.

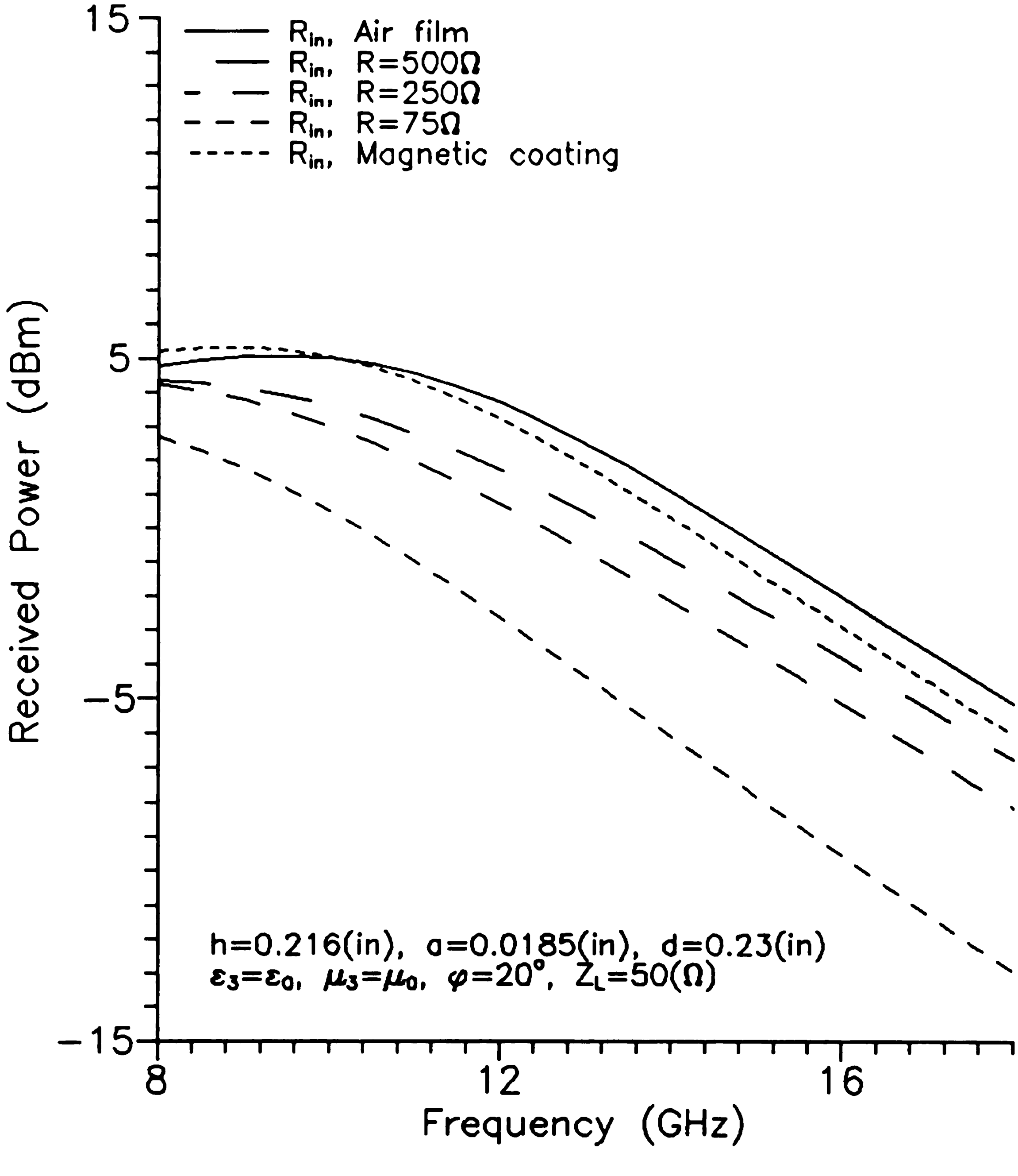

Figure 7.1.16 Received power of imaged monopole in tri-layered media with foam substrate and different superstrates.

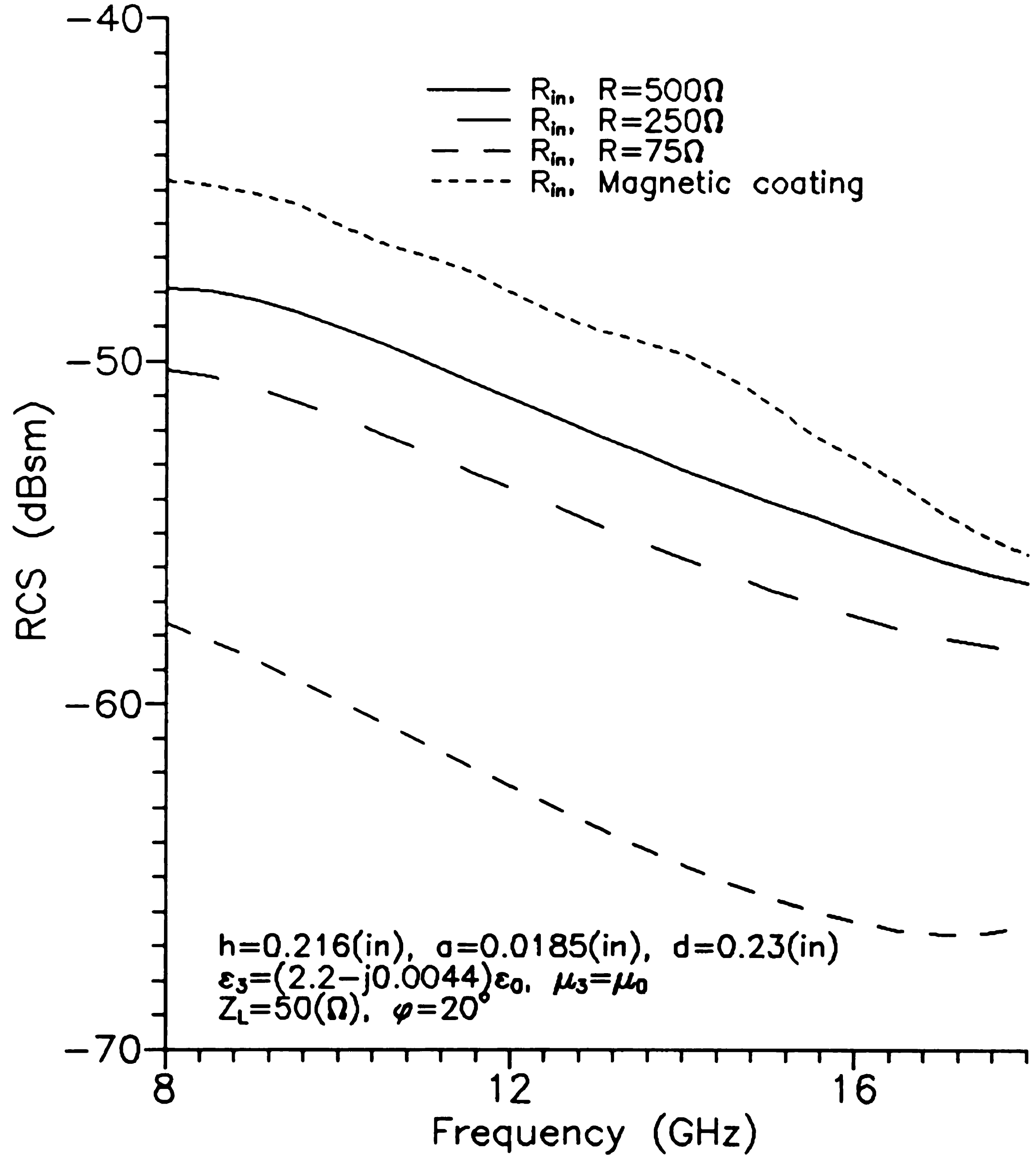

Figure 7.1.17 Radar cross section of imaged monopole in tri-layered media with PTFE substrate and different superstrates.

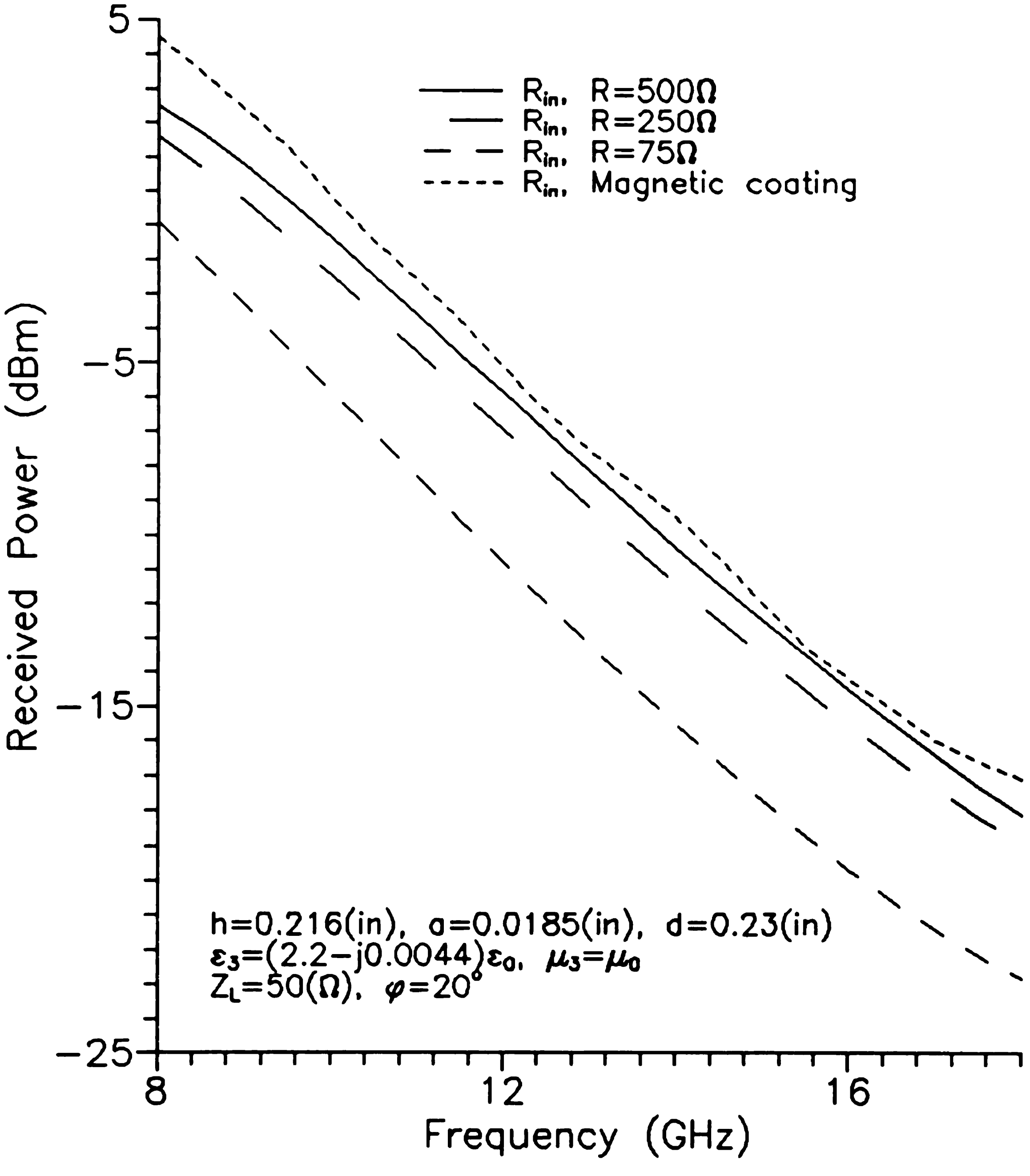

Figure 7.1.18 Received power of imaged monopole in tri-layered media with PTFE substrate and different superstrates.

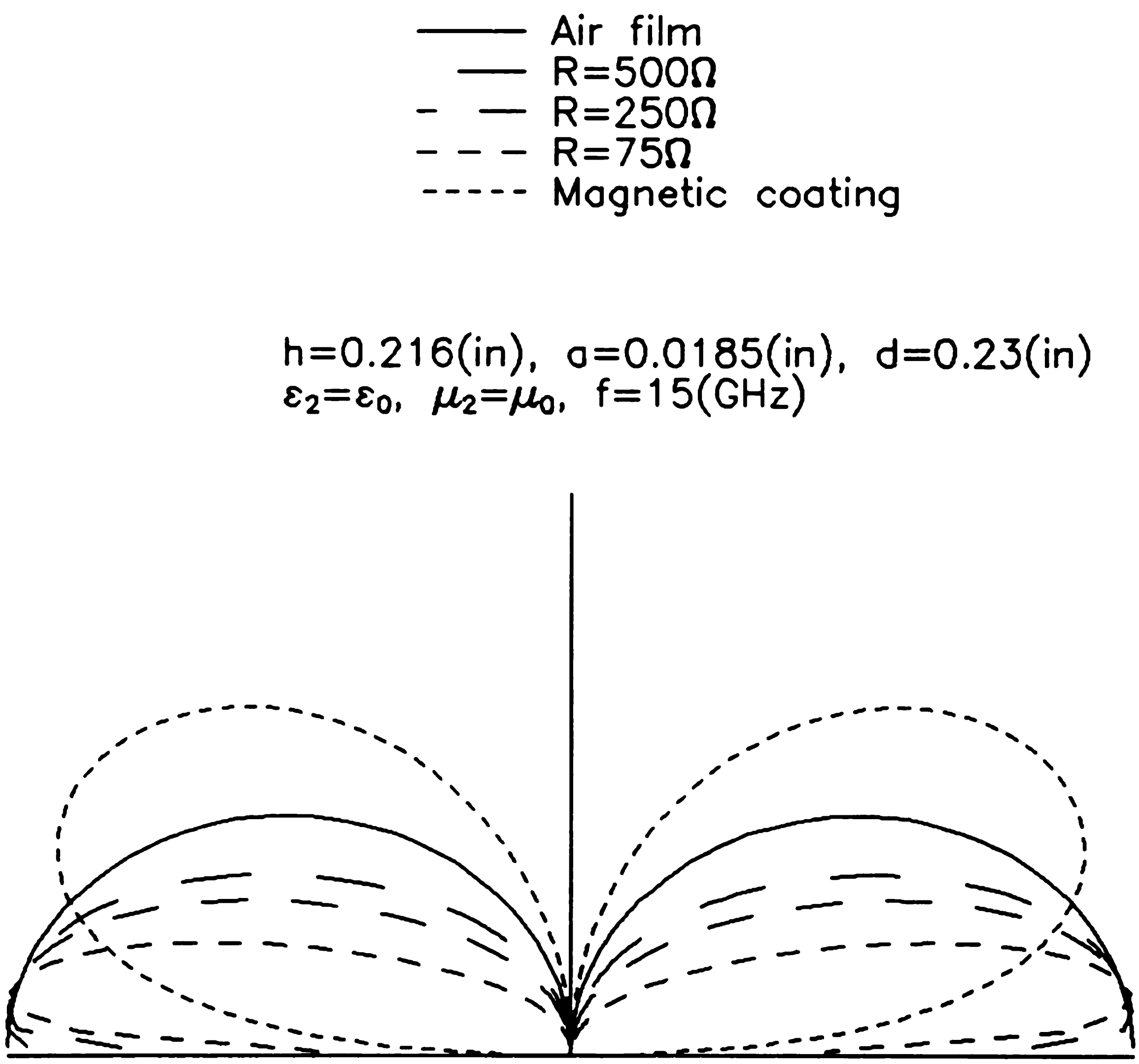

Figure 7.1.19 E-plane radiation pattern of imaged monopole in tri-layered media with foam substrate and different superstrates.

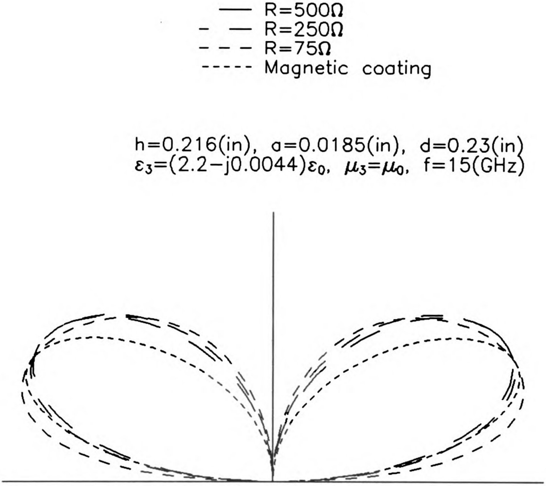

Figure 7.1.20 E-plane radiation pattern of imaged monopole in tri-layered media with PTFE substrate and different superstrates.

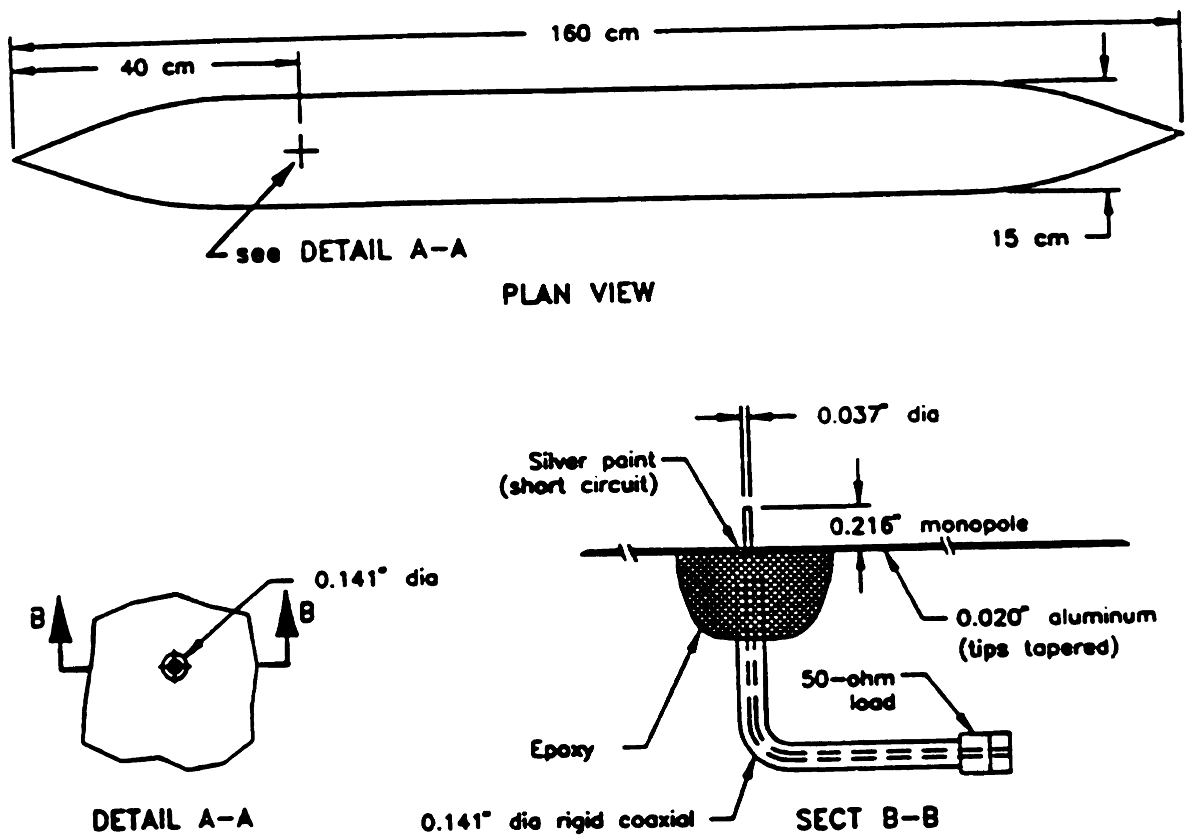

Figure 7.1.21 Drawing of vacuum kayak measurement platform.

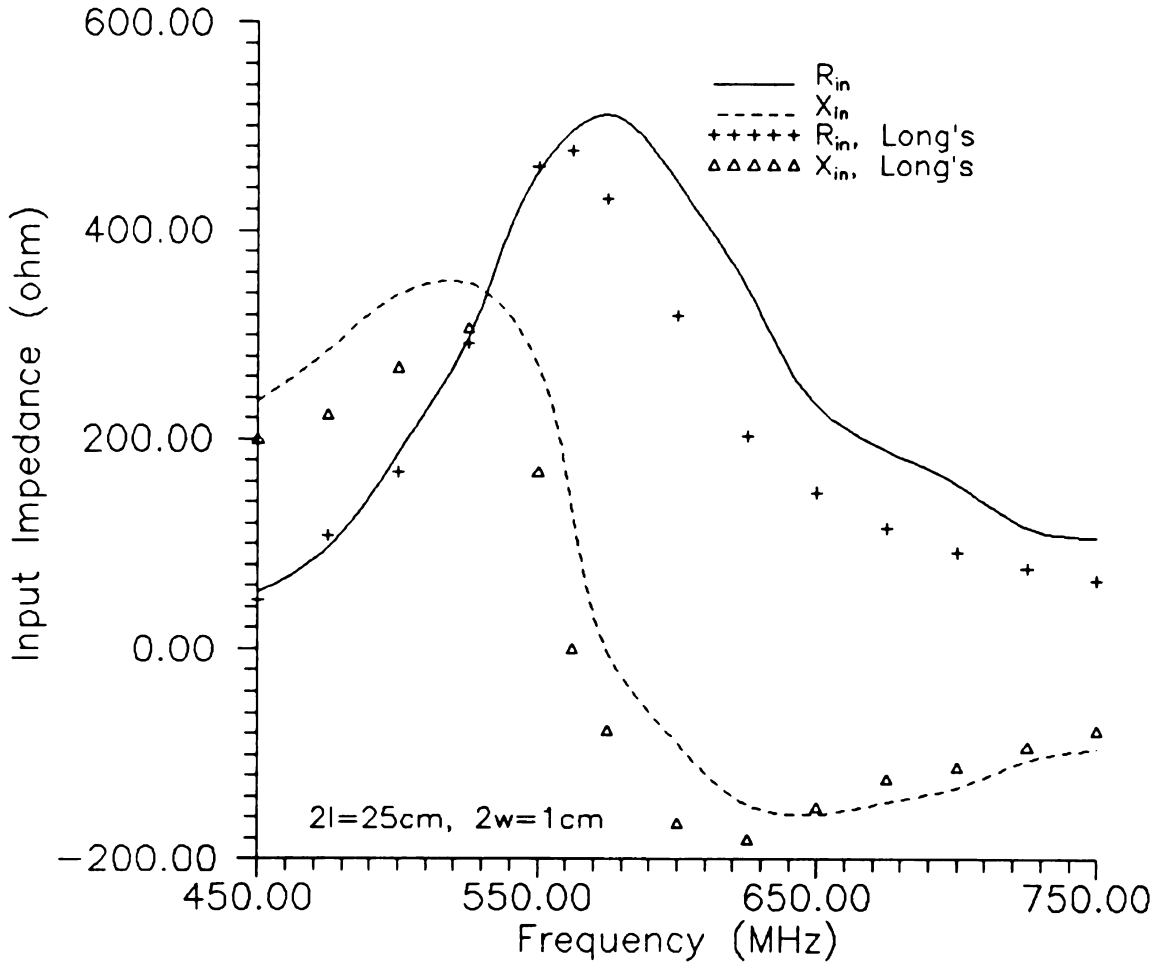

Figure 7.2.1 Input impedance of open slot antenna.

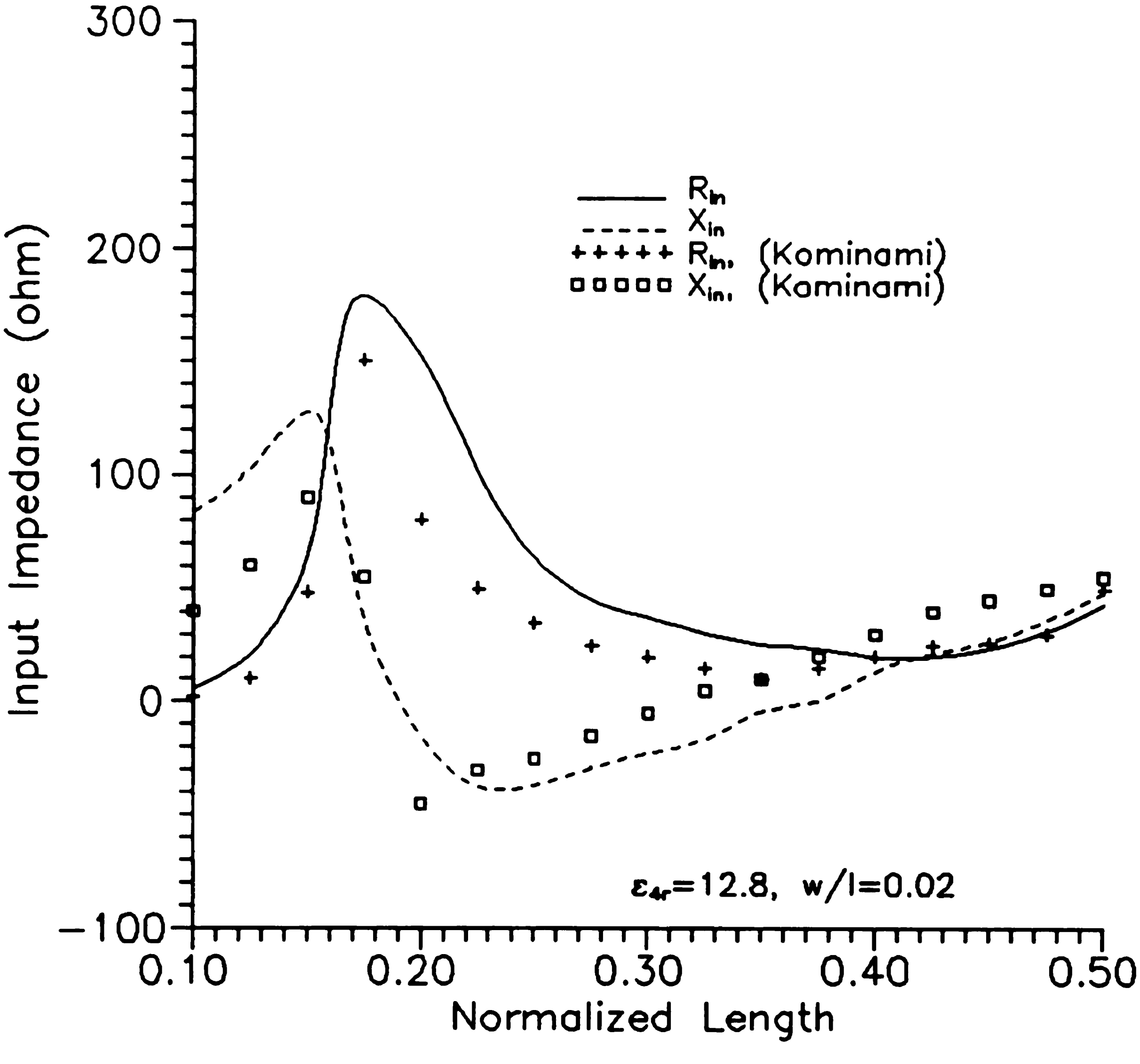

Figure 7.2.2 Input impedance of slot on semi-infinite GaAs substrate.

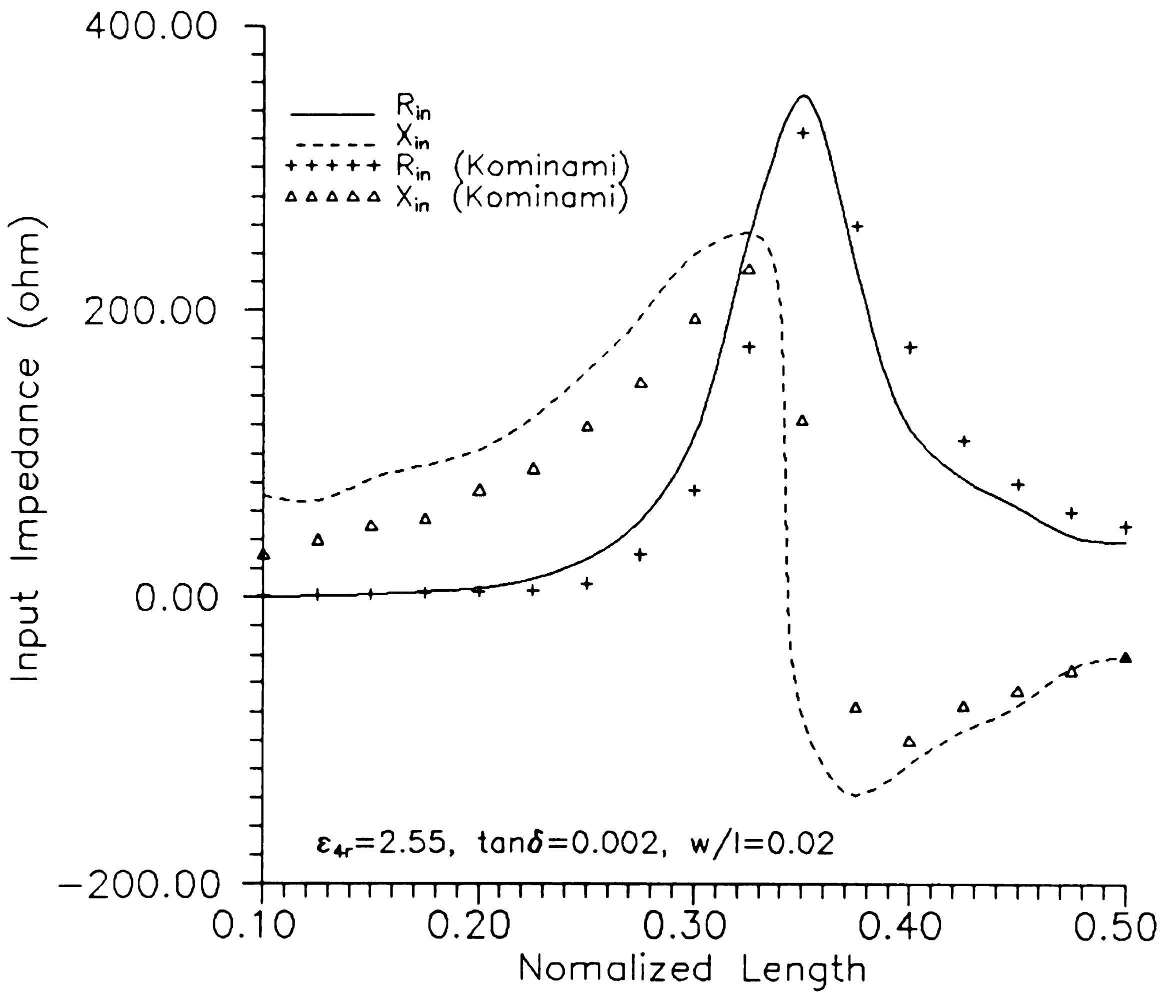

Figure 7.2.3 Input impedance of slot on semi-infinite PTFE substrate.

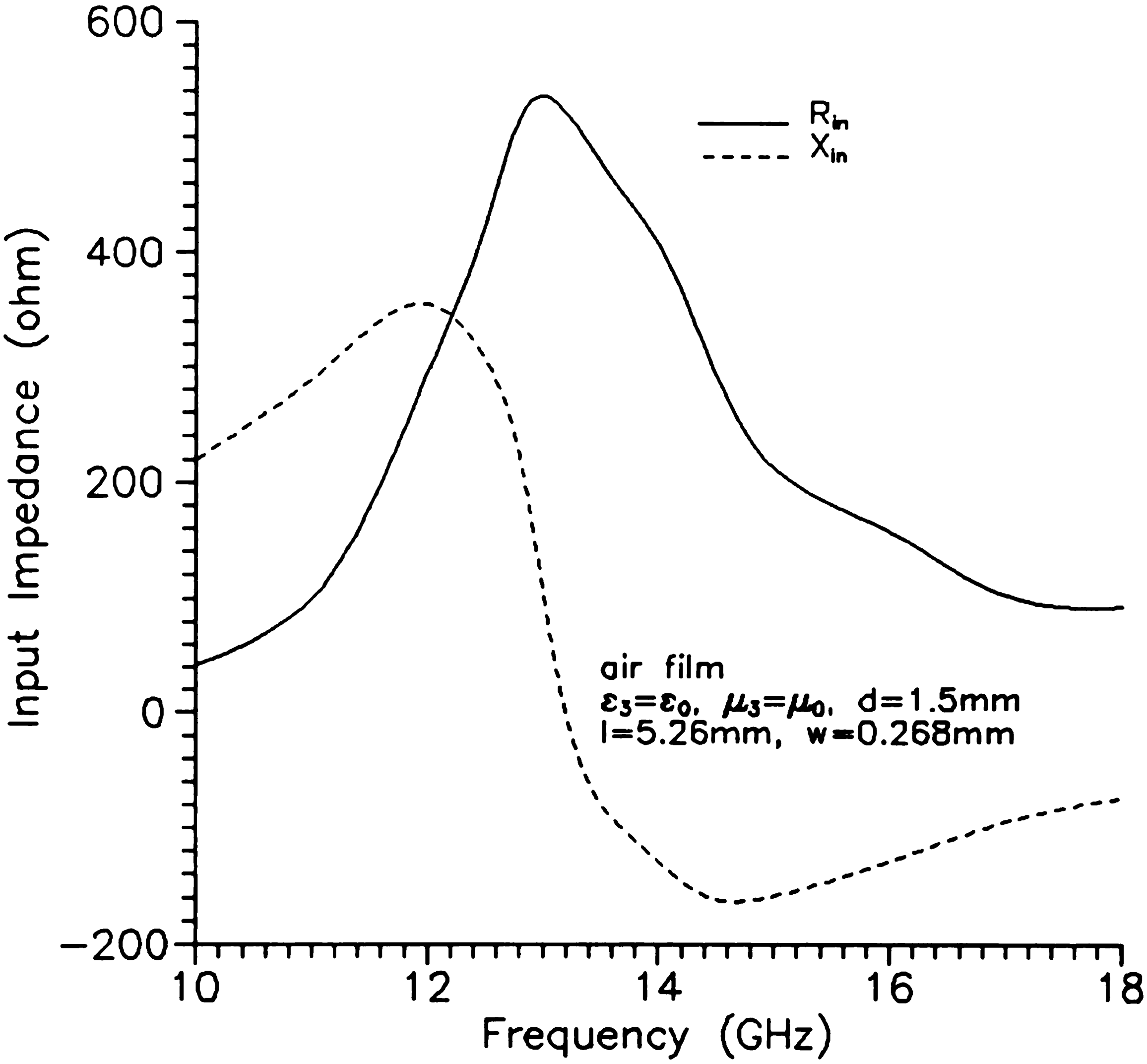

Figure 7.2.4 Input impedance of slot in tri-layered media with air film and foam substrate.

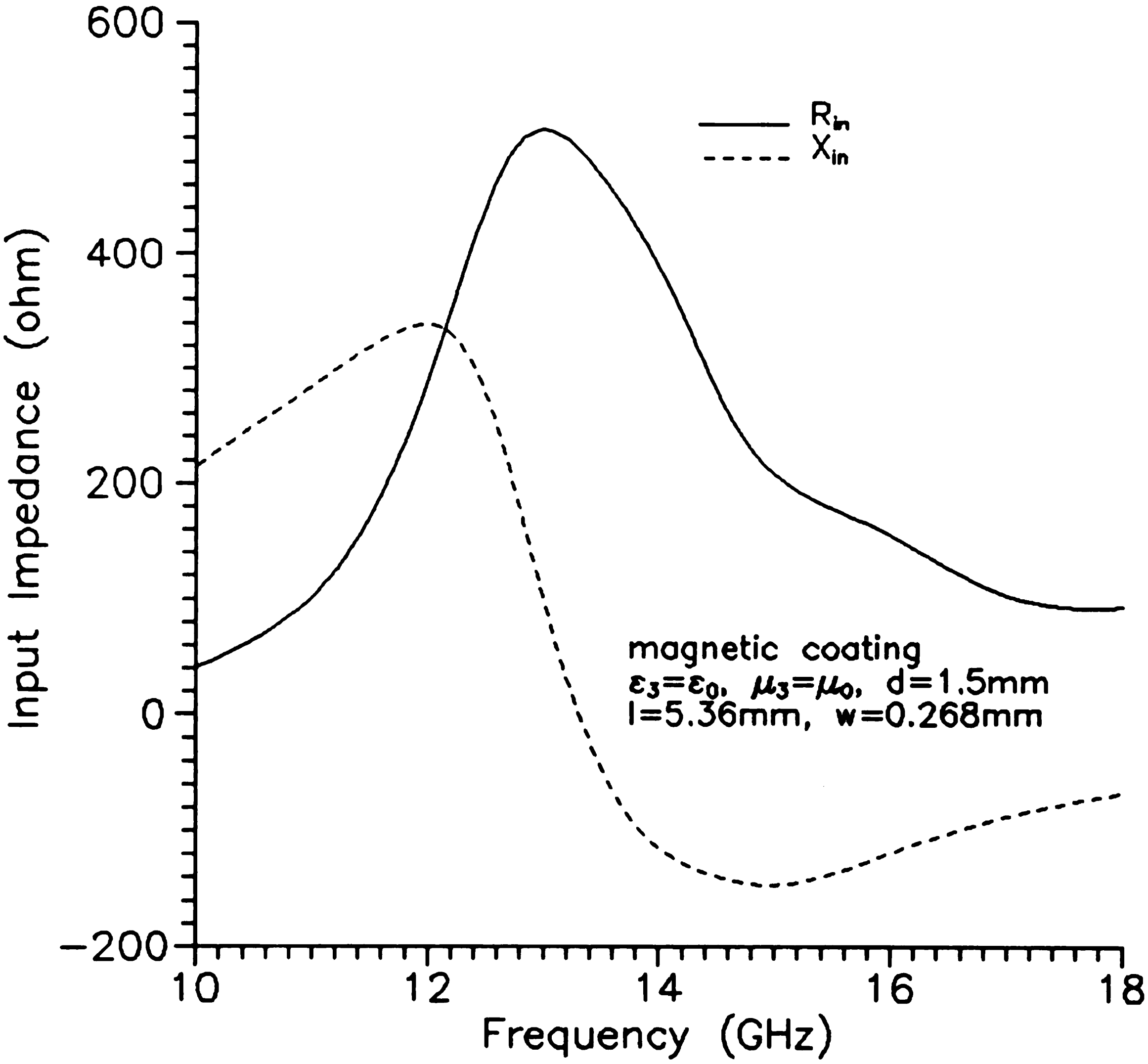

Figure 7.2.5 Input impedance of slot in tri-layered media with magnetic coating and foam substrate.

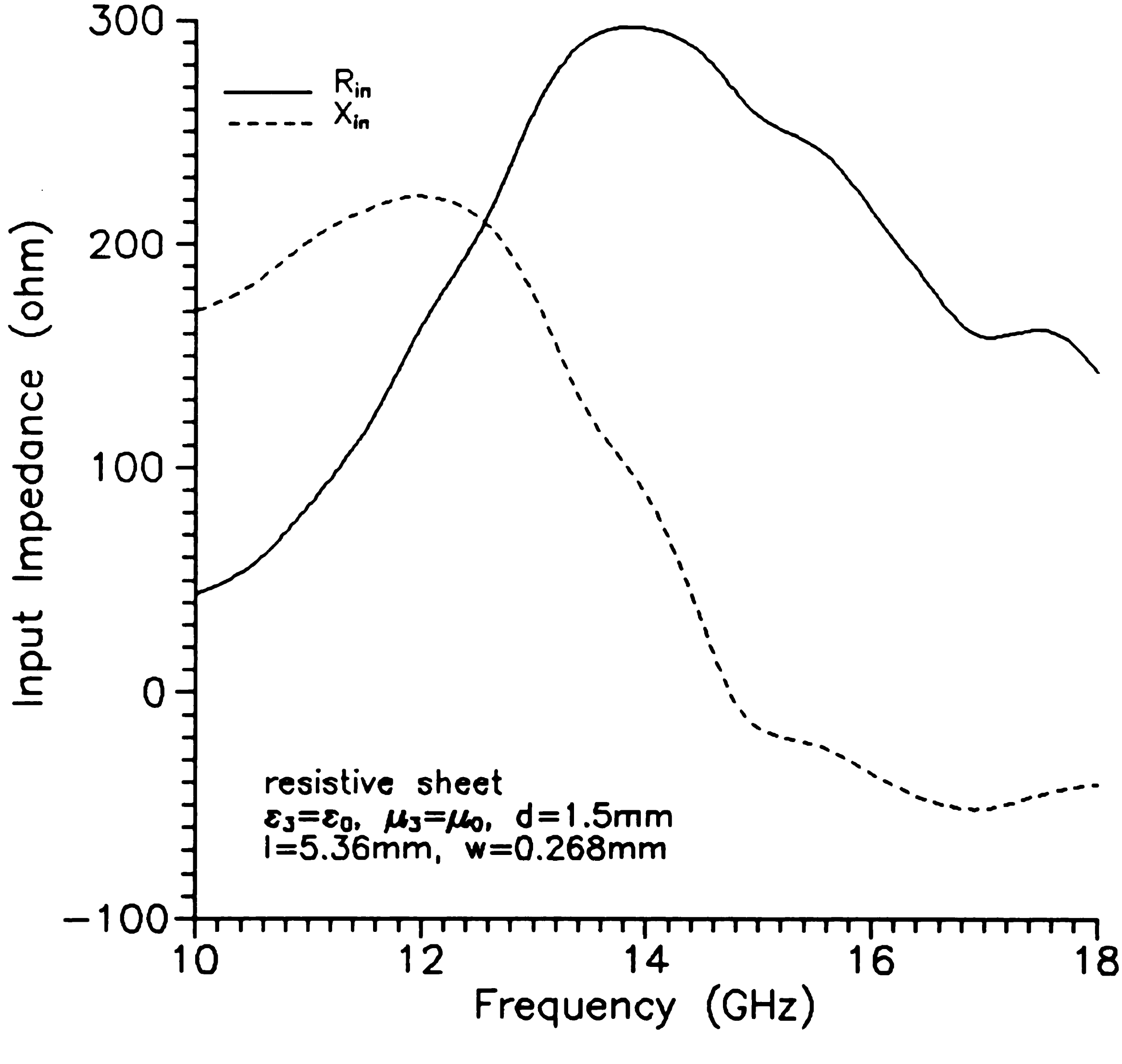

Figure 7.2.6 Input impedance of slot in tri-layered media with resistive sheet and foam substrate.

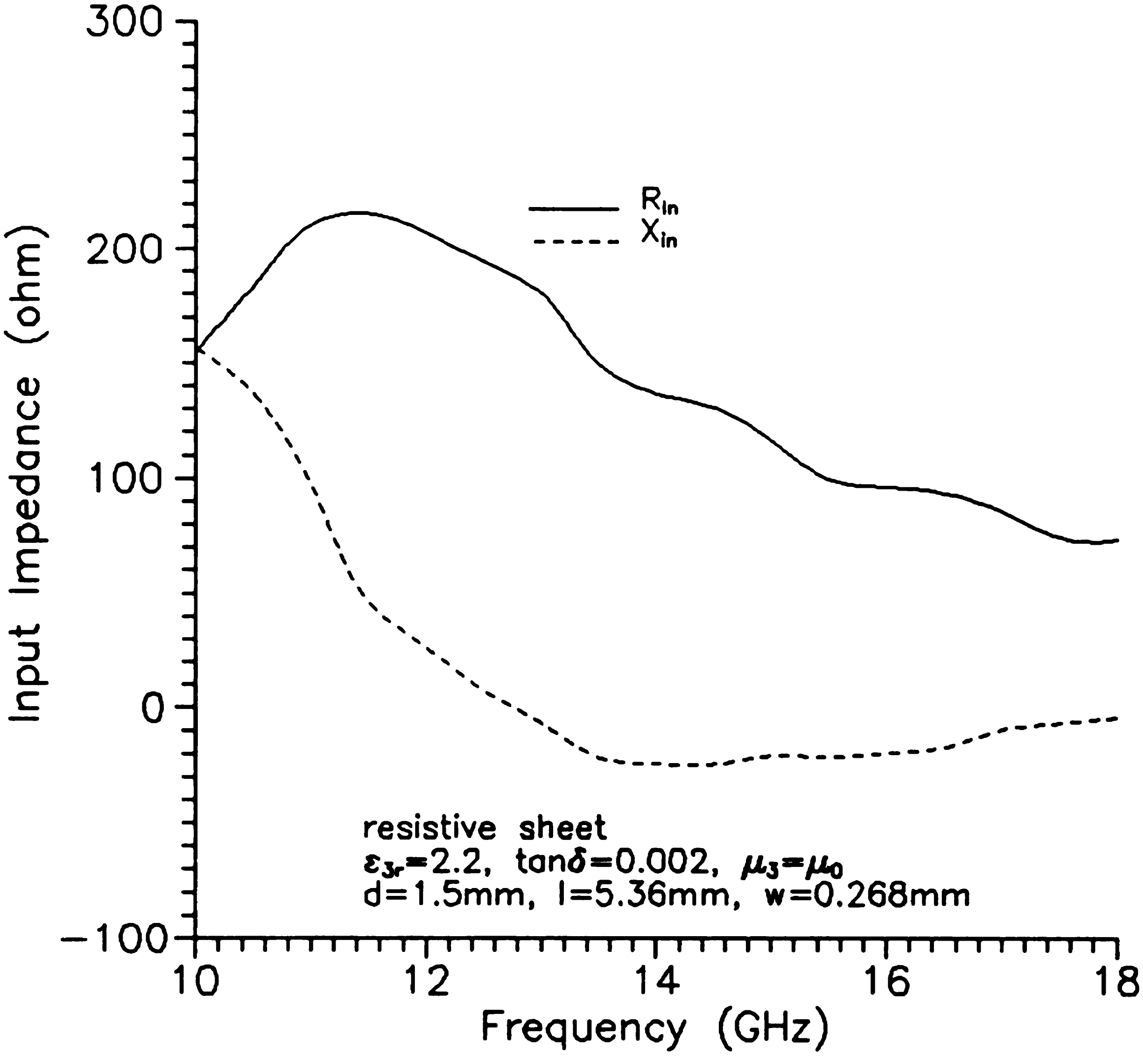

Figure 7.2.7 Input impedance of slot in tri-layered media with resistive sheet and PTFE substrate.

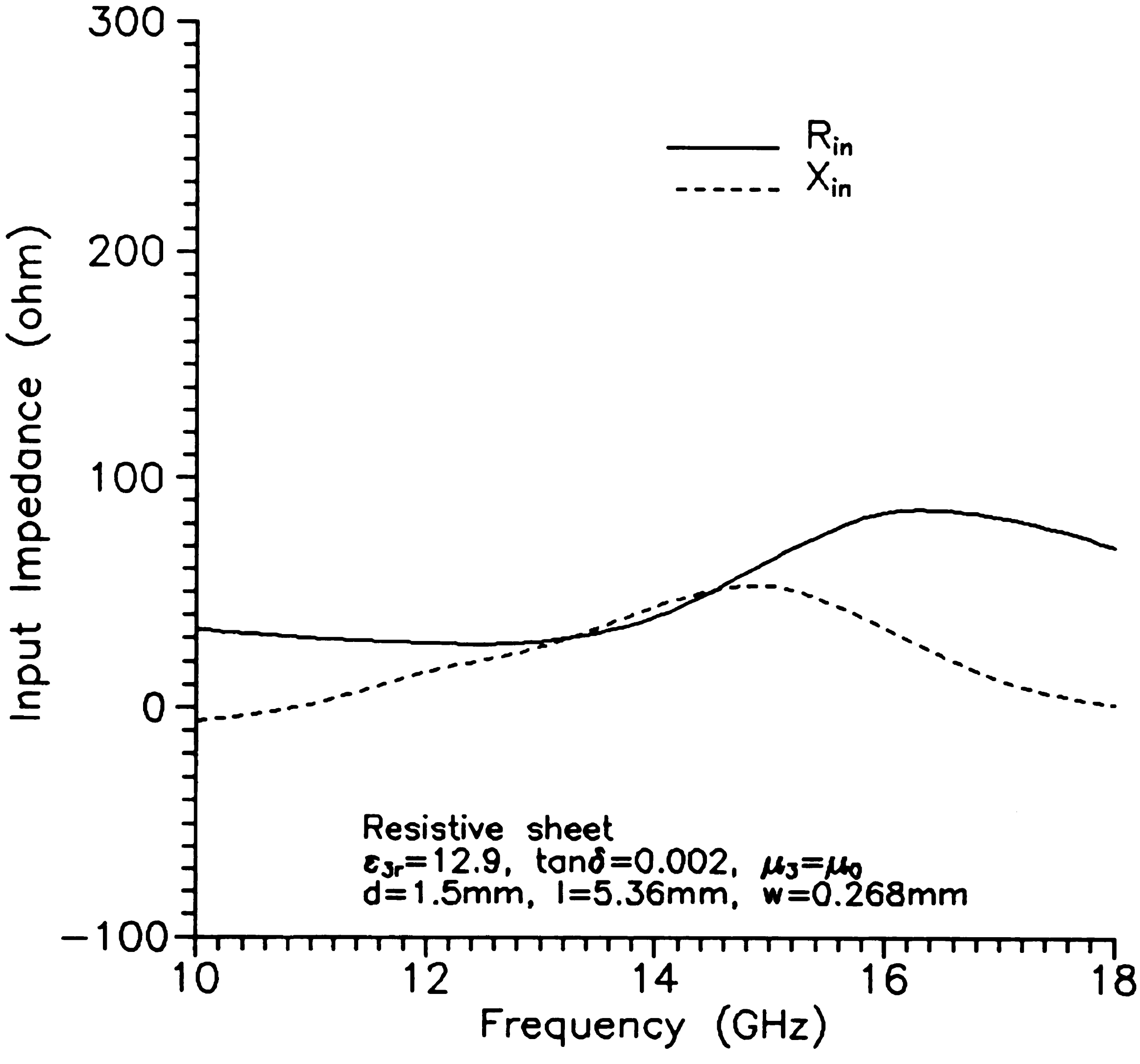

Figure 7.2.8 Input impedance of slot in tri-layered media with resistive sheet and GaAs substrate.

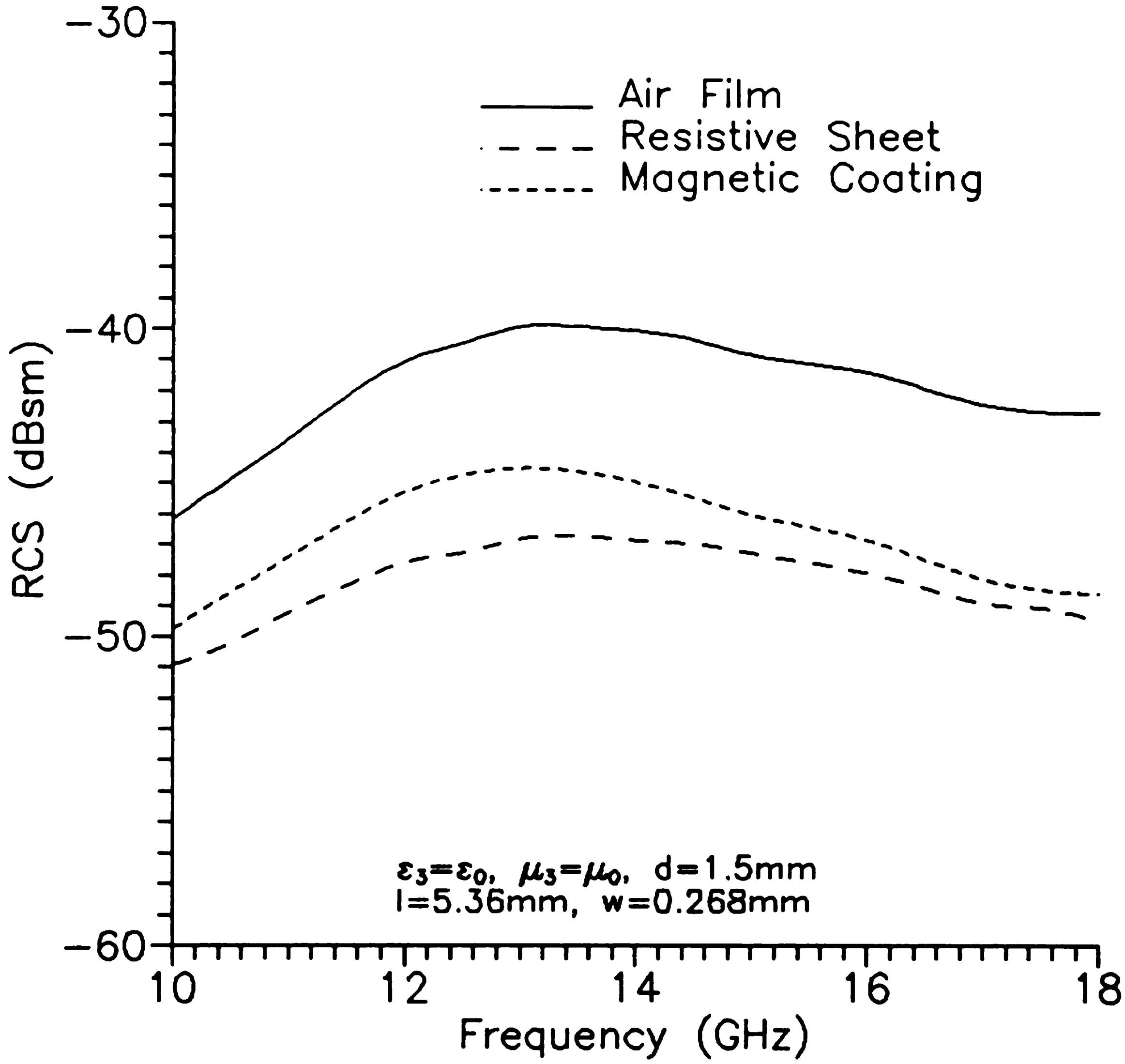

Figure 7.2.9 Radar cross section of slot in tri-layered media with foam substrate and different superstrates.

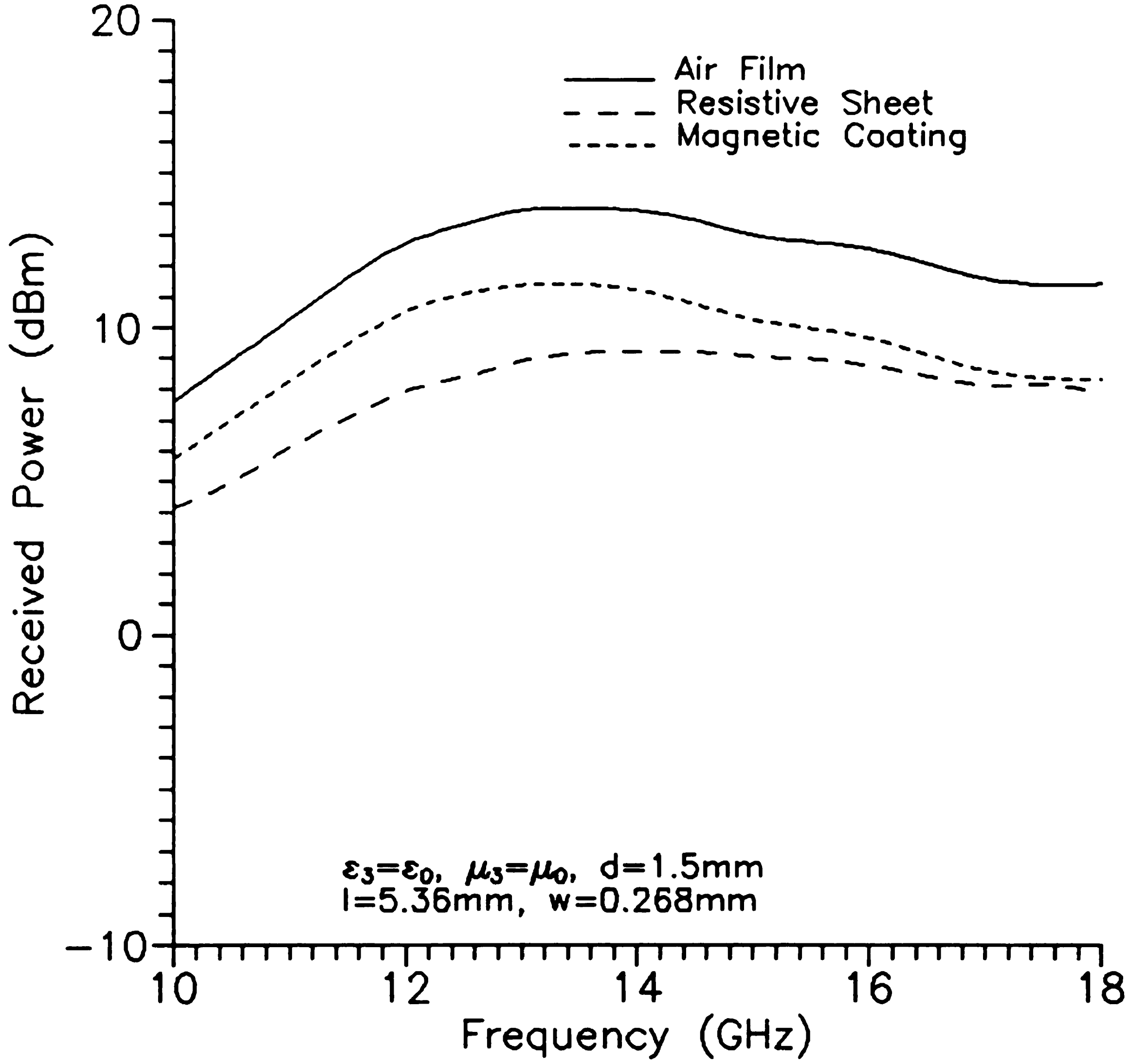

Figure 7.2.10 Received power of slot in tri-layered media with foam substrate and different superstrates.

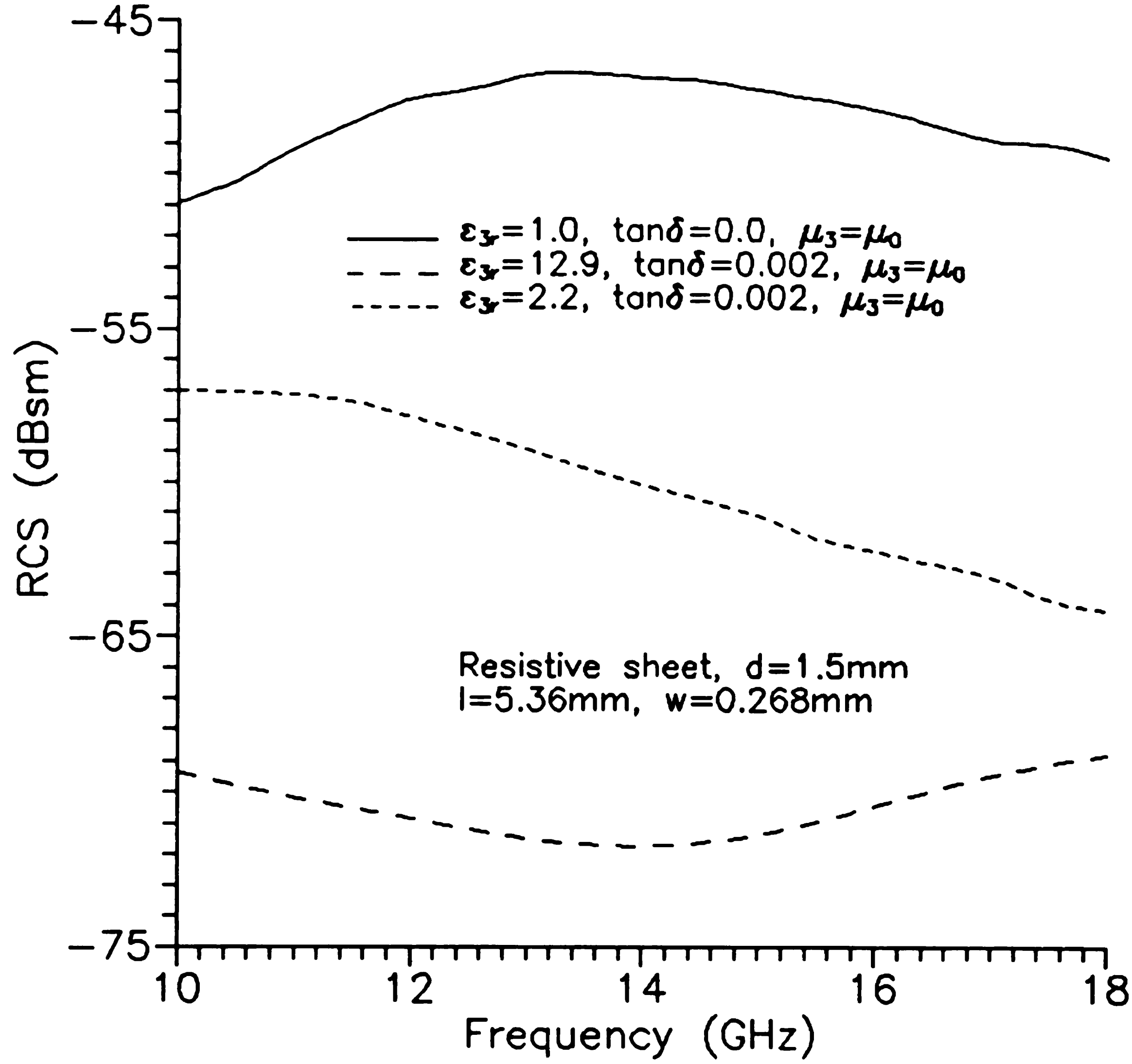

Figure 7.2.11 Radar cross section of slot in tri-layered media with resistive sheet and different substrates.

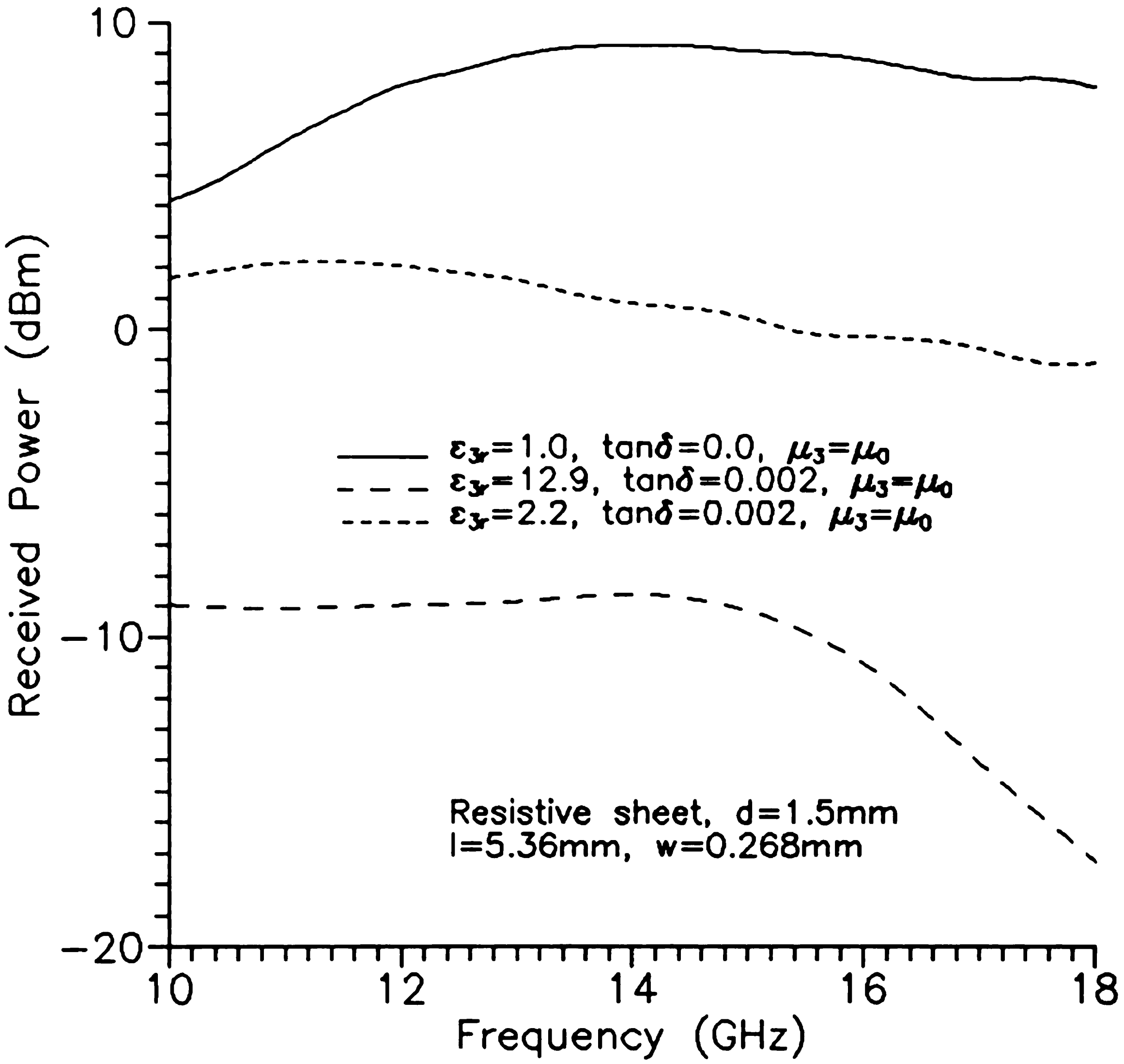

Figure 7.2.12 Received power of slot in tri-layered media with resistive sheet and different superstrates.

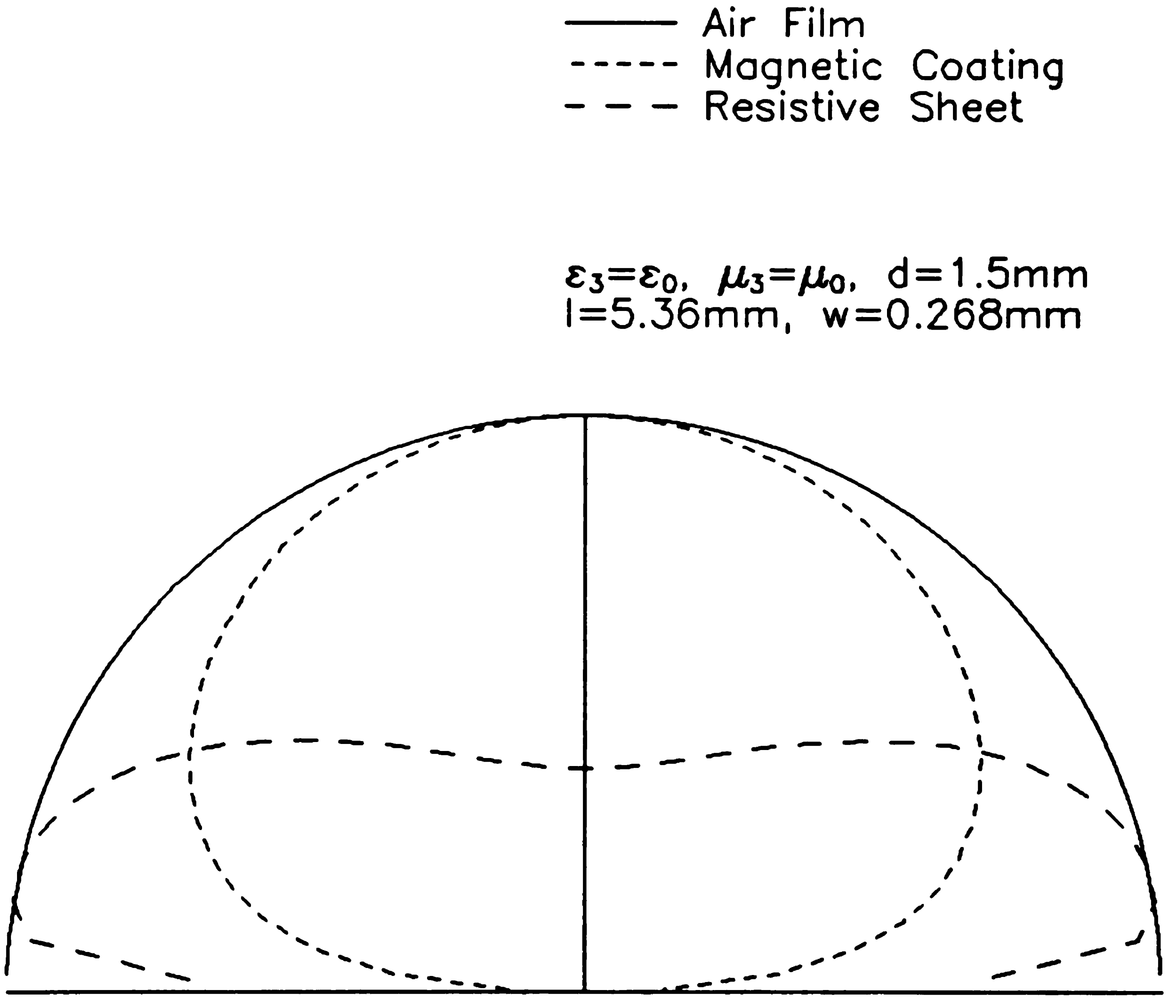

Figure 7.2.13 E-plane radiation pattern of slot in tri-layered media with foam substrate and different superstrates.

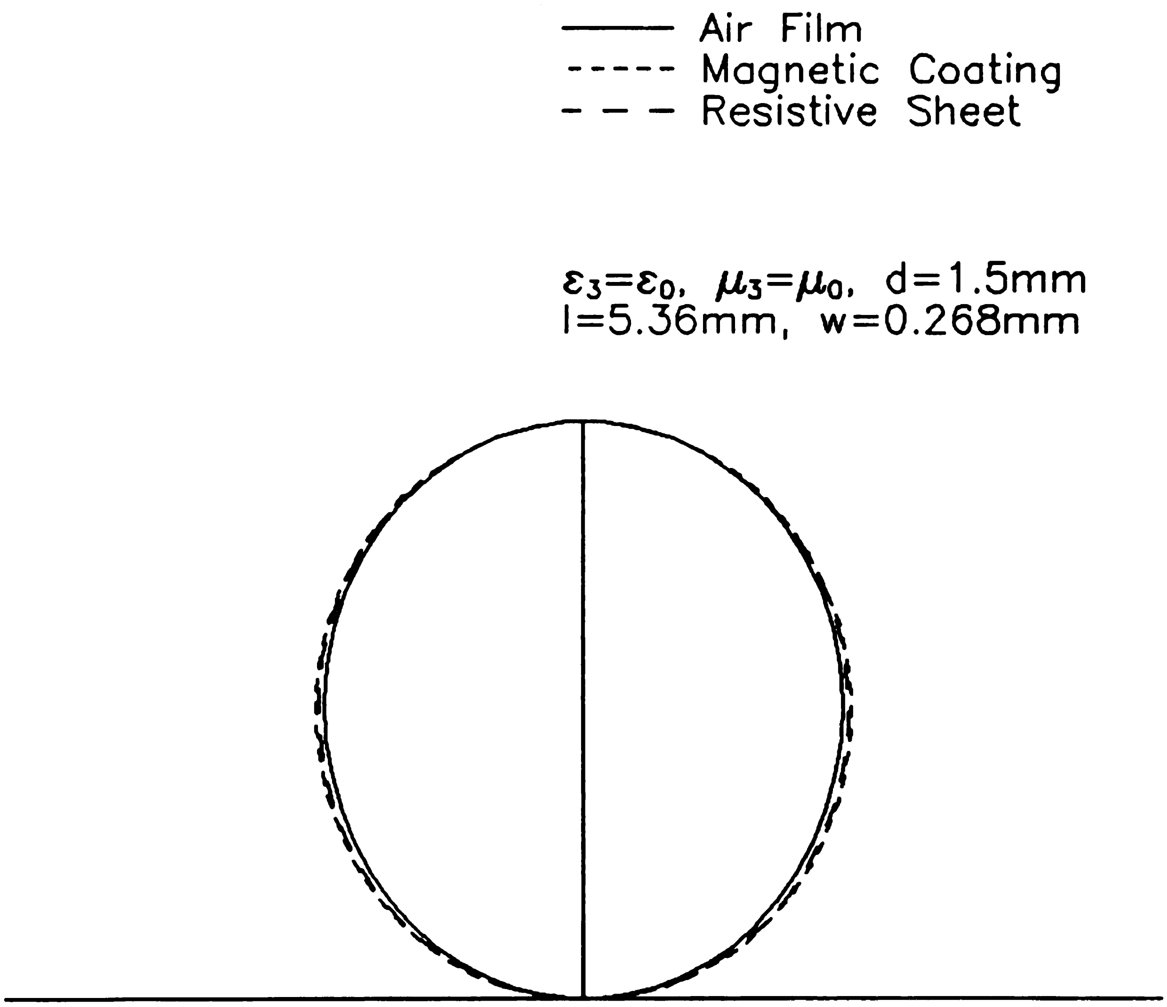

Figure 7.2.14 H-plane radiation pattern of slot in tri-layered media with foam substrate and different superstrates.

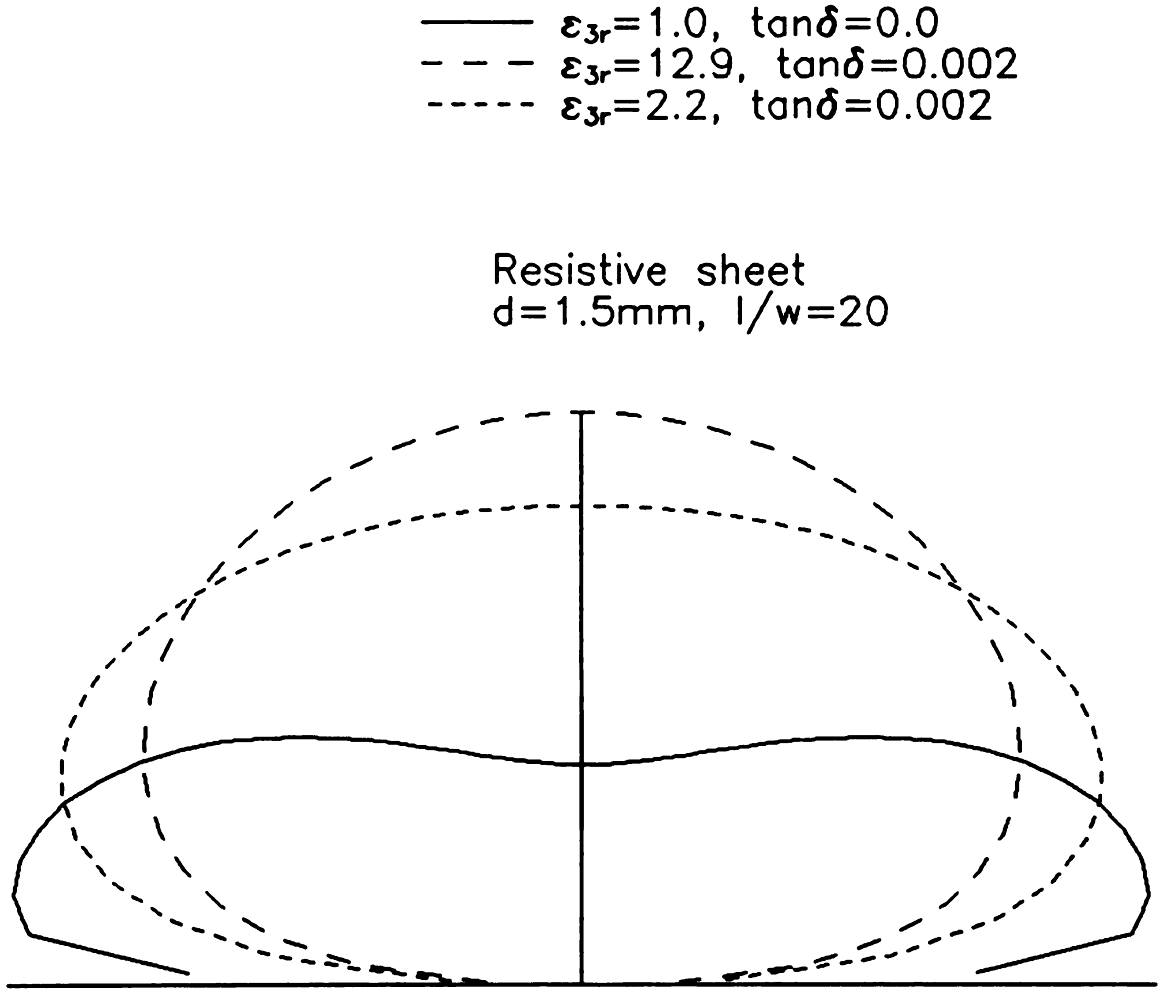

Figure 7.2.15 E-plane radiation pattern of slot in tri-layered media with resistive sheet and different substrates.

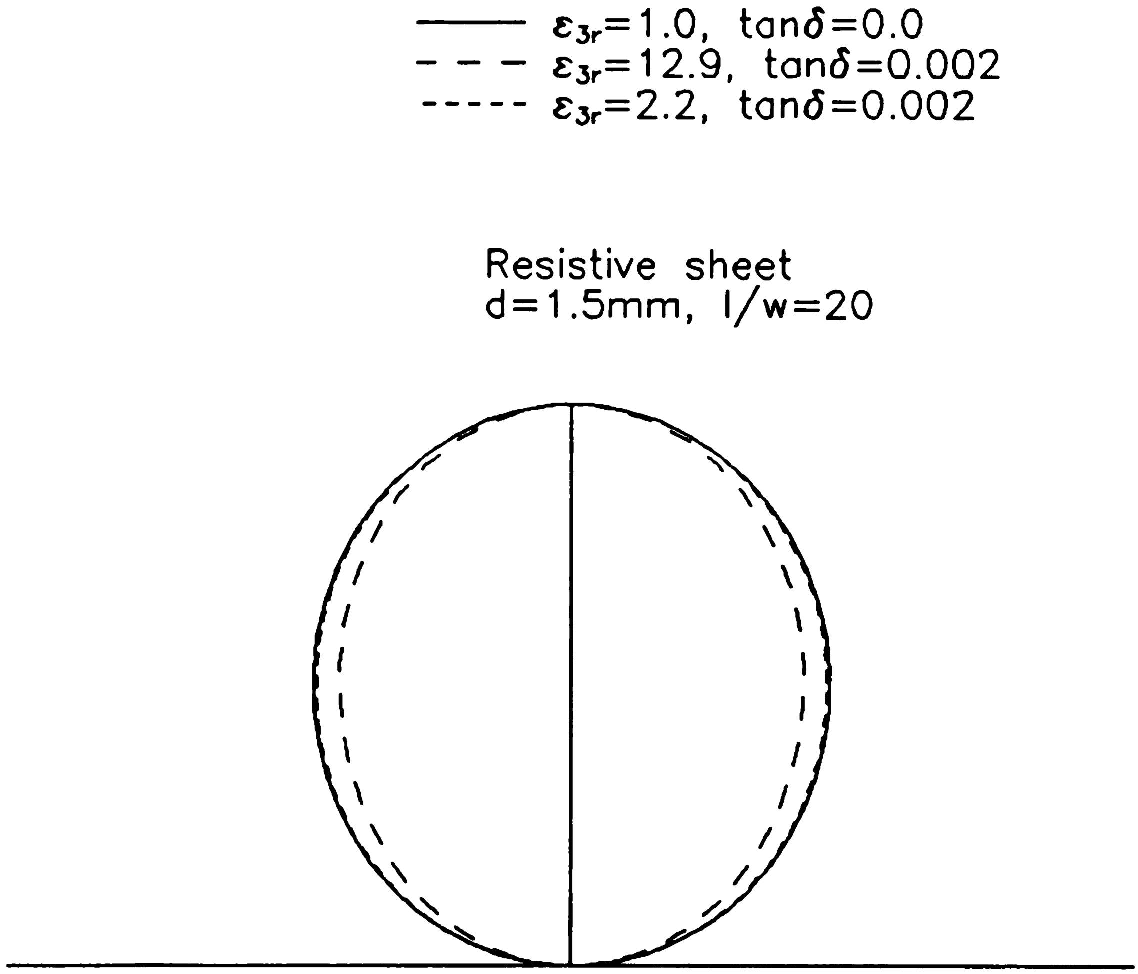

Figure 7.2.16 H-plane radiation pattern of slot in tri-layered media with resistive sheet and different substrates.

CHAPTER EIGHT

CONCLUSIONS

The scattering and receiving characteristics of imaged monopoles and slots in tri-layered media have been investigated in this dissertation. Emphasis is placed on the effects of lossy superstrates on the scattering and receiving characteristics. Basic electromagnetic parameters of monopoles and slots, such as input impedance, radiation pattern, radar cross section, and received power, have been studied by the full-wave integral equation approach.

Electric and magnetic Hertzian potentials have been used to facilitate the derivation of electric and magnetic dyadic Green's functions in tri-layered media. The dyadic Green's functions for electric Hertzian potential, magnetic Hertzian potential, electric field, and magnetic field in tri-layered media have been derived and expressed in terms of Sommerfeld integrals. An electric field integral equation (EFIE) and a magnetic field integral equation (MFIE) are converted to Hallen-type integral equations (HTIE) and the HTIEs are solved by the method of moments to obtain unknown electric and equivalent magnetic currents.

The existence of a lossy superstrate shifts all the surface wave poles of Sommerfeld integrals off the real axis of the complex λ-plane. This fact makes it possible to evaluate the impedance and admittance matrix entries via real axis spectral integration. The stationary phase method is used to compute the scattered far field.

Two representative antennas, an imaged vertical monopole and a narrow rectangular slot, in tri-layered media have been investigated numerically. The results are compared with published data whenever possible. In the case of a monopole shorted to the ground plane in tri-layered media, theoretical results are compared with experimental ones. The numerical results demonstrate that, for an antenna in tri-layered media with a lossy superstrate, the reduction in radar cross section is greater than the reduction in received power. The theory developed in this research can aid in the design of antennas with good transmitting and receiving capabilities and low radar cross sections.

In the case of a slot in tri-layered media, it is a very demanding computational task to fill the admittance matrix. Further research is needed to find efficient and robust analytical and numerical techniques for the evaluation of admittance matrix elements.

In most applications, another ground plane or a cavity is placed under the slot to make it unidirectional and to provide more practical feeding mechanisms. The current theory can be extended to analyze a cavity backed or microstrip fed slot. The kernel of the integral equation for such an antenna system will be even more complicated. The challenge is find efficient matrix filling methods to keep the computer cost in check.

BIBLIOGRAPHY

BIBLIOGRAPHY

[1] R.S. Elliott, *Antenna Theory and Design*, Prentice-Hall, Inc., New Jersey, 1981.

[2] R.C. Johnson and H. Jasik, *Antenna Engineering Handbook*, McGraw-Hill, New York, 1984.

[3] R.E. Collin and F.J. Zucker, *Antenna Theory*, McGraw-Hill, New York, 1969.

[4] R.W.P. King, *The Theory of Linear Antennas*, Harvard University Press, Cambridge, 1956.

[5] A. Sommerfeld, *Partial Differential Equations in Physics*, Academic Press, New York, 1949.

[6] Weng Cho Chew, *Waves and Fields in Inhomogeneous Media*, Van Nostrand Reinhold, New York, 1990.

[7] R.F. Harrington, *Fields Computation by Moment Methods*, The Macmillan Company, New York, 1968.

[8] R. Mittra, Ed, *Numerical and Asymptotic Techniques in Electromagnetics*, Spring-Verlag, New York, 1975.

[9] R. Mittra, Ed, *Computer Techniques for Electromagnetics*, Pergaman Press, Oxford, 1973.

[10] D.P. Nyquitst, *Advanced Topics in Electromagnetics*, EE929 Class Note, Department of Electrical Engineering, Michigan State University, Fall 1987.

[11] M.A. Blischke, *Broadband analysis of radiation, receiving and scattering characteristics of microstrip antennas and arrays*, Ph.D. dissertation, Department of Electrical Engineering, Michigan State University, 1989.

[12] Arthur D. Yaghjian, "Electric Dyadic Green's Functions in the Source Region," *Proceedings of the IEEE*, vol. 68, pp. 248-263, Feb. 1980.

[13] P. Katehi, "A space domain integral equation approach in the analysis of dielectric-covered slots," *Radio Science*, vol. 24, pp. 253-260, March-April 1989.

[14] P. Katehi, P. Katehi, *The Green's function for a slot on the ground of a dielectric slab*, Radiation Lab. Report RL-841, Department of Electrical Engineering and Computer Science, University of Michigan, June 1987.

[15] C.M. Butler, Y. Rahmat-Samii, and R. Mittra, "Electromagnetic penetration through apertures in conducting surfaces," *IEEE Trans. Antennas Propag.*, vol. AP-26, pp. 82-93, Jan. 1978.

[16] C.M. Butler, and D.R. Wilton, "General analysis of narrow strips and slot," *IEEE Trans. Antennas Propag.*, vol. AP-28, pp. 42-48, Jan. 1980.

[17] R.D. Nevels, and C.M. Butler, "Electromagnetic diffraction by a slot in a ground screen covered by a dielectric slab," *IEEE Trans. Antennas Propag.*, vol. AP-30, pp. 390-395, May 1982.

[18] P. Bhartia, K.V.S. Rao, and R.S. Tomar, *Millimeter-Wave Microstrip and Printed Circuit Antennas*, Artech House, Boston, 1991.

[19] P. Katehi, *A generalized solution to a class of printed circuit antennas*, Doctoral dissertation, Department of Electrical Engineering, University of California, Los Angeles, June 1984.

[20] K.R. Carver and J.W. Mink, "Microstrip antenna technology," *IEEE Trans. Antennas Propag.*, vol. AP-29, pp. 2-24, Jan. 1981.

[21] R.H. Jansen, "The spectral-domain approach for microwave integrated circuits," *IEEE Trans. Microwave Theory Tech.*, vol. MTT-33, pp. 1043-1056, Oct. 1985.

[22] W.C. Chew and L. Gurel, "Reflection and transmission operators for strips or disks embedded in homogeneous and layered media," *IEEE Trans. Microwave Theory Tech.*, vol. MTT-36, pp. 1488-1497, Nov. 1988.

[23] D.R. Jackson and N.G. Alexopoulos, "Gain enhancement methods for printed antennas," *IEEE Trans. Antennas Propagat.*, vol. AP-33, pp. 976-987, Sept. 1985.

[24] K.A. Michalski and D. Zheng, "Electromagnetic scattering and radiation by surface of arbitrary shape in layered media," *IEEE Trans. Antennas Propagat.*, vol. AP-38, pp. 335-353, March 1990.

[25] Y.L. Chow, J.J. Yang, D.G. Fang, and G.E. Howard, " A closed-form spatial Green's function for the thick microstrip substrate," *IEEE Trans. Microwave Theory Tech.*, vol. MTT-39, pp. 588-592, March 1991.

[26] N.G. Alexopolous, P.B. Katehi, and D.B. Rutledge, "Substrate optimization for integrated circuit antennas," *IEEE Trans. Microwave Theory Tech.*, vol. MTT-31, pp. 550-557, July 1983.

[27] N.G. Alexopoulos, D.R. Jackson, "Fundamental superstrate (cover) effects on printed circuit antennas," *IEEE Trans. Antennas Propagat.*, vol. AP-32, pp. 807-816, Aug. 1984.

[28] D.R. Jackson and N.G. Alexopoulos, "Analysis of planar strip geometries in a substrate-superstrate configuration," *IEEE Trans. Antennas Propagat.*, vol. AP-34, pp. 1430-1438, Dec. 1986.

[29] M. Kominami, D.M. Pozar, and D.H. Schaubert, "Dipole and slot elements and arrays on semi-infinite substrates," *IEEE Trans. Antennas Propagat.*, vol. AP-33, pp. 600-607, June 1985.

[30] Y. Yoshimura, "A microstripline slot antenna," *IEEE Trans. Microwave Theory Tech.*, vol. MTT-20, pp. 760-762, Nov. 1972.

[31] R. Shavit and R.S. Elliott, "Design of transverse slot arrays fed by a boxed strip-line," *IEEE Trans. Antennas Propagat.*, vol. AP-31, pp. 545-552, July 1983.

[32] S.A. Long, "Experimental study of the impedance of cavity-backed slot antennas," *IEEE Trans. Antennas Propagat.*, vol. AP-23, pp. 1-7, Jan. 1975.

[33] D.M. Pozar, "A reciprocity method of analysis for printed slot and slot-coupled microstrip antennas," *IEEE Trans. Antennas Propagat.*, vol. AP-34, pp. 1439-1446, Dec. 1986.

[34] P.L. Sullivan and D.H. Schaubert, "Analysis of an aperture coupled microstrip antenna," *IEEE Trans. Antennas Propagat.*, vol. AP-34, pp. 977-984, Aug. 1986.

[35] S.L. Dvorak, *Accurate and efficient numerical analysis of printed strip dipole antennas in layered media*, Doctoral dissertation, Department of Electrical and Computer Engineering, University of Colorado, 1989.

[36] W.A. Johnson and D.G. Dudley, "Real axis integration of Sommerfeld integrals: source and observation points in air," *Radio Science*, vol. 18, pp. 175-186, March-April 1983.

[37] P. Katehi, and N.G. Alexopoulos, "Real axis integration of Sommerfeld integrals with application to printed circuit antennas," *J. Math. Phys.*, 24(3), pp. 527-533, 1983.

[38] W.C. Chew, "A quick way to approximate a Sommerfeld-Weyl-type integral," *IEEE Trans. Antennas Propag.*, vol. AP-36, pp. 1654-1657, 1988.

[39] S.L. Dvorak and E.F. Kuester, *Numerical Computation of the Incomplete Lipschitz-Hankel Integral Je0(a,z)*, Scientific Report No. 89, Electromagnetic Laboratory, Department of Electrical and Computer Engineering, University of Colorado, Boulder, Colorado 80309, 1987.

[40 D.G. Fang, J.J. Yang and G.Y. Delisle, "Discrete image theory for horizontal electric dipoles in a multilayered medium," *IEE Proceedings*, vol. 135, Pt. H, Oct. 1988.

[41] C.L.Chi and N.G. Alexopolous, "An efficient numerical approach for modeling microstrip-type antennas," *IEEE Trans. Antennas Propagat.*, vol. AP-38, pp. 1399-1404, Sept. 1990.

[42] H.Y. Yang, A. Nakatani, and J.A. Castaneda, "Efficient evaluation of spectral integrals in the moment method solution of microstrip antennas and circuits," *IEEE Trans. Antennas Propagat.*, vol. AP-38, pp. 1127-1130, July 1990.

[43] J.R. Mosig and F.E. Gardiol, "Analytic and numerical techniques in the Green's function treatment of microstrip antennas and scatters," *Inst. Elec. Eng. Proc.*, vol. 130, pt. H, pp. 175-182, Mar. 1983.

[44] D.M. Pozar, "Improved computational efficiency for the method of moments solution of printed dipoles and patches," *Electromagn.*, vol. 3, pp. 299-309, July-Dec. 1983.

[45 C.L. Chi and N.G. Alexopoulos, "Radiation by a probe through a substrate," *IEEE Trans. Antennas Propag.*, vol. AP-34, pp. 1080-1091, Sept. 1986.

[46] F.M. Tesche, "On the behavior of the thin-wire antennas and scatterers arbitrarily located within a parallel-plate region," *IEEE Trans. Antennas Propag.*, AP-20, pp. 482-486, July 1972.

[47] E.J. Rothwell, W.J. Gesang, and K.M. Chen, *Receiving and scattering characteristics of an imaged monopole beneath a lossy sheet*, Technical Report No. 3, Department of Electrical Engineering, Michigan State University, East Lansing, 1990.

[48] D.P. Nyquist, *Antennas*, EE926 Class Note, Department of Electrical Engineering, Michigan State University, Fall term 1987. pp. 110-114.

[49] D.C. Champeney, *A Handbook of Fourier Theorems*, Cambridge University Press, Cambridge, 1987.

[50] A. Papoulis, *The Fourier Integral and Its Applications*, New York: McGraw-Hill, 1962.

[51] I.S. Gradshteyn, I.M. Ryzhik, *Tables of Integrals, Series, and Products*, Academic Press, 1980.

[52] M. Abramowitz, I.E. Stegun, *Handbook of Mathematical Functions with Formulas, Graphs, and Mathematical Tables*, U.S. Government Printing Office, Washington, D.C., 1972.

[53] W.H. Beyer, Ed., *CRC Standard Mathematical Tables*, CRC Press, 1973.

[54] W. Press, et. al., *Numerical Recipes*, Cambridge University Press, 1986.

[55] Robert E. Collin, *Field Theory of Guided Waves* , IEEE Press, New York, 1991.

[56] Kun-Mu Chen, *Electromagnetic Theory*, EE835 Class Note, Department of Electrical Engineering, Michigan State University, 1987.

[57] K.A. Michalski, "On the efficient evaluation of integrals arising in the Sommerfeld halfspace problem," *Inst. Elec. Eng. Proc.*, vol. 132, pt. H, pp. 312-318, Aug. 1985.

[59] K.A. Michalski and C.M. Butler, "Evaluation of Sommerfeld integrals arising in the ground stake antenna problem," *Inst. Elec. Eng. Proc.*, vol. 134, pt. H, pp. 93-97, Feb. 1987.

[60] K. Aki and P.G. Richard, *Quantitative Seismology - Theory and Methods*, vols. I and II, Freeman, New York, 1980.

[61] R. Shavit and R.S. Elliott, "Design of transverse slot arrays fed by a boxed stripline," *IEEE Trans. Antennas Propag.*, vol. AP-31, pp. 545-552, July 1983.

[62] R.J. Mailloux, "On the use of metallized cavities in printed slot arrays with dielectric substrates," *IEEE Trans. Antennas Propag.*, vol. AP-35, pp. 477-487, May 1987.

[63] J.S. Bagby and D.P. Nyquist, "Dyadic Green's function for integral electronic and optical circuits," *IEEE Trans. Microwave Theory Tech.*, vol. MTT-35, pp. 206-210, Feb. 1987.

[64] M.S. Voila and D.P. Nyquist, "An observation on the Sommerfeld-integral representation of the electric dyadic Green's function for layered media," *IEEE Trans. Microwave Theory Tech.*, vol. MTT-36, pp. 1289-1292, 1988.